

**Electroanalytical Studies
of Some Species of Clinical Importance**

by

Martin Telting Diaz

**A Thesis submitted
to Dublin City University
for the degree of Doctor of Philosophy**

**School of Chemical Sciences
Dublin City University**

September 1990

This thesis is dedicated to the memory
of my good friend and colleague
Francis Regan

ACKNOWLEDGEMENTS

I would like to express my gratitude to my supervisors Dr. Dermot Diamond and Dr. Malcolm R. Smyth for their continuous support and encouragement during the course of this work. In particular, I wish to acknowledge their considerable patience and attention to detail during the preparation of this thesis.

I wish to thank Prof. Paulino Tunon Blanco for the opportunity and privilege of working with his research group at the University of Oviedo, Asturias, Spain.

I would like to acknowledge the technical staff of the school of chemical sciences at Dublin City University for their excellent help and assistance.

I wish to acknowledge my fellow post graduate students, both at DCU and University of Oviedo, for their help, cooperation and friendly advice during my research work. In particular, I would like to thank Aodhmar Cadogan, Francis Regan and Philip O'Dea.

I wish to thank Prof. Albert Pratt as head of the school of chemical sciences for the use of facilities at the university.

I wish to express my particular gratitude to Dr. Eileen Buckley and Dr. Jose Maria Fernandez Alvarez for their unceasing support during my time at the university.

I would like to acknowledge Mr. Gerry O'Sullivan and Mr. Peter Mc Gaffney from the pathology laboratories at St. James Hospital, Dublin, for useful discussion and the provision of clinical samples.

Finally, I wish to thank my friend Josephine for her unending support and friendship.

This thesis is submitted in fulfilment of the requirements for Doctor of Philosophy, by research and thesis. It has not been presented as an exercise for a degree at this or any other university. Except where otherwise stated, this work has been carried out by the author alone, on a full time basis between 1987 and 1990, at Dublin City University.

Martin Telting Diaz

Dr. Dermot Diamond

Dr. Malcolm R. Smyth

ABSTRACT

Solvent polymeric membrane electrodes incorporating p-t-butyl hexaethyl ester and hexaethyl ester calix[6]arene as neutral carriers have been constructed for use in caesium selective electrodes. The potentiometric sensing electrodes including 2-nitrophenyloctyl ether as solvent mediator exhibit near-Nernstian behaviour in the range 1×10^{-4} M to 1×10^{-1} M CsCl. The pattern of selectivity encountered for a range of common interferents is not modified by the inclusion of potassium tetrakis(p-chlorophenyl)borate as ion-exchanger in the case of the hexaethyl ester although some improvement in sensitivity is obtained in the case of the hexaethyl ester. The hexaethyl ester is superior with respect to rubidium and potassium selectivities, with the coefficients being of the order of 3×10^{-2} and 2.7×10^{-3} respectively. Both electrodes are relatively stable and responses are essentially complete within seconds.

Different types of sodium electrodes have also been constructed using two tetrameric calixarene ionophores, namely methyl p-t-butylcalix[4]aryl acetate and the methyl tetraketone derivative of p-t-butylcalix[4]arene. The selectivity of both electrodes is similar although discrimination against ammonium ions is improved by a factor of ten in the case of the methyl tetraketone based electrode. The selectivities against lithium, potassium and hydrogen ions are improved in comparison to other commercially available ionophores. Response times, stability, reproducibility and life time characteristics agree well with the requirements made of these devices for clinical applications. On the assessment of a large number of blood plasma samples, the methyl ester tetrameric based electrode exhibits excellent correlation when compared to two hospital based auto-analysers and to flame photometry. The residual standard deviation is typically within 1 to 3 mmol/l and highly influenced by the dipping method employed for the determination. Optimisation of the selective membrane in the case of methyl tetraketone based electrodes also give excellent results for the analysis of sodium in plasma samples, although in this case correlation with the above mentioned reference methods is higher and the residual standard deviation is lower. The incorporation of the methyl ester calix[4]arene electrode in a flow injection system has proven advantageous in improving both precision and accuracy in comparison to the dipping technique.

Solid-state monomeric and polymeric calixarene based electrodes have been constructed and found to exhibit promising features to varying degrees. Thus, platinum coated electrodes based on the methyl tetraketone calix[4]arene gave similar performance to the conventional sort in terms of Nernstian response, selectivity and response time, although the electrodes are less stable. Another chemically modified tetrameric calixarene (monomer VI) has been found to be responsive to potassium ions. Copolymerisation of two monomeric calixarenes with methyl methacrylate carried out have led to non-responsive electrodes while other polymers exhibited sub-Nernstian slopes to sodium and caesium.

Amperometric studies have been also carried out to assess the voltammetric behaviour of pipemidic acid. The drug has been investigated by linear sweep, differential pulse and square wave voltammetry at a hanging mercury drop electrode. Two reduction processes were observed in Britton-Robinson buffer in acidic solutions, whereas only one or two processes were observed in alkaline solutions, depending on the pH of the buffer employed. Adsorptive effects have been used to accumulate the drug onto the electrode and linear calibration graphs were obtained in the range 2.5×10^{-9} to 1×10^{-7} M. A simple procedure of extraction has been employed for the determination of pipemidic acid in urine samples.

Table of Contents

<u>Chapter 1</u>	Construction and Characterisation of Calixarene Based Ion-Selective Electrodes	
1.1	INTRODUCTION	2
1.2	Potentiometric Measuring Cell	5
1.2.1	Liquid Junction Potential	9
1.3	Activity Coefficient	11
1.4	Selectivity	12
1.4.1	Separate Solution Method	14
1.4.2	Mixed Solution Method	14
1.5	Ion Selective Electrodes Based on Neutral Carriers	16
1.5.1	Characteristics of Neutral Carriers for ISEs	17
1.5.2	Solvent Polymeric Membrane Ion-Selective Electrodes	21
1.5.2.1	Polymer Matrices	22
1.5.2.2	Solvent Mediator	23
1.5.2.3	Ion-Exchanger	24
1.5.3	Design of Polymer Membrane Electrodes	25
1.6	Response Time of ISEs	26
1.6.1	Membranes with Incorporated Ion-exchanger Sites	26
1.6.2	Membranes without Ion-exchanger	27
1.7	Life Time of Solvent Polymeric Membranes	29
1.8	EXPERIMENTAL WORK	31
1.8.1	Calixarene Ligand Molecules	31

1.8.2	Copolymerisation Procedure	35
1.8.3	Membrane Preparation	37
1.8.4	Electrode Construction	38
1.8.4.1	Glass Pipette Electrodes	38
1.8.4.2	Catheter Electrodes	40
1.8.4.3	Macroelectrodes	42
1.8.4.4	Coated Wire Electrodes	42
1.8.4.5	Glassy Carbon Electrodes	43
1.8.5	Materials	43
1.8.6	Potentiometric Apparatus and Measurements	44
1.9	RESULTS AND DISCUSSION	44
1.9.1	Caesium Electrodes	44
1.9.2	Sodium Electrodes	49
1.9.2.1	Methyl p-t-butylcalix[4]aryl acetate ionophore	49
1.9.2.1.1	Electrode Response	49
1.9.2.1.2	Injection Experiments	52
1.9.2.1.3	Determination of Selectivity Coefficients	56
1.9.2.1.4	Life time	60
1.9.2.2.	Methyl Tetraketone Calix[4]arene	60
1.9.2.2.1	Glass Pipette Electrodes	60
1.9.2.2.1.1	Electrode Response	62
1.9.2.2.1.2	Injection Experiments	65
1.9.2.2.2	Solvent Polymeric Membrane Electrodes	67
1.9.2.2.2.1	Optimisation of the ISE Membrane	70
1.9.2.2.2.2	Membrane Response	71
1.9.2.2.2.3	Injection Experiments	72

1.9.2.2.2.4	Determination of Selectivity Coefficients	73
1.9.2.2.2.5	Life Time	76
1.9.2.2.3	Coated Wire Electrodes	78
1.9.2.2.3.1	Electrode Response	79
1.9.2.2.3.2	Selectivity Coefficients	81
1.9.3	Polymeric Calixarene Compounds	81
1.9.3.1	Monomers I and II	83
1.9.3.1.1	Copolymerisation	83
1.9.3.1.2	Picrate Extraction	85
1.9.3.1.3	Membranes	85
1.9.3.1.4	Photopolymerisation	86
1.9.3.2.	Polymers IV, V and Monomer VI	86
1.9.3.3	Results and Discussion	86
1.10	Conclusions	89
1.11	References	93

Chapter 2 Application of Tetrameric Calixarene Based ISEs
to the Detrmination of Sodium in Plasma Samples

2.1	INTRODUCTION	100
2.2	Clinical Background to Sodium Analysis	102
2.2.1	Composition of Blood	102
2.2.2	The Role of Sodium in Blood Plasma	103
2.2.3	Pathological Conditions Involving Sodium Disturbances	103
2.3	Concentration Vs Activity	105

2.3.1	Sodium Bound to Proteins	107
2.3.2	Sodium Bound to Hydrogen Carbonate	108
2.3.3	Red Blood Cell Effect	108
2.3.4	Matrix Effect	109
2.3.5	Importance of Activity-Concentration in Clinical Assays	109
2.3.5.1	Hyperproteinaemia	110
2.3.5.2	Hyperlipoproteinaemia	110
2.4	Characteristics of ISE Membranes in the Analysis of Biological Samples	111
2.4.1	Stability	111
2.4.2	Selectivity	114
2.5	Liquid Junction Potential	114
2.6	Calibration of ISEs in Biological Samples	115
2.7	EXPERIMENTAL WORK	117
2.7.1	Introduction	117
2.7.2	Electrode and Membrane Construction	117
2.7.3	Materials and Samples	117
2.7.4	Potentiometric Cell	118
2.7.5	Procedures	118
2.7.5.1	Measurements from Calibration Curve	119
2.7.5.2	Measurements from Standard Addition	121
2.8	RESULTS AND DISCUSSION	121
2.9	Conclusions	139
2.10	References	141

Chapter 3 **Performance of p-t-ButylCalix[4]aryl Acetate ISEs
in a Flow Injection System**

3.1	INTRODUCTION	147
3.2	Continuous Flow Analysis	149
3.3	Flow Injection Analysis	150
3.4	Theoretical Models of FIA	154
3.5	FIA and Other Continuous Flow Techniques	156
3.6	Instrumentation	158
3.6.1	Pump	160
3.6.2	Injection Valve	160
3.6.3	Manifold/Reactor System	160
3.6.4	Flow Cells and Detectors	162
3.6.4.1	ISE Flow-through Cells	162
3.6.4.2	ISFETs	166
3.6.5	Computerisation	166
3.7	Some Characteristics of ISEs in Flowing Systems	167
3.7.1	Response Time	167
3.7.2	Liquid-Junction and Reference Electrode	168
3.7.3	Streaming Potential	169
3.8	Potentials of FIA	170
3.9	Some Applications of ISEs in FIA	173
3.10	EXPERIMENTAL WORK	176
3.11	Apparatus	177
3.12	Materials and Samples	177

3.13	Membrane and Electrode Preparation	178
3.14	FIA Arrangement	178
3.15	Electrode Response	182
3.16	Optimisation of the ISE Response	187
3.16.1	Injection Volume	187
3.16.2	Effect of Flow Rate	188
3.16.3	Manifold Length	192
3.16.4	Carrier Composition	192
3.17	Analytical Procedure	200
3.17.1	Calibration	200
3.17.2	Analysis of Blood Plasma Samples	203
3.17.2.1	Flame Photometry	207
3.18	Conclusions	214
3.19	References	217

Chapter 4 Adsorptive Stripping Voltammetric Behaviour of
Pipemidic Acid

4.1	INTRODUCTION	222
4.2	Electrochemical Analysis in Clinical Chemistry	225
4.2.1	Organic Polarography	227
4.2.1.1	Electroreducible Molecules	227
4.2.1.2	Electrooxidisable Molecules	227
4.2.1.3	Molecules originating Anodic Processes with the Metal Electrode	228
4.2.1.4	Molecules originating Catalytic Processes	228

4.2.1.5	Molecules Adsorbing at Mercury Electrodes and originating Tensammetric Processes	228
4.2.1.6	Derivatisation	228
4.2.2	General Features of Voltammetric Techniques	229
4.3	Theory of Electroanalytical Techniques	231
4.3.1	Introduction	231
4.3.2	Polarographic Techniques	231
4.3.2.1	Classic Direct Current Polarography	231
4.3.2.2	Differential Pulse Polarography	232
4.3.2.3	Alternating Current Polarography	233
4.3.2.4	Square Wave Polarography	233
4.3.2.5	Stripping Voltammetry	234
4.3.2.5.1	Anodic Stripping Voltammetry	235
4.3.2.5.2	Cathodic Stripping Voltammetry	236
4.3.2.5.3	Adsorptive Stripping Voltammetry	237
4.4	EXPERIMENTAL WORK	245
4.4.1	Apparatus	245
4.4.2	Materials	245
4.4.3	Method	246
4.5	RESULTS AND DISCUSSION	246
4.5.1	Cyclic Voltammetry	246
4.5.2	Influence of pH	248
4.5.3	Adsorptive Stripping Voltammetric Behaviour of Pipemidic Acid	250
4.5.3.1	Effect of Accumulation Potential	251

4.5.3.2	Accumulation under Convective Transport	251
4.5.3.3	Influence of Electrolysis	253
4.5.3.4	Effect of Scan Rate	253
4.5.3.5	Effect of Accumulation Time	257
4.5.3.6	Effect of Concentration of Pipemidic Acid in Solution	259
4.5.3.7	Differential Pulse and Square wave Voltammetry	261
4.5.3.7.1	Differential Pulse Voltammetry	263
4.5.3.7.2	Square Wave Voltammetry	265
4.5.3.8	Application of Adsorptive Stripping Voltammetry to the Determination of Pipemidic Acid in Urine	266
4.5.3.8.1	Extraction Procedure	266
4.5.3.8.2	Effect of Concentration of Pipemidic Acid in the Presence of Urine Extracts	271
4.5.3.8.3	Standard Addition	274
4.5.3.9	Conclusions	277
4.6	References	279
	Concluding Remarks	282

CHAPTER 1

Construction and Characterisation

of Calixarene Based

Ion-Selective Electrodes

1.1 INTRODUCTION

The dynamic progress of ion-selective electrodes (ISEs) in the last two decades led to the most spectacular achievements in the fields of chemical analysis. The remarkable output of published literature on ion-selective electrodes shows the vitality of this area, and is evidenced by comprehensive periodical reviews in prestigious journals [1-3]. References to books dealing entirely or partially with ISEs, citations to specialised reviews and the generation of several hundred research papers every year indicate a continuing high level of activity in this field.

From an historical point of view, the beginnings of ion-selective electrodes can be traced to the discovery of the pH electrode by Cremer (1906) [4] and Haber and Klemensiewicz (1909) [5] who found that certain glasses responded to hydrogen ion activity. However, the pH electrode did not become commonly employed until about 20 years later. Consideration of the causes of the "alkaline error" lead to the modification of the Nernst equation by Nicolsky (1937) [6] to incorporate the concept of selectivity coefficients, which would account for the effect of interfering ions on the response of an ion-selective electrode. The studies carried out by Karrenman and Eisenman (1962) [7] and the work of Stephanova et al (1963) [8] provided the insight necessary for the development of new ISEs. A great contribution came from the work of Stefanac and Simon (1967) [9,10], whose development of the first neutral carrier based ISE for potassium ions marked the beginning of new and efficient electrodes for a variety of alkali and alkaline earth metal ions. At present there are about 30 cations and anions which can be detected selectively by direct potentiometry with different types of ion-selective electrodes. Other analytes of interest include gas molecules (e.g. NH_3 , CO_2),

pharmaceuticals (digoxin, penicillin, etc.), organic species (urea, glutamine, etc.) Further examples can be found in a comprehensive review [11].

In the last few years, the development of electrodes has been mainly directed towards enzyme and immuno electrodes (biosensors) as well as neutral carrier based ion-selective electrodes. Although, glass membrane electrodes are still widely used in biology and medicine for determination of hydrogen and sodium ions, neutral carrier based ion-selective electrodes have become extremely important for the measurement of pH and alkali and alkaline earth metal cations. It is in fact the development of neutral carriers which has opened up the possibility of preparing liquid membrane ion-selective electrodes for different ions and of different selectivities. The satisfactory selectivities of the ligand membranes, the availability of membrane components and the easy construction have prompted the replacement of a large number of other type of membranes, including the hydrogen and sodium glasses.

Ion-selective electrodes are in many aspects ideal sensors. Thus their prime advantage is their insensitivity to sample colour, viscosity or suspended solids. These parameters make their use preferable to many photometric procedures. Long life time, adequate selectivity and response time of the order of tens of milliseconds are attractive features connected with their behaviour. Furthermore the electrodes may be used for measurement over a very wide concentration range (10^{-1} M - 10^{-5} M) and they are, with few exceptions, generally tolerant of small changes in pH. An additional advantage for analytical methods involving ISEs is that they are relatively simple, and cheap to develop, set up and use.

All of these inherent features of ISEs, plus the development observed in the last 20 years has brought about a remarkable revival in potentiometry.

Miniaturization of sensors has led to important applications in the fields of laboratory diagnostics, intensive therapy and biology research [12-14]. The combination of enzyme development with the ISE methodology has produced novel biosensors with many applications in clinical analysis. The alliance between the ever progressing semiconductor technology and potentiometric techniques has resulted in ion-selective field effect transistors for multi-channel sensing purposes. In addition advances in computer control have allowed the automation of many of the steps involved in analytical procedures and have in turn boosted the development of more efficient multi-ion sensor array devices [15].

Obviously, overall progress in potentiometry has been firmly based on the invention of more efficient sensors. Consequently, the aim of this chapter is to present experimental work carried out towards the evaluation of newly synthesised neutral carriers for use in ion-selective electrodes. Chemically modified tetrameric, hexameric and polymeric calixarene compounds as complexing agents for sodium, potassium and caesium ions will be presented. The construction of liquid pipette, catheter-type, coated wire and conventional macro-electrode designs incorporating the calixarene neutral carriers will be described. The characterisation of such electrodes in terms of their most important characteristics (sensitivity, selectivity, response time, stability reproducibility and life time) has been investigated. As present trends in neutral carrier based membrane electrodes are directed to covalently bound compounds so as to produce 'solid-state' devices, attempts to bind monomeric calixarene ligands to a support matrix by copolymerisation will be described. To place the experimental work in context, the principles of potentiometry will be discussed to some extent, as will the general properties and characteristics of neutral carrier based ISEs. However it is not the purpose of this chapter

to abound in extensive theoretical considerations, only the most relevant aspects and progress in the field of ISEs will be covered.

1.2 POTENTIOMETRIC MEASURING CELL

A potentiometric measuring cell is formed by an indicator electrode, a reference electrode and a solution in contact with both. When an ISE is placed in solution containing only i^+ , a momentary flux of this ion occurs across the selective membrane in the direction of the solution which contains the lower activity of i^+ . This flux causes a build up of positive charge on the low activity side of the membrane and a build up of negative charge on the high activity side of the membrane. Hence, an electrical potential is set up which opposes further ionic migration and eventually an equilibrium membrane potential (E_m) is established. This potential so established prevents further transfer of i^+ .

The utility of ion-selective electrodes depends upon the determination of membrane potentials. The potential difference between an ion-selective membrane and the adjacent solution is not directly measurable. Since it is generated by an ion exchange between the two phases, which does not involve the fundamental step of electrochemistry i.e. charge transfer between ionic and electronic conductors, the two phase system must be extended by adding phases to both electrolytes so that a complete electrochemical cell with electrodes as terminals is formed. The potential difference of interest (membrane potential) is one of several galvanic potentials which together constitute the electromotive force (emf) of the cell, i.e. the measurable quantity (Fig. 1.1) Thus the membrane potential of the cell

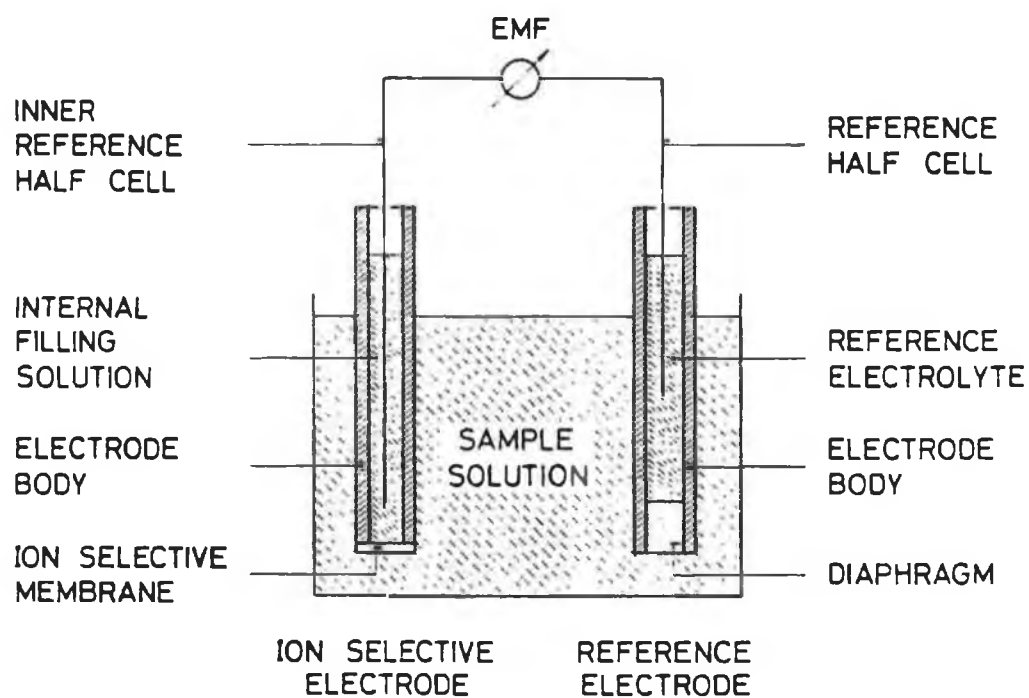


Fig. 1.1 Schematic diagram of a potentiometric measuring cell incorporating an ion-selective membrane electrode.

Electrode A/ext solution/Membrane/int solution/electrode B		
Electrode potential	Membrane potential	Electrode potential

may be considered as the electric potential difference between the internal and external solutions and includes both the diffusion potential E_D and the internal and external phase boundary potentials E'_B and E''_B respectively (Donnan potential), thus we can write:

$$E_m = E'_B + E''_B + E_D \quad (1.1)$$

ideally, E'_B and E_D are constant, while E''_B is variable and depends on the activity of the primary ion (a_i). The conditions under which this ideality is realised may be deduced by deriving the Nernst equation. Thus provided $E_m = E''_B$, the membrane potential given by the Nernst equation [16,17] is:

$$E''_B = S \log a_i \quad (1.2)$$

with S being the Nernst slope factor and given by:

$$S = 2.303 R T / z_i F = 59.16 \text{ mV}/z_i (25^\circ\text{C}) \quad (1.3)$$

where, R is the gas constant, T is the absolute temperature, z is the charge of the ion and F is the faraday constant.

However, as an isolated membrane potential cannot be measured directly,

the ISE must be incorporated into the electrochemical cell (Fig. 1.1). As ion-selective electrodes respond logarithmically to the activity of the primary ion (i), the ISE potential is described by:

$$E_{\text{ISE}} = E_{\text{ISE}}^0 + S \log a_i \quad (1.4)$$

where E_{ISE}^0 incorporates constant contribution from E'_B , E_D , the internal electrode/electrolyte contact and potentials generated in the ISE leads/connections to the millivolt meter. The intercept E_{ISE}^0 is a temperature dependent constant.

Now in the reference half cell (Fig. 1.1), E_{ref} is ideally independent of the sample composition. It includes contributions from the internal electrolyte/electrode boundary and potentials generated in the leads to the millivolt meter. Often a junction potential (E_j) is superimposed (see section 1.2.1).

Overall the cell potential is described thus:

$$E_{\text{cell}} = E_{\text{ISE}} - E_{\text{ref}} \quad (1.5)$$

then by combining eqn.(1.4) and eqn.(1.5) we can write;

$$E_{\text{cell}} = E_{\text{cell}}^0 + S \log a_i \quad (1.6)$$

where E_{cell}^0 incorporates all 'constant' potentials in the cell including: E_{ref} , E_D and E'_B . The only variable is E''_B which is accounted for in 'S log a_i '.

From these theoretical considerations, it can be concluded that a Nernstian response will be obtained to changes in primary ion activities in the sample solution i.e. $59.16 \text{ mV}/Z_i$ per decade change in a_i at 25°C . Thus a change in the emf of 1 mV will correspond to a relative change in the activity of a monovalent ion of around 4 %

Inaccuracies may arise from:

1. Variation in the reference electrode junction potentials (section 1.2.1). This is recognised as being matrix dependent. Hence sample and standard matrices should be matched.
2. Incorrect matching of leads. Only good quality leads/connectors should be used.
3. Mismatching of electrode/meter impedances. Only good quality meters with high input impedance should be used (preferably $> 10^9 \Omega$) to minimise the potential drop on connecting the cell.

1.2.1 Liquid Junction Potential

Although it is often assumed that the liquid junction potential (E_j) generated at the interface (diaphragm, free flowing junction, etc.) between the reference electrolyte (salt bridge) and the sample solution is not influenced greatly by the sample composition, it may in fact vary considerably. At the boundary between two dissimilar solutions, a junction potential generated by the unequal diffusion of cations and anions is always set up. Contributing factors such as the solvents, the nature of the electrolytes, and the concentration of a given electrolyte can all differ from sample to sample. Hence fluctuations in E_j can be expected where solution concentrations on

matrices vary significantly. These fluctuations contribute to the overall cell potential and are therefore a source of error in ISE measurements.

Equations for the calculation of E_j are available from the theories of Plank [18,19] and Henderson [20,21]. The Henderson approximation is more frequently applied because of its simplicity:

$$E_D = \frac{\sum z_i u_i a_i(o) - \sum z_i u_i a_i(d)}{\sum z_i^2 u_i a_i(o) - \sum z_i^2 u_i a_i(d)} \cdot \frac{RT}{F} \ln \frac{\sum z_i^2 u_i a_i(o)}{\sum z_i^2 u_i a_i(d)} \quad (1.7)$$

where

z_i : charge number of the ion i ;

u_i : absolute mobility of the ion i ($\text{cm}^2 \text{s}^{-1} \text{J}^{-1} \text{mol}$);

a_i : single-ion activity of the ion i in the sample solution (mol l^{-1})

a_i' : single-ion activity of the ion i in the reference electrolyte (or salt bridge) of the reference electrode (mol l^{-1}).

A more simplified presentation of Plank's approach for the calculation of E_j has been developed by Morf [22].

In order to reduce the magnitude of the liquid junction potential, highly concentrated solutions of 1:1 electrolytes consisting of ions with similar mobilities are used either as bridges between reference and sample solution or as a solution of the reference electrode itself, which then forms its own salt-bridge. The most commonly employed equi-transferent solutions are saturated (4.2 M at 25°C) or 3 M KCl solutions. In some cases, bridges with electrolytes other than KCl e.g. NH_4Cl , LiOAc , KNO_3 and NH_4NO_3 , must be applied in order to avoid contamination of the sample solution.

The liquid junction potential is constant as long as a steady state is maintained at the boundary between the two solutions. The magnitude of the potential depends on the geometry of the interface. The structure of the reference electrode tip (at which the junction is formed) is thus of great practical importance. In order to assure high stability and reproducibility of the liquid junction various designs, have been employed for diverse practical applications (see section 2.8, chapter 2).

1.3 ACTIVITY COEFFICIENT

The measurement of species with ISEs in terms of concentration is based on the convenient relationship between the ISE response and log activity. The activity coefficient (f), of an electrolyte is related to the activity (a), by the following equation

$$a_i = c_i f_i \quad (1.8)$$

Due to deviations from ideal behaviour, the activity of an ion in solution is not identical to its concentration. Factors like electrostatic interactions will result in a predominance of ions of opposite charge around a particular ion, thus preventing it from exerting its full electrochemical influence (e.g. decrease in activity). Ion-solvent interaction is another factor which contributes to this situation. Ions tend to attract polar solvent molecules, holding them in solution. This prevents the molecules from generating their full solvent vapour pressure and therefore decreasing the activity of the solute.

These factors obviously become less significant in more dilute solutions

and when the ionic strength is relatively small. Thus, when concentration tends to zero, the activity coefficient tends to 1 and activity and concentration are practically equal.

Therefore, the activity coefficient takes account of the factors that separate the solution from a presumably ideal solution. Its value depends on the ionic strength (I) of the solution.

$$I = 1/2 \sum C_i z_i^2 \quad (1.9)$$

where C_i is the molar concentration of specie i and z charge of i. The activity coefficient of a solution may be estimated from the ionic strength by means of the extended Debye-Huckel equation [23]

$$\log f_i = -A z_i^2 \left[\frac{\mu^{1/2}}{1 + \mu^{1/2}} - 0.2 \mu \right] \quad (1.10)$$

where A is a solvent dependent constant. This equation may be used for solutions with ionic strength up to 0.1 or slightly higher.

1.4 SELECTIVITY

In practice an ideal Nernstian membrane electrode response as described so far (equation 1.3) can not usually be observed. Additional contributions to the measured activity that result from the presence of interfering ions (j) in the sample solution must be taken into account. A quantitative description of the electrode selectivity is given by the selectivity coefficient, which can be interpreted with reference to the Nicolsky-Eisenman equation [6]:

$$E = E_i^0 + S \log \left[a_i + K_{ij}^{\text{pot}} (a_j)^{z_i/z_j} \right] \quad (1.11)$$

Thus, the selectivity coefficient theoretically enables the activity of the primary ion to be determined, even in the presence of various interfering ions which contribute to the ISE potential.

However, the variability of these selectivity coefficients (e.g. dependence on the method of determination, the activity level of the interfering ions, the ion activity ratio of the ions to be determined and the interfering ions, and other factors [23]) is well recognized and has been reflected in the abandonment of the original term 'selectivity constant'. This problem has been further emphasised in the literature by the lack of uniform approach to the evaluation of selectivity coefficients. In fact, the numerical values of selectivity coefficients for identical electrodes evaluated by different authors show significant discrepancies. This is clearly seen from the work of Hulanicki and Augustowska [24] which summarises the published data from various workers for some Orion ISEs. As an example, the published selectivity coefficient of the Orion calcium electrode (92-20) against sodium ions varies from 10^{-4} to 0.42 when determined by different methods. A difference of two orders of magnitude is still observed when the same measuring method is used. Less spectacular but still significant differences are observed for the Orion 92-32 divalent cation electrode [24].

Regardless of the variability of selectivity coefficients, they are valuable in determining the suitability of an ISE for a particular analytical application. Two methods described below are normally employed, although other methods have also been described [23,25].

1.4.1 Separate Solution Method (SSM)

Although SSM method does not present a realistic situation as to the conditions faced by an ISE in sample solution, it has become widely adopted to allow simple comparison of newly introduced electrodes.

According to the SSM, values of K^{pot}_{ij} can be calculated from:

$$\frac{E_2 - E_1}{S} = \log K^{pot}_{ij} + (z_i/z_j - 1) \log a_i \quad (1.12)$$

for $a_i = a_j$

where E_1 and E_2 are the measurements of separate solutions of primary and interfering ion respectively at the same activity.

1.4.2 Mixed Solution Method (MSM)

Two procedures are available in this case:

(a) fixed level of interfering ion (j) in the presence of a variable primary ion concentration, usually 10^{-6} M to 10^{-1} M. Extrapolation of the straight line of the response curve Fig. 1.2 gives the activity of the primary ion producing the same potential as the fixed activity of the interfering ion. The selectivity is then given by the following equation:

$$a_i = K^{pot}_{ij} (a_j)^{z_i/z_j} \quad (1.13)$$

Often the response at lower activities of the primary ion is difficult to measure precisely and the intersection cannot be located exactly. A solution is to find where the curves A and B (Fig. 1.2) differ by $18 \text{ mV}/z_i$, and then use equation (1.13).

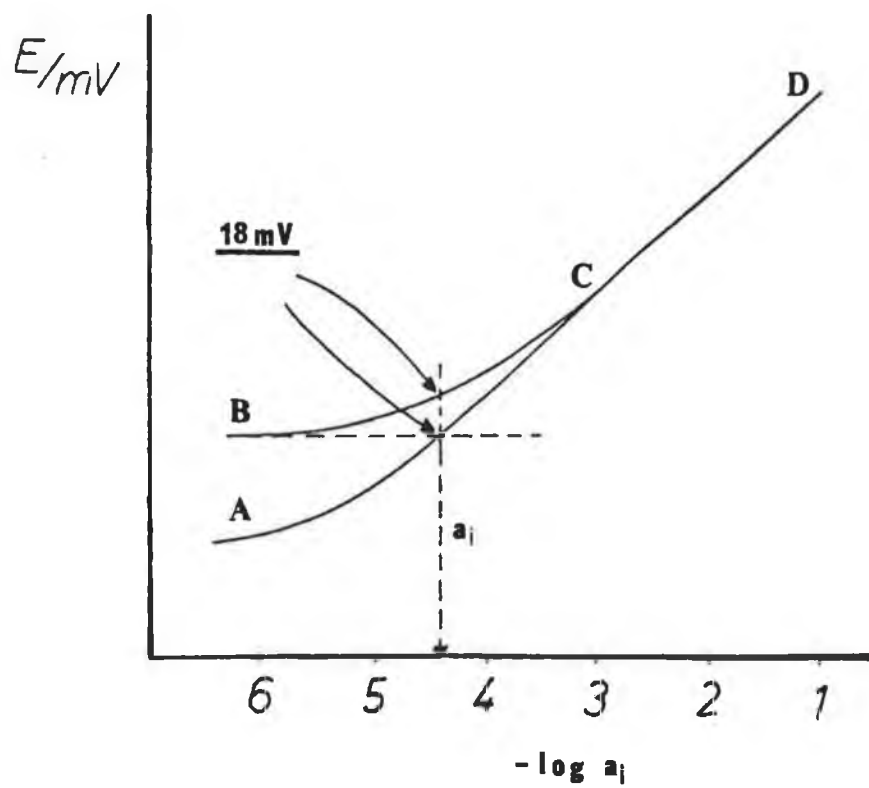


Fig. 1.2 Selectivity coefficients by the mixed solution method, a.
B-C response to (i) and (j); A-D response to (i) only.

(b) this procedure consists of fixing the level of the primary ion and varying the activity of the interfering ion. The method is frequently applied to examine the influence of pH over a particular membrane electrode.

1.5 ION-SELECTIVE ELECTRODES BASED ON NEUTRAL CARRIERS

In 1964 Moore and Pressman [26] discovered that the antibiotic valinomycin exhibited selectivity for alkali cations. Two years later it was shown by Stefanac and Simon [10] that valinomycin could be used in artificial membranes for analytical purposes. Unfortunately, of the large number of antibiotics with ionophoric properties, only the potassium-selective carrier valinomycin [27] and the ammonium-selective nonactin [27] have found widespread use in potentiometry with ion-selective electrodes. It was after the introduction of the crown ethers by Pedersen in 1967 [28] that the use of synthetic carriers expanded rapidly. However, it was only after several years that new crown compounds were employed successfully as components in liquid membrane electrodes [29-32]. Intensive research led to the synthesis of new classes of ionophoric compounds based on macrocyclic (hemyspherands, bis-crown ethers, calixarenes) and non-cyclic structures (lipophilic oxa amides) [33,34]. Those which exhibited high selectivities were introduced for use in membrane electrodes.

While organic ion-exchangers 'charged carriers' such as organophosphates or tetraphenylborate (cation exchangers) and tetraalkyl ammonium ions (anion exchangers) have gained considerable importance as complexing agents, this chapter is centered exclusively towards the role of neutral carriers. Comments on ion-exchangers will be only made in relation to their use as additives in solvent polymeric membrane electrodes.

1.5.1 Characteristics of Neutral Carriers for Ion-Selective Electrodes

The most successful illustration of the search for selectivity was the introduction by Ammann et al [35,36] of a number of non-macrocyclic molecules (see Fig. 1.3) with remarkable selectivities towards alkali and alkaline metal ions. From this work, several neutral-carriers have been successfully commercialised and are in widespread use today. This has led to the conclusion that ionophores have to fulfill certain requirements in order to behave as analytically useful sensing agents for ion-selective electrodes [37].

- a) Lipophilicity: The ligand and the complex have to be sufficiently soluble in the membrane phase. It has been pointed out [38] that for a continuous life time of at least one year for a solvent polymeric membrane, a partition coefficient (K) of the ionophore between the aqueous sample and the membrane phase larger than 10^5 has to be achieved (in favour of the membrane phase).
- b) Mobility: Both ligand and complex must have an adequate mobility in the membrane phase. This is possible only if the over-all dimensions of the carrier remain within limits, but are still compatible with high-lipid solubility
- c) Selectivity Coefficient (K_{ij}^{pot}): The ideal electrode responds only to the primary ion (i) i.e. $K_{ij}^{pot} = 0$ for all interfering ions (j), and the Nicolsky equation (eqn. 1.11) reduces to the Nernst equation. In reality, a good electrode should approach this ideal behaviour as closely as possible, with K_{ij}^{pot} being as small as possible for all common interfering ions.
- d) Ion-exchange kinetics: the ion-exchange kinetics for the exchange reaction of cations of the same charge

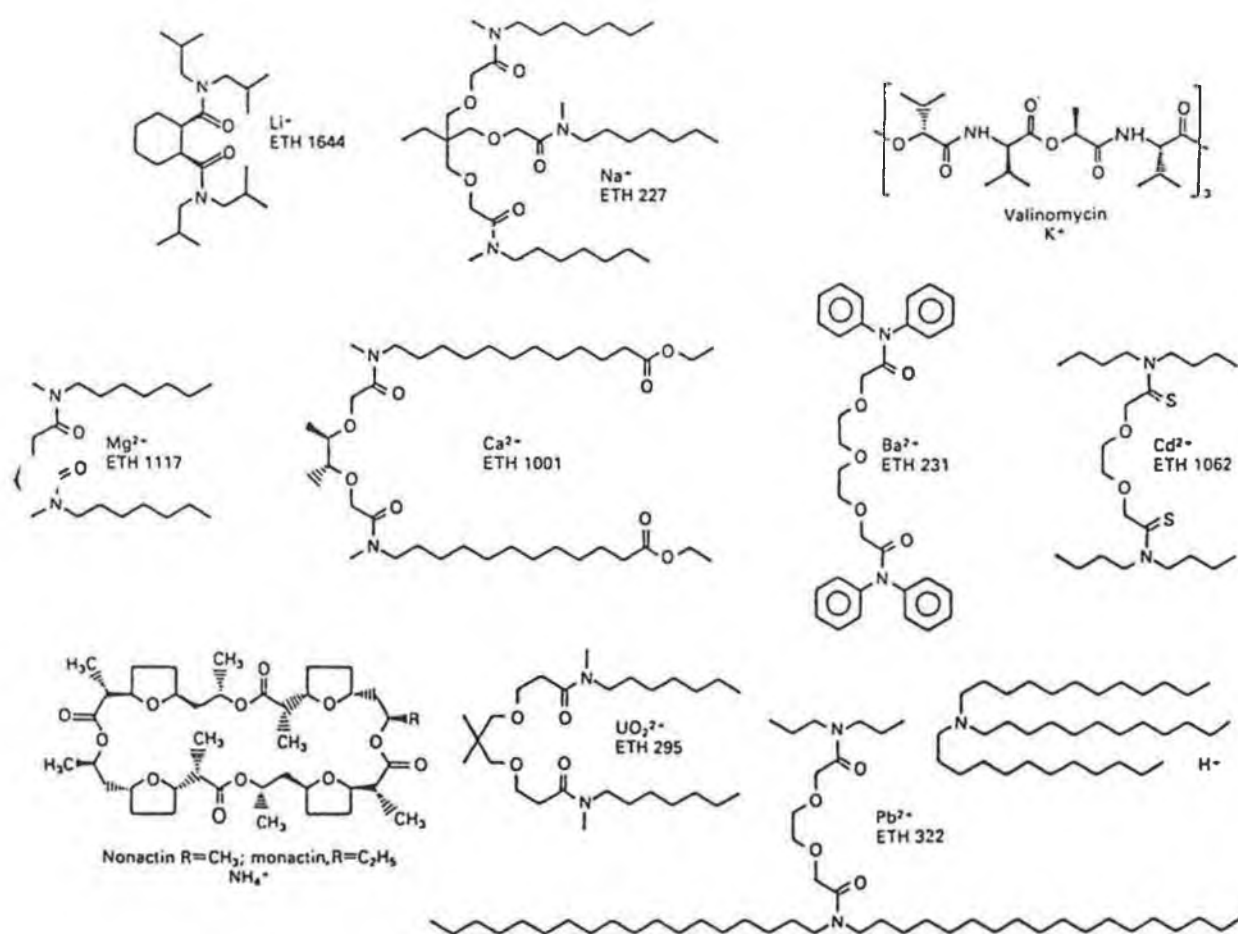


Fig. 1.3 Chemical structures of some commonly used neutral carriers in ISEs.



(where S_n is the electrically neutral ligand), has to be compatible with the required response time of the membrane electrode.

The most important 'molecular parameters' a complexing agent that fulfills the requirements mentioned above are:

Coordination sites: attractive binding sites are ligand atoms that are capable of replacing the hydration shell of the aquo-ion. Polar coordinating groups should include preferably oxygen as the ligand atom. Amine nitrogen and sulphur atoms have also been used. However, other properties of the binding sites besides the actual coordinating groups e.g. dipole moment, polarisability, van der Waals radius, may have a considerable influence on the magnitude of the ion-dipole interaction [39].

Coordination number, cavity: a carrier molecule should be a multidentate ligand in which the stable conformation is a relatively rigid cavity; the cavity formed by a given number of polar coordinating groups should be suited for the uptake of the primary ion, while the non-polar groups form a lipophilic shell around the coordination centre to shield the solvent from the cation charge. Ideally the shape and size of the cavity should be complementary to the ion in question. The coordination number and cavity size determine the preference for a certain cation. Cations larger than the cavity will deform the optimal arrangement while smaller cations will not fill the available space. Unfortunately, the planning of optimum designed cavities is impeded by the uncertainty involved in predicting the equilibrium conformations and

stoichiometries of the complexes.

Arrangement of the coordination centers: the centers should be facing into the cavity.

Size of the ligand: an important contribution to the stabilities of the complexes and the cation selectivities of the carrier is made by the electrostatic interactions between the charged complexes and the surrounding membrane solvent. A small thickness of the ligand layer around the central atom leads to a preference of divalent relative to monovalent cations of the same size; this effect is particularly important when using polar membrane solvents with high dielectric constants.

Evidently among all the parameters mentioned the complexing properties of a particular ligand are stored in the molecular structure as a whole. It is in fact virtually impossible to modify one parameter without affecting others that may have a key influence over the extraction capability of a particular ion. Thus, for instance, the change of a thioether sulfur atom to an oxygen atom in a coordination site not only affect the dipole moment of the coordinating site, but also the polarisability, the size of the ligand atom and the topology about this binding site. In addition the same consideration may apply for other properties of the ligands in analytically important ISEs. For example, the high stability constants obtained between cryptands and certain cations limits the use of these compounds in ISEs due to their rather slow exchange kinetic rate. A key compromise must then be found between a flexible conformation of the ligand to permit a sufficiently fast ion exchange with the demands posed on the stability constant of the formed complex.

Over the past years, a great deal of attention has been given to model calculations such as mechanical, electrostatic, computer-aided and quantum

chemical models for the development of effective neutral carriers. Although these models base their principles from theoretical and semi-empirical considerations and are a major aid in the design of new compounds, they have proven unsuccessful in the design of new relevant compounds for use in ISEs. To a large extent, the search for successful ligands is still basically a trial and error process.

1.5.2 Solvent Polymeric Membrane Ion-Selective Electrodes

For analytical applications neutral carriers are introduced into solvent polymer matrix systems. The procedure requires a mixture of the polymer matrix, the ion-selective molecule, plasticiser and generally (although not always) an ion-exchanger. These systems possess similar properties to their 'pure' liquid membrane counterparts (ionophore incorporated in a non-miscible water solvent), but have the added advantages of extended life time, robustness and considerable economy of sensor materials [40]. In addition they also offer various possibilities of electrode design and subsequently an extension of the scope of the electrodes. These attractive features have led to the increasing popularity of neutral carrier-based solvent polymeric membrane electrodes.

The properties of neutral carrier-based solvent polymeric membranes have been extensively investigated. Thus many studies on molecular aspects such as ion-ligand interaction in membranes [41], ion-exchange kinetics [42], carrier-exchange kinetics, and bulk diffusion and interfacial diffusion [43] have been dealt with. In addition, practical aspects such as membrane preparation, incorporation of membranes in electrode arrangements and construction of electrode bodies have been extensively treated [44] and helped

to allow optimisation of liquid membranes with respect to selectivity, membrane resistance, life time and emf stability.

1.5.2.1 Polymer Matrices

Many different polymer matrices have been investigated and suggested for use in ISEs [45-48] although poly(vinyl)chloride (PVC) is by far the most common. PVC [49] and silicone rubber [50] yield membranes of good mechanical and chemical stability and excellent electromotive properties. Additional desirable characteristics for polymer matrices include biocompatibility, clean surface of the resulting membrane (no pores) and chemical inertness i.e. no competition with the ligand complex formation process (no coordinating sites, no charged sites). With respect to the latter aspect, Meyerhoff et al [51] have recently discussed the potential advantages of functionalised PVC matrices i.e. aminated and carboxylated PVC. From their work, it has been shown for the first time that a variety of ISEs can be prepared in a chemically non-inert PVC matrix without significant losses in selectivity and response time. Moreover, it has been demonstrated that these types of matrices may prove successful as substrates for covalently attaching proteins to the surface of the electrode without adversely affecting the electrode response and thus opening a new approach to biosensor design.

Solvent polymeric membranes typically contain about 30 wt.% PVC [52]. Lower contents result in fragile membranes, while higher content values produce a substantial increase in electrical resistance [53] and a sluggish response [52]. Also an increase in the amount of matrix material strongly influences the diffusion coefficient of the ligand and other components in the membrane phase. The dependence of carrier and plasticiser diffusion coefficients on the

PVC content may become apparent by the rate of the loss of these components from the membrane phase.

1.5.2.2 Solvent Mediator

The solvent mediator in which the neutral carrier is dissolved also functions as a plasticiser for the PVC. In addition it plays auxiliary roles in controlling the relative permittivity of the final organic phase, the mobility of the ion exchanger sites according to the viscosity of the mediator and site density by variation of the concentration of ion exchanger. These auxiliary roles can influence the extent of enhancement of the partition coefficient for a particular ion, with consequent effects on electrode selectivity. The ligand membrane selectivity depends to a great extent on the dielectric constant (ϵ) of the membrane phase. The relatively high amount of solvent mediator normally used in solvent polymeric membranes (i.e. 60 - 66 %) dictates to a large extent the dielectric constant of the membrane. Research into the factors controlling the preference of ligands for monovalent over divalent cations [54] indicate that solvent-mediators of low ϵ favour divalent cations, especially when $\epsilon < 10$. Both membrane solvents of low ϵ (adipates, sebacates, phthalates ($\epsilon \sim 4$)) and relatively high ϵ (nitroaromatics ($\epsilon \sim 24$)) are available. The influence of the dielectric constant on the membrane selectivity stems from the contribution of the dielectric medium to the free energy of transfer. The term is described by the Born equation:

$$\Delta G_B = - \frac{(Z e_0)^2}{2(r_{ion} + s)} \left(1 - \frac{1}{\epsilon} \right) \quad (1.14)$$

where ΔG_B describes the free energy of transfer of a neutral carrier complex from the gas phase into a dielectric medium (membrane). Since the value of ΔG_B is proportional to the square of the charge of the ion to be complexed, an increased preference of the membrane for divalent over monovalent cations is expected with an increase in the polarity of the membrane solvent. Equation 1.14 also contains another molecular parameter, namely the average thickness (s) of the ligand layer; its influence depends on the ion charges and the dielectric constant.

Whatever the complete role of solvent mediators, the choice will be dictated by several criteria (i.e. chemical stability, chemical inertness, low vapour pressure, adequate viscosity, adequate , solubilisation properties for ligand and membrane additives, high lipophilicity, efficient plasticising properties) of this component which will in turn affect other parameters (i.e selectivity, membrane resistance, life time and stability). These parameters can then be optimised by the correct choice of solvent mediator. Although, this choice can lead to marked improvements in membrane behaviour, the response and selectivity of ligand-free plasticiser-PVC membranes should also be examined carefully. Studies demonstrate that plasticisers may partly behave as ionophores [55].

1.5.2.3 Ion-Exchanger

Additives consisting of lipophilic anionic sites [56] (e.g. alkali tetra arylborates) are commonly used in neutral carrier based cation-selective electrodes. The incorporation of these cation-exchange sites into the membrane are beneficial in many respects. The lipophilic anion reduce or eliminate the tendency of other lipophilic anions from the sample solution to penetrate the

membrane phase [57]. In addition they may modify the membrane selectivity (increased divalent/monovalent selectivity), reduce the electrode response time, improve the cation sensitivity in the case of carriers with poor extraction properties, and considerably reduce membrane resistance [57]. Sodium tetraphenylborate and potassium tetrakis(p-chlorophenyl)borate are the most commonly used salts. Advantages provided by the inclusion of these ion exchangers have been demonstrated by many authors [58-60]. However, the amount of added salt must be strictly limited, since excessive concentrations can lead to drastic changes in membrane selectivity [61]. Depending on the stoichiometry of the complex, an increase over a given molar ratio of ion-exchanger/ligand yields a membrane with the properties of a classical cation-exchanger. Pretsch et al [62] have demonstrated that this drawback can be avoided if both cation and anion are lipophilic.

1.5.3 Design of Polymer Membrane Electrodes

Solvent polymeric membranes are usually fabricated to designs similar to the conventional glass electrodes. However a remarkable advantage of these type of electrodes is that the design can be modified to suit various measuring situations. For example, very little volumes e.g. 1 ml, can be treated by sandwiching between a specially prepared flat surface of a reference electrode fabricated from a glass cone and socket and a PVC electrode of conventional design [63]. Flow injection analysis samples can be analysed by suitable thin film membrane ISEs (see section 3.14, chapter 3) or by ISE based on tubular membranes [64]. Measurements in biological cells can be achieved by means of specially designed microelectrodes with PVC matrix membranes and conventional inner filling solutions [65].

1.6 Response Time of Ion-Selective Electrodes

The overall response time of an ion-selective electrode is affected by multiple aspects [66-68] i.e. time constant of the measuring instrument [69], the impedance of the equivalent electrical circuit of the membrane [70], the rate of ion-transfer reaction across the membrane/sample interface [71], the diffusion of the analyte ion through the stagnant layer in the sample [72], the diffusion within the selective-membrane [73] and the establishment of a liquid-junction at the reference electrode. These aspects have been extensively treated by many researchers and the comments have reached more or less a mature state, reflected in the formulation of detailed mathematical models [68]. Response times are only meaningful if the overall response time of the potentiometric system is governed by the properties of the membrane. For neutral carrier based electrodes two type of behaviour are recognised.

1.6.1 Membranes with Incorporated Ion-exchanger Sites

In this case, the response is represented by an exponential function which actually describes the response of the cell assembly. Here, as the composition of the membrane remains approximately constant, the diffusion processes of ions passing through the membrane becomes negligible in the absence of interfering ions. As a result, the dynamic response characteristic is governed by the transport processes in the aqueous diffusion layer, which depends on the shape and condition of the membrane surface, as well as the composition of the sample. This type of response behaviour is markedly influenced by the direction of the activity change in the solution. The response is described by eqn. (1.15):

$$E_t = E_{\infty} + S \log \left(1 - \left(1 - \frac{a_i^0}{a_i} \right) e^{-t/\tau'} \right) \quad (1.15)$$

$$\text{with } \tau' = \frac{\delta^2}{2D'} \quad (1.16)$$

where, E_t and E_{∞} are cell potential at time t and at equilibrium potential ($t = \infty$) respectively (mV); a_i^0 and a_i activities of primary ion in the bulk of the solution at $t < 0$ and $t > 0$ respectively (mol l^{-1}); D' is the mean diffusion coefficient in the adhering aqueous layer ($\text{cm}^2 \text{s}^{-1}$); and δ is the thickness of the adhering aqueous layer (cm).

1.6.2 Membranes without Ion-exchanger

In this case diffusion of ions into the membrane may occur and a steady-state is attained slowly compared to the diffusion in the internal and external aqueous phases. The rate limiting process is determined to a large extent by the dynamic behaviour of the processes within the membrane itself. The response curve is described by eqn. (1.17):

$$E_t = E_{\infty} + S \log \left[1 - \left(1 - \frac{a_i^0}{a_i} \right) \frac{1}{\sqrt{t/\tau}} \right] \quad (1.17)$$

$$\text{with } \tau = \frac{DK^2\delta^2}{D'^2} \quad (1.18)$$

where K is the partition coefficient between the aqueous and the membrane phase.

According to these equations, the response time can then be reduced by:

- 1.- minimising the thickness of the adhering aqueous layer (e.g. fast stirring or flowing systems and by minimisation of the membrane surface.

- 2.- using samples of higher activities (only in the case of membranes incorporating ion-exchanger sites).
- 3.- reduction of the diffusion coefficient in the adhering aqueous layer: since the diffusion coefficient of the carrier complex salt is approximately proportional to the mobility of the sample anion in the membrane [74], the permeability of the membrane with respect to sample anions should be low. This can be achieved by using a highly viscous membrane phase.
- 4.- reduction of the partition coefficient between the aqueous and membrane phase: the extraction of the salt into the membrane is kept low if non-polar membrane phases are used [74]. In addition, the neutral carrier should be a relatively weak complexing agent (stability constant around 10^5) and should be incorporated into the membrane at low concentrations. The sample solution should not contain lipophilic anions since they enhance the salt extraction into the membrane phase.

The response time of ISEs is a critical and limiting factor for many applications. Further studies reflecting the importance of the experimental design [75], evaluation of the rate limiting step [73], theoretical description of response curves [76], effect of the neutral carrier membrane composition [77], and practical definitions of response time have been reported. With respect to response time definitions, there is certain amount of ambiguity in the literature. Thus IUPAC has recommended that response times should be defined as the time required for the emf to undergo 90% of its total change (t_{90}). However, many different definitions (t_{α} ($\alpha = 50, 90, 95, 99$)) adopted by workers are still in use. Guibault et al [78], proposed the response time (t^*) which was that time required for the emf to approach within 1 mV of its final value. This has, however, been discarded since the

t^* values yield different results for monovalent and divalent ISEs and for activity steps of different size. Recently another definition of response time which is independent of the knowledge of the final emf value has been proposed [79].

1.7 Life Time of Solvent Polymeric Membranes

An important characteristic of any ISE is its operative life time for a particular application. In fact, the life time demands made on the ISE will be dictated mainly by its particular use. In clinical analysis, PVC membranes should be suitable for continuous use in undiluted biological fluids (whole blood, plasma, urine, etc.) for at least a few months if intended for use in clinical analysers. In electrophysiology, microelectrodes based on liquid membranes need to have life times of hours or days.

Excluding factors such as mechanical defects, electrical shunts, chemical deterioration or surface contamination, the life time of PVC electrodes is limited by the loss of the neutral carrier and/or plasticiser from the membrane into the sample solution. These components usually exhibit a rather low molar mass (500 to 1000 g mol⁻¹), and so the mobility of these molecules in the membrane phase is relatively high. As the lipophilicity of membrane components is determined by the relative solubility of these in the membrane and sample phases, a gradual loss of components from the membrane phase occurs. In PVC membranes, a loss of the plasticiser down to a level of less than 30 wt.% plasticiser will result in an extremely high membrane resistance, with consequent adverse effects on the performance of the ISE. On the other hand a loss of ionophore from the membrane causes a deterioration in the electrode selectivity and sensitivity particularly when the ionophore concentration in

the membrane phase drops below about 10^{-4} M [80].

Several theoretical models have been used to predict the life time of neutral carrier membranes [80]. These models are based on the kinetics of component loss from the membrane phase into the sample solution. One of the methods proposed to estimate the suitability of membrane materials includes partition with 1-octanol and the use of lipophilicity increments [81]. Here a partition coefficient of $10^{5.5}$ is the estimated requirement for a membrane life time of about one year [82]. The following equation may be used to calculate approximative life times [80]:

$$\text{Life time} = (10^3 K_d + 1.3 \times 10^7 d^2) \ln (c_o / C_{\text{lim}}) \quad (1.19)$$

where, K_d = The partition coefficient between water and 1-octanol

C_o = The initial concentration of the component

d = membrane thickness in cm

C_{lim} = limiting concentration of the component required for the ISE to function.

Thus by using a sufficient membrane thickness, a high initial concentration of ionophores and using materials of high lipophilicity, electrodes of suitable life times can be fabricated.

1.8 EXPERIMENTAL WORK

1.8.1 CALIXARENE LIGAND MOLECULES

The calixarene compounds used here form part of a number of neutral carriers synthesised by Prof. McKervey and coworkers [83]. Some of these compounds have been used in this research as recognition systems for use in ion-selective electrodes, while others have already been reported as sensing agents in ISEs.

Calixarene compounds [83,84] are considered as cyclic oligomers of phenolformaldehyde condensates. In essence these neutral carriers are a class of [1n] metacyclophanes comprising cyclic arrays of phenolic residues attached by methylene groups at the ortho position to the hydroxyl group. The compounds are ideally suited for structural modification at different locations (Fig. 1.3). Derivatives containing pendant ether, amide, ketonic and ester groups have been synthesised and shown to exhibit different degrees of ionophoric activity [83]. The size of the macrocycle can be modified by changing the number of ring units, as in the case of compounds used here. Thus those compounds with a six membered ring correspond to ligands exhibiting caesium selectivity (Fig. 1.4) (hexameric calixarenes) while those with four membered rings (tetrameric calixarenes) accommodate in their cavity ions of smaller ionic radius e.g. sodium (Fig. 1.5).

The modified compounds employed here involve two main types of elaboration at the phenolic portions. With the hexameric calixarenes there are two esters (p-t-butyl hexaethyl ester and hexaethyl ester, Fig. 1.4) and with the tetrameric calixarenes, one ester (methyl p-t-butylcalix[4]aryl acetate, Fig. 1.5a), and one ketone, (the methyl ketone derivative of p-t-butylcalix[4]arene, Fig. 1.5b). The polymeric ligands used (Fig. 1.6), although

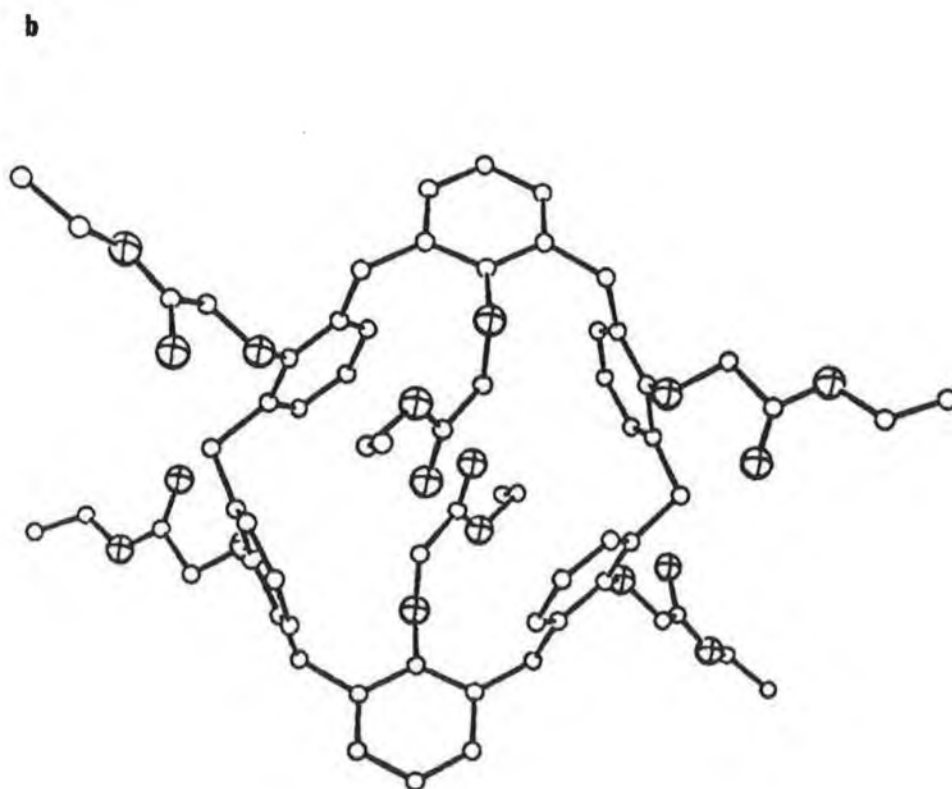
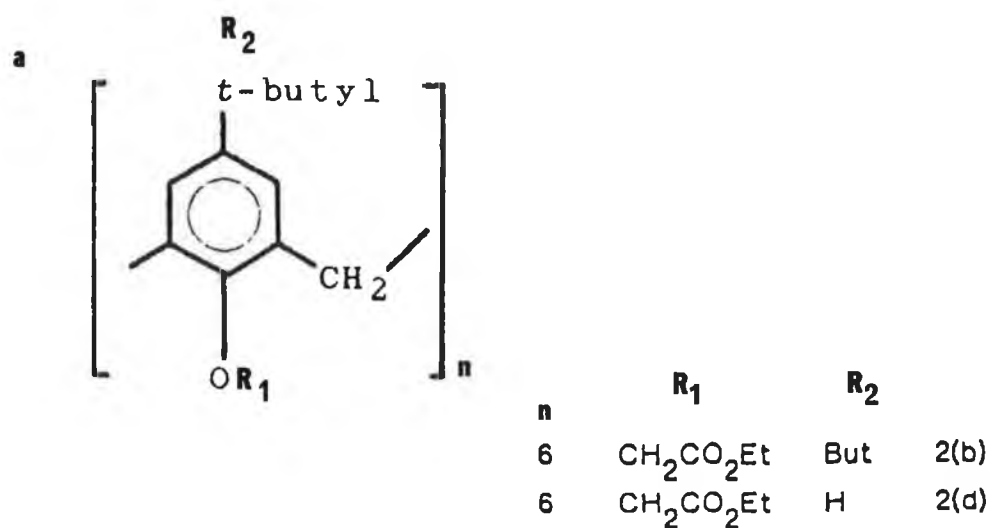


Fig. 1.4 (a) Structure of p-t-butylcalix[6]arene where the substituents R₁ and R₂ correspond to the ionophores used in this research. (b) Hexamer (2d) has a 0.404 and 0.42 nm separation between adjacent phenolic oxygen atoms (oxygen atoms marked with a cross).

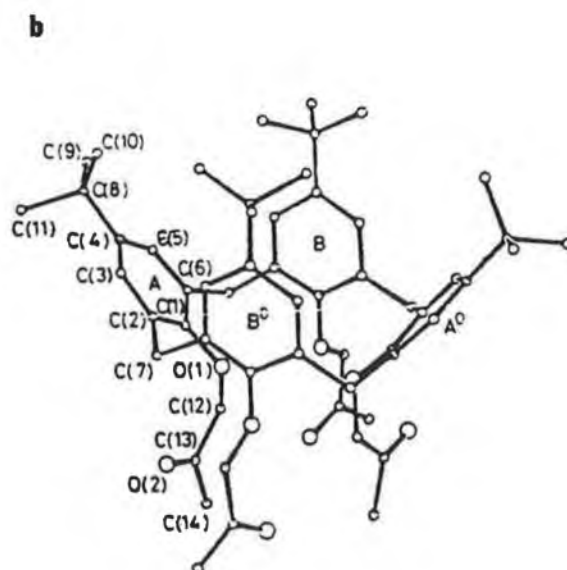
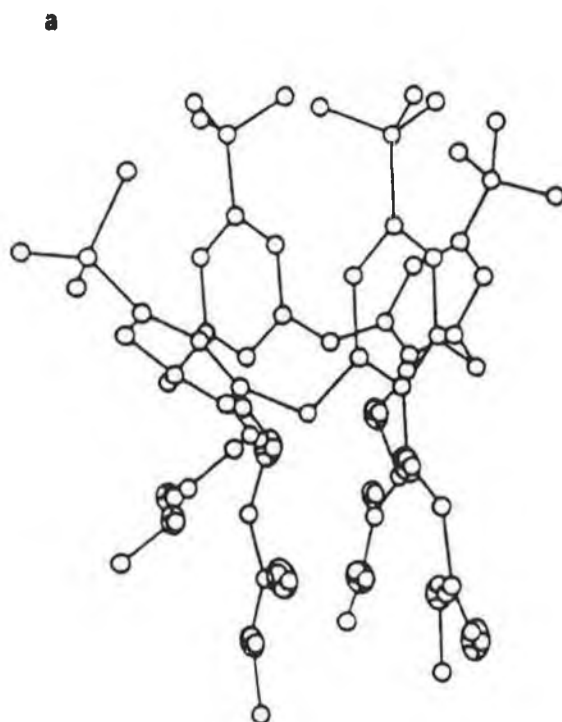


Fig. 1.5 (a) Methyl *p*-*t*-butylcalix[4]aryl acetate. Separation between adjacent phenolic oxygen atoms is 0.31 - 0.33 nm. (b) Methyl tetraketone derivative of *p*-*t*-butylcalix[4]arene.

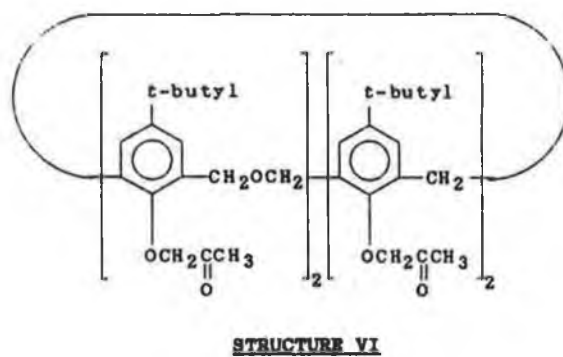
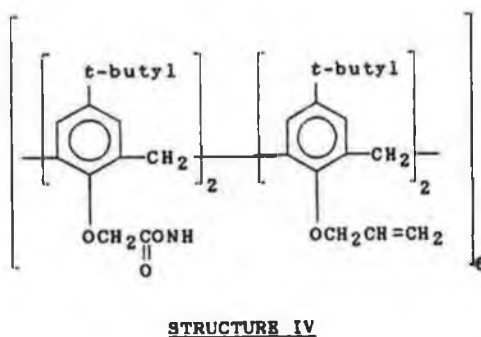
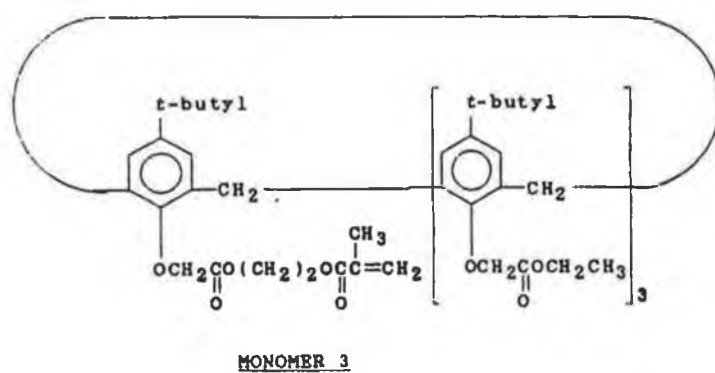
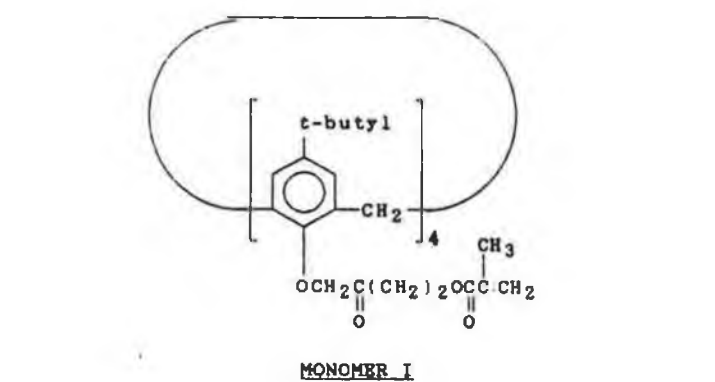


Fig. 1.6 Monomeric and polymeric calixarene inophores investigated for use in ISEs.

possessing more complex structures, can be assigned a semi-systematic name based on generalised rules for calixarene nomenclature viz; 1. specifying the size of the macrocycle by a bracketed number inserted in the 'calix-arene' stem, and specifying the nature and position of substitution on the aromatic rings by appropriate prefixes and suffixes. Thus a cyclic tetramer derived from p-tert-butyl phenolic and methylene units is named as p-t-butylcalix[4]arene (Fig 1.4a).

Clearly, the ionophores presented (Fig. 1.4, Fig. 1.5a 1.5b, and Fig.1.6) seem to meet the structural requirements outlined previously in section 1.5.1. Hence, the molecules present inward facing polar coordinating groups (nitrogen, oxygen) suitably orientated for complexation with metal ions, and outward facing non-polar groups (aryl, alkyl) responsible for the solubility of the ion carrier complex in the membrane phase.

The anticipated ionophoric behaviour is confirmed by results of phase transfer studies (Table 1.1) [83]. From these data, it can be clearly seen that the tetrameric calixarenes present by far the largest preference for sodium ions, while the hexameric compounds are relatively more efficient at extracting caesium ions.

1.8.2 Copolymerisation Procedure

Based on the structural requirements that an ionophore must have as outlined in section 1.5.1, it was decided to copolymerize monomer I (Fig. 1.6) with another monomer, namely methyl methacrylate, intending to disperse the number of polar groups in the ligand sphere, which might lead to a more sensitive response and possible selectivity.

Prior to copolymerization, methyl methacrylate (b.p. 92 - 94°C) was

Compound	Li ⁺	Na ⁺	K ⁺	NH ₄ ⁺	Rb ⁺	Cs ⁺
^a Butyl ethyl ester	11.4	50.1	85.9	—	88.7	100.0
^a ethyl ester	4.7	10.4	51.3	—	94.1	94.6
^b Methyl ester	6.7	85.7	22.3	—	9.8	25.5
^b Methyl tetraketone	31.4	99.2	84.1	23.0	53.7	83.8

Table 1.1 Percent extraction of alkali metal picrate into CH₂Cl₂ at 20°C for some hexameric and tetrameric compounds used in this research. 2.5x10⁻⁴ M compound in CH₂Cl₂; 2.5x10⁻⁴ M picric acid in 0.1 M aqueous MOH.

vacuum distilled to remove any inhibitor and thus allow it to participate in the copolymerisation. Copolymerisation was carried out as follows:

Copolymer 1: a 250 ml three necked round bottom flask, equipped with a stirrer, nitrogen gas inlet tube, thermometer and a reflux condenser was charged with 0.25 g monomer I, 2.5 g methyl methacrylate, 25 - 50 mg azobisisobutyronitrile (AIBN) initiator (1 - 2 % m/m relative to methyl methacrylate) and approximately 40 ml toluene. Nitrogen was bubbled vigorously through the solution for 15 minutes. The temperature was raised to 80 - 90°C by means of an oil bath and maintained for 5 - 6 hours under a nitrogen atmosphere. The solution was then allowed to cool and the polymer was formed by controlled precipitation in 400 ml of diethylether, under vigorous stirring. The product was collected using a sintered glass crucible and dried in the vacuum oven.

Copolymer 2: For copolymer 1, a monomer/methylmethacrylate ratio of 1:10 was employed, whereas in this case a ratio of 1:5 was used and the procedure followed through. However in this occasion petroleum ether (b.p. 40 - 60) was used as the precipitating solvent. The product formed was too fine to collect by any means. It was therefore necessary to evaporate off the petroleum ether and toluene to approximately 10 ml and precipitate into diethylether. Using this approach, a product was eventually collected.

An attempt was made to purify copolymer 2 to try to remove possible unreacted monomer. This was done by dissolving the product in dichloromethane, filtering it and adding it to 400 ml of petroleum ether as before. The product was collected in the same manner as previously. The copolymers were characterised by IR, UV and NMR spectroscopy and incorporated into plasticized membranes which were subsequently used to construct catheter type and coated wire electrodes.

1.8.3 MEMBRANE PREPARATION

Liquid membranes unless stated otherwise, were prepared according to a generalised procedure which consisted of:

0.66 wt.% calixarene ionophore was weighed into a 2 ml sample bottle together with 66.1 wt.% of solvent-mediator. In the case of membranes which contained ion-exchanger, 0.16 wt.% potassium tetrakis(p-chlorophenyl)borate was added to the mixture. In every instance this was slightly heated and stirred over a hot magnetic plate for at least 5 to 10 minutes. The solution was left to cool for a few minutes. Addition of 33.0 wt.% of poly(vinyl)chloride PVC was carried out only when the mixture was completely transparent. The resulting paste was stirred vigorously and an excess of tetrahydrofuran was

added thus avoiding the mixture to turn tacky while dissolving into the THF. Once it was completely dissolved, controlled evaporation of the THF left a 'runny-honey' type consistence of the membrane cocktail.

1.8.4 ELECTRODE CONSTRUCTION

Several type of electrodes were constructed during this work (Fig. 1.7).

These included:

- Glass pipette electrodes
- Catheter type electrodes
- Conventional macroelectrodes
- Coated wire electrodes
- polymeric film membranes deposited on glassy carbon electrodes

1.8.4.1 Glass Pipette Electrodes

(i) A 0.1 mm diameter trimel enamel coated, (Johnson Matthey U.K.) was cut to about 20 cm length. At both ends, the silver wire was bared by softening the trimel enamel with 50:50 mixture of nitric/sulphuric acid (immersed for about 20-25 seconds), after which the enamel was carefully pulled from the wire by hand under a gentle stream of running water. A critical step here is not to over expose the wire to the $\text{HNO}_3/\text{H}_2\text{SO}_4$ mixture in order to avoid the possibility of oxidation of the silver

(ii) the silver wire was then chloridised in a 14 % solution of sodium hypochlorite for 30 minutes.

A stable voltage depends on the reversible reaction between the chloride ions in the internal filling solution of the electrode and the solid AgCl of the internal reference. Silver wires can also be chlorided electrolytically

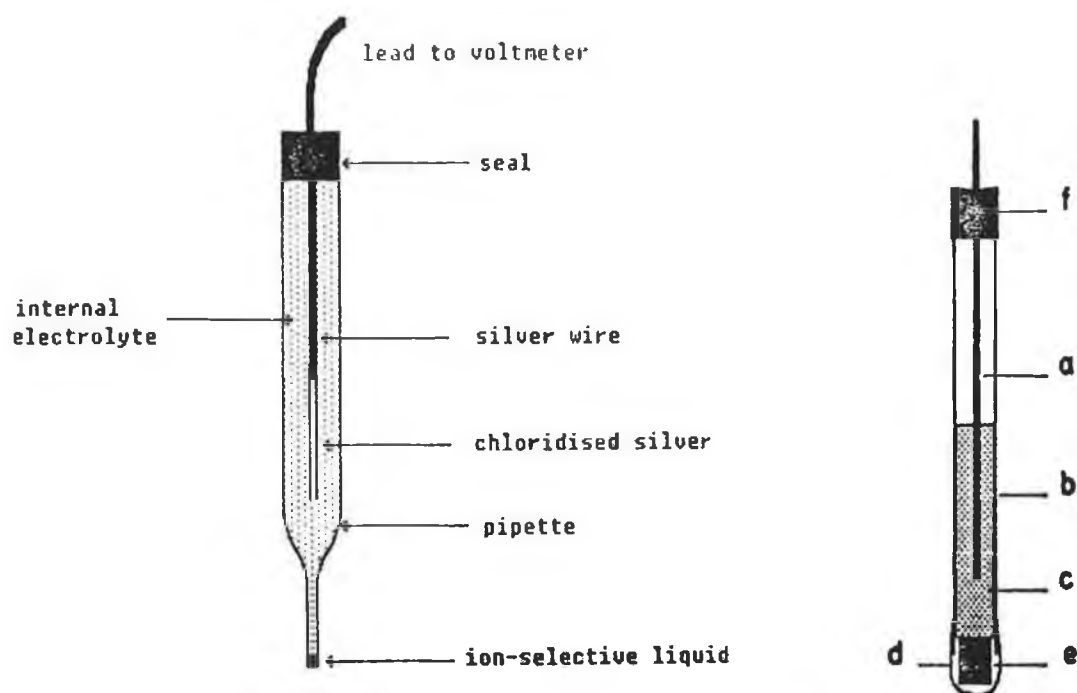


Fig. 1.7 Schematic of different type of electrodes constructed during research.

1) Glass pipette electrodes; 2) Catheter type electrodes: (a) silver wire, (b) internal reference solution, (c) PVC tubing, (d) PVC ion-selective membrane, (e) porcelain tip and f) 2 mm electrical plug; 3) conventional bench electrodes;

e.g. 0.1 M KCl at 10 mA/cm² for 15 minutes [85]. Electrolytic coating is claimed to produce a lower resistance and a more stable potential but the layer of AgCl is easily damaged [86]. Another approach is the dipping of the Ag wire into molten AgCl. In this case the coating is thicker and stronger but it has a higher electrical resistance

(iii) the chloridised silver wire was inserted through the broad end of a pasteur pipette, leaving 1 cm projecting from the narrow tip. In the broad end the wire was soldered to a 2 mm electrical plug and this was then fitted and sealed with silicone rubber

(iv) once the rubber hardened after few hours, the pipette was filled with internal filling solution (0.1 M NaCl) to within 1 - 2 mm of the pipette tip using a suitable syringe. Finally the liquid membrane solution containing the ionophore (liquid membrane without PVC matrix) was placed into the remaining space with a fine syringe and the electrode left to condition in 0.1 M NaCl for 30 minutes (Fig. 1.7).

1.8.4.2 Catheter Type Electrodes

A 16 cm length of PVC tubing, was used as the electrode body (EMS Medical Group Ltd., Stonehouse, Glos, U.K.) (1 mm i.d.). A chloridised silver wire, made as described above for pipette glass electrodes, was introduced through the tube. One end of the wire was soldered to a 2 mm plug which was subsequently fixed to the tube by glueing with an epoxy resin. At the other end, the wire was cut to size and a 2 - 3 mm porcelain tip (Morgan Matroc Products Ltd.) previously modelled to suitable shape was inserted so that half of its length protruded from the tube. The porcelain tip was then fixed in position with a drop of THF. To build the solvent polymeric membrane onto the

porcelain tip, it was dipped into the membrane cocktail briefly. The procedure was repeated at least four times until a suitable coating is observed. Thereafter the THF of the coating cocktail was then left to evaporate for 24 hours at room temperature. Internal filling solution (0.1 M solution of the primary ion) was then injected with a fine syringe through an opening in the tubing wall. The opening was then sealed with epoxy resin and the electrode was left to condition for at least 30 minutes in 0.1 M solution of the primary ion prior to use (Fig. 1.7).

The coating seems to play an important role in the performance of electrodes of this type. Both the magnitude of the electrical resistance and the slope of some electrodes seemed to have been related to some extent to the coating procedure. Although the dipping technique does not pose major problems (provided that no air bubbles are formed on the coated surface and that the coatings are evenly built up), the consistency of the prepared cocktail seems to be a key aspect. Thus the consistency dictates to a large extent the number of dipping cycles and therefore the thickness of the resulting coating. While coatings with a rather viscous cocktail membrane can still be made by an experienced practitioner, this is most likely to lead to electrodes exhibiting less efficient performance with high impedance and voltage readings which are dependent on the stirring rate of the solution being measured. In addition, variations on the measured slopes of some electrodes to some extent seemed to be a function of the membrane thickness. Although no study is presented here in relation to the thickness of the membrane coating, this factor had a clear influence on the work of Lev et al [87]. These workers investigated thick membranes containing Valinomycin or Nonactin neutral carriers dissolved in heptane and concluded that the resistance of a thick membrane is a linear

function of the membrane thickness, with a constant term corresponding to the surface resistance. However, once sufficient experience of the coating procedure is obtained, highly stable electrodes with reproducible response behaviour can be manufactured to this design.

1.8.4.3 Conventional Macroelectrodes

A classical bench electrode body (Russell gas sensing electrode model ISE 97-7809) was used. In this case the solvent polymeric membrane was prepared following a traditional procedure described by Moody and Thomas [88] (see also details in section 3.13, chapter 3). A 9 mm diameter disk was cut from the master membrane and inserted into the cap of the electrode, leaving a membrane of 7 mm diameter exposed to the sample solution. The electrode design enables the membrane disks to be clipped to the electrode caps rather than being glued. The electrodes were filled with 0.1 M NaCl as internal reference solution and left to soak for conditioning in 0.1 M NaCl for at least 30 minutes.

1.8.4.4 Coated Wire Electrodes

A 1.5 cm platinum wire (1 mm diameter) previously roughened with a metallic file to improve adherence of the membrane matrix was soldered to an approximately 10 cm copper conductor (0.5 cm diameter). The copper wire was soldered to a 2 cm electrical plug and then the whole body insulated with heat shrink. The joint between the platinum and the conductor was sealed with a layer of PVC to avoid any shorting out of the membrane when the electrode was placed in solution. The platinum end (previously washed with dilute nitric acid, deionised water and dried with acetone) was dip-coated with the membrane

cocktail 5 to 8 times with drying periods of at least 15 minutes in between the dipping cycles. A uniform thickness of the coating through the 1 cm length was difficult to achieve and a rather spheroidal shape was obtained at the far end of the wire. The THF in the membrane was left to evaporate for 24 hours and 30 minutes conditioning of the electrode in 0.1 M NaCl followed before measurements were performed.

1.8.4.5 Glassy Carbon Electrodes

These electrodes were used to investigate the properties of some polymerisable calixarenes, with the objective of producing a solid-state electrode. A glassy carbon electrode body was fixed to a metallic pin conductor with silver epoxy resin and left to harden in an oven at 80°C for 12 hours. The glassy carbon electrode surface was treated as follows. The electrode was polished with emery paper, followed by an alumina slurry on a woollen polishing cloth. Once a freshly polished surface was obtained, 5-50 μ l of solution membrane was placed onto the surface of the electrode and photopolymerised under UV light for 30 - 40 minutes, after which time, a transparent film formed on the surface. The electrode was conditioned in milli-Q water for 15 minutes.

1.8.5 MATERIALS

Analar grade chlorides of alkali metal and alkaline earth metal ions (NaCl, KCl, LiCl, CsCl, RbCl, NH_4Cl , CaCl_2 , MgCl_2) and potassium phthalate hydrogen salts were obtained from Riedel-de-Haen. Solutions and working buffers were prepared in distilled-deionised water. Solvent-mediators: dioctyl sebacate (DOS), 2-nitrophenyl octyl ether (2-NPOE); ion exchanger

potassium tetrakis(p-chlorophenyl)borate (KpTCPB); polymer matrix: poly(vinyl)-chloride (PVC); and tetrahydrofuran (THF) were all supplied by Fluka. Solvent-mediators phenyl phthalate (PP) and dioctyl phenyl phosphonate (DPP) were from Aldrich and Sigma, respectively. Salts of tris buffer were also obtained from Sigma.

All other reagents used were of the best analytical grade available. Calixarene ionophores were obtained from the organic synthetic group at UCC directed by Prof. McKervey..

1.8.6 POTENTIOMETRIC APPARATUS AND MEASUREMENTS

Measurements were taken with a Philips PW9421 digital pH meter (0.1 mV resolution) or alternatively with a Corning 240 pH/millivoltmeter coupled to a Fluka 8060A digital multimeter to obtain 0.01 mV resolution. External reference electrodes used were Ag/AgCl and saturated calomel. Two different types of saturated calomel electrodes (SCE) (free flowing liquid junction, Metrhom ref. 60.705.000; and the usual ceramic frit type of junction) were used according to availability. For injection experiments with the methyl tetraketone based electrode, the transient response-time curves were observed on a monitor screen of a BBC microcomputer using in-house software. Additional injection experiments and results of drift studies were recorded in a Linseis 16512 chart recorder.

1.9 RESULTS AND DISCUSSION

1.9.1 CAESIUM ELECTRODES

At present, methods to determine caesium make use of flame photometry or

atomic absorption, although lately ICP has been used. The importance of measuring caesium ions derive mainly from its role in nuclear fission processes. Ion-selective electrodes lend themselves nicely to the determination of alkali metal ions although no real effort has been directed to develop electrodes for caesium. Certain crown ether compounds [89-90] and a cryptahemispherand [91] have been shown to exhibit caesium complexing properties. Hexameric calix-arene compounds (Fig. 1.4) have shown excellent sensitivity to caesium ions and good selectivity against a range of alkali and alkaline earth metal ions. Earlier work [92] has demonstrated the benefits of incorporating ion exchanger KpTCPB to improve the electrode response, although the ion-exchanger itself has been found to exhibit ionophoric activity towards caesium ions.

Solvent polymeric membranes incorporating the two ionophores shown in Fig. 1.4, were prepared according to the procedure already outlined in section 1.8.3. The ionophores were incorporated in 2-NPOE solvent mediator with and without ion-exchanger (KpTCPB). In those membranes which incorporated KpTCPB, a 1:4 m/m proportion ion-exchanger/ligand was added. Catheter type electrodes were made up and the electrode response assayed in CsCl calibration solutions ranging from 10^{-6} M to 10^{-1} M and in separate solutions of alkali and alkaline earth metal ions at the 0.1 M concentration level.

Thus from the results obtained (Table 1.2), it can be seen that both the butyl substituted hexameric calixarene ester and the unsubstituted derivative electrode show good sensitivity to CsCl solutions either incorporating or excluding the ion-exchanger from the membrane. The responses are linear in the range 10^{-4} to 10^{-1} M CsCl. Further observation from table 1.2 seems to indicate that a real improvement in sensitivity is obtained in the membranes

<u>Response (mV) to Change in Concentration</u>					
<u>- log [Cs⁺]/M</u>					
Electrode	4	3	2	1	Slope(mV/dec)
2b	246.5	296.9	352.3	406.5	53.5
2b	287.0	333.7	389.2	443.2	52.4
2b	239.7	289.7	344.6	398.5	53.1
2b [*]	249.3	295.7	351.2	403.7	51.9
2d	406.1	459.9	514.6	467.2	53.8
2d	395.0	449.9	504.4	557.0	54.1
2d	427.0	480.8	534.0	587.2	53.4
2d [*]	350.0	400.5	455.9	509.4	53.4

Table 1.2 Caesium electrode response and electrode slope function to CsCl calibrating solutions ranging from 10⁻⁴ M to 10⁻¹ M.

* indicates the absence of KpTCPB in the electrode membrane

<u>Selectivity Coefficients log K_{csj}^{pot}</u>			
<u>interfering</u>	<u>electrodes based on ligand</u>		
<u>ion</u>	2b	2d	2d [*]
H ⁺	-3.17	-3.00	-3.10
K ⁺	-0.67	-2.66	-2.57
Na ⁺	-2.37	-3.59	-3.52
Li ⁺	-3.37	-4.40	-4.29
Ca ²⁺	-3.72	-4.05	-3.97
Mg ²⁺	-3.15	-3.70	-3.75

Table 1.3 Selectivity coefficients for PVC Cs⁺ electrodes.

Separate solution method 0.1 M

* membrane without ion-exchanger.

containing KpTCPB in comparison to those which did not contain the lipophilic anion. However, another trend encountered was that the incorporation of ion-exchanger did not produce any major visible difference on the stability of the electrodes. The electrodes behaved relatively stable with drifts not more than 0.5 mV during a 3 minutes reading.

According to the selectivity data presented in table 1.3, and calculated by the separate solution method, there is a higher preference for Cs^+ ions against interfering ions with the unsubstituted hexaethylcalix[6]arene ligand than with the butyl substituted one. This preference is, however, not enhanced by the introduction of the ion-exchanger. Interestingly enough the selectivity trend obtained follows closely the alkali metal picrate salt extraction figures for both ligands. Thus the trend favours Cs^+ with respect to interfering ions in the order $\text{K}^+ < \text{Na}^+ < \text{Li}^+$.

Unfortunately no data was obtained in this work for rubidium ions. Nevertheless, selectivity coefficients have been recently reported for rubidium employing both ligands in a PVC membrane, plasticised with 2-NPOE solvent mediator [93]. Thus this selectivity data obtained by Cadogan et al [93] using the same technique confirms largely the one obtained here and adds coefficients for Rb^+ and NH_4^+ ions, the values being ($\log K_{\text{Cs}}^{\text{pot}}$):

p-t-Butyl hexamer (KpTCPB added) $\text{Rb}^+ = -0.99$ and $\text{NH}_4^+ = -2.06$,

ethyl hexamer (KpTCPB added) $\text{Rb}^+ = -1.52$ and $\text{NH}_4^+ = -2.75$

The dynamic response behaviour of these electrodes was observed by recording their change in potential to shifts in concentration. The magnitude of the jump indicates the preference established in the selectivity studies

with the largest jump being for caesium ions followed by K^+ and Na^+ while the lowest change in potential is that observed for Li^+ ions (Fig. 1.8).

Response times were fast ($t_{90\%}$ ~ few seconds) in every case.

1.9.2 SODIUM ELECTRODES

The best known sodium ISE is the sodium glass electrode, which has been in common use since the late 1950s. The principal interferents of sodium glass are hydrogen and silver ions; potassium ions interfere to a lesser extent. Consequently, since silver ions are rarely present as a sample constituent, problems are restricted to pH adjustment in sample solutions. However, further problems are encountered with sodium glass electrodes will be discussed in chapter 2. Several sodium electrodes based on neutral carriers recently developed offer certain advantages over traditional glass electrodes [94-96].

The novel sodium sensors described here are based on derivatives of the tetramer p-t-butylcalix[4]arene (Fig. 1.5) [83].

1.9.2.1 METHYL p-t-BUTYLCALIX[4]ARYL ACETATE

1.9.2.1.1 Electrode Response

PVC membranes were prepared according to the procedure outlined in 1.8.3. Typically these membranes contained 2.0 mg ionophore, 200.0 mg plasticizer 2-NPOE, 0.5 mg ion-exchanger and 100 mg PVC. Batches of electrodes were made up and the response of the electrodes measured in 10^{-6} M to 10^{-1} M of pure NaCl solutions against a calomel electrode with a free flowing junction. The response for a batch of 5 electrodes based on the methyl ester derivative measured sequentially in gently stirred sodium solutions at $24 \pm 1^\circ C$

Sodium Activity	<u>Electrode Response (mV)</u>					Slope mV/dec
	30 sec	60 sec	90 sec	120 sec	150 sec	
1×10^{-4}	17.2	17.9	17.4	17.3	17.5	
1×10^{-3}	75.3	75.3	75.4	75.4	75.4	
1×10^{-2}	132.8	132.8	132.7	132.8	132.8	
1×10^{-1}	189.2	189.1	189.1	189.1	189.1	59.4
					59.4	
1×10^{-4}	13.8	14.1	14.2	14.3	14.2	
1×10^{-3}	71.4	71.5	71.7	71.6	71.6	
1×10^{-2}	129.3	129.4	129.5	129.5	129.5	
1×10^{-1}	186.0	186.1	186.1	186.2	186.2	59.5
					59.5	
1×10^{-4}	16.7	17.0	17.1	17.2	17.3	
1×10^{-3}	75.6	75.7	75.7	75.7	75.7	
1×10^{-2}	133.0	133.2	133.3	133.4	133.5	
1×10^{-1}	189.9	190.0	190.1	190.2	190.2	59.8
					59.8	
1×10^{-4}	13.3	13.6	13.9	14.0	14.2	
1×10^{-3}	71.5	71.6	71.6	71.7	71.7	
1×10^{-2}	129.6	129.7	129.7	129.8	129.8	
1×10^{-1}	186.0	186.1	186.2	186.3	186.3	59.6
					59.6	
1×10^{-4}	15.8	15.8	15.9	16.0	15.9	
1×10^{-3}	73.6	73.6	73.6	73.6	73.6	
1×10^{-2}	131.7	131.7	131.8	131.8	131.8	
1×10^{-1}	188.6	188.7	188.7	188.7	188.8	59.7

Table 1.4 Methyl p-t-butylcalix[4]arene PVC based electrode response to pure sodium solutions.

is illustrated in table 1.4.

The results of the 5 electrodes indicate a Nernstian response for the sodium range 10^{-4} M to 10^{-1} M (calculated from values taken at two and a half minutes). The results of the freshly prepared set showed excellent reproducibility and stability. In fact, these features can be both obtained if considerations such as those discussed in section 1.8.4.2 (electrode construction) are carefully observed. In addition it is equally important to consider the multiple sources of error introduced in potentiometric measurement [97]. Durst [97] has extensively reviewed this matter and suggested that, since batch measurements are strongly affected by chemical and mechanical interference (washing, cleaning, changing solutions) experimental procedures should be carried out in a reproducible way. Temperature effects, reference electrode stability and its liquid junction are also key aspects to consider to avoid irreproducible results and variations in slopes.

However, inherent characteristics of the electrode performance still lead to some degree of imprecision. This is observed in the above results (Table 1.4) by the tendency to drift shown by some of the electrodes. The drift profile was examined for all of the 5 electrodes over 1 hour period. The electrodes were placed in gently stirred 1×10^{-2} M NaCl solutions and exhibited an average positive drift of 0.5 mV per hour under non-thermostatted conditions (max. temperature change 0.4°C over a 5 hours period). A more detailed investigation of the drift involved the measurement over a 24 hour period with 2 electrodes which had been used and stored in 0.1 M NaCl for about 10 days. The drift this time in thermostatted 1×10^{-2} M NaCl solutions amounted to 1.7 ± 0.1 mV in each case.

To assess the reproducibility of the electrodes, they were transferred

from a 10^{-3} M into a 10^{-2} M NaCl solution five times sequentially and the measurements taken every two minutes. The results showed a highly reproducible response (± 0.08 mV) on transfer of the electrode from a 10^{-3} to a 10^{-2} M solution, while a lower precision of ± 0.22 mV was obtained when the transfer was done in the opposite direction (average of five measurements in each case).

Measurements of resistance were carried out in unstirred 0.1 M NaCl solutions for 5 newly constructed electrodes. The electrodes, which had been stored in 0.1 M NaCl previous to measurement, gave an average resistance of 1.03 ± 0.04 M. The resistance found is in accordance with typical values observed for solvent polymer membrane electrodes, and is significantly less than resistances found with glass electrodes.

1.9.2.1.2 Injection Experiments

A rough guide to electrode selectivity may be obtained by injecting known amounts of ions into a sample solution containing the primary ion. In addition, extra information is also obtained regarding the dynamic response of the electrode to transient shifts in the measured analyte.

Thus aliquots of 450 μ l of 0.1 M solutions of alkali and alkaline earth metal ions were injected manually into 50 ml of 10^{-4} M solutions of the primary ion. The response traces recorded on the chart recorder are shown in Fig. 1.9.

The results in the case of the Na^+ injection (involving a step change in concentration of nearly one order of magnitude, 10^{-4} M to 10^{-3} M) showed a practically Nernstian response. The response was very fast (almost instantaneous) and was probably limited by the stirring rate. As expected from selectivity data obtained from previous work [92], the responses to other

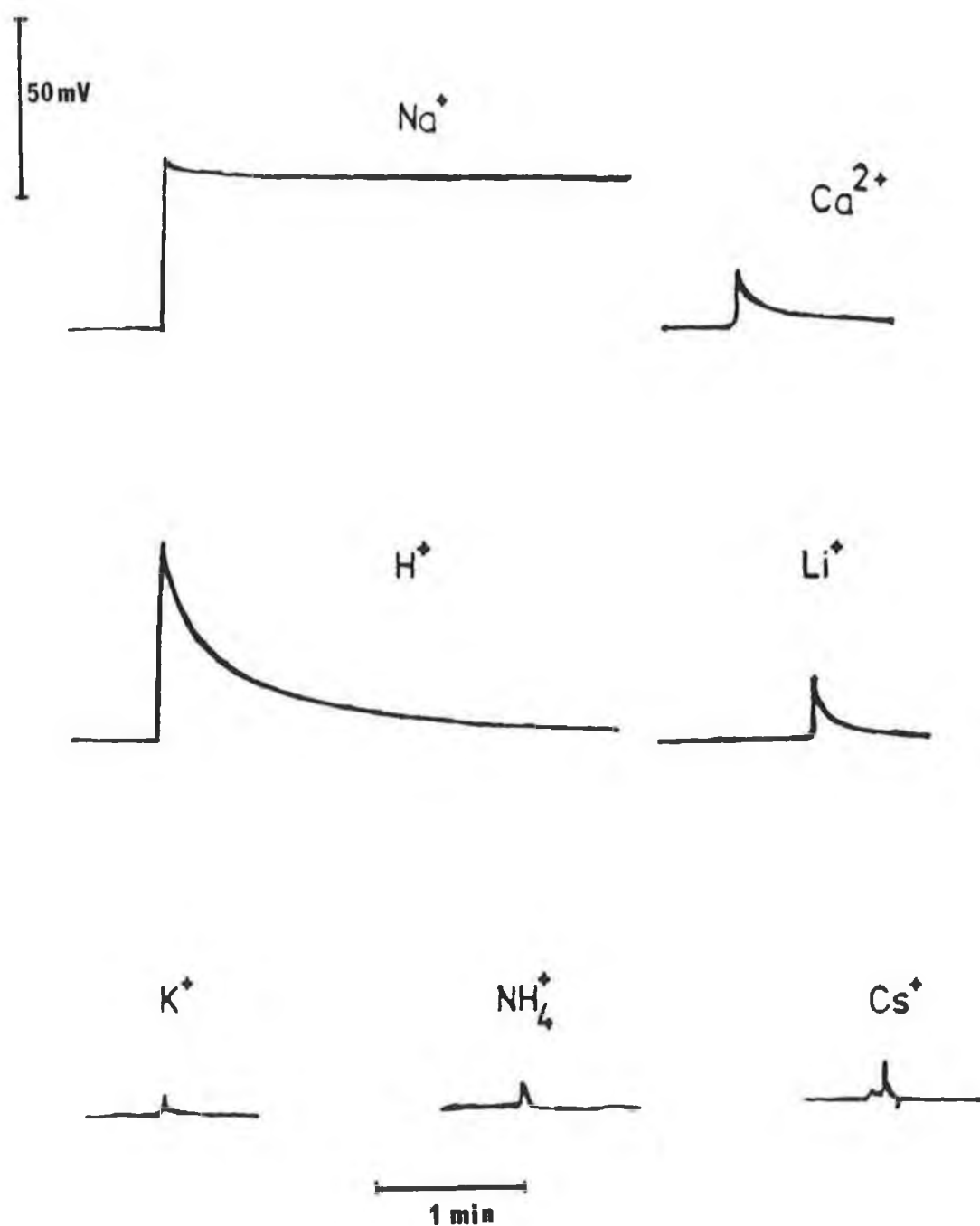


Fig. 1.9 Transient response to a 10-fold increase in sodium concentration (10^{-4} - 10^{-3}) for a methyl ester tetramer based catheter electrode.

alkali and alkaline metal ions was small. However, when the injection of HCl was performed a very fast and large transient amounting nearly 60 mV was obtained. The magnitude of the response decreased with time and became negligible in comparison to the sodium response only after a couple of minutes. This transient is in contrast to that previously reported [92] in which the response amounted no more than 3 millivolts. The cause of this difference on the initial response of the electrode to hydrogen ions is not clear but it could be related to the different ionophore/ion-exchanger ratio used. The apparent time dependent selectivity against hydrogen ions is further discussed in chapter 2.

Further injections of sodium were performed to try to assess the response time of the electrode to the step-change in concentration considered above. The monitoring of the response at two chart speeds is shown in Fig. 1.10.

Although, by no means a detailed study, it certainly gives an indication of the fast response time of these electrodes. The shape of the traces is highly distorted probably by the way the analyte is presented to the surface of the electrode. Unfortunately it is not easy to create a concentration step at an electrolyte/electrode interface and unless conditions are strictly designed for response time experiments, the measured data lacks reproducibility. However, Lindner et al [68] have suggested that even with an ideal step-change in the sample concentration, where a very fast concentration change is assured at the electrode surface, the electrode may still be in contact with parts of the solution containing different concentrations leading to mixed potentials that may distort the response curve. In addition, as mentioned in theoretical considerations (see section 1.6) the response time functions are not controlled exclusively by the electrolyte/electrode interface, but by other factors such

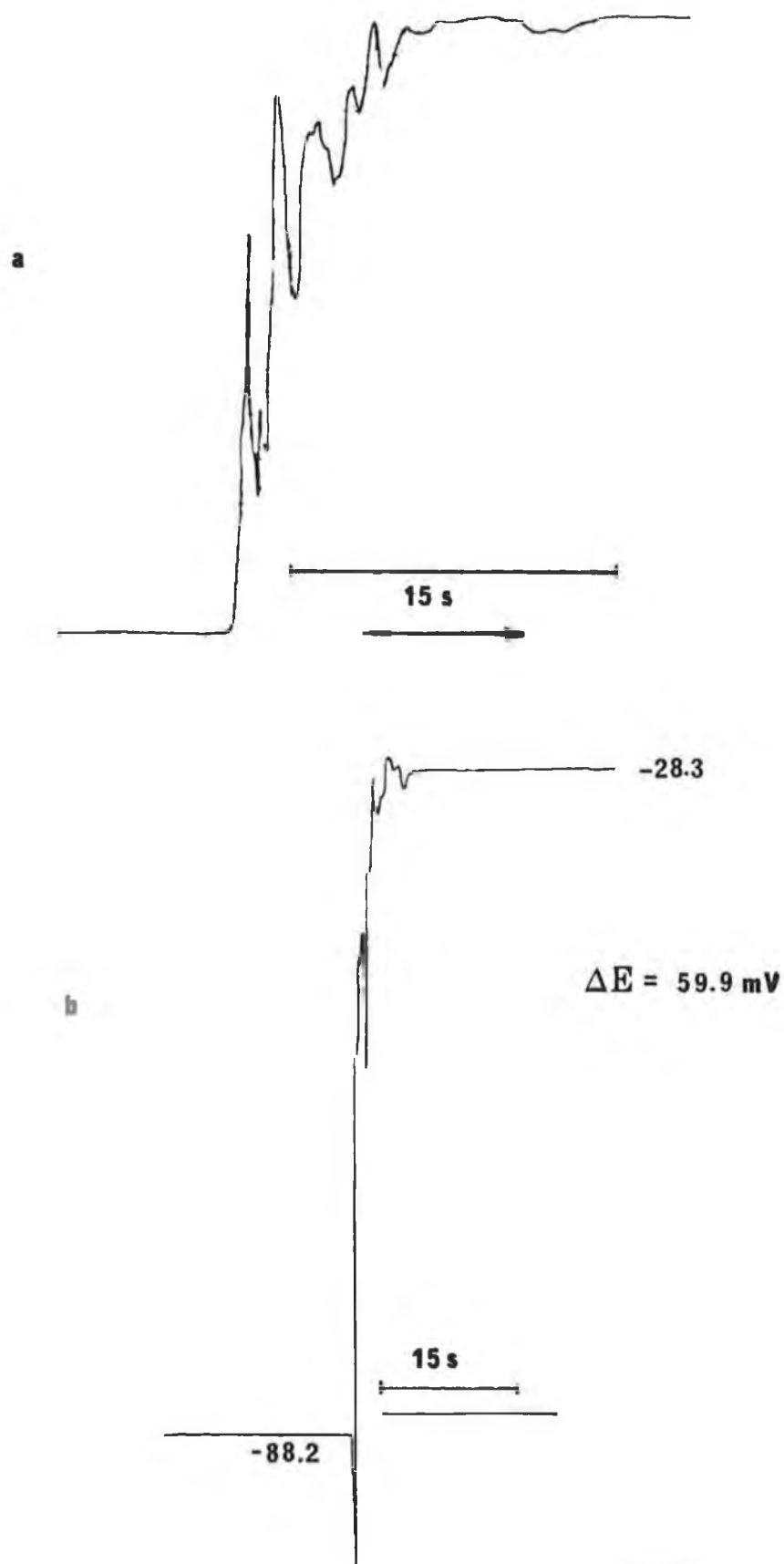


Fig. 1.10 Transient response to a 10-fold increase in sodium concentration (10^{-4} - 10^{-3} M) for a methyl ester tetramer based catheter electrode.

a) chart speed 300 mm/min, and b) 120 mm/min.

as the measuring technique and the design and geometry of the cell. In this respect several workers have reported specially designed cells to avoid these problems [75]. Despite these problems under the simple injection experiments employed during this work the response time (t_{90}) of the electrodes was less than 5 seconds. From theoretical considerations (section 1.6.2) it is believed that the response time can be even further reduced and perhaps the 'true' electrode response time determined, for example by means of carefully designed flow-injection analysis experiments (FIA).

1.9.2.1.3 Determination of Selectivity Coefficients

The electrode response was measured in a range of solutions (10^{-6} M - 10^{-1} M) of alkali and alkaline earth metal ions and the calibration curves constructed as shown in Fig. 1.11. The results again show a Nernstian response to sodium ions with a second and third preference for caesium and hydrogen ions respectively. Responses to the latter two ions increase with concentration but not in a Nernstian fashion.

To determine selectivity coefficients, potential measurements were made in 0.1 M solutions of interfering ions. The final measurement was the reading averaged at 10 and 15 minutes. A problem that soon became apparent when measuring solutions other than sodium was the larger drift associated with the measurements. Thus, to ensure reproducibility in the measurements and avoid the influence of this drift to a minimum selectivity coefficients were measured in the following way:

the slope of the electrode function in 10^{-4} M to 10^{-1} M NaCl solutions was measured 3 times and the results averaged. Once the slope of the electrode had been determined, the 0.1 M solution was measured once and subsequently the

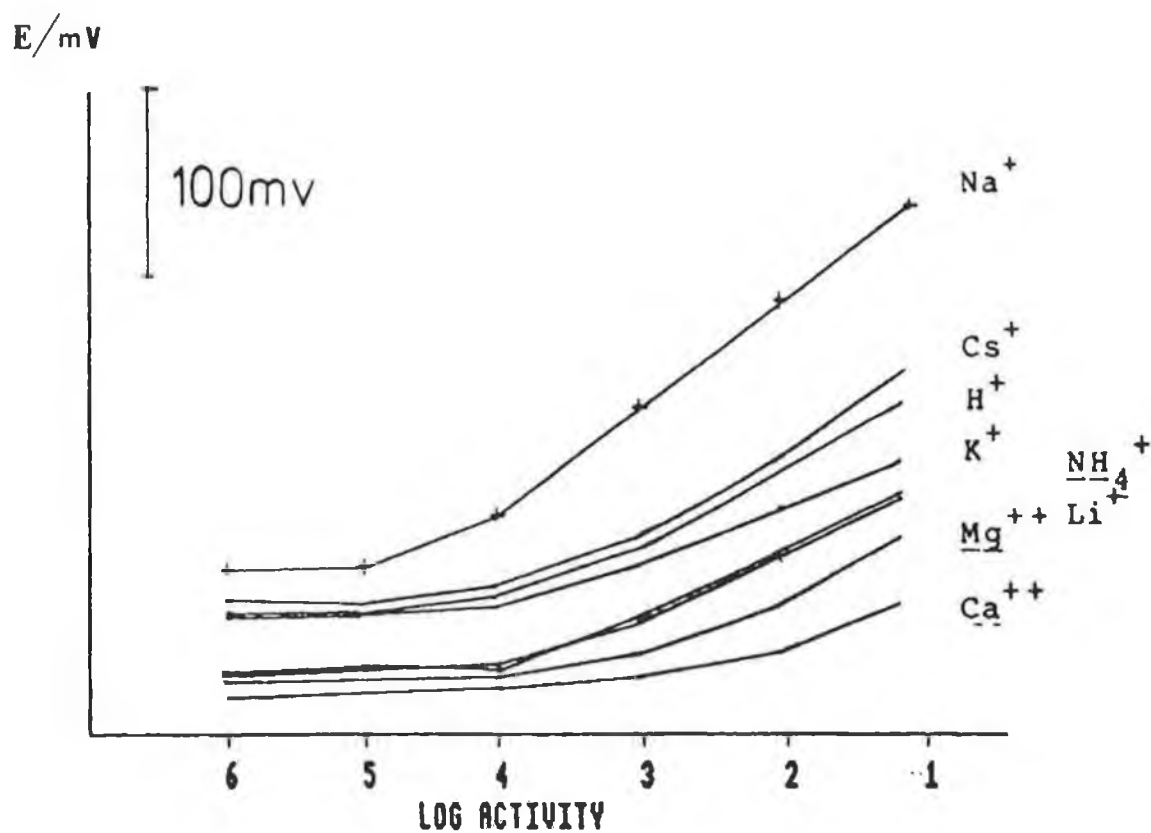


Fig.1.11 Calibration curves for alkali and alkali earth metal ions as performed by catheter type electrodes based on ligand methyl p-t-butylcalix[4]arene.

interfering solution (0.1 M) was measured three times. The NaCl 0.1 M solution was then measured twice and the results so obtained were averaged. The selectivity coefficients for the rest of the interfering ions were then measured using the same procedure with the same electrode. The results so obtained are shown in table 1.5 and compared to the glass electrode and other available sodium electrodes based on neutral carriers.

From these results it is evident that the electrode exhibits excellent selectivity against a range of common alkali and alkaline earth metal ions with an order of preference following the sequence:



Thus the order of preference obtained is similar to that obtained from phase transfer studies of salt picrate extraction performed by McKervey et al [98] and following closely the values of selectivity coefficients previously reported for the same electrode [92]. From the comparison with other available sodium electrodes it can be seen that the methyl ester derivative, although not possessing as good selectivity as the sodium glass electrode with respect to Cs^+ , K^+ and NH_4^+ , is by far more H^+ selective and nearly similar with respect to Li^+ selectivity. With regard to the other sodium selective ligands, the methyl ester calixarene exhibits better selectivity towards K^+ , Li^+ and H^+ . While the importance of a good discriminating sodium electrode against potassium and lithium is fundamental in clinical assays, the selectivity against hydrogen ions is a characteristic welcome in any application. The electrode lithium selectivity can become particularly important while measuring sodium in patients undergoing lithium therapy. This

Selectivity Coefficients ($\log K_{ij}^{\text{pot}}$)				
ION	Methyl-Ester	ETH 227	bis(12-crown-4)	Na ⁺ Glass
Cs ⁺	-1.51	-2.4	—	—
H ⁺	-1.88	-0.1	—	3.0
K ⁺	-2.47	-2.0	-1.85	-3.0
NH ₄	-2.74	-1.7	—	-4.5
Li ⁺	-2.78	0.5	-1.80	-3.0
Mg ⁺⁺	-3.12	-2.2	-3.15	—
Ca ⁺⁺	-3.74	-1.5	-3.68	—

Table 1.5 Selectivity coefficients ($\log K_{\text{Na}^+}^{\text{pot}}$) for solvent polymeric membranes and sodium glass electrode by the separate solution method (0.1 M). The values for the membrane ETH 227 have been obtained by Simon and co-workers [96], and for the bis(12-crown-4) by Moody and Thomas [60].

is the case with patients suffering from maniac depression during which the administration of lithium salts can be as high as to produce serum concentrations of 1.5 mmol l^{-1} [99].

The selectivity against hydrogen interferences was also investigated by the mixed solution method, by varying the pH of 10^{-3} and 10^{-2} M NaCl solutions. Insignificant variations ($< 1.0 \text{ mV}$) in the electrode potential between pH 10.5 and 5.5 were obtained indicating a good selectivity over hydrogen ions under these conditions.

1.9.2.1.4 Life Time

As indicated in the theoretical treatment of this chapter, the life time of ion-selective electrodes can be an important consideration, the degree of importance of which depending upon the particular application. Although no systematic study of life time was intended, the performance of the electrode was observed during a 1 month period by measuring the slope of the electrode function. The electrode was regularly utilised during the month in question and was permanently stored in NaCl 0.1 M solutions when not in use. The slopes vs time plots (Fig. 1.12) indicate that life times of at least one month are possible in aqueous solutions. A more detailed study of the electrode life time has been recently published [100]. In this work a life time of at least one year in aqueous solutions has been deduced from considerations made on membrane resistance.

1.9.2.2 METHYL TETRAKETONE CALIX[4]ARENE

1.9.2.2.1 Glass Pipette Electrodes

To assess the potential use of methyl tetraketone derivative of

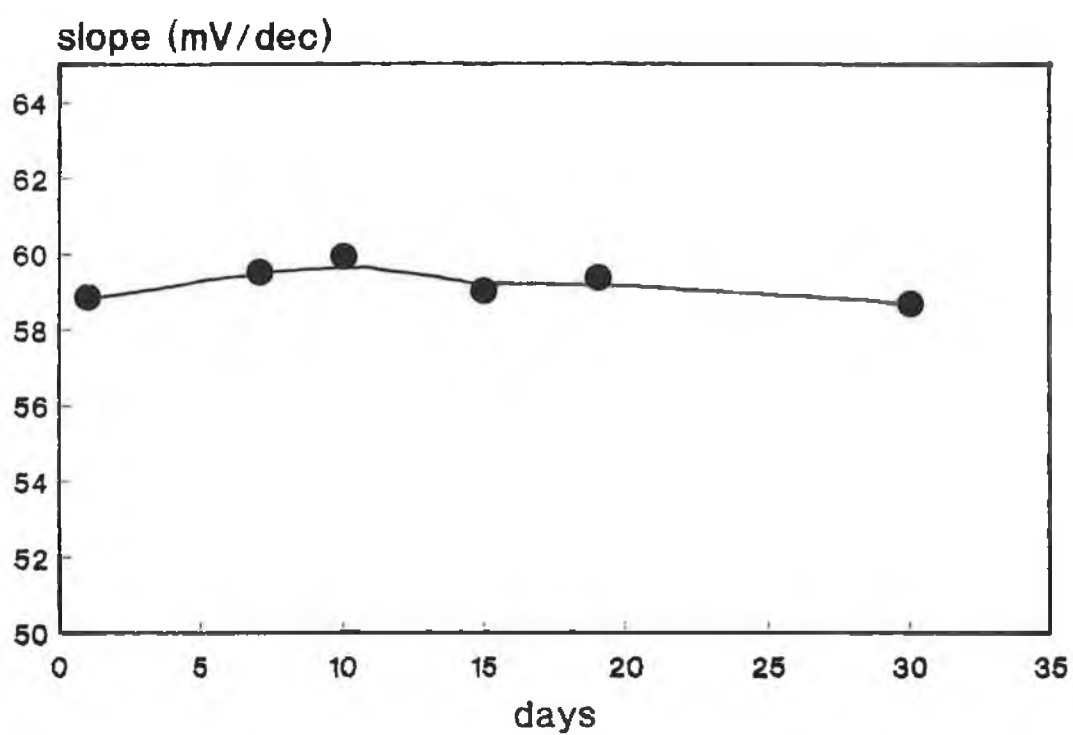


Fig. 1.12 Variation of electrode slope function with time. Details as in text.

<u>Solvent</u>	<u>Ionophore Solubility</u>
Toluene	soluble
Dichloromethane	soluble
Nitrobenzene	insoluble
1,3,5,trichlorobenzene	insoluble
<u>Plasticiser</u>	
2-NPOE	soluble
Diethyl phthalate	soluble
Diethyl phosphonate	soluble
Diethyl sebacate	soluble

Table 1.6 Solubility of 0.5 - 1 wt.% methyl tetraketone derivative in some common organic solvents and plasticisers

p-t-butyl calix[4]arene as a sensing agent in ion-selective electrodes, the ligand was dissolved in several organic solvents and plasticisers (Table 1.6).

The methyl tetraketone derivative had a good solubility in the solvent mediator 2-NPOE, yielding a yellowish transparent solution after dissolving 1 mg in 100 mg of plasticiser. This solution was placed in glass pipette electrodes as described in section 1.8.4.1 and batches of up to 10 electrodes were constructed.

1.9.2.2.1.1 Electrode Response

The electrode response was measured against an Ag/AgCl external reference for separate solutions of alkali and alkaline earth metal ions at two different concentrations i.e. 10^{-4} M and 10^{-1} M (dilution of 0.1 M aliquot to its final concentration was prepared without incorporating ionic buffers).

A considerable drift amounting at least a few millivolts per hour was observed once the electrodes were placed in the 10^{-4} M NaCl solution. Consequently, the measurements were taken only after 10 minutes when the potential had become acceptably stable. The results obtained for five electrodes (Table 1.7) showed a clear response of the electrodes to sodium ions when the solution was changed from 10^{-4} M to 10^{-1} M. Although the results obtained among the 5 electrodes were different in absolute voltage reading (Table 1.7 shows only ΔE), the overall pattern in every case indicated preference for sodium with an average response of 152.4 mV and with the second and third largest difference obtained for CaCl_2 (86.6 mV) and CsCl (77.2 mV), respectively for the concentration step considered.

Ion	$\log [\text{Na}^+] / \text{M}$									
	ΔE mV									
	-4	-1	-4	-1	-4	-1	-4	-1	-4	-1
Na^+	158		150		155		151		148	
K^+	55		67		52		58		41	
Cs^+	76		75		86		78		81	
Li^+	53		40		33		55		26	
NH_4^+	47		38		43		46		29	
Ca^{2+}	95		82		86		89		81	
Mg^+	49		54		64		67		56	

Table 1.7 Potential difference (ΔE) in millivolts for 5 glass pipette electrodes to two molar concentration of different cations.

The absolute millivolt reading, which expresses to some extent the reproducibility in the construction of a set of electrodes, showed considerable variation among electrodes. This seemed to be due to factor such as the lack of control over the geometry of the tip, slight cracks suffered during measurements, differences in membrane thicknesses and variations in stirring rate. In fact one of the problems constantly faced with this electrode was the rather fragile tip design. The electrode tip was easily cracked during handling if extreme precautions were not taken. In addition, a very low stirring rate had to be used in order to avoid the membrane falling off the tip.

An interesting aspect of the results obtained in table 1.7 was the near-Nernstian behaviour obtained. This is shown by the magnitude of the potential jump observed for the concentration step involved. Thus electrode 1 exhibited a change of 158 mV, with the expected Nernstian value for the range of concentrations assayed of 177.4 mV.

The near-Nernstian behaviour was in fact confirmed when the ionophore was included in membrane solutions which this time incorporated 0.25 wt.% ion-exchanger. The electrode response function measured in NaCl solutions ranging from 10^{-6} M to 10^{-1} M is depicted in Fig. 1.13 for a set of 3 electrodes. The results show that a linear response is obtained in the 10^{-4} to 10^{-1} activity range. Moreover one of the electrodes (3) shows a practically Nernstian response (59.0 mV dec^{-1}) which confirms the excellent extraction capability of the ionophore for sodium in accordance with McKervey's data (Table 1.1).

Another aspect observed was the improvement in the general stability of the electrode in the various sample solutions with the incorporation of KpTCPB

in the membrane. The drift was smaller, which allowed the measurements to be taken at 5 minutes, rather than 10, and the signal was less affected by noise. Although no resistance measurements were taken at this stage, the improvements may have been due to the introduction of the ion-exchanger KpTCPB. These improved characteristics are in fact widely mentioned in the literature in association with the role of ion-exchangers in liquid membranes and have been already discussed in section 1.5.2.3.

Although the practical applicability of glass pipette electrodes is limited they are useful at least for a rough assessment of new potential ionophores, although the response does certainly lack reproducibility. This is clearly reflected in the values obtained for the slope function of the 3 electrodes depicted in Fig. 1.13 which were measured in the same calibration solutions.

1.9.2.2.1.2 Injection Experiments

The procedure adopted was to add 1 ml 0.1 M solutions of alkali and alkaline earth metal ions into 40 ml of a 10^{-4} M NaCl solution. The responses are then compared to that provided by the injection of sodium ion at the same concentration. A theoretical response of 83.1 mV was calculated for the sodium injection according to the following equation:

$$E = S \log C_{\text{final}}/C_{\text{start}} \quad (1.20)$$

The transient responses to these injections are reported in table 1.8. Thus, a value of 75 mV (which approximates closely to the calculated value of 83.1 mV) was obtained for the sodium response. A fast response time (t_{90}),

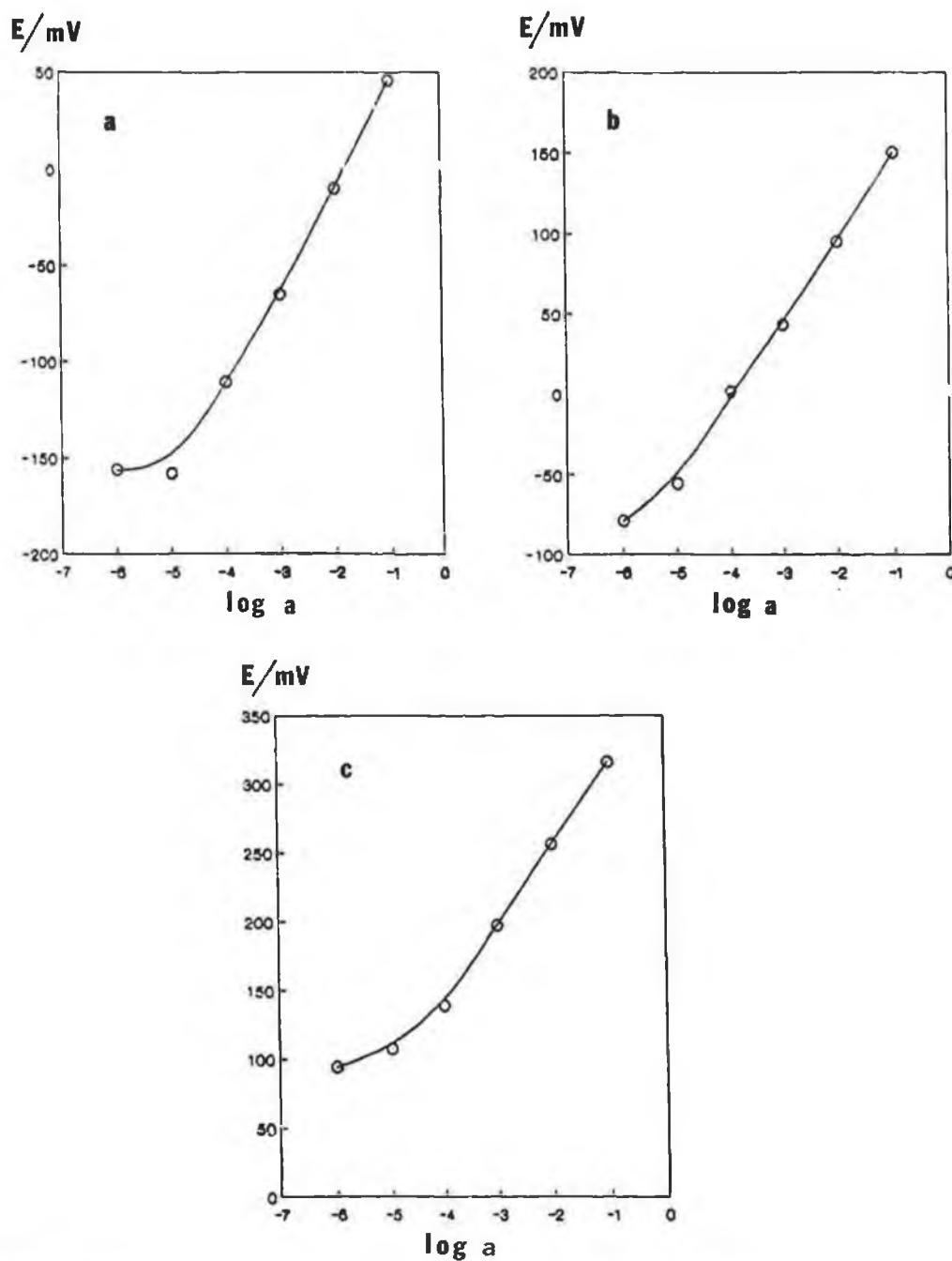


Fig. 1.13 Calibration curves for glass pipette electrodes based on methyl tetraketone calix[4]arene. The slopes of the electrodes in the 10^{-4} to 10^{-1} M range are: a) 54.6 mV Dec^{-1} , b) 49.9 mV Dec^{-1} and c) 59.0 mV Dec^{-1} .

generally within 10 seconds was observed for the same injection. The response of the electrode to similar activity changes for the other alkali and alkaline earth metal ions is clearly insignificant in comparison to the sodium response. However the second largest response was that obtained for the injection of potassium ions, which seems to agree with the data of picrate salt extraction of alkali ions presented by McKervey [98].

Ions	Sodium Solution	Sodium Solution	E_2-E_1 (mV)
	10^{-4} M (mV)	10^{-1} M (mV)	
Na^+	-120	-45	75
Cs^+	-19	-12	7
K^+	-6	7	13
Li^+	-1	-7	6
NH_4	2	2	0
Ca^{2+}	-6	3	9
Mg^{2+}	-1	-4	3

Table 1.8 Response of glass pipette electrodes containing methyl tetraketone derivative to injections of alkali and alkaline metal ions.

1.9.2.2.2 Solvent Polymeric Membrane Electrodes

Batches of catheter type and conventional macroelectrodes were constructed as described earlier. Typical membrane mixtures contained 2.0 mg ionophore, 200.0 mg plasticiser, 100.0 mg PVC and KpTCPB as ion exchanger. Membranes with varying amounts of ion exchanger were initially tested in electrodes that contained 2-NPOE as plasticiser in order to assess its

KpTCPB		Electrode Response (mV)			
50 % mol		Time (min)			
ratio	$-\log a_{\text{Na}}$	1	2	Slope mV/dec	Resistance M Ω
0				57.9	5.3
	-4	-139.4	-139.4		
	-3	-82.2	-82.4		
	-2	-26.1	-26.2		
	-1	28.3	28.3		
25				59.5	2.9
	-4	-140.9	-141.0		
	-3	-82.5	-82.5		
	-2	-24.9	-24.8		
	-1	31.3	31.4		
50				59.7	1.3
	-4	-135.5	-135.3		
	-3	-76.9	-76.8		
	-2	-19.0	-19.1		
	-1	37.3	37.4		
75				59.4	1.0
	-4	-134.5	-134.4		
	-3	-76.3	-76.1		
	-2	-18.8	-18.6		
	-1	37.4	37.7		

Table 1.9 Response in mV and resistance of methyl tetraketone calix[4]arene electrodes containing varying amounts of ion-exchanger in the plasticised membrane (plasticiser = 2-NPOE). The results represent only one electrode, although other electrodes gave an identical pattern for the parameters being discussed.

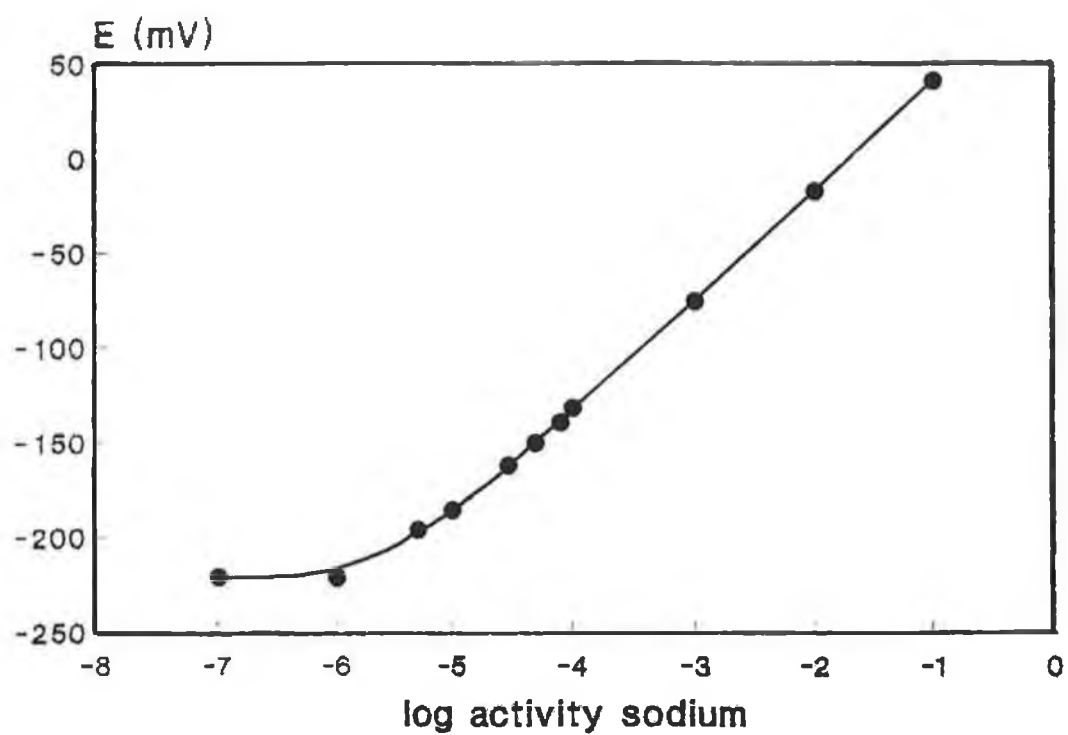


Fig. 1.14 Calibration curve for methyl tetraketone calix[4]arene in pure sodium solutions ranging from 1×10^{-7} M to 1×10^{-1} M

influence on the electrode performance (table 1.9).

From the results obtained in table 1.9 for electrodes containing 2-NPOE as membrane plasticiser, it was soon realised that the incorporation of KpTCPB had a marked influence on the electrode sensitivity and resistance. This aspect was taken into consideration and further membranes described here all contain 50 % mol ratio KpTCPB as ion-exchanger relative to the ionophore.

As expected from the results obtained with glass pipette electrodes, the methyl tetraketone derivative showed a reproducible Nernstian response in NaCl solutions, with a linear range between 3×10^{-5} M to 1×10^{-1} M (Fig. 1.14). From the data obtained (Table 1.9), it seems apparent that the Nernstian response of the electrode is only obtained with the addition of small quantities of ion-exchanger in the membrane, although the proportion of ion-exchanger/ligand in this is not critical.

The resistance of the electrodes as seen from table 1.9 using 2-NPOE plasticiser is low and well within the order of magnitude characteristic to these electrodes (~ 1 M). The resistance decreases according to the amount of KpTCPB added.

1.9.2.2.2.1 Optimisation of the ISE Membrane

When a polymeric ion-selective membrane is prepared, the type and amount of the polymer matrix, the membrane solvent (plasticiser) and the ligand must be chosen so as to produce to best possible electrode response. As described in section 1.5.2.1 PVC is the most suitable polymer for membrane purposes.

With regard to the membrane plasticiser, 2-NPOE, DOS, DPP, PP were investigated. The membranes contained approximately 1 % ionophore and 50 % mol

ratio of KtPCPB relative to ionophore. Membranes based on 2-NPOE plasticiser without the ion-exchanger were also investigated.

1.9.2.2.2 Membrane Response

The results of electrode slope function measured in NaCl solutions ranging from 1×10^{-7} M to 1×10^{-1} M prepared by serial dilution and measured at $25 \pm 1^\circ\text{C}$ are shown in table 1.10, together with other data i.e. resistance, drift and detection limit.

Electrodes based in 2-NPOE and DOS plasticiser provided Nernstian responses (59.7 and 60.3 mV dec. $^{-1}$, respectively) in the sodium range 3×10^{-5} to 1×10^{-1} M, while those electrodes based in dioctyl phenyl phosphonate and 2-NPOE without KpTCPB showed only near-Nernstian responses (57.9 and 53.6 mV dec. $^{-1}$, respectively) in the 1×10^{-4} to 1×10^{-1} M range. The membranes based in phenyl phthalate were sub-Nernstian (31 mV dec. $^{-1}$) and therefore they were not considered for further examination.

Plasticiser	KpTCPB	Slope	Resistance	Detection	Drift
	50% mol	mV/Dec	M Ω	limit/M	mV/h
2-NPOE	0	57.9	5.3	2.8×10^{-6}	+ 2.1
2-NPOE	50	59.7	1.3	2.3×10^{-6}	+ 0.1
DOS	50	60.3	57.8	3.1×10^{-6}	+ 3.0
DPP	50	53.6	3.4	8.7×10^{-5}	+ 0.4
PP	50	~31	10.3	_____	_____

Table 1.10 Electrode function, resistance, detection limits and drift of catheter sodium electrodes incorporating the methyl tetraketone derivative as ionophore in different membrane solvents.

The resistance measurements conducted in 0.1 M NaCl in freshly constructed electrodes and maintained in 0.1 M NaCl for 24 hours (Table 1.10) indicated that the lowest resistances are found using 2-NPOE as membrane solvent, and as indicated above, the incorporation of ion-exchanger decreases the resistance. The more lipophilic membrane solvent DOS exhibits a resistance ($57.8 \text{ M}\Omega$) which is comparatively 50 times higher than the membranes incorporating 2-NPOE ($1.3 \text{ M}\Omega$). The high resistance found for the DOS based membranes resulted in noisy signals, particularly at low concentration levels.

The membranes containing DOS plasticiser also exhibited the largest drift when this parameter was examined in 0.1 M NaCl solutions (thermostatted cell at 25°C). A monotonous positive drift that amounted as much as 3 mV per hour was found for the DOS based electrodes, while values of only 0.1 mV and 2.1 mV per hour were found for the 2-NPOE electrodes, with and without ion exchanger respectively. Although the drift exhibited by the DOS based membranes was rather significant, it was shown to have a constant profile against time when assessed at 4 different concentrations i.e. 10^{-1} , 10^{-2} , 10^{-3} and 10^{-4} M NaCl solutions. Nevertheless the fact that the drift is fairly constant allows the possibility of correction, thus permitting measurements to be carried out without need for frequent recalibration of the electrodes.

1.9.2.2.2.3 Injection Experiments

Following the same procedure outlined previously for the methyl calix[4] arene ester derivative injection experiments were carried out. In this occasion the response curves to injections of alkali and alkaline earth metal ions were observed via BBC microcomputer and the magnitude of the change

in potential to the step change in concentration followed using pH meter. Figure 1.15 shows a large jump in potential for sodium ions which remains constant with time. The response is achieved rapidly within a few seconds. The response for the rest of group I ions is minimal and no larger than 5 mV in all instances at most. The response to alkaline earth metal ions and hydrogen ions however show a rapid large transient response followed by a decrease with time to the initial baseline value in the case of calcium and magnesium. Especially important is the magnitude in the change of potential exhibited by hydrogen ions. This in fact gives a response which is comparable to that of sodium ions, decreasing only slightly after a few minutes. The selectivity against hydrogen is examined in the next section.

1.9.2.2.4 Determination of Selectivity Coefficients

The selectivity coefficients for the methyl tetraketone calix[4]arene membrane containing different solvent mediators were measured according to the procedure described in section 1.9.2.1.3 for the methyl ester derivative in 0.1 M solutions of alkali and alkaline earth metal ions by the separate solution method. For electrodes containing 2-NPOE plasticiser with ion-exchanger, the mixed solution method was also employed. Here the procedure was to add a constant level of interfering ion i.e. 1×10^{-3} M, to NaCl solutions ranging from 1×10^{-6} M to 1×10^{-1} M. To evaluate the interference of hydrogen ions on the electrode response of 2-NPOE membranes with KpTCPB, the selectivity was determined by varying the pH of solutions with a fixed background of primary ion (i.e. 10^{-2} and 10^{-3} M NaCl). These solutions were adjusted to pH 10.5 with ammonia solution (ca. 1 M) and the pH subsequently varied according to the desired value by adding concentrated HCl. In another

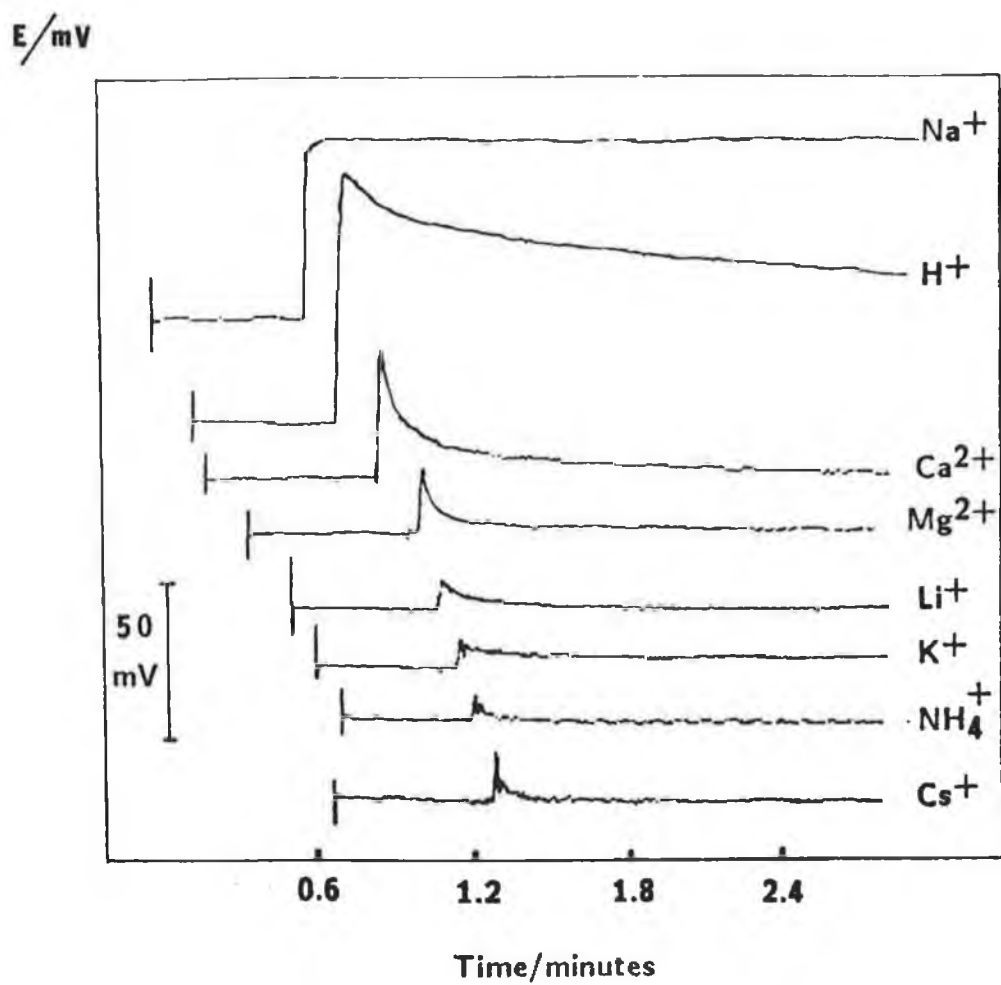


Fig. 1.15 Transient response of catheter electrodes based on methyl tetraketone ionophore to a 10-fold increase in sodium concentration (10^{-4} - 10^{-3}).

Selectivity Coefficients							
$\log K_{ij}^{\text{pot}}$							
Plasticiser	KpTCPB	K ⁺	Li ⁺	NH ₄ ⁺	Cs ⁺	Mg ²⁺⁺	Ca ²⁺
2-NPOE	0	-2.44	-2.37	-3.32	-3.57	-2.10	-2.59
2-NPOE	50	-2.44	-2.46	-3.50	-3.81	-2.18	-2.63
DOS	50	-2.42	-2.46	-3.37	-3.60	-2.22	-2.57
DPP	50	-1.49	-0.54	-0.49	-1.92	-2.02	-2.32

Table 1.11 Selectivity coefficients as performed by SSM in 0.1 M solutions.

experiment, sodium calibration curves (10^{-6} M to 10^{-1} M) were prepared in different acidic media (i.e HCl pH = 2; phthalate buffers pH = 3 and 4; tris buffer pH = 7 and 8) and the sodium electrode function measured in the 10^{-4} - 10^{-1} M range.

From the results summarised in table 1.11 it can be seen that the incorporation of different solvent mediators in the membrane composition resulted in no drastic changes in those membranes containing 2-NPOE and DOS plasticiser, whereas the membranes plasticised with DPP exhibited a large decrease in selectivity for all the alkali ions. The incorporation of the ion exchanger did not show any marked influence on electrode selectivity when it was present in a 50 % mol ratio with respect to the ionophore. With the exception of DPP based electrodes, a high selectivity for all the ions tested was generally obtained and compared favourably with selectivities previously

obtained for the methyl ester calixarene electrode (see Table 1.5).

The results from the mixed solution method indicated close agreement with the SSM for the ions tested i.e. K^+ , Li^+ and Ca^{2+} . Typical results in all cases originated selectivity coefficients of the same order of magnitude i.e. $\log K_{ij}^{pot} < -2$.

The selectivity against hydrogen assessed by the mixed solution method showed little influence of pH over the range 10.5 - 5.0. Typical results reflected an emf change no larger than 1.0 mV in both 10^{-2} M and 10^{-3} M NaCl solutions over this pH range. The electrode slope function was however lost at pH values lower than 4, due to the high levels of hydrogen activity.

1.9.2.2.5 Life Time

The operative life time of the electrodes based on different solvent mediators was studied by measuring periodically the electrode slope in 10^{-4} to 10^{-1} M NaCl solutions and measuring the resistance in 0.1 M NaCl. The investigation was carried out for approximately four months and all electrodes were stored in a 0.1 M NaCl solution between tests.

The results (shown in Fig. 1.16a and 1.16b) indicate that life times over 4 months could be expected for those electrodes based on DOS and 2-NPOE plasticisers. This is shown by the small variation in electrode slope exhibited in aqueous solutions during this period of time. The presence or absence of KpTCPB in the 2-NPOE based electrodes seemed to have little if any influence on the life time of the electrodes. The absence of ion exchanger in the 2-NPOE membrane did however produced a faster increase in membrane resistance, with values approaching 20 M Ω at the end of four months, while values of only around 3 M Ω were typical of the membranes with ion-exchanger at

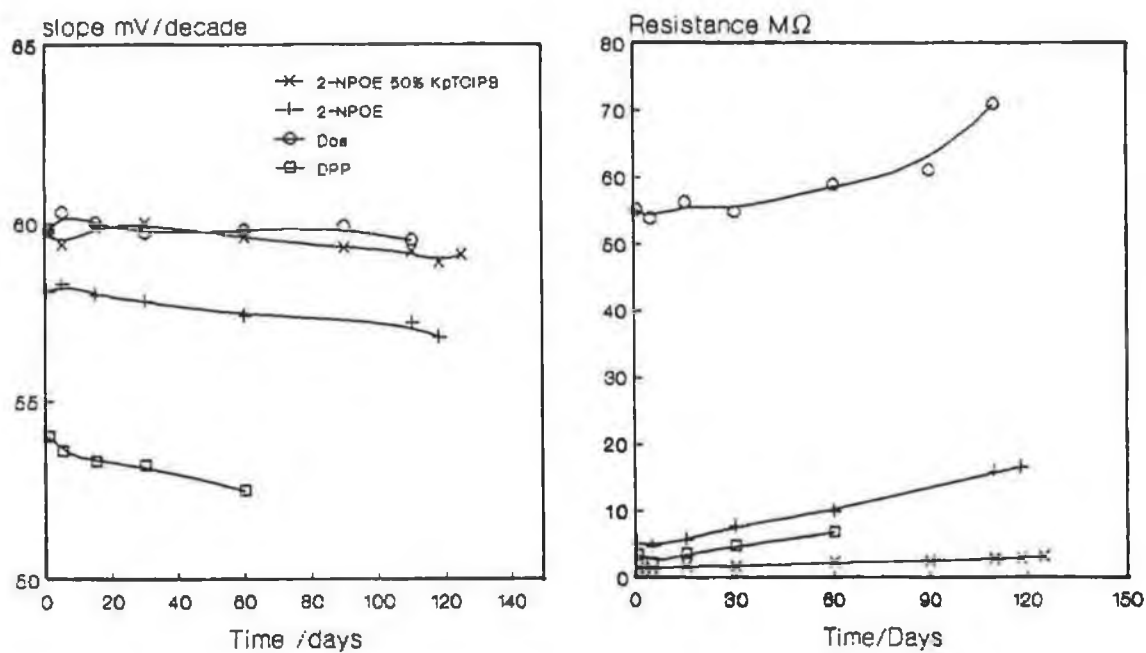


Fig. 1.16 Electrode function (a), and resistance (b) for methyl tetraketone calix[4]arene electrodes as measured over a period of four months. Symbols in (a) indicate membrane composition.

the end of the same period. However an even more noticeable increase in resistance ($70 \text{ M } \Omega$) and a general deterioration in the stability of the electrodes based in DOS plasticiser was observed at the end of the trial period. Although the electrode slope with this plasticiser is not affected to any extent, the rather high instability of the electrode poses limitations in its use. A limited performance was also apparent with the DPP based electrodes. The sub-Nernstian slope of this electrode rapidly deteriorated within the first two months and the resistance increased. Evidently, the type of sample being analysed will dictate finally the operative life time of an electrode. Thus for instance, in biological fluids the non-water fraction represented by a high content of proteins and lipids will enhance the solubility of lipophilic membrane components in the aqueous phase and reduce the electrode life time. It would then be expected that more lipophilic membrane components such as DOS plasticiser would give a more extended life time than those membranes incorporating the 2-NPOE mediator.

1.9.2.2.3 Coated Wire Electrodes (CWEs)

CWEs differ from ISEs, in that the ion-selective PVC membrane is formed directly over a solid conducting substrate (usually metallic), and therefore lack the internal reference solution of the ISE. This makes fabrication simpler, but the lack of a stable inner boundary potential can cause problems. As the PVC membranes employed are identical to those used in ISEs, a brief study of the effectiveness of calixarene-based CWEs was carried out.

1.9.2.2.3.1 Electrode Response

Batches of electrodes based on methyl tetraketone calix[4]arene were prepared according to the construction procedure outlined in section 1.8.4.4. Typically, membranes contained: ionophore, 2-NPOE solvent mediator, KpTCPB ion-exchanger and PVC, the composition of which was the one already outlined (1.8.3).

The electrode response was assessed in NaCl solutions ranging from 1×10^{-4} M to 10^{-1} M using a thermostatted cell at $25 \pm 0.5^\circ\text{C}$. The response was Nernstian and linear over the range of concentrations assayed. The electrode response over a 3 hour period for one of the electrodes constructed are shown in table 1.12.

The results obtained with this electrode are similar to those obtained with several CWEs. The CWEs were found to be generally less stable than the corresponding ISEs (see Table 1.12). In fact, when placed in contact with a solution the electrodes show a clear tendency to drift to negative values with magnitudes of around 2 mV over a 3 minute period. However this drift is relatively constant, as evidenced by the high regression coefficient obtained in every instance. There does seem to be a slight tendency for the electrode to drift more at lower concentration levels, leading to a progressive decrease in the slope with time.

The resistance for 3 of the newly constructed electrodes in 0.1 M NaCl gave values slightly lower than those found for catheter type electrodes based on the same membrane composition (i.e. 0.76, 0.86 and 1.04 M Ω average of 5 measurements in each case).

Another batch of electrodes prepared separately during this investigation gave conflicting results. These electrodes showed slope values

Electrode Response (mV)						
[Na ⁺]/M	30s	60s	90s	120s	150s	(Hour)
1x10 ⁻⁴	315.2	315.1	315.3	315.7	316.5	First
1x10 ⁻³	378.8	377.6	377.2	377.1	377.3	
1x10 ⁻²	439.4	437.7	437.0	436.8	436.6	
1x10 ⁻¹	497.3	495.8	495.2	494.9	494.7	
slope	60.7	60.2	60.0	59.7	59.4	
r	.9998	.9999	.9999	.9999	.9999	Second
1x10 ⁻⁴	318.9	318.3	318.3	318.5	319.0	
1x10 ⁻³	380.4	379.1	378.6	378.4	378.3	
1x10 ⁻²	440.5	438.7	438.1	437.8	437.5	
1x10 ⁻¹	497.7	496.3	495.7	495.4	495.2	
slope	59.7	59.4	59.2	59.0	58.8	Third
r	.9999	.9999	.9999	.9999	.9999	
1x10 ⁻⁴	322.6	321.2	320.4	319.9	319.5	
1x10 ⁻³	380.6	379.3	378.8	378.5	378.3	
1x10 ⁻²	439.7	438.2	437.7	437.4	437.1	
1x10 ⁻¹	497.8		495.0		494.7	
slope	58.5		58.3		58.4	
r	.9999		.9999		.9999	

Table 1.12 Coated wire electrode response during a three hour period measurement.

ranging from 52.0 mV to 60.3 mV. Although no systematic study was carried out on these electrodes, it is believed that variations in the number of coating layers arising from the manual procedure was the cause for slope fluctuations. This problem has been reported by some workers who have found that an optimisation in the number of layers is necessary for best electrode performance [29]. In fact to build a reproducible and uniform layer over the metal surface of the electrode (which was the problem faced here), the electrode should preferably be held by a laboratory clamp and the consistency of the membrane cocktail should be such as to minimise drop formation at the tip of the wire.

1.9.2.2.3.2 Selectivity Coefficients

The selectivity coefficients for the CWE were calculated by the separate solution method classically in 0.1 M solutions of alkali and alkaline earth metal ions. The measuring procedure was that outlined in section 1.9.2.1.3 and measurements were taken at three minutes after immersion in the solution. The results are the average of 2 electrodes presenting slopes of 58.9 and 59.2 mV/decade in sodium activity.

The selectivity coefficients obtained (Table 1.13) show the pattern similar to that of the corresponding ISEs with little or no variation as a result of the CWE. Thus the selectivity obtained for the CWEs confirms the selectivity data previously presented for the methyl tetraketone calix[4]arene electrode.

1.9.3 POLYMERIC CALIXARENE COMPOUNDS

Traditionally and as performed so far in the course of this

<u>IONS</u>	$\log K_{Na,j}^{pot}$		
	<u>Methyl Tetraketone</u>		<u>Methyl Ester</u>
	Catheter Electrode	CWE	Catheter Electrode
K ⁺	-2.44	-2.08	-2.47
Li ⁺	-2.46	-2.44	-2.78
NH ₄	-3.50	-3.36	-2.74
Cs ⁺	-3.81	-----	-1.51
Ca ⁺⁺	-2.63	-2.59	-3.74
Mg ⁺⁺	-2.18	-2.12	-3.12

Table 1.13 Selectivity data for catheter type and coated wire electrodes based on methyl tetraketone derivative of calix[4]arene. Methyl ester p-t-butylcalix[4]aryl acetate ionophore is also included for comparison

investigation, ISEs incorporating solvent polymeric matrices require that the ionophoric compound be dissolved in an involatile non-polar solvent and the resulting solution subsequently entrapped in PVC.

One important disadvantage of this approach is that the ionophoric material, plasticiser and ion-exchanger can leach out of the PVC matrix into the sample solution thus limiting the life time of the electrode. This becomes especially problematic in flowing systems as well as in the already mentioned biological fluids due to the the high lipophilicity of the sample.

Currently there is a growing interest in developing solid state electrodes and special attention is being given to covalently bound sensing compounds which can also adhere to different electrode substrates. The asymmetric membranes so developed should lead to the development of cheap disposable sensors which can be mass produced.

This experimental section examines briefly some characteristics of monomeric and polymeric calixarene structures when incorporated in ISEs.

1.9.3.1 Monomers I and II

1.9.3.1.1 Copolymerisation

Copolymers were prepared according to the procedure already described in section 1.8.2 and were subsequently examined by UV, IR and NMR techniques. The resulting information obtained is described below:

Ultra-Violet Spectra: Spectra of all materials including monomer I, methyl methacrylate and prepared copolymer showed the same characteristics over the wavelength range 190-700nm. Samples were dissolved in toluene and run against a toluene blank. Maximum absorption occurred at 280nm (for spectroscopic data, refer to Appendix).

Infra-Red Spectra: All samples were run as potassium bromide discs. The carbon-carbon double bond is normally observed at a frequency of ca. 1630 cm^{-1} . As expected, both monomers showed noticeable bands in this region. However, the copolymers also showed a slight absorption, thus indicating that the polymerisation reaction may not have gone to completion and some amount of unreacted monomer was still present. This was checked by thin layer chromatography (TLC) using a mobile phase of 70:30 petroleum ether:ethyl acetate, with the samples dissolved in toluene. No detectable monomer was observed in the copolymer (see appendix).

Nuclear Magnetic Resonance Spectra: Samples were dissolved in either deuterated chloroform or dimethyl sulfoxide(DMSO) containing tetramethylsilane marker. DMSO itself exhibits 2 absorption bands at 2.5 and 3.3 ppm. Methyl methacrylate yielded the simplest NMR spectra with the following absorption bands: 1.9ppm($-\text{CH}_3$), 3.7ppm($-\text{OCH}_3$) and 5.5-6ppm(vinyl protons). The latter are indicative of the presence of double bonds in the sample. Monomer I presented the same bands plus some additional features. The large broad peak at the start of the spectra correspond to the tertiary butyl groups of the monomer, the peaks at 6.8ppm are indicative of aromaticity while the bands at 4-5ppm may possibly be due to the CH_2 groups.

Thus, the copolymer spectra had all the above features except that there was no evidence of the presence of vinyl protons, thus implying that the quantity of monomer present in the copolymer was very small.

The analytical techniques used here do not offer any conclusive evidence about the structure or nature of the copolymer. Hence additional information such as molecular weight, nature of copolymer (e.g. block, alternating, random) and the relative reactivities of each monomer are necessary in order to

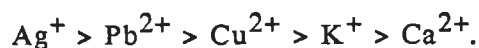
optimise the conditions for preparation and characterisation of the polymers. However no further investigation was carried out in relation to characterisation of the copolymers and the products so obtained were at this stage considered suitable for incorporation in ISEs.

1.9.3.1.2 Picrate Extraction

Previous to preparation of the corresponding ISE membranes, picrate extraction experiments were carried out on these copolymers to assess the possible extraction capabilities. However, since it was not feasible to prepare a definite concentration of copolymer in the organic phase, it was not possible to carry out detailed extraction studies.

For the picrate extraction experiments approximately 3 mg of copolymer was dissolved in dichloromethane and aqueous solutions of available picrate salts (Ag^+ , K^+ , Ca^{2+} , Pb^{2+} , Cu^{2+}) were prepared so that the final concentration was 2.5×10^{-4} M. Subsequently, 5 ml of the dichloromethane solution containing the copolymer were shaken with 5 ml of the picrate salt solution for 3 minutes and the relative extraction of metal picrates into the organic phase was determined by measuring the increase in absorbance of the dichloromethane at 380 nm.

The results obtained showed extraction capabilities in the order:



1.9.3.1.3 Membranes

Previous to membrane preparation the solubility of the copolymers was tested in toluene, dichloromethane and different plasticisers (2-NPOE, DOS,

DPP, PP). The results of these solubility tests showed that the copolymers were insoluble in all of the plasticisers attempted and only soluble in dichloromethane and toluene. Toluene was chosen as the membrane solvent and the membranes cast using a dipping technique similar to that described in section 1.8.3 without incorporating ion-exchanger. Catheter type (internal filling solution 0.01 M KCl) and coated wire ISEs were prepared and preconditioned in water for one hour previous to measurements. (see results and discussion).

1.9.3.1.4 Photopolymerisation

The photopolymerisation of monomers I and II was carried out directly on glassy carbon electrode surface according to the procedure described in section 1.8.4.5. Once the photopolymerisation was achieved, the glassy carbon electrodes were soaked in milli-Q water for about 30 minutes previous to measurements.

1.9.3.2 Polymers IV, V and Monomer VI

These ionophores were incorporated in typical solvent polymeric membranes described in section 1.8.3 with the exception that they did not contain ion-exchanger. The membranes were tested in either catheter type or coated wire electrodes. The internal reference electrolyte of catheter type electrodes was 0.1 M of the primary ion being investigated.

1.9.3.3 RESULTS AND DISCUSSION

The properties of electrodes incorporating the copolymerised materials polymers and monomer VI were evaluated by the slope and linear range

of calibration curves. Calibration curves for Na^+ , K^+ , Li^+ , NH_4^+ , Ca^{2+} , Mg^{2+} , Cs^+ (all chloride salts) over the range 10^{-4} M to 10^{-1} M were measured.

The results (Table 1.14) indicated that the only trend obtained for glassy carbon electrodes with the photopolymerised materials was a sub-Nernstian response to sodium ions (slope 37 mV) with monomer I. A major difficulty with the experimental setup used was trying to ensure reproducibility of the membrane surface from one batch to the next. The electrodes were conditioned prior to use in milli-Q water, which was found to be a suitable conditioning medium. Conditioning in salt solutions tended to impart memory effects to the electrodes.

Electrode	Ionophore	Slope (mV/decade)	Ion	Resistance $\text{M}\Omega$
Glassy C	I	37	(Na^+)	0.88
Pt CW	IV	45	(K^+)	2.03
Pt CW	IV	54	(Cs^+)	1.92
Mini-ISE	V	47	(Na^+)	2.43
Mini-ISE	IV	54	(Cs^+)	2.30
Mini-ISE	VI	55	(K^+)	1.98

Table 1.14 Electrode function and resistance measurements of some polymeric and monomeric calixarene structures investigated

Response to other ions followed no set patterns, but gave steady readings, as would be expected from a low resistance membrane (typically 0.88 M Ω). The sodium responses obtained were irreproducible.

Equally disappointing were the results obtained with copolymers. The attempt to chemically modify the monomers by copolymerisation was successful but on incorporation of the compounds into catheter type and coated wire electrodes, no responses were obtained. In the case of copolymer I, this lack of response might be attributed to the excess activity around the binding sites (contains 4 unsaturated groups / monomer) thus giving rise to a highly branched polymer. Copolymer based on monomer II showed also no response. The membrane resistances in this case were so large (not measurable) with extreme drift, that the results obtained were completely irreproducible.

Polymer materials incorporated either in catheter type or coated wire electrodes showed promising results. Thus polymer IV exhibited near-Nernstian responses to Cs⁺ ions and consistently gave slopes of 45 mV/decade for K⁺ ions over the range of concentrations assayed. The same polymer showed also some response to NH₄⁺ ions which was evidenced by reproducible changes of about 100 mV over the concentration range. The slopes obtained were reproducible and the resistance measurements gave typical values around 2 M Ω .

The results obtained for the mixture of polymer I/monomer I (50 :50) indicated a sub-nerstian slope to Na⁺ of 47 mV/decade for the same range of concentrations. The triplicated measurement over a three hour period produced in fact very stable readings with low resistance values. Although no further investigation of these compounds was made it would be reasonable to assume at this stage that the pure polymeric form of III may yield electrodes with enhanced performance for sodium ions.

The results of coated wire electrodes with monomer VI gave a near-Nernstian behaviour of 55 mV/decade for potassium ions.

1.10 CONCLUSIONS

In this research, several types of ion-selective electrodes incorporating neutral carriers as sensing agents have been constructed. Glass pipette, catheter type and conventional macroelectrodes were suitable for the analytical purposes intended. The electrodes are simple to construct, provided reliable results and the cost associated to their construction is minimal. The advantage of glass glass pipette electrodes is that they can be used to assess rapidly the general performance of a new compound. The electrode however is very fragile and if extreme care is not taken the results, are subject to variations due to irreproducibility of the tip surface.

Caesium electrodes were studied and the results indicated that the best electrode is that based on the hexaethyl derivative incorporating 1:4 ligand ion exchanger in a 2-NPOE plasticised membrane. Both electrodes investigated gave rapid responses to changes in concentration with near-Nernstian behaviour and very favourable selectivities against common interferents.

Tetrameric ligands sensitive to sodium ions were incorporated in ISEs. Methyl p-t-butylcalix[4]aryl acetate and methyl tetraketone calix[4]arene both exhibited Nernstian responses and a linear range between 3×10^{-5} to 1×10^{-1} M NaCl. The methyl ester derivative showed response times of less than 5 seconds and the selectivity coefficient data was comparable to the sodium glass electrode but with better discrimination against hydrogen ions. Generally the selectivity against other interfering ions was superior to other neutral carrier based ion-selective electrodes presently available. The

electrode based in this ligand possessed good stability and reproducibility especially when the change in concentration was towards increasing concentrations. The life time of the electrode in pure NaCl solutions indicated that the electrode remained functional for at least one month during which the membrane resistance was slightly over 1 M . More extensive work on life time previously reported has however indicated that the life time of the electrode goes beyond 5 months [100].

The methyl tetraketone calix[4]arene based ISE behaved comparably well, but seemed to be even more stable than the methyl ester tetrameric calixarene. The incorporation of ion-exchanger (KpTCPB 50 % mol ratio with respect to ionophore) in the 2-NPOE plasticised membranes markedly influenced characteristics such as slope, resistance and general stability, although the selectivity was not improved by the addition. DOS based membranes also showed excellent results, although the resistances exhibited with this membrane solvent were higher and the drift of the electrode was extensive. The use of dioctyl phenyl phosphonate did not produce any improvement in electrode behaviour. The slopes were near-Nernstian and the selectivity coefficients were much lower. The selectivity exhibited by electrodes incorporating 2-NPOE and DOS was similar. Good discrimination against interferents was indicated by the separate solution method and confirmed by the mixed interferent method in the case of the 2-NPOE plasticised membrane. Selectivity data from the methyl tetraketone derivative were improved for caesium and ammonium ions in comparison to the methyl ester derivative, but showed a decrease for calcium and magnesium. The selectivity against that of potassium and lithium remained unchanged. Interference due to hydrogen ions for both the methyl ester and the methyl tetraketone based electrodes was negligible over a wide range of pH when

measured at steady state values in 10^{-2} and 10^{-3} M NaCl solutions.

The desire to miniaturise, simplify and produce less expensive ion-selective electrodes has drawn a lot of attention to the field of membranes based on solid-state configuration. Accordingly, coated wire electrodes incorporating the methyl tetraketone calix[4]arene ionophore were prepared. These electrodes exhibited Nernstian responses and low resistance but generally they proved inferior to the conventional sort with respect to drift and reproducibility. The selectivity data encountered with these electrodes was however in accordance with the catheter type electrodes.

Coated wire electrodes may have potential for the future development of miniaturised sensors such as ChemFETs, since such devices also contain these asymmetrically arranged membranes.

Coated wire electrodes incorporating polymers IV and V showed some promise. Of special interest was polymer IV which exhibited a near-Nernstian response to caesium, while also exhibiting some response to potassium ions. Polymer V (which was actually a mixture of monomer I and polymer I) gave consistent slightly sub-Nernstian responses to sodium ions. The fact that the ionophore material is not pure suggests that the response can be improved if polymeric forms of monomer I are introduced in ISEs.

The copolymerisation of monomer I and II was achieved but on introduction of the resulting materials into ISEs no responses were obtained. Generally the responses were very unstable and irreproducible. The same applied to photopolymerisation of the same compounds on glassy carbon electrode surfaces. Here the reproducibility of the methodology employed was probably a major drawback in obtaining functioning membranes. However, these are only preliminary results in a new and complex area, and more detailed investigations

into the development of solid-state devices based on polymerisable calixarenes will follow.

The introduction of a new calixarene monomer (monomerVI) into coated wire electrodes provided a near-Nernstian slope for potassium ions and also exhibited low resistance. The response obtained by monomer VI confirms that a new range of compounds could probably be developed by focusing on the chemical modification of the methylene bridging groups.

1.11 REFERENCES

1. Solsky, R.L., Anal. Chem., 1988, 60, 106R.
2. Koryta, J., Anal. Chim. Acta, 1988, 206, 1.
3. Moody, G.J. and Thomas, J.D.R., Ion-Sel. Electrode Rev., 1986, 8(2), 209.
4. Cremer, M., Z. Biol., 1906, 47, 562.
5. Haber, F. and Klemensiewicz, Z., Z. Phys. Chem., 1909, 67, 385.
6. Nicolsky, B.P., Zh. Fiz. Khim., 1937, 10, 495.
7. Karrenman, G. and Eisenman, G., Bull. Math. Biophys., 1962, 24, 413.
8. Stephanova, O.K., Shultz, M.M., Materova, E.A. and Nicolsky, B.P., Vestn. Leningrad, Univ., 1963, 4, 93.
9. Stefanac, Z. and Simon, W., Chimia (Switzerland), 1966, 20, 436.
10. Stefanac, Z. and Simon, W., Microchem. J., 1967, 12, 125.
11. Arnold, M.A. and Solsky, R.L., Anal. Chem., 1986, 58, 84R.
12. Havas, J., Ion-and Molecule-Selective Electrodes in Biological Systems, Springer-Verlag, Berlin, 1985.
13. Collison, M.E. and Meyerhoff, M.E., Anal. Chem., 1990, 62, Report.
14. Ammann, D., Ion-Selective Microelectrodes, Principles, Design and Application, Springer-Verlag, Berlin, 1986.
15. Beebe, K., Uerz, D., Sandifer, J. and Kowalski, B., Anal. Chem. 1988, 60, 66.
16. Nernst, W., Z. Phys. Chem., 1888, 2, 613.
17. Nernst, W., Z. Phys. Chem., 1889, 4, 129.
18. Plank, M. Ann. Phys. Chem., 1890, 39, 161.
19. Plank, M. Ann. Phys. Chem., 1890, 40, 561.
20. Henderson, P., Z. Phys. Chem., 1907, 59, 118.

21. Henderson, P., Z. Phys. Chem., 1908, 63, 325.
22. Morf, W.E., Anal. Chem., 1977, 49, 810.
23. Moody, G.J. and Thomas, J.D.R., Selective Ion Sensitive Electrodes, Merrow, Watford UK, 1971.
24. Hulanicki, A. and Augustowska, Z., Anal. Chim. Acta, 1975, 78, 261.
25. Gadzekpo, V.P.Y. and Christian, G.D., Anal. Chim. Acta, 1984, 164, 279
- 26.. Moore, C. and Pressman, Biochem. Biophys. Res. Commun., 1964, 15, 562.
27. Koryta, J., Anal. Chim. Acta, 1977, 91, 1.
28. Pendersen, C.J., J. Am. Chem. Soc., 1967, 89, 7017.
29. Tamura, H., Kimura, K. and Shono, T., Anal. Chem., 1982, 54, 1224.
30. Kimura, K., Oishi, H., Miura, T. and Shono, T., Anal. Chem., 1987, 59, 2331.
31. Assubaie, F.N., Moody, G.J. and Thomas J.D.R., Analyst, 1988, 113, 61.
32. Moody, G.J., Owusu, R.K. and Thomas, J.D.R., Analyst, 1988, 113, 65.
33. Beer, P.D., in "Chemical Sensors", Edmonds, T.E. (ed.), Blackie, Chapman and Hall, New York, 1988, p. 18.
34. Morf, W.E. and Simon, W., in "Ion Selective Electrodes in Analytical Chemistry", Freiser, H. (ed.), Plenum Press, 1978, Vol. 1, p. 211.
35. Ammann, D., Pretsch, E. and Simon, W., Tetrahedron. Lett., 1972, 2473.
36. Ammann, D., Pretsch, E. and Simon, W., Helv. Chim. Acta., 1973, 56, 1780.
37. Ammann, D., Bissig, R., Cimerman, Z., Fiedler, U., Guggi, M., Morf, W.E., Oehme, M., Osswald, H., Pretsch, E. and Simon, W., in "Proceedings of the International Workshop on Ion Selective Electrodes and on Enzyme Electrodes in Biology and Medicine", Urban & Schwarzenberg, Munich-Berlin-Vienna, 1976, p. 22.
38. Oesch, U. and Simon, W., Anal. Chem., 1980, 52, 692.

39. Ammann, D., Morf, W.E., Anker, P., Meier, P.C., Pretsch, E. and Simon, W., *Ion-Sel. Electrode Rev.*, 1983, 5, 3.
40. Moody, G.J. and Thomas, J.D.R., in reference 34, p. 287..
41. Buck, R.P., *Sens. Actuators*, 1981, 1, 197.
42. Stefanova, O.K. and Shultz, M.M., in "Progress in Surface and Membrane Science", Cadenhead, D.A. and Danielli, J.F. (eds.), Academic Press, New York, 1981, Vol. 14, p. 131.
43. Horvai, G., Toth, K. and Pungor, E., *Anal. Chim. Acta*, 1989, 216, 163.
44. Koryta, J., *Anal. Chim. Acta*, 1982, 139, 1.
45. Shijo, Y., *Bull. Chem. Soc. Jpn.*, 1975, 48, 1647.
46. Hassan, S.K.A., Moody, G.J. and Thomas, J.D.R., *Analyst*, 1980, 105, 147.
47. Fiedler, U. and Ruzicka, J., *Anal. Chim. Acta*, 1973, 67, 179.
48. Schafer, O.F., *Anal. Chim. Acta*, 1976, 87, 495.
49. Moody, G.J., Oke, R.B. and Thomas, J.D.R., *Analyst*, 1970, 95, 910.
50. Pick, J., Toth, K., Pungor, E., Vasek, M. and Simon, W., *Anal. Chim. Acta*, 1973, 64, 477.
51. Ma, S.C., Chaniotakis, N.A. and Meyerhoff, M.E., *Anal. Chem.*, 1988, 60, 2293.
52. Griffiths, G.H., Moody, G.J. and Thomas, J.D.R., *Analyst*, 1972, 97, 420.
53. Buck, R.P., *Ion-Sel. Electrode Rev.*, 1982, 4, 3.
54. Simon, W., Morf, W.E. and Meier, P.C., in "Structure and Bonding", Dunitz, J.D., Hemmerich, P., Ibers, J.A., Jorgensen, C.K., Neilands, J.B., Nyholm, R.S., Reinen, D. and Williams, R.J.P., (eds.), Vol. 16, Springer-Verlag, Berlin, 1973, p. 113.
55. Bluoën, S., Dale, J. and Lund, W., *Anal. Chim. Acta*, 1986, 185, 347.
56. Ammann, D., Pretsch, E., Simon, W., Lindner, E., Bezegh, A. and Pungor,

- E., *Anal. Chim. Acta*, 1985, 171, 119.
57. Morf, W.E., *The Principle of Ion-Selective and of Membrane Transport*, Akademiai Kiado, Budapest, 1981.
 58. Imato, T., Katahira, M. and Ishibashi, N., *Anal. Chim. Acta.*, 1984, 165, 285.
 59. Okada, T., Hiratani, K. and Sugihara, H., *Analyst*, 1987, 112, 587.
 60. Moody, G.J., Saad, B.B. and Thomas, J.D.R., *Analyst*, 1989, 114, 15.
 61. Meier, P.C., Morf, W.E., Laubli, M. and Simon, W., *Anal. Chim. Acta*, 1984, 156, 1.
 62. Pretsch, E., Wegmann, D., Ammann, D., Bezegh, A., Dinten, O., Laubli, M.W., Morf, W.E., Oesch, U., Sugahara, K., Weiss, H. and Simon, W., in "Recent Advances in the Theory and Application of Ion-Selective Electrodes in Physiology and Medicine, Kessler, M., Harrison, D.K. and Hoper, J., (eds.), Springer-Verlag, Berlin, 1985.
 63. Thomas, J.D.R., in "Ion-Selective Electrodes", Pungor, E., (ed), Akademiai, Kiado, Budapest, 1978, p. 175.
 64. Meyerhoff, M.E. and Kovach, P.M., *J. Chem. Educ.* 1983, 60, 766.
 65. Brown, H.M., Pemberton, J.P. and Owen, J.D., *Anal. Chim. Acta*, 1976, 85, 261.
 66. Shatkay, A., *Anal. Chem.*, 1976, 48, 1039.
 67. Buck, R.P., *Anal. Chem.*, 1976, 48, 23.
 68. Lindner, E., Toth, K. and Pungor, E., *Dynamic Characteristics of Ion-Selective Electrodes*, CRC Press, Boca Raton, Florida, 1988.
 69. Oehme, M. and Simon, W., *Anal. Chim. Acta*, 1976, 86, 21.
 70. Buck, R.P., *Ion Sel. Electrode Rev.*, 1982, 4, 3.
 71. Morf, W.E., Lindner, E. and Simon, W., *Anal. Chem.*, 1975, 47, 1596.

72. Markovic, P.L. and Osburn, J.O., *AIChE J.*, 1973, 19, 504.
73. Lindner, E., Toth, K. and Pungor, E., *Anal. Chem.*, 1976, 48, 1071.
74. Morf, W.E. and Simon, W., in reference 34, p. 259.
75. Lindner, E., Toth, K., Pungor, E., Berube, T. and Buck, R.P., *Anal. Chem.*, 1987, 59, 2213.
76. Lindner, E., Toth, K. and Pungor, E., *Anal. Chem.*, 1982, 54, 202.
77. Lindner, E., Toth, K., Pungor, E., Morf, W.E. and Simon, W., *Anal. Chem.*, 1978, 50, 1627.
78. Uemasu, I. and Umezawa, Y., *Anal. Chem.* 1982, 54, 1198.
79. Lindner, E., Toth, K., Pungor, E. and Umezawa, Y., *Anal. Chem.*, 1984, 56, 808.
80. Ammann, D., Morf, W.E., Anker, P., Meier, P.C., Pretsch, E. and Simon, W., *Ion Selec Electrode Rev.* 1983, 5, 3.
81. Morf, W.E., Whurmann, P. and Simon, W., *Anal. Chem.*, 1976, 48, 1031.
82. Oesch, U. and Simon, W., *Anal. Chem.*, 1980, 52, 692.
83. Arnaud-Neu, F., Collins, E., Deasy, M., Ferguson, G., Harris, S., Kaitner, B., Lough, A.J., McKervey, M., Marques, E., Ruhl, B.L. Schwing-Weill, M.J. and Seward, E., *J. Am. Chem. Soc.*, 1989, 111, 8681.
84. Gutsche, C.D., *Calixarenes*, RSC monographs in supramolecular chemistry no.1, RSC, Cambridge (UK), 1989.
85. Treasure, T. and Band, D.M., *J. Med. Eng. Tech.*, 1977, 1, 271.
86. Thomas, R.C., *Ion Sensitive Intracellular Microelectrodes*, Academic Press, London, 1978, p. 22.
87. Lev, A.A., Malev, V.V. and Osipov, V.V., in "Membranes", Eisenman, G. (ed.), M. Dekker, New York, Vol. 2, 1973.
88. Moody, G.J. and Thomas, J.D.R., in reference 33, p. 76.

89. Kimura, K., Maeda, T., Tamura, H. and Shono, T., *J. Electroanal. and Interfacial Electrochem.*, 1979, 95, 91.
90. Attiyat, A.S., Ibrahim, Y.A. and Christian, G.D., *Microchem. J.*, 1988, 37, 122.
91. Cram, D.J. and Ho, S.P., *J. Am. Chem. Soc.*, 1986, 108, 2998.
92. Diamond, D., Svehla, G., Seward, E. and McKervey, A., *Anal. Chim. Acta*, 1988, 204, 223.
93. Cadogan, A., Diamond, D., Smyth, M.R., Svehla, G., MacKervey, A., Seward, E. and Harris, S., *Analyst*, in press.
94. Jeng, J. and Shih, J.S., *Analyst*, 1984, 109, 641.
95. Zhou, X., Luo, Y., Wu, C., Zou, Z. and Hu, Q., *Anal. Chim. Acta*, 1988, 212, 325.
96. Anker, P., Jenny, H-B., Wuthier, U., Asper, R., Ammann, D. and Simon, W., *Clin. Chem.*, 1983, 29, 1508.
97. Moody, G.J., Saad, B.B. and Thomas, J.D.R., *Analyst*, 1989, 114, 67.
98. Durst, R.A., in reference 34, p. 311.
99. Xie, R.Y. and Christian, G.D., *Analyst*, 1987, 112, 61.
100. Diamond, D. and Regan, F., *Electroanalysis*, 1990, 2, 113.
101. McKervey, M.A., Seward, E.M., Ferguson, G., Ruhl, B. and Harris, S.J., *J. Chem. Soc., Chem. Commun.*, 1985, 388.

CHAPTER 2

Application of Tetrameric Calixarene

Based ISEs to the Determination of

Sodium in Plasma Samples

2.1 INTRODUCTION

Sodium and potassium are among the most frequently demanded analysis by clinicians in hospital laboratories. As reported recently [1] an average sized district general hospital in the United Kingdom which serves a population of approximately 250,000 carries out between 150 to 250 analyses of sodium and potassium each working day. As the workload in clinical laboratories increases, analytical techniques have evolved towards more efficient, inexpensive and rapid analyses, characterised by high precision and accuracy. Ion-selective electrodes satisfy these requirements and it is in fact, these characteristics which have made ion-selective electrodes an indispensable tool in most clinical laboratories.

The earliest measurements of sodium in blood serum [2-4], were based on adaptation of the zinc uranyl precipitation technique [5]. The introduction of flame photometry brought a significant improvement [1], enabling both a large number of assays to be carried out on a reduced volume of sample and giving an acceptable degree of clinical accuracy and analytical precision. Flame photometry thus enjoyed an unbalanced supremacy for many years in electrolyte determination. Although the technique is still widely used, the advent of ion-selective electrodes to chemical analysis provided analytical chemists with an alternative method. Over the past twenty years, there has been a gradual replacement of the photometric technique by electrode-based measurements. This increasing popularity has arisen from advantages such as the removal of the gas supply, the possibility of measuring ionic activity instead of concentration, the non-destructive characteristic of the analysis and less expensive instrumentation.

Nowadays ion-selective electrodes incorporated in clinical analysers

perform the vast majority of routine measurements of the most relevant physiological ions, e.g. Na^+ , K^+ , Ca^{2+} , NH_4^+ , H^+ , Li^+ [6,7]. As regards sodium, the sodium glass ISE was the first electrode to be used for sodium determination. The electrode has been commonly applied to the determination of this ion in various biological fluids such as whole blood [8], serum [9,10], plasma [8,11] and urine [8,9,12]. At present most of the modern equipment in clinical laboratories employ the sodium glass electrode for routine analysis. However, on account of the advantages that solvent polymeric membranes exhibit over their glass counterparts [13], much research is today directed towards the development of lipophilic complexing agents in order to provide electroanalysts with improved sensors for sodium and other clinically important ions [14-18].

The main disadvantages of the sodium glass membranes are the rather high electrical resistance [19], the poor hydrogen selectivity [20], deposition of biological components on the glass surface (e.g. proteins) [21], a time dependent response to changes in potassium concentration that can lead to significant errors in the sodium measurement in the clinical laboratory [22] and the provision of leak-proof joint between the glass-membrane electrode body and the channel of miniaturised flow systems found in clinical analysers [10]. This latter problem is compounded by the fact that solvent polymeric ion-selective membranes are used in clinical analysers for the determination of potassium and calcium in plasma samples. The use of a sodium selective PVC membrane would enable a single coherent ISE block to be manufactured, which would greatly reduce the engineering problems associated with the hybrid blocks used in analysers at present. The fact that PVC membranes can overcome these disadvantages has been widely recognised [13].

The present chapter aims to describe the application of the tetrameric calixarene ionophores introduced in chapter 1 in the biomedical field. The determination of sodium in plasma samples will be presented and the results obtained will be discussed in comparison to flame photometry and to two clinical analysers, namely the Smac Technicon Analyser 3 and the Hitachi 704. For an electrode to be successfully applied to clinical analysis, it must satisfy a complete spectrum of requirements encompassing selectivity, sensitivity, lifetime and response time. The importance of these properties will therefore be discussed in some detail.

A brief introduction on relevant aspects of the use of ion-selective electrodes in clinical analysis will follow prior to presentation of experimental research.

2.2 CLINICAL BACKGROUND TO SODIUM ANALYSIS

2.2.1 Composition of Blood

The plasma and the cellular elements of the blood fill the vascular system and together comprise the total blood volume. The blood is the vehicle for metabolic communication between the organs of the body. The blood is very complex in its chemical composition since it carries a large number of nutrients, metabolites, waste products and inorganic ions, making possible the coordinated interplay and integration of metabolism.

About one half of the blood volume is the blood plasma, which is 90 % water and 10 % dissolved matter. Over 70 % of the plasma solids is composed of proteins, and about 20 % of organic metabolites. The remaining 10 % of plasma solids consists of inorganic salts.

Sodium is the major cation component of the inorganic salts present in

plasma with a concentration of about 140 mmol l^{-1} , whereas in the red cells it is only 4 mmol l^{-1} . Conversely, potassium has a concentration of 3 mmol l^{-1} and 110 mmol l^{-1} in plasma and red cells respectively.

2.2.2 The Role of Sodium in Blood Plasma

Because of the relatively large amount of sodium in the body, this electrolyte is by far the most important substance influencing the distribution and retention of body water, as also is potassium. Sodium is largely associated with chloride and bicarbonate in the regulation of acid-base equilibrium [23]. The other important function is the maintenance of the osmotic pressure of body fluids and thus the protection of the body against excessive fluid loss. It also functions in the preservation of normal irritability of muscle tissue and the permeability of cells [24]. The mechanism that maintains the sodium concentration, 'the sodium pump' is related to intra and extracellular water content, and hydrogen ion concentration [25]. Disturbances in these mechanisms can arise from several different pathological conditions (see below). Hence sodium measurements in plasma samples can be regarded as a general indicator of patient well-being.

2.2.3 Pathological Conditions Involving Sodium Disturbances

As this thesis is concerned with the analytical aspects of physiology a detailed description of blood biochemistry will not be presented. However, a brief outline of some of the most frequent and important pathological states affecting sodium plasma balance will be mentioned.

When there is loss of fluids or electrolytes through the gastrointestinal tract, urinary tract, sweat, extensive burns, etc. or gain through intravenous

hypertonic salts, excessive intake of liquids, etc., measurements of sodium and potassium concentration in plasma provide strong evidence of water or electrolyte imbalances and may also be helpful in the supervision of a particular therapy. Additional information can be obtained by measuring sodium urinary levels, since about 95 % of sodium that leaves the body is excreted in the urine [26]. These measurements thus indicate how and to what extent water and/or electrolyte imbalance is occurring.

As already mentioned, the clinical conditions involving changes in plasma sodium concentration must affect the state of hydration and osmolality, owing to the close relationship between water balance and extracellular sodium concentration.

Pathological states involving sodium disturbance can be categorised as follows:

(a) Hypernatraemia: An increase of sodium over the acceptable limit is known as hypernatraemia [27]. It is a sign of hyperosmolality and therefore indicative of reduction of water volume (dehydration). Hyponatraemic states may occur as result of Cushing's disease [28] which causes hyperactivity of the adrenal cortex, tumours secreting excess of corticotropin (ACTH) [28] or tumours producing an excess of sex hormones [28]. Intravenous administration with drugs such as glucocorticosteroids or the fast intravenous administration of sodium salts may also lead to hypernatraemia [29]. Elevated levels of plasma sodium may arise from conditions which generate a rapid loss of water [30] such as diarrhoea, vomiting, diabetes insipidus or insensitve losses as occur during during raised body temperature).

(b) Hyponatraemia: A reduced sodium concentration in plasma may be an indication of hypoosmolality. However, the levels of sodium as measured in the

plasma may not reflect accurately the total body sodium. This is so when patients are given large quantities of hypotonic fluids [32]. Here the distal tubules in the kidneys act to retain sodium and consequently excretion of the additional plasma water is suppressed. Hence, although the plasma sodium levels are reduced, the total amount of sodium present is normal. Conditions like these can be observed in edematous states like cirrhosis, congestive heart failure, or some renal illnesses where the sodium rather than low may be normal or even high. However in clinical conditions where real reduction of sodium does occur, the low plasma sodium truly indicates depletion of the total body sodium. This is common with excessive loss of water such as insensitve loss, gastrointestinal loss, impaired renal sodium excretion, in Addison's disease (reduction of cortisol) [28], hypoaldosteronism [28] or low production of antidiuretic hormone [28]. Therapy with some commonly used diuretics often seem to be the cause of hyponatraemia, specially when the therapy is extensive and in high doses [33].

Obviously the measurement of plasma sodium is important in clinical diagnosis, but this provides only a limited amount of information regarding electrolyte imbalance. It is only from the combined measurement of sodium urinary and plasma levels that clinicians can obtain valuable information for patient diagnosis.

2.3 THE CONCENTRATION VS ACTIVITY CONTROVERSY

The introduction of ion-selective electrodes in the clinical field has facilitated the development of two types of instruments [1]:

a) the high capacity clinical analysers of the type developed by Technicon, with which indirect potentiometric measurements are carried out on diluted

samples, and

b) low capacity instruments for direct potentiometric measurements, requiring no pre-dilution step. These instruments are designed for use in intensive care units where rapid assessment of electrolyte activities is required to avoid the so called 'turn around time' in hospitals [34]. They are used frequently for single patient sampling. Analyses of whole blood electrolytes or hyperlipidaemic samples (see section 2.5.4.2) are made with low capacity instruments.

The measurements of sodium by flame photometry expressed in concentration and by direct or indirect potentiometry expressed in activity can lead to divergent results and problems in the clinical interpretation of these results. The discrepancy of the measurements has given rise to the question of which of the methods provides the most clinically and analytically significant information. This has become known as the activity concentration controversy [35]. Worth [1] has discussed the problem at length. From his data (Table 2.1), he states that using direct potentiometry a sodium concentration of 140 mmol l^{-1} will have an activity coefficient corresponding approximately to that of a molality of 0.1, namely 0.778. However, the total ionic strength of a solution will also affect the activity coefficient of each ion. In plasma the total molality is approximately 0.2 Kg^{-1} , giving an activity coefficient for sodium of about 0.74. In indirect potentiometry with a 1 : 200 dilution step, the total molality would be approximately 0.001. From the same work, Worth [1] points out that a concentration of 140 mmol l^{-1} measured by flame photometry, would only be 135 mmol l^{-1} (dilution 1 : 200) as measured by indirect potentiometry, while 104 mmol l^{-1} is found by measuring with ISEs without dilution step involved. The different results observed have been the

Activity Coefficient	
Molality	NaCl
0.001	0.966
0.005	0.928
0.01	0.905
0.05	0.821
0.1	0.778
0.5	0.678

Table 2.1 Activity coefficients from emf measurements at 25°C

matter of extensive literature discussions [36] and owe their basis from factors arising in the unequal nature of plasma or serum and aqueous solutions. These factors are discussed below.

2.3.1 Sodium Bound to Proteins

It is a well known fact that there are many substances (e.g. metabolites, drugs, hormones and ions), that are transported in the blood stream to varying extents in protein-bound form. Albumin accounts for most of these substance-protein complexes. A significant percentage of calcium is bound to albumin and is normally not detected when calcium concentration is measured with ion-selective electrodes. However, methods have been proposed for measurements of total serum calcium, thus including bound and non-bound calcium [37]. Although there are authors who support the idea of sodium-protein binding [38], there are others who suggest that there is not evidence of such

complexation [39]. Whatever the real situation is, the amount of protein-bound sodium is believed to be small although in-vitro experiments [40] have indeed demonstrated the existence of these sodium-albumin complexes.

2.3.2 Sodium Bound to Hydrogen Carbonate

It has been shown that by arranging a system where the sodium and potassium concentrations and total ionic strength is kept constant and the hydrogen carbonate is increased, the activity of both sodium and potassium measured by direct potentiometry will decrease, while the concentration of the same as measured by flame photometry remains constant [41]. In one study, the presence of hydrogen carbonate at a concentration of 25 mmol l^{-1} was found to decrease the sodium and potassium content measured by direct potentiometry by 2 % and 3.1 % respectively from their original normal plasma concentrations. It has been suggested however that this could be due to changes in liquid junction potential [42], rather than the formation of sodium and potassium complexes.

2.3.3 Red Blood Cell Effect

The existence of the red blood cell effect is a matter of debate. Results 1.55 % higher for sodium have been found by some workers with direct potentiometric measurements in whole blood when compared to plasma at physiological levels [43]. Other studies [44] suggest no significant differences. However, advisable careful handling and mixing of samples should be observed to avoid possible increased potassium levels due to leakage from damaged cells. Even when collection and processing of samples is carefully carried out [45], some workers have found significant discrepancies between

plasma and whole blood sodium determinations. Bijster et al [46] supported the observation that there is a significant increase in sodium and potassium using blood compared with plasma samples, but they have also shown that this is due to the use of an open static liquid junction between the selective and reference electrodes.

2.3.4 Matrix Effects

The volume occupied by the plasma matrix (e.g. macromolecules such as proteins and lipoproteins) is significant and not available to low molecular weight substances such as electrolytes unless they are bound to these macromolecules. The plasma matrix is estimated to be 8 % of the total and therefore the measurements of electrolyte activity are determined in a volume which is 8 % smaller than the total sample volume. This means that the values of activity measured by direct potentiometry are higher than those provided by flame photometry and indirect potentiometry. Indirect potentiometry is comparable to the photometric technique since the dilution step reduces the matrix effect, so the volume available to ions is not significantly different from the total volume. Experiments have shown [9] that the addition of physiological amounts of proteins or lipids to sodium chloride solutions had little or no effect on sodium activity measurements made by direct potentiometry. On the other hand the sodium concentration measured by flame photometry showed the predicted reduction of around 8 % [9].

2.3.5 Importance of Activity-Concentration in Clinical Assays

It is well accepted that physiological mechanisms are controlled by the activity of their components. Therefore, it would appear that plasma activity

is the physiologically important parameter, rather than concentration [47,48]. In general, the factors discussed above do not cause significant problems in sodium determination, and can in the most part be compensated for using calibration procedures. Unfortunately, this is not the case with matrix effects where protein and lipoprotein content may vary significantly from sample to sample [49,50]. As explained previously, the matrix effect on ion concentration is due to changes in plasma water fraction and affects every ion to the same extent.

Increase in plasma protein and lipoprotein may occur in several pathological conditions leading to significant differences in the analysis of sodium and potassium by flame photometry and direct potentiometry.

2.3.5.1 Hyperproteinaemia

In this case the total protein concentration is much larger than normal. Values of 100 g l^{-1} to 200 g l^{-1} are commonly observed (normal value $60 - 80 \text{ g l}^{-1}$). Different studies show that when no sodium depletion has occurred and no electrolyte disturbance is seen in these patients, the flame photometry results indicate that the patients are hyponatraemic, whereas direct potentiometric measurements show the correct normonatraemic state [51].

2.3.5.2 Hyperlipoproteinaemia

An excessive lipid concentration causes also a reduction in the plasma water fraction. Conditions such as uncontrolled diabetes, hypertrigliceridaemias, hyperlipidaemias and others [52] may cause elevated lipids levels. In all instances, flame photometry incorrectly gives lower values for sodium in comparison to direct potentiometry (pseudohyponatraemia).

Therefore, care must be exercised when low sodium levels are found by flame photometry. In such cases, the protein and lipid plasma content should be checked before hyponatraemia is diagnosed. Where pseudohyponatraemia is not recognised, excess sodium may be administered to a patient in order to raise the apparent low sodium blood level to the normal range. This incorrect therapy has already caused at least one death [53]. In cases like these, assays should be carried out by direct potentiometry.

2.4 CHARACTERISTICS OF ISE MEMBRANES IN THE ANALYSIS OF BIOLOGICAL SAMPLES

2.4.1 Stability

The stability and reproducibility of emf measurements depends both on the type of electrode being used and the experimental design. For instance, the reproducibility of precision on measurements in biological samples is claimed to be about 10 times better than that of routine measurements and according to Ammann [54] can approach limits only imposed by the electronic measuring equipment. Since the demands on the precision may differ between clinical laboratories, Oesch et al [13] have suggested the five-fold subdivision of the physiological normal range of electrolytes with a 95 % confidence limit for comparison purposes between electrodes. If the normal physiological range of plasma sodium is 135 mmol l^{-1} to 150 mmol l^{-1} , (see table 2.2) this proposal implies that a precision better than 0.1 mV is required for the analysis. Current mV-meters have an accuracy of $\pm 0.1 \text{ mV}$. An inaccuracy of 0.1 mV in the sodium measurements would introduce an error of 0.5 mmol l^{-1} which is considered to be within a realistic clinical tolerance error of 2 mmol l^{-1} [55].

ION	Physiological range mmol/l mmol/l	Required precision/ mmol l ⁻¹	mV range at 25°C	Required precision/mV
K ⁺	3.5-5.0	0.1	9.2	0.5
Na ⁺	135-145	0.5	1.8	0.1
Li ⁺ *	0.7-1.5	0.04	19.6	0.97
Ca ⁺⁺	1.0-1.2	0.02	2.3	0.12
Cl ⁻	95-110	0.75	3.8	0.19
HCO ₃ ⁻	21.3-26.5	0.26	5.6	0.28

Table 3 Physiological range and required precision for some commonly determined ions using ion-selective electrodes.

* Therapeutic range

Leaving aside factors such as the ISE membrane, electrical circuitry, and the reference electrode which undoubtedly affect the stability and the reproducibility of the emf, important criteria concerning stability in biological samples are:

- 1.- shift in the standard potential (E^0)
- 2.- drift
- 3.- residual standard deviation
- 4.- reproducibility

Oesch et al [13] suggest that in batch determinations the reproducibility of the measurement is the relevant stability criterion. This is based on the

assumption that a long term drift does not influence the measurements because sample /calibration intervals are usually of the order of one minute or less. However with continuous in-vivo applications, the same authors recognise that the stability will be dictated by the drift and residual standard deviation since intermittent calibrations can no longer be performed.

A further consideration regarding precision involves the shift in standard potential (E^0) frequently observed when an ISE is first placed in a solution containing proteins (see section 3.16.2, Fig. 3.24, Chapter 3). The E^0 shift is believed to be due to interfacial changes (sample/membrane) caused by the deposition of proteins onto the surface of the electrode. Adsorption of even small amounts of proteins on the membrane surface will change the physical characteristics of the membrane. Consequently a shift in potential will be observed since the internal reference electrolyte interface remains basically unaltered.

Another factor highlighted by Oesch et al [13] is that the sample/membrane interface may be altered due to the extraction of marginally lipophilic membrane components by samples containing protein or lipid. Thus the mobility of membrane components is not fast enough to replace the extracted molecules in the sample-side of the interface. The generation of these slight interfacial imbalances clearly will cause changes in the ISE potential which are typically manifested by drift.

To tackle the problem of deposition of macromolecules on the electrode surface, several workers have used exclusion membranes over the ISE sensor [56]. However, the use of such membranes sometimes fails to inhibit relatively low molecular weight plasma components and may also generate additional potential differences [57].

2.4.2 Selectivity

Clinical samples of normal individuals have well-defined physiological concentration ranges for all electrolytes of clinical importance. Thus using the Nicolsky equation (eqn. 1.11, chapter 1) and assuming physiological concentration ranges, required selectivity coefficients have been calculated according to the following equation [13], below:

$$K_{ij}^{pot} = \frac{a_{imin}}{a_{jmax}} \frac{P_{ij}}{100} \quad (2.1)$$

where, K_{ij}^{pot} is the highest tolerable value of the selectivity coefficient

a_{imin} is the lowest expected activity of the measuring ion i^{z_i}

a_{jmax} is the highest expected activity of the interfering ion j

P_{ij} is the highest tolerable error in the activity a_i due to interferences of a_j (in percent).

The required sodium selectivity coefficient for a maximal interference of 1 % (worst case) by a common range of electrolytes present in plasma samples according to eqn. (2.1) is presented in table 2.3.

From the data seen in table 2.3, it is clearly seen that all ionophores listed in table 1.5 (chapter 1) satisfy the selectivity requirements imposed for clinical applications, excepting that of the ETH 227 ionophore in the presence of therapeutical concentrations of lithium.

2.5 Liquid-Junction Potential

In measurements carried out in biological systems, the assumption that the liquid junction potential is minimum and constant is not valid during the course of calibration and measurements due to the extremely complex composition

Required Selectivity Coefficient K_{ij}^{pot}						
	H^+	Li^+	$*Li^+$	K^+	Mg^{2+}	Ca^{2+}
Na^+	4.4	2.1	-0.1	-0.6	-1.2	-1.3

Table 2.3 Required selectivities for sodium electrodes for plasma applications. Therapeutic level (*)

of plasma samples. Therefore some fluctuation must be allowed for liquid junction potential between the reference system and the biological fluid. Tolerances in accuracy of 10 % for sodium require reproducibilities of 0.3 mV. Thus reference and bridge solution, as well as carefully matched matrices between standards and samples for calibration purposes must be given special attention.

2.6 CALIBRATION OF ISEs IN BIOLOGICAL SAMPLES

To solve problems due to varying ionic strength and thus measure the activity of the analyte as reliably as possible, all activity coefficients in the calibrants should try to closely match those in the samples. This is achieved by making up standards in a matrix with a background of a constant ionic strength that approximates to that of the plasma sample ($I \sim 0.15$).

However, the situation is complicated by the fact that plasma samples do not have a constant ionic strength (especially in pathological states). Even where samples do have a fairly constant ionic strength, different commercial instruments and different workers tend to use different calibrants which may have different ionic strengths. It is not real surprise therefore that some

commercial instruments have been shown to produce considerable inter-instrumental deviations [58,59]. In comparative studies several calibration procedures have been published [60] and proposals for a unified approach for measurement of biological samples with ion-selective electrodes form the basis of recommendations by the International Federation of Clinical Chemists [61].

2.7 EXPERIMENTAL WORK

2.7.1 Introduction

The following experimental work describes the use of methyl p-t-butylcalix[4]aryl acetate and the methyl tetraketone derivative of p-t-butylcalix[4]arene based PVC electrodes in the analysis of sodium in plasma samples. The determinations were carried out under steady-state conditions (dipping method) and compared to the results previously obtained for the same samples by two continuous flow analysers employing the sodium glass electrode (the Smac Technicon 3 and the Hitachi 704) and by flame photometry.

2.7.2 Electrode and Membrane Construction

Catheter type and conventional macroelectrodes of the type described in chapter one were used. The construction of catheter type and macroelectrodes followed the procedures described in sections 1.8.4.2 and 1.8.4.3 respectively.

Membrane preparation for catheter type electrodes was that outlined in section 1.8.3 (chapter 1), while those membranes used for macroelectrodes are described in chapter 3 (section 3.13).

2.7.3 Materials and Samples

All chemicals used for electrolyte solutions were of analytical reagent grade and the solutions were prepared in distilled deionised water. Membrane components were from the same sources already described in section 1.8.5 (chapter 1). Salts of tris buffer were obtained from Sigma, D-glucose was obtained from BDH and urea from Riedel-de Haen.

Plasma samples were obtained from the Biochemistry departments at St.

James and Beaumont Hospitals, Dublin. Each site provided their respective results for the sodium analysis. The St. James results were obtained with a Technicon Smac 3 Analyser, while those from Beaumont Hospital were obtained with the Hitachi 704 Analyser. Flame photometric data were also obtained from Beaumont Hospital.

2.7.4 Potentiometric Cell

Measurements were conducted under ambient temperature conditions, except when indicated otherwise and when using standard addition method in which the temperature was maintained at $25 \pm 0.5^{\circ}\text{C}$, using a thermostatted polarographic cell. A Philips PW9421 digital pH meter (0.1 mV resolution) or alternatively a Corning 240 pH millivoltmeter coupled to a Fluka 8060A digital multimeter (total resolution 0.01 mV) were used for measurements. The reference electrode was a saturated calomel electrode (SCE) with a free flowing liquid junction (Metrohn ref. 60.705.000), except when indicated otherwise.

Overall the electrochemical cell can be represented by:



2.7.5 Procedures

Plasma samples were stored at 4°C . At least one hour was allowed after removal from storage for temperature equilibration to occur before measurements were taken. Samples and standards were stirred slowly during measurements. Results were obtained both from a calibration curve, and by the standard addition method.

In every instance, previous to plasma measurements sets of up to 5

electrodes were constructed, conditioned in 0.1 M NaCl solutions and their electrode slope function tested in six sodium calibration solutions ranging from 1×10^{-6} M to 1×10^{-1} M. Drift and resistance of the electrodes was also examined previous to plasma measurements. The electrode which presented best performance characteristics was used to perform the analysis.

2.7.5.1 Measurements from Calibration Curves

(a) In an initial approach, the procedure for electrodes containing methyl p-t-butylcalix[4]aryl acetate was as follows:

to determine the emf of plasma samples, six sodium calibration solutions were made up and the slope of the electrode function measured in these solutions. Stock solutions contained 50.0, 125.0, 140.0, 155.0, 200.0, and 500.0 mmol l⁻¹ of Na⁺ with a constant ion background of K⁺ (4.0 mmol l⁻¹), Ca²⁺ (1.1 mmol l⁻¹) and Mg²⁺ (0.6 mmol l⁻¹). When taking measurements, 1 ml of each stock solution was removed, 2 ml of tris buffer added (pH 7.4) and the volume made up to 10 ml (all salts present as chlorides).

A similar procedure was used with blood samples, i.e. 2 ml of tris buffer (pH 7.4) were added to 1 ml of blood plasma and the total volume made up to 10 ml. For the batches of samples analysed under this procedure, the plasma was obtained after centrifugation of heparinised blood at 3500 rev min⁻¹ for 10 min. After every third or fourth sample the electrode response was checked in the calibration solutions. Potentials were measured against a calomel reference electrode with a constrained ceramic junction (Metrohm AG 9100, Herisan). A total of 44 samples were processed under this procedure. The emf values used for calculations were the mean of the potential measured at 10 and

15 minutes after immersing the electrodes in the sample.

(b) In another approach which was adopted subsequently for electrodes based on both methyl p-t-butylcalix[4]aryl acetate and the methyl tetraketone derivative of p-t-butylcalix[4]arene, calibration solutions consisted of five artificial plasma samples containing 100.0, 125.0, 140.0, 155.0 and 180.0 mmol l⁻¹ NaCl respectively, with a fixed background of K⁺ (4.4 mmol l⁻¹), Ca²⁺ (2.4 mmol l⁻¹), Mg²⁺ (0.8 mmol l⁻¹), glucose (4.7 mmol l⁻¹) and urea (2.5 mmol l⁻¹). An identical procedure was adopted for the calibration solutions and the plasma samples. The procedure was as follows:

1 ml aliquots of the calibrant solutions and plasma samples were diluted 10-fold by adding 9 ml of a diluent (pH 7.4 tris buffer in 0.11 M LiCl). The high background concentration of LiCl in the solution dominates the ionic strength, and gives a relatively constant sodium activity coefficient ranging from 0.758 to 0.754 in the calibrants, (see Table 2.4). This enables the ion-selective electrodes to be calibrated in terms of sodium concentration rather than activity. From the data obtained in chapter 1, section 1.2.9.1.3 (Table 1.5) and section 1.9.2.2.2.4 (table 1.11) it is known that both ISEs are very selective against lithium ions, and at this level, lithium does not affect the response of the sodium electrodes.

Under the above mentioned procedure the measurements were recorded every 30 seconds after immersing the electrodes in the sample solutions and the value at two minutes was chosen for calculations. Recalibration was carried out after 5 samples in every instance.

2.7.5.2 Measurements by Standard Addition

For the standard addition method the following routine was employed:

1 ml of plasma was diluted and the emf of the cell was recorded (E_1).

After addition of a standard solution of known sodium concentration, a second emf value was obtained (E_2). The concentration of the analyte (C_a) can then be calculated using equation (2.2), below [62]:

$$C_a = \frac{V C_s}{V_0 \left[\text{antilog} \left(\frac{E_2 - E_1}{S} \right) \right] \left(\frac{V}{V_0 + V_r} + 1 \right)^{-1}} \quad (2.2)$$

where v_0 is the known volume of plasma sample containing an unknown sodium concentration C_a , C_s is the concentration of a standard sodium solution of volume V_d added to the sample, V_r is the total volume of reagents added to the sample (diluent buffer) and S is the calibration slope of the electrode. After addition of a diluent volume V_d (as for V_r) the emf (E_3) was obtained and the slope S calculated according to equation (2.3), below [62]:

$$E_2 - E_3 = S \log \left(\frac{V_0 + V + V_d}{V_0 + V} \right) \quad (2.3)$$

A schematic diagram of the standard addition procedure is shown in table 2.4.

2.8 RESULTS AND DISCUSSION

As mentioned in section 2.7.5.1, a first approach to measure plasma samples with electrodes based on methyl ester calix[4]arene, involved the

Standard Addition Procedure

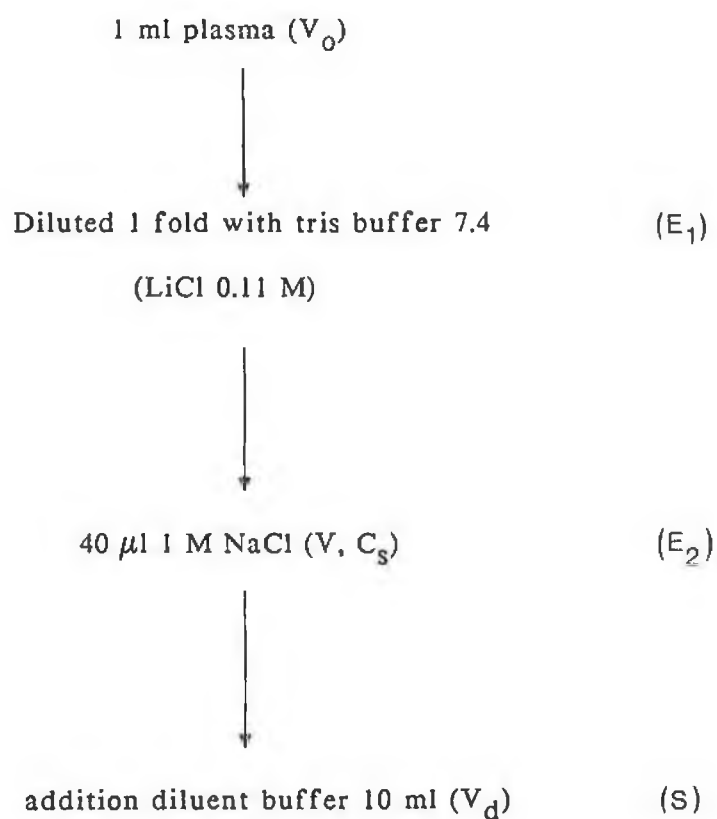


Table 2.4 Diagram of the standard addition method used for determination of sodium in plasma samples.

determination of a set of 44 samples divided into two batches. The electrodes were calibrated in six standard solutions designed to bracket the expected values of sodium plasma. The response proved to be linear in triplicated measurements with slopes ranging from 54 to 58.5 mV dec⁻¹.

As plasma sodium levels outside the range 70 - 170 mmol l⁻¹ are pathological the performance of the electrode over the range 50 mmol l⁻¹ to 200 mmol l⁻¹ only is relevant. Although in every day practice, pathological values rarely exceed 20 mmol l⁻¹ above and below the physiological range the electrodes shown here covered the complete pathological range as depicted in Fig. 2.1. In fact, from the calibration curve shown, it can be seen that the electrodes behaved exceptionally well in the standard calibration solutions, with the regression coefficients being normally superior to 0.9999. Thus in order to ensure maximum electrode efficiency, plasma samples were analysed only when the electrode slope was Nernstian or near-Nernstian and the calibration curve exhibited a correlation coefficient above 0.9999. The results of indirect potentiometric measurements compared to the Smac Technicon Analyser for batches of 24 and 20 samples are shown in table 2.5 and Fig. 2.2a and 2.2b, respectively.

The regression data obtained for the ISE based on the methyl ester derivative showed good correlation ($r = 0.94$) with the hospital based analyser. A more careful inspection of the data showed however that a small but systematic error was evident. This was reflected as a positive bias that amounted an average of 3.1 mmol l⁻¹ (values over the segmented line which denotes the ideal correlation in Fig. 2.2a). The second batch of 20 plasma samples showed a similar pattern (Fig. 2.2b) with a good correlation ($r = 0.95$) but with an average negative error of 4.6 mmol l⁻¹ in this

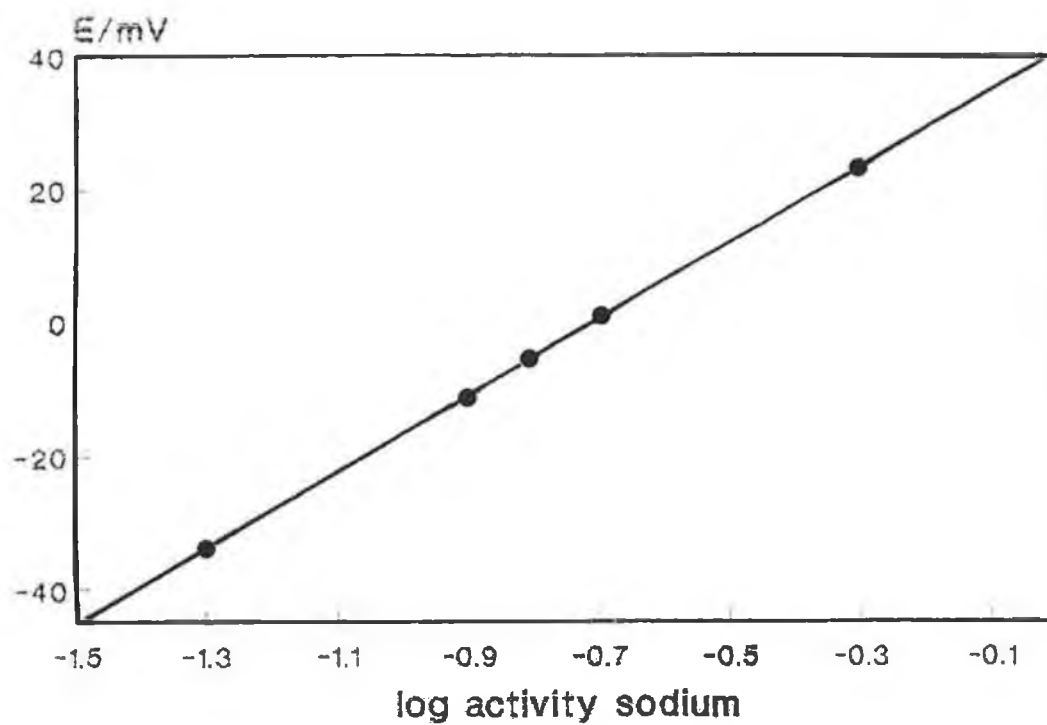


Fig. 2.1 Calibration curve in sodium aqueous standards for the analysis of sodium in plasma samples.

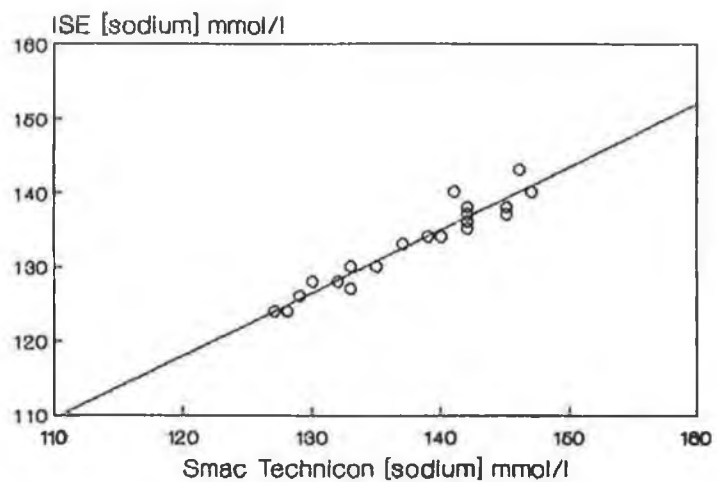
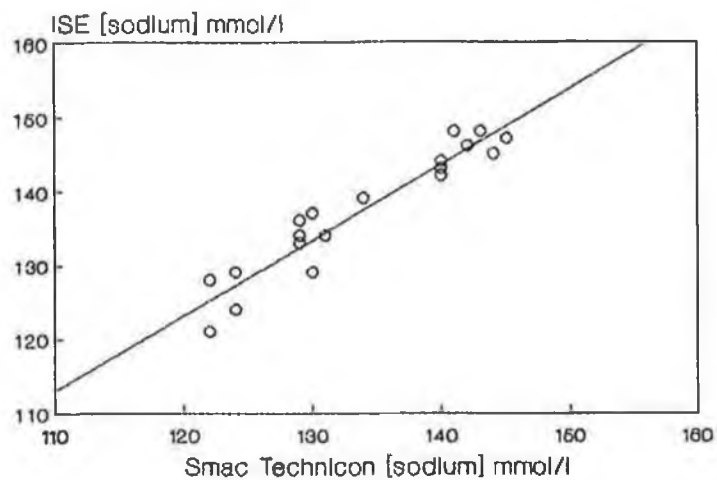


Fig. 2.2 Correlation of sodium measurements in plasma samples. (a) slope 0.975, $r = 0.94$; (b) slope 0.847, $r = 0.95$.

Sample	Concentration Na ⁺ mmol/l			
	ISE	Smac Technicon	ISE	Smac Technicon
1	121	122	124	127
2	128	122	124	128
3	124	124	126	129
4	129	126	128	130
5	133	129	128	132
6	134	129	130	133
7	136	129	127	133
8	129	130	130	135
9	137	130	133	137
10	129	130	134	139
11	134	131	134	140
12	139	134	140	141
13	139	134	135	142
14	139	134	137	142
15	143	140	136	142
16	142	140	138	142
17	143	140	138	145
18	144	140	137	145
19	143	140	143	146
20	148	141	140	147
21	146	142		
22	148	143		
23	145	144		
24	147	145		

Table 2.5 Results of sodium determination in plasma samples by PVC catheter type electrodes based on methyl p-t-butylcalix[4]arene ionophore and by Smac Technicon Analyser.

instance (results below the segmented line in Fig. 2.2b).

The high correlation obtained in both cases confirms that the electrodes can be used for blood sodium determination with confidence. The constant bias most likely arises from the procedure used to calibrate the electrode, as each individual calibration point is subject to error arising from signal drift and noise. Factors which may contribute to the bias are discussed in detail below.

While accepting that the main sources of error are probably related to the dipping method adopted in this study, it must be pointed out that the hospital results are also subject to error. Batch to batch variation in the Smac Technicon standards or the ISE standards (as the calibrants used in the ISE methodology were from different stock) might contribute to some extent to the observed error. However, variations in the Smac Technicon calibrants are unlikely with present day manufacturing methods and quality control. More common sources of error affecting the standard potential of the measuring cell will be discussed in relation to the ISE methodology employed here.

It is important to emphasise that for precise work, the cell temperature, the reference electrode potential and the liquid junction potential must all be controlled to within an acceptable margin of error. The sensitivity of the cell to temperature fluctuations depends on the difference between the temperature coefficients (dE^0/dT) of the indicator and the reference electrodes, temperature hysteresis, and the actual dependence of the electrode slope response on temperature. Depending on the type of electrode and the experimental tolerances temperature control to $\pm 0.5^\circ\text{C}$ is usually sufficient for most applications. Under non-thermostatted conditions, the cell temperature might change by $1 - 2^\circ\text{C}$ during the course of an experiment. This would produce a change of less than 0.5 mV/decade in the electrode slope, as

well as affecting the standard cell potential and the activity coefficients of the ions. While these fluctuations will contribute to electrode drift, recalibration of the electrode after every five samples minimises this error.

In relation to the liquid junction, which is recognised to be another important contributor to the standard cell potential, the use of equi-transferent solutions is required for most applications. Nevertheless, since the blood plasma samples and standards prepared here had a fairly regulated ionic composition, the contribution from liquid junction potential was expected to be small and was further minimised by using a saturated KCl bridge. In connection with liquid junction effects, Simon and co-workers [63] have reported values as small as 70 μV , which correspond to relative errors of $\sim 0.3\%$ for monovalent ions in blood serum when using appropriate salt bridges. In the same biological medium, the use of, for example, isotonic NaCl i.e. 0.15 M, as bridge electrolyte, results in changes of the liquid junction of up to 0.5 mV which would correspond to a 2 % relative error. Although the magnitude of the liquid junction potential does not explain the total differences observed in both batches of samples, variation in the junction stability will contribute in unquantifiable error to the results. This is however expected to be small, given that complementary analytical data provided by the hospital analysers indicated that none of the samples were grossly abnormal.

Another source of error which is particularly problematic in clinical samples arises from the blockage of the reference electrode liquid junction. The obstruction may appear as a result of proteins clogging at the tip of the reference electrode or by crystallisation of KCl from the bridge electrolyte if temperature variations occur. Polyelectrolytes and colloidal or suspended

particles in biological samples can also affect the junction potential [63]. Generally, these blockages give rise to moderate and monotonic drift, although considerable changes in the junction potential could be expected if the the degree of obstruction is large. Thus, when working with biological samples, the form or configuration of the liquid junction is a vital consideration in determining the overall performance of the reference electrode. Various types of liquid junctions have been designed and are readily available. The choice of which to use is mainly dictated by the composition of the sample solution and its tolerance to contamination by the salt bridge electrolyte. The most commonly used junctions are the constrained type junctions, of which the ceramic plug (which was used in these initial studies), is probably the best general purpose junction. This junction performs reasonably well for measurements in small volumes and in extremely dilute samples. However in biological samples, the presence of macromolecules make them prone to contamination and they are particularly likely to produce misleading results [64]. Errors of 10 mV or even more have been claimed to be common in some commercial reference electrode half-cells with restrained liquid junctions [65]. With respect to solutions that may clog the small orifice, such as solutions containing proteins, a free-flowing free diffusion liquid junction is recommended.

In addition to errors arising from the reference electrode, the ISE potential may be affected by poisoning of the membrane by sample protein or leaching of the membrane components into highly lipophilic samples (see section 2.4.1).

From this discussion, it is clear that numerous factors contribute to errors in ISE measurements in plasma samples. In an attempt to minimise

errors, the experimental procedure was modified in the following way:

1. Other common components of plasma were introduced into the standards at their normal levels (i.e. glucose, urea), to give a closer matrix match with plasma samples.
2. Tris buffer pH 7.4 containing 0.11 M LiCl was used as the diluent rather than pure water. The high background concentration of LiCl in samples and standards ensures a relatively constant ionic strength and activity coefficients for sodium.
3. A free flowing liquid junction reference electrode was used instead of the ceramic frit electrode in order to minimise the liquid junction problems outlined above.

Figure 2.3 shows the ISE results obtained with this method plotted against the respective reference method, i.e. Hitachi plasma analyser (a) and the Smac Technicon analyser (b).

From the data obtained, excellent agreement was found when comparing either to the Hitachi or the Smac Analyser. In fact for a batch of 59 samples the regression coefficient found was 0.816, with a residual standard deviation of 2.6 mmol l^{-1} . In the case of the Smac Technicon analyser the correlation coefficient was similar ($r = 0.827$) while the residual standard deviation was only 1.3 mmol l^{-1} (see Table 2.6).

In the light of these results, a clear correlation between the ISE and the reference methods is evident. However a small variation in the slope is observed for the data corresponding to the two different analysers, thus perhaps reflecting some degree of inter-instrumental variation. The probable reasons for these differences can be explained in terms of calibrant formulation and correction factors built into the microprocessor software. To

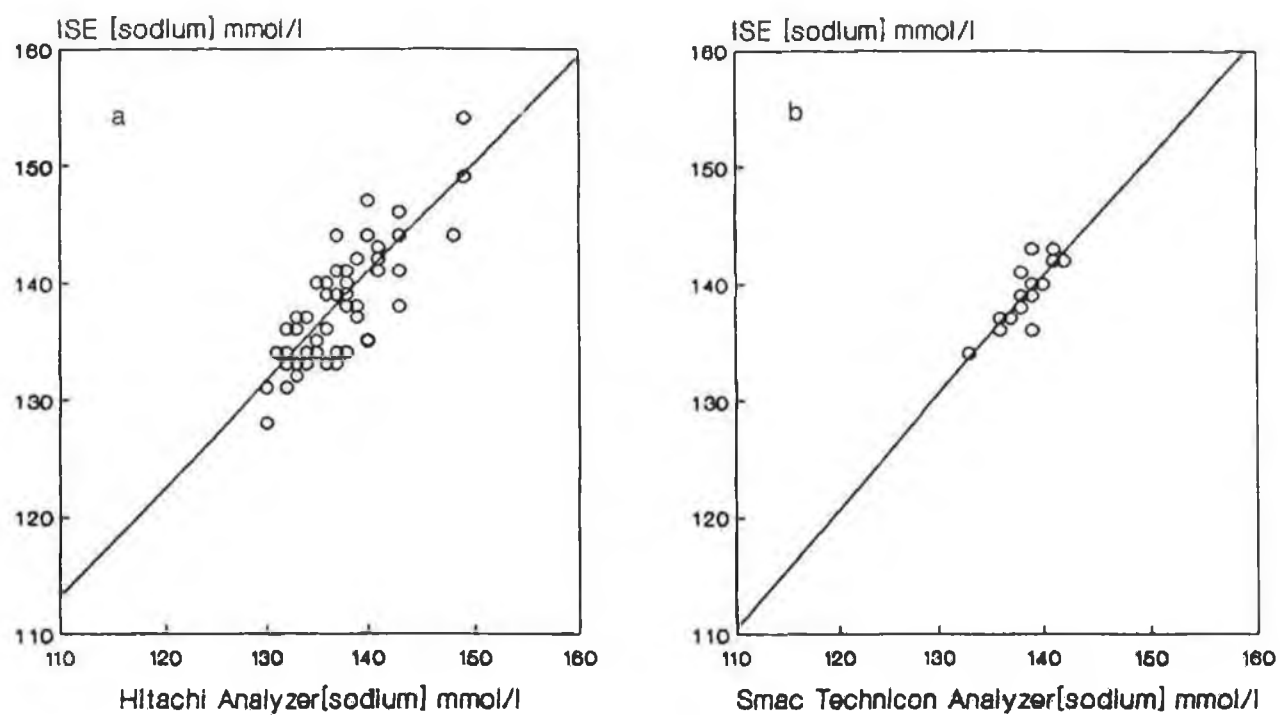


Fig. 2.3 Correlation for sodium measurements in plasma samples between the ISE and (a) Hitachi Analyser and (b) Smac Technicon Analyser.

n	assay	slope	intercept	r	residual SD mmol/L
61 ^a	Hitachi	0.93	5.85	0.820	±3.0
59 ^a	Hitachi	1.01	-0.37	0.816	±2.6
18 ^a	Technicon Smac	1.11	-15.03	0.827	±1.3
17 ^b	Hitachi	1.02	-1.95	0.792	±3.2
7 ^a	Flame Photometry	1.000	-1.14	0.904	±1.4

Table 2.6 Comparison of linear regression data for plasma sodium determination by different methods vs mini-ISE based on methyl p-tert-butylcalix[4]aryl acetate.

^amini-ISE results obtained using a calibration curve.

^bperformed by standard addition method.

obtain linear agreement with flame photometry, manufacturers use standards of different ionic strength rather than one fixed value, leading in some cases to considerable instrumental variations. This is usually prevented by periodical control assessments during electrolyte determinations. However, as pointed out by Cowell and McGrady [66] these control assessments lack reliability in certain cases since the comparison is usually based on agreement with a single calibration point. This type of assessment is not sufficient to guarantee the reliability of the analyser results for this type of comparative study. In this respect a more convenient and widely reliable method which is adopted by many workers for the assessment of new ISEs is the flame photometric technique. Although the slight variation in the slope when comparing to both different methods can also be ascribed to a simple population bias, the difference is rather small and for the purposes of comparison this deviation could be well within the precision of the type of technique employed.

A further factor observed in the comparison of both methods was however a difference in the residual standard deviation of the batches. Thus the better precision encountered with the Technicon method could have been due to the much cleaner aspect of the plasma samples in comparison to the samples provided by Beaumont hospital. The samples analysed by the Hitachi analyser were typically more opalescent, and high degree of hemolysis was rather common. Although hemolysed samples were avoided, visual inspection of the samples at times may not reveal microscopic fragments of erythrocytes present in plasma. Thus for accurate measurements it is always advisable to handle plasma or serum samples as carefully as possible.

The good correlation exhibited by the ISE was further confirmed by the analysis of a similar number of samples in a related study [67]. These

measurements were typically obtained one minute after immersion of the electrodes in the sample, and compared to results obtained with the Hitachi Analyser. The results shown in Fig. 2.4 and included in table 2.6 showed similar correlation for a batch of 61 samples ($r = 0.820$). Furthermore, the standard residual deviation obtained (3.0 mmol l^{-1} , 61 samples) was highly close to that obtained in this research (2.6 mmol l^{-1} , 59 samples).

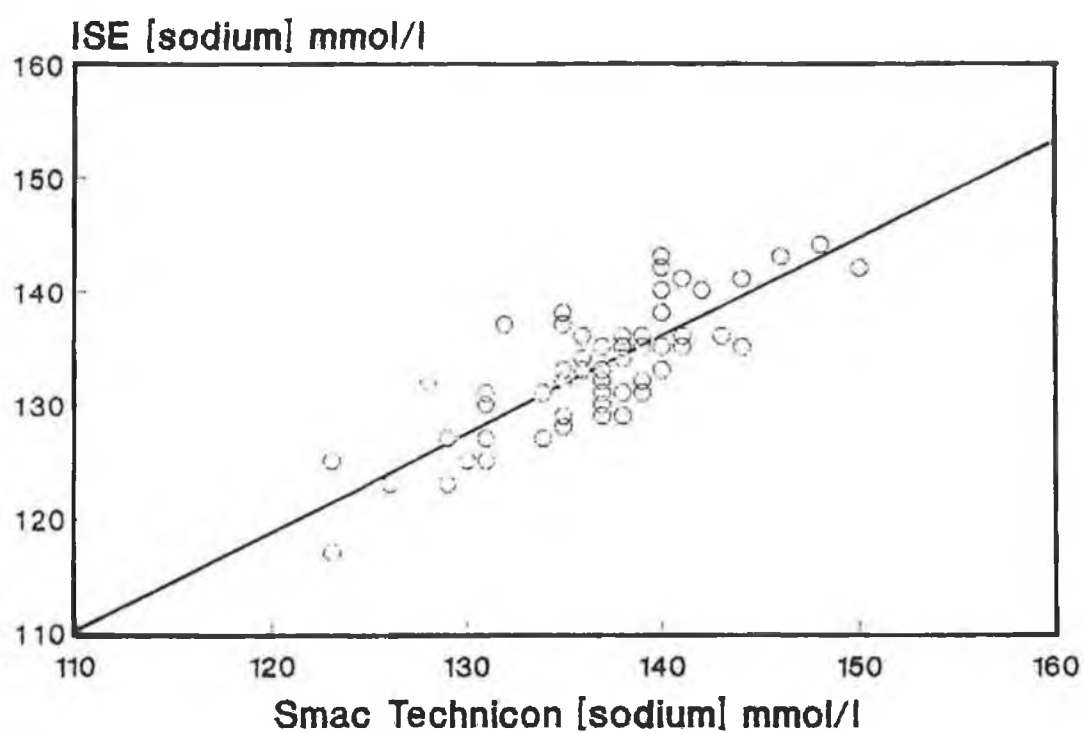
However, some deviation was observed in the slope of the correlation of both plots. Several reasons may be probably involved in such variations and the ones already mentioned i.e. batch to batch variation, liquid junction effects, ISE membrane fouling, could perfectly apply to this observation. Calibration in the previous study [67] was carried out after every 20 samples in contrast to the procedure used in this work (after every five samples) and this might account for differences in the results.

sample	Mini-ISE ^a	Flame Photometry	Hitachi analyzer (glass electrode)
1	138	140	139
2	138	138	137
3	130	133	133
4	140	140	139
5	140	142	141
6	136	135	136
7	136	138	137
regression coefficient			
	ISE vs Hitachi	ISE vs Flame Photometry	Flame Photometry vs Hitachi
	0.932	0.905	0.979

Table 2.7 Sodium concentration (mmol l^{-1}) and correlation coefficient measured for plasma samples by two different ISEs and flame photometry.

^aresults obtained from calibration curve.

^bperformed by standard addition method.



61 plasma samples

Fig. 2.4 Correlation for sodium measurements between the ISE and Hitachi analyser. Reading taken at one minute.

In another batch of samples, the ISE results (Table 2.7) showed improved agreement when compared with flame photometry, although smaller number of samples was assayed. The standard addition technique did not improve the correlation with the Hitachi analyser, although the regression coefficient and residual standard deviation were highly comparable (Fig. 2.5, table 2.6).

During sodium plasma determination carried out with electrodes based on the methyl tetraketone derivative of p-t-butylcalix[4]arene, the electrodes were similarly calibrated every 5 samples and all measurements were carried out under carefully controlled temperature conditions. The results obtained from calibration curve are shown in Fig. 2.6. In the analysis of 10 samples, the results gave a high correlation between the tetraketone based ISE and the Hitachi analyser ($r = 0.979$) and the flame photometric data ($r = 0.987$, $n = 10$), with residual standard deviation of 1.1 mmol l^{-1} and 0.9 mmol l^{-1} respectively. In the case of the Technicon analyser, the results did not agree as well as for the Hitachi analyser, and a regression coefficient $r = 0.951$ and a residual standard deviation of 1.8 mmol l^{-1} was found ($n = 10$).

In comparing both electrodes (those based on the tetramethyl ester and the tetramethyl ketone tetramers) in the analysis of sodium in plasma samples it seems clear that much better agreement and precision was normally found with electrodes based in the methyl tetraketone derivative. One of the reasons which may well account for the improved results may be the temperature control. However, another important consideration is the lower tendency to drift exhibited by the tetraketone based electrodes. In fact, during the course of measurements the electrodes exhibited improved stability in comparison to the methyl ester calixarene. However, it must also be appreciated that the number of analysed plasma samples was smaller when assessing the methyl tetraketone

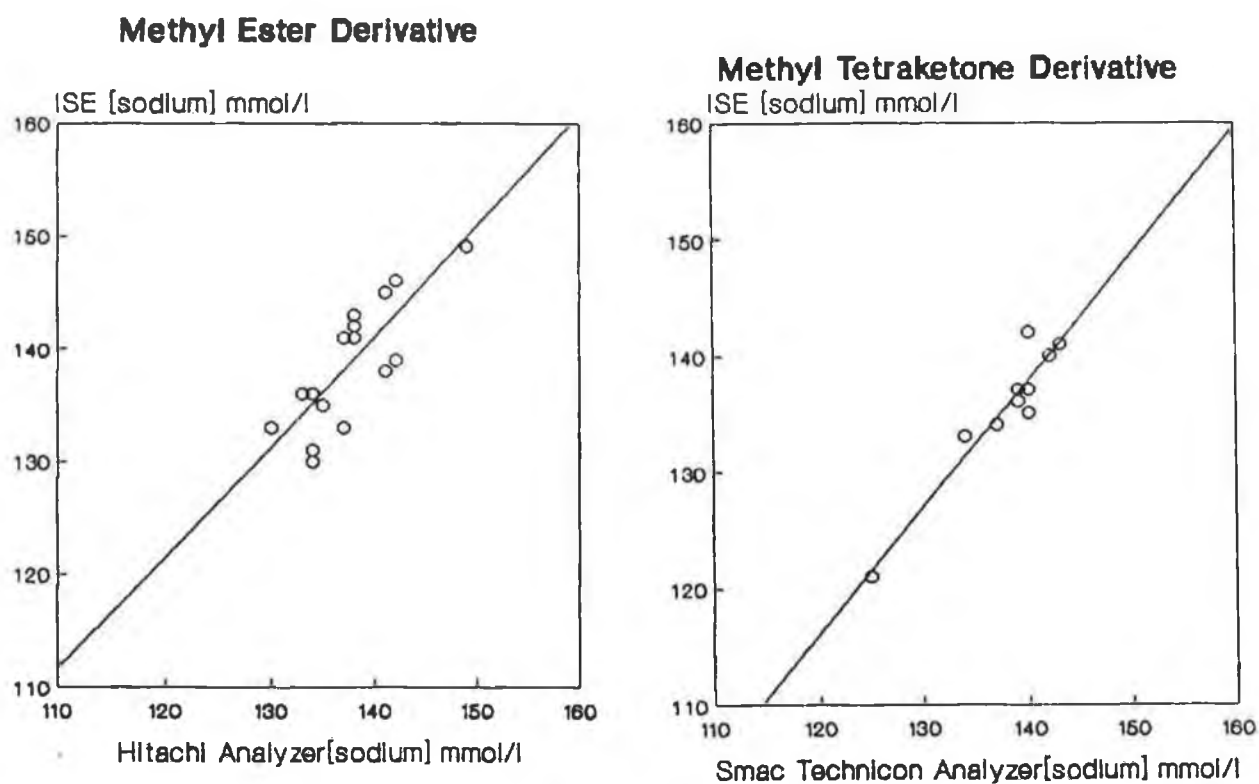


Fig. 2.5 Correlation between calixarene based ISEs and two hospital based analysers. The results obtained for the ISEs were performed by standard addition method.

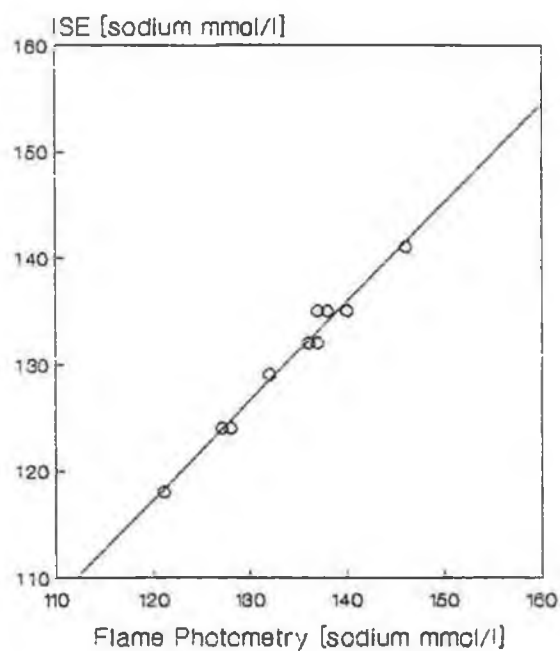
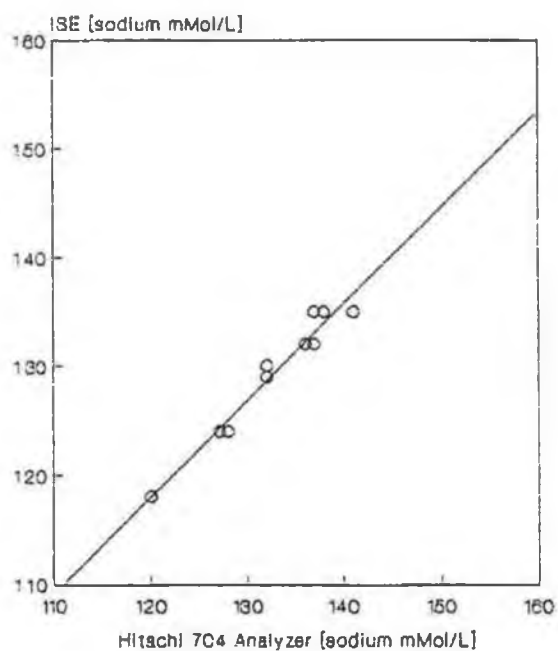


Fig. 2.6 Correlation for sodium measurements in plasma samples between methyl teraketone calix[4]arene based ISE and (a) Hitachi Analyser and (b) Flame photometry.

electrodes, and in general, the greater the number of samples, the lower the correlation coefficient will be.

2.9 CONCLUSIONS

The electrodes presented here have been successfully applied to the determination of sodium in blood plasma samples. The results obtained by using both electrodes were in good agreement with results obtained with the Hitachi and Smac Technicon Analysers. The electrodes showed comparable correlation in each case and the standard residual deviation varied from 1-3 mmol l⁻¹. The comparison with the traditional flame photometry technique seemed to improve the regression data in each case although batches of no more than 10 samples were analysed when comparing top flame photometry. The standard addition technique confirmed the agreement of the results with the analysers, although no major improvement was observed in precision. Some inconsistency was observed in the slope of the correlation plots for some batches of samples. The source of this inconsistency remained unclear but several factors influencing the use of ion selective electrodes in biological samples may be attributed. Overall, the electrodes showed excellent performance in plasma samples and can be regarded as proven sodium sensors for clinical analysis. However, it is necessary to keep in mind that a precision better than 1 % is desirable when measuring plasma sodium. Since the physiological range is relatively narrow, represented only by a short millivolt span, good accuracy and precision is difficult to achieve. This problem is further compounded with simple dipping type measurements where several physical and mechanical interferences are prone to introduce errors. However, this study has shown that it is possible to obtain remarkably close results to the more

sophisticated analysers, by using the inexpensive ISE/bench meter setup.

However, the use of the electrodes in a flow injection analysis approach will certainly improve the precision and accuracy of plasma sodium determinations.

2.10 REFERENCES

1. Worth, H.G.J., *Analyst*, 1988, 113, 373.
2. King, E.J., Haslewood, G.A.D., Delory, G.E. and Beall, D., *Lancet*, 1942, 1, 207.
3. Trinder, P., *Analyst*, 1951, 76, 596.
4. Lochhead, H.B. and Purcell, M.K., *Am. J. Clin. Pathol.*, 1952, 21, 877.
5. Barber, H.H. and Kolthoff, I.M., *J. Am. Chem. Soc.*, 1928, 50, 1625.
6. Lutsgarten, J.A., Wenk, R.E., Byrd, C. and Hall, B., *Clin. Chem.*, 1974, 20, 1217.
7. Solsky, R.L., *Anal. Chem.*, 1988, 60, 106R.
8. Ladenson, J.H., *Clin. Chem.*, 1979, 25, 757.
9. Langloff, E. and Seiness, I., *Clin. Chem.*, 1982, 28, 170.
10. Anker, P., Jenny, H.B., Wuthier, U., Asper, R., Ammann, D. and Simon, W., *Clin. Chem.*, 1983, 29, 1508.
11. Preusse, C.J. and Fuchs C.J., *J. Clin. Chem. Clin. Biochem.*, 1979, 17, 639.
12. Graves, S.W., Koch, D.D. and Ladenson, J.H., *Clin. Chem.*, 1982, 28, 1631.
13. Oesch, U., Ammann, D. and Simon, W., *Clin. Chem.*, 1986, 32, 1448.
14. Morf, W.E. and Simon, W., in "Ion-Selective Electrodes in Analytical Chemistry", Freiser, H. (ed.), Vol. 1, Plenum Press, 1978, p. 211.
15. Cadogan, A.M., Diamond, D., Smyth, M.R., Deasy, M., McKervey, M.A. and Harris, S.J., *Analyst*, 1989, 114, 1551.
16. Zhou, X., Luo, Y., Wu, C., Zou, Z. and Hu, Q., *Anal. Chim. Acta*, 1988, 212, 325.
17. Meier, P.C., Ammann, D., Morf, W.E. and Simon, W., in "Medical and

- Biological Applications of Electrochemical Devices", Koryta, J. (ed.), John Wiley & Sons, Chichester, 1980, p. 13.
18. Tamura, H., Kimura, K. and Shono, T., Anal. Chem., 1982, 54, 1224.
 19. Bates, R.G., Determination of pH, Theory and Practice, John Wiley & Son, New York, 1973, p. 351.
 20. Ammann, D., Bissig, R., Cimerman, Fiedler, U., Guggi, M., Morf, W.E., Oehme, M., Osswald, H., Pretsch, E. and Simon, W., in "Ion and Enzyme Electrodes in Biology and Medicine", Kessler, M., Clark Jr., L.C. and Lubbers, D.W. (eds.), Urban & Schwarzenberg, Munchen-Berlin-Wien, 1976, p. 23.
 21. Simon, W., Ammann, D., Anker, P., Oesch, U. and Band, D.M., Ann Ny Acad Sci 1984, 428, 279.
 22. Vitiello, J.D., Kenney, S.D., Czaban, J.D. and Cormier, A.D., Clin. Chem., 1980, 26, 1021.
 23. Havas, J., Ion-and Molecule-Selective Electrodes in Biological Systems, Springer-Verlag, Berlin, 1985, p. 13.
 24. Henry, J.R., Cannon, C.D. and Winkelman, W.J., Clinical Chemistry, Vol. 2, Harper & Row, Publishers Inc., Maryland, 1980, p. 643.
 25. Skou, J.C., Physiol. Rev., 1965, 45, 596.
 26. Mikal, S., Homeostasis in Man, Little Brown and Company, Boston, 1969, p. 13.
 27. Friedman, S.M. and Wong, S.L., J. Appl. Physiol., 1963, 18, 950.
 28. Krupp, M.A. and Chatton, J.M., Current Medical Diagnosis and Treatment, Lange Medical Publications, New York, 1981, pp.763-850.
 29. Bochner, F., Carruthers, G., Kampmann, J. and Steiner, J., Handbook of Clinical Pharmacology, Little Brown and Company, Boston, 1980, 197.

30. Cecil, R.L. and Beeson, P., Internal Medicine, 9th ed., Lange Medical Publications, Cal. 1978, p. 578.
31. Amper, H.A., Rodwell, V.W. Mayes, P.A., Review of Physiological Chemistry, Lange Medical Publications, Cal., 1977, p.254.
32. Levinsky, N., in "Harrison's Principles of Internal Medicine, Thorn, G., Adams, R., Braunwald, E. and Iselbacher, K. (eds.), Harrison, T.R., 1977, 8, p. 364.
33. Chamberlain, J., Analysis of Drugs in Biological Fluids, CRC Press, Boca Raton, Florida, 1986, p. 140.
34. Collison, M.E. and Meyerhoff, M.E., Anal. Chem., 1990, 62, Report.
35. Maas, A.H.J., Siggard-Andersen, O., Weisberg, H.F. and Zijistra, W.G., Clin. Chem., 1985, 31, 482.
36. Arnold, M.A. and Solsky, R.L., Anal. Chem., 1986, 58, 84R.
37. Anker, P., Wieland, E., Ammann, D., Dohner, R.E., Asper, R. and Simon, W., Anal. Chem., 1981, 53, 1970.
38. Harry, D.J., Davidson, B. and Kenny, M.A., Clin. Chem., 1980, 26, 992.
39. Dahms, H., Rock, R. and Seligson, D., Clin. Chem., 1968, 14, 859.
40. Mohan, M.S., Bates, R.G., Hiller, J.M. and Brand, M.J., Clin. Chem., 1978, 24, 580.
41. Coleman, R.L. and Young, C.C., Clin. Chem., 1981, 27, 1983.
42. Czaban, J.D., Cormier, A.D. and Legg, K.D., Clin. Chem., 1982, 28, 1936.
43. Patel, S. and O'Gorman, P., Clin. Chem., 1978, 24, 1856.
44. Ladenson, J.H., Clin. Chem., 1977, 23, 1912.
45. Foch-Andersen, N., Wimberley, P.D., Thode, J. and Siggaard-Andersen, O., Clin. Chem., 1984, 30, 433.
46. Bijster, P., Vader, H.L. and Vink, C.L.J., Ann. Clin. Biochem., 1983, 20,

116.

47. Gosling, P., *Ann. Clin. Biochem.*, 1970, 7, 131.
48. Mohan, M.S., Bates, R.G., Hiller, J.M. and Brand, M.J., *Clin. Chem.*, 1978, 24, 580.
49. Steffes, M.W., and Freier, E.F., *J. Lab. Clin. Med.*, 1976, 88, 683.
50. Ladenson, J.H. and Koch, D., *Clin. Chem.*, 1981, 27, 1094.
51. Forrest, A.R.W. and Shenkin, A., *Lancet*, 1980, 2, 1256.
52. Dunne, M.J., Shenkin, A. and Imrie, C.W., *Lancet*, 1979, 1, 211.
53. Aw, T.C. and Keichle, F.L., *Am. J. Emerg. Med.*, 1985, 3, 236.
54. Ammann, D., *Ion-Selective Microelectrodes*, Spriger-Verlag, Berlin, 1986, p. 81.
55. Martin, M.J. and Rolfe, P., *Anal. Proc.*, 1986, 23, 303.
56. Kimura, K., Oishi, H., Miura, T. and Shono, T., *Anal. Chem.*, 1987, 59, 2331.
57. Gadzekpo, V.P.Y., Moody, G.J. and Thomas, J.D.R., *Analyst*, 1986, 111, 567.
58. Broughton, P.M.G., Smith, S.C.H. and Buckley, B.M., *Clin. Chem.*, 1985, 31, 1765.
59. Degiampietro, P., Peheim, E. and Colombo, J.P., *Clin. Chem.*, 1985, 31, 302.
60. Mohan, M.S. and Bates R.G., *Clin. Chem.*, 1975, 21, 864.
61. Maas, A.H.J., Siggaard-Andersen, O., Weinsberg, H.A. and Ziglotre, W.G., *Int. Fed. Clin. Chem. News*, 1982, 31, 5.
62. Midgley, D., *Analyst*, 1987, 112, 557.
63. Anker, P., Wieland, E., Ammann, D., Dohner, R.E., Asper, R. and Simon, W., *Anal. Chem.*, 1981, 53, 1970.

64. Durst, R., in "Ion-Selective Electrodes in Analytical Chemistry", Freiser, H. (ed.), Vol. 1, Plenum Press, New York, 1978, p. 326.
65. Illingworth, J.A., Biochem. J., 1981, 195, 259.
66. Cowell, D.C. and Mc Grady, P.M., Clin. Chem., 1985, 31, 2009.
67. Regan, F., Private Data.

CHAPTER 3

Performance of

p-t-ButylCalix[4]aryl Acetate ISEs

in a Flow Injection System

3.1 INTRODUCTION

Present progress in analytical chemistry is based on complex technologies and on the use of sophisticated instruments. As quantitation of analytes in various matrices is a major activity in many laboratories, these have been equipped with a large variety of different instruments for automated analysis. Advances in this area have been stimulated by recognised advantages of automation, such as increased precision, reduction cost of individual sample assay and the satisfactory reliability of automated equipment.

The field in which the automatic methods of analysis have had most significant influence is that of clinical chemistry. Medicine at present relies on a large number of clinical parameters for diagnosis. Diagnosis based on the patient-physician relationship through dialogue and physical examination, has been slowly substituted by the clinical data obtained by the analysis of blood and urine. In whichever direction this important aspect of our society has taken, it is easy to understand the necessity of obtaining a large number of analytical data rapidly and at low cost, in a hospital laboratory during each working day.

At present, methods which have been mostly developed to satisfy these requirements are fundamentally based on the continuous flow analysis concept introduced by Skeggs in 1957 [1]. The proposed approach led to the successful Auto-analyzers of the type produced by Technicon which are based on Skegg's idea. Continuous flow methods form an indispensable part of any clinical laboratory and find an increasing number of applications in other types of routine laboratory analysis. It is this analytical methodology which produced to a great extent the remarkable progress achieved by ISEs in the clinical

field. Their widespread use as flow-through detectors in automated analysers for electrolyte determination and the characteristics of such membrane sensors in continuous flow analysis has been the focus of numerous comprehensive reports [2-4].

Flow injection analysis (FIA) constitutes a relatively recent and important innovation in analytical chemistry [5]. Its attractive characteristics are based in a simple concept, a low cost set-up, simple and easy operation and a great capacity to obtain results with speed, accuracy and precision. It is, however, its versatility which differentiates it from most of the new analytical techniques. It can adapt itself easily to most types of analysis without complex technical changes and it is relatively easy for an analytical researcher to intervene directly in its functioning allowing optimisation of the system and control over the chemical variables. Since FIA has been recognised as a very efficient way of improving wet chemical methods with respect to sample handling and processing, it is not surprising that ISEs are able to benefit enormously from it in terms of the various types of detection systems utilised. However, despite the rather large number of publications including the use of potentiometric sensors as detectors in FIA systems, commercialisation has been disappointingly slow.

The purpose of this chapter is to summarise the concept of continuous flow analysis, with further discussion of the present theory of FIA. In addition, some of the diverse techniques and applications to date of ISEs in FIA will be reviewed. Finally, design considerations for a flow injection analysis system incorporating sodium ion-selective membrane electrodes based on calixarene ionophores and their application to the determination of sodium in human plasma samples will be presented.

3.2 CONTINUOUS FLOW ANALYSIS

In the mid 1950s, the work load in routine laboratories had been increased so much that some kind of automation had become an urgent necessity. At that time, only manual and time-consuming methods were available. It was in 1957 that Skeggs introduced the continuous flow analysis (CFA) technique which proved to be suitable for the automation of wet chemical analysis. Skegg's technique was based on the reaction of samples aspirated from their individual containers, at regular intervals of time, into a tube containing appropriate reagent(s) in a flowing stream. In this way, the samples became a part of a continuously moving stream into which at pre-determined points, reagents were added at fixed flow rates from connecting tubing coils. The treated stream flowed through a cell which was part of the detection system and then passed to waste. The continuous signal so obtained was collected by a recorder and the measurement typically performed in the steady state. Every sample generated a transient signal which had the shape of a curve whose features, such as the maximum height, could be related to the parameter to be determined in every sample. The base line between curves corresponded to the time in which no sample or product of its reaction passed through the detector. The movement of all streams in the channels of continuous flow analysers was controlled by a peristaltic pump which was also responsible for the aspiration of the samples. Through the multiple channels of the analysers the samples could be divided for multiple analysis, and several chemistries performed over the flowing stream by means of diverse separation methods such as dialysis, extraction, filtration, decantation and also distillation.

To overcome an important disadvantage of the concept of continuous flow which is the liability to contamination from the preceding sample (carry over),

air segmentation was also proposed. These methods, which introduce air bubbles to avoid mutual contamination between samples, constitute historically the classical automated methods of analysis developed by the Technicon technology and have received the name of 'segmented flow analysis' (SFA). Such denomination makes reference to the partition of the flow in separated plugs (segmented) which were recognized to promote three primary functions: (1) to limit sample dispersion; (2) to promote mixing of the sample with reagents by generating turbulent flow; and (3) to scrub the walls of the tubes in the system. The development of the required instrumentation resulted in the various 'auto-analysers' used in clinical analysis today.

3.3 FLOW INJECTION ANALYSIS

The absence of air bubbles in a FIA system and the variation of geometric and hydrodynamic characteristics in comparison to segmented flow methods (SFA) constitute the basis of this relatively new methodology.

FIA implies discrete and controlled injection of a sample solution into an unsegmented carrier/reagent moving stream. Thus, at the point of injection, the carrier/reagent solution is pushed aside and a well-defined sample zone or 'plug' is formed and subsequently transported to a flow-through detector cell. Although the detector may record an inherent property of the sample solution (e.g. pH), usually, a selective or preferably a specific reaction will be required to discriminate analyte from sample interferences. Therefore, during its transport to the detector the plug can mix with reagent(s) to induce a chemical reaction. The species formed by a particular reaction (e.g. coloured) can be sensed while passing through the detector cell. The typical recorded signal has the shape of a sharp peak, the height of which is related to the

concentration of the analyte. The sample solution may commonly reach the detector well before steady-state conditions have been achieved.

Non-equilibrium measurements are allowed as long as the timed processes in the analytical conduits of the system are completely reproducible. This leads to relatively short residence times and consequently to high sample throughput.

The experimental working conditions of FIA causes an incomplete mixing of the sample plug which is characterized by two aspects:

- (a) it is variable with time, and therefore is different in every point of the FIA system, and
- (b) this variability must be very reproducible, which means that when the same volume of sample is injected successively, the degree of mixing must be the same at every stage of the transport of the sample to the detector.

These aspects result in a concentration gradient of the sample plug which is variable with time.

The technique of FIA is based on three basic concepts:

- (1) controlled sample injection,
- (2) reproducible timing of the movement of the injected sample from the injection valve to the detector, and
- (3) controllable sample dispersion.

Dispersion, which is the main principle to be considered here, is the physical process of mixing of the injected sample with its surrounding environment. This process, in a dynamic flowing stream, ultimately leads to the dilution of the sample. The dispersion coefficient (D), introduced by Ruzicka and Hansen [6], is defined as the ratio of the concentration of sample solution before (C^0) and after (C^{\max}) the dispersion process has taken place.

$$D = C^0/C^{\max} \quad (3.1)$$

The parameter then describes the degree of dilution of the injected sample in a given time and has a corresponding value at every point of the FIA peak. In this respect, equation (3.1) represents the dispersion coefficient at the maximum of the peak. This dispersion is easily measured for FIA systems with spectrophotometric detection by comparing the absorbance shown by the undiluted sample with its maximum absorbance after dilution. An approach to determine the dispersion coefficient for systems with electrochemical detection has been described recently [7].

The dispersion can be manipulated by adjusting parameters such as sample volume, flow rate, reaction coil, length and inner diameter of tubing. Several researchers have investigated the influence of these [8,9] and other variables, e.g. temperature [10] and flow cell characteristics [11], on the dispersion. Peak width is an appropriate measure to evaluate dispersion. In principle, the dispersion increases with increasing sample volume, residence time, and flow cell size [8,9,11], whereas it decreases with increasing temperature [10]. The fact that dispersion can be manipulated to suit exactly the requirements of an individual analytical procedure it has permitted the classification of the degree of dispersion involved i.e. limited, medium or large [12].

Two mechanisms contribute to the dispersion of the sample zone:

- (1) convective transport developed in conditions of laminar flow, which yields a parabolic velocity profile in the direction of the flow, and
- (2) diffusional transport (predominantly radial diffusion), which promotes mixing perpendicular to the direction of the flow.

An illustration of the net transport result is shown in Fig. 3.1.

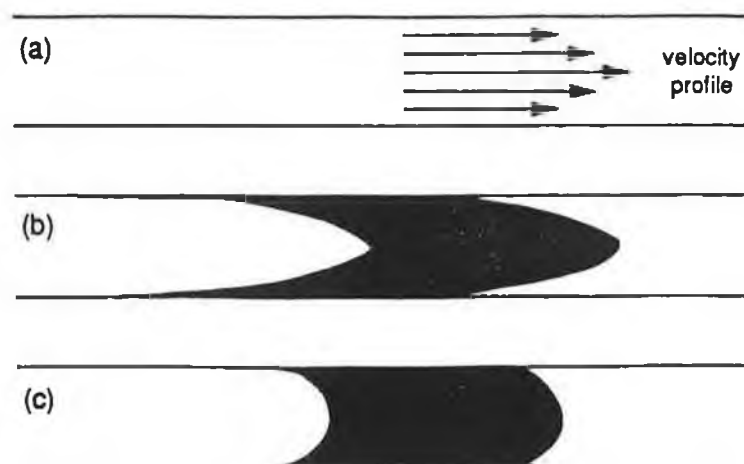


Fig. 3.1 Dispersion of a sample plug in FIA: (a) laminar-flow velocity profile; (b) dispersion of the sample plug caused by convection; (c) dispersion of the sample plug caused by convection and molecular diffusion.

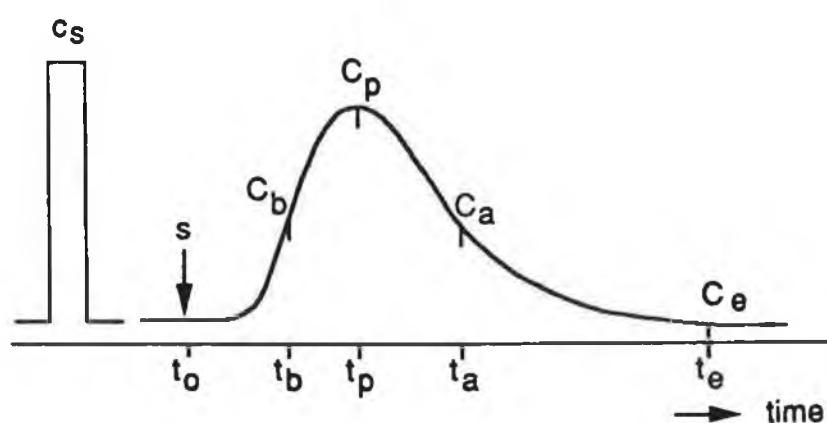


Fig. 3.2 Undiluted concentration, C_s , at time of injection, t_o , and the concentration profile after dilution in the FIA system showing a well defined concentration, C_t , at each time, t_t (t_b , t_a : time before and after peak maximum; t_p : time at peak maximum; t_e : time at end of peak, return to base line).

Although this presentation is useful to understand the effects of the physical processes, one should not be led to think that the plug zone is short and compact. A real behaviour of a sample plug as demonstrated by Tyson [13] shows that a 10 μ l sample injected into a 0.5 mm bore tube would occupy a length of about 5 cm at $t = 0$, before any dispersion has occurred.

Finally, the concentration profile produced over a time period as measured by the detector is illustrated in Fig. 3.2. The original concentration, C_s at time of injection, $t = t_0$, is diluted to C_t at time t_t due to dispersion. Based on the FIA fundamentals, the concentration is well defined at each time.

3.4 THEORETICAL MODELS OF FIA

Having discussed the general characteristics of FIA, attention must now be given to the problem of establishing a theoretical model. The main goal of theoretical modelling is to derive a general expression for the concentration-time function ($C=f(t)$). This function should permit one to define the peak characteristics (eg. starting time, residence, width and peak height or area) and interrelate them with the experimental variables of the system (flow, length of manifold). It would be important however, to stress that it is difficult to predict the behaviour of an injected sample for two reasons:

a) It is not easy to assess the contribution to dispersion of elements such as injection, connections, geometry of the flowing cell, etc. Only empirical relationships between these parameters have been determined.

b) Frequently FIA systems incorporate more than one conduit, hence the effect of mixing tees (size and geometry) must be taken into account, by means of more complex theoretical models.

Two well accepted models to describe the concentration-time function are the 'axial-dispersion' model and the 'tanks-in-series' model. By solving the corresponding differential equations, the concentration profile at a given time can be calculated. However these equations are usually complicated and hence, hard to solve in a direct way. Therefore the time dependent concentration function is commonly obtained by using numerical methods such as the Laplace transformation. The Laplace transformed function allows direct derivation of the statistical moments (i.e. mean and variance), which correspond with residence time and dispersion in the FIA system respectively.

The entire peak profile will depend on the dispersion process and the additional chemical (reaction) and physicochemical processes (extraction or dialysis) if they are present in the FIA system. The overall dispersion as expressed by the variance can be described as a summation of the variances of the individual parts of the system:

$$\sigma^2_{\text{overall}} = \sigma^2_{\text{inj}} + \sigma^2_{\text{transp}} + \sigma^2_{\text{chem}} + \sigma^2_{\text{det}}$$

A complete theoretical model should take into consideration all of the processes already mentioned, i.e., the contributions of elements such as injection operation (σ^2_{inj}), the connectors and tubing (σ^2_{transp}), the additional chemical processes (σ^2_{chem}) and the geometry and size of the flow cell (σ^2_{det}). Theoretical studies have been extensively reviewed by Horvai and Pungor [14].

Currently, the number of these studies is rapidly growing. Recent works investigate aspects such as consecutive reaction kinetics in an FIA system [15], a theoretical description of the dispersion taking into account

simultaneous contributions of injection, transport and detection [16-18], optimisation of confluent mixing [19], and a theoretical model with kinetics and reagent dispersion [20]. Despite the fairly simplified approach of the true systems, theoretical studies permit one to assess to some extent the optimal experimental FIA conditions.

3.5 FIA AND OTHER CONTINUOUS FLOW TECHNIQUES

The continuous flow concept is usually identified with three techniques: FIA, SFA and liquid chromatography. As has been already mentioned, SFA mainly differs from FIA by the use of air segmentation. Air segments are introduced to limit the dispersion of a single sample and so prevent carry-over between subsequent samples. These air segments have to be removed before they reach the detector, although, measurements without debubbling have recently been described [21]. Another inherent characteristic of SFA is that detection typically occurs at steady-state conditions. LC mainly differs from FIA by the use of a chromatographic separation column. The principal objective in LC is the detection of several components from a single injected sample, which obviously involves the separation of sample components prior to detection. Although, it is always possible to interface short chromatographic columns or columns to effect ion exchange, oxidation or reduction with FIA systems, the main objective of FIA has been to automate wet chemical methods.

Differences and similarities in the three techniques become apparent in the instrumentation applied (Fig. 3.3). Further differences from an experimental point of view include the following:

- work pressure: low pressure in SFA and FIA, and high pressure in LC;
- sample introduction: continuous aspiration in SFA, and discrete sample

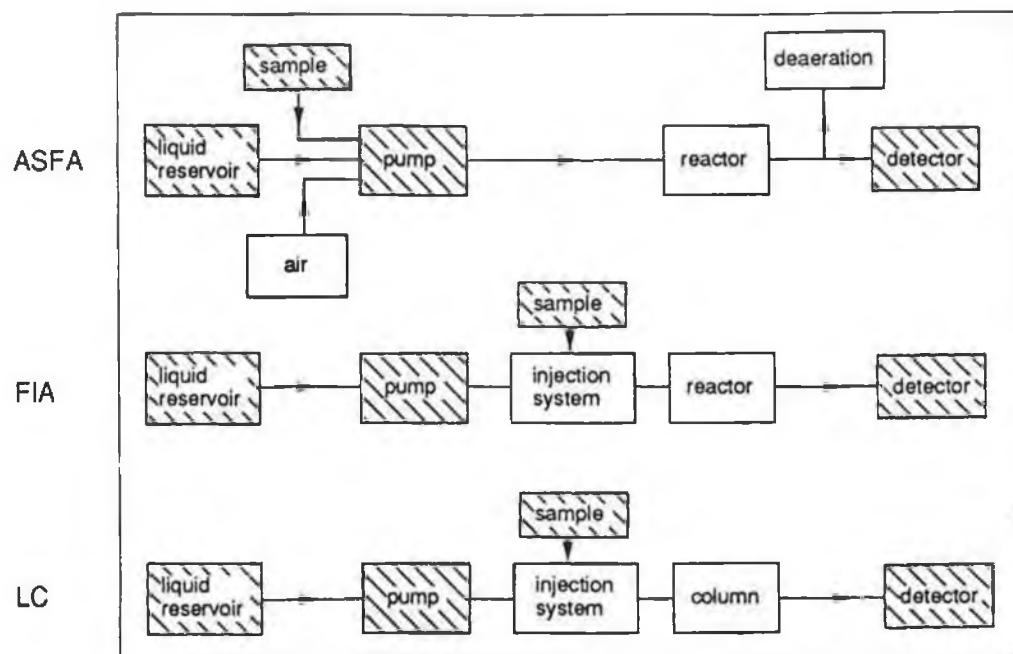


Fig. 3.3 Comparative diagram of continuous flow techniques. The open blocks show instrumental differences of the techniques.

injection in FIA and LC;

- sample throughput: up to 60/h in SFA, up to 15/h in LC and up to 250/h in FIA

Naturally, from experimental considerations, it can be seen FIA complements both SFA [22] and LC [23].

3.6. INSTRUMENTATION

The basic essential parts of a simple FIA system (Fig. 3.4) include the following:

a) a pump to propel the flowing stream through the different elemental units. This must deliver a constant and regular flow, which must be free from pulsation and perfectly reproducible;

b) an injection valve to introduce very precise and accurate sample volumes;

c) a manifold system to connect the different elements and permit the flow and mixing of the sample with the carrier stream(s). In cases where the mixing is not adequate for the analysis or a reaction and division of the stream is required accessory elements can be introduced such as mixing chambers, differing reactor types and mixing tees;

d) a detection system that permits the continuous measurement of the analyte by some means.

These very simple instrumental requirements facilitate experimentation with FIA. Naturally, the performance of each of the basic components can vary from simple and/or cheap to advanced and/or expensive. Recent advances in FIA instrumentation, and its extension in relation to the use of potentiometric detectors will be discussed below.

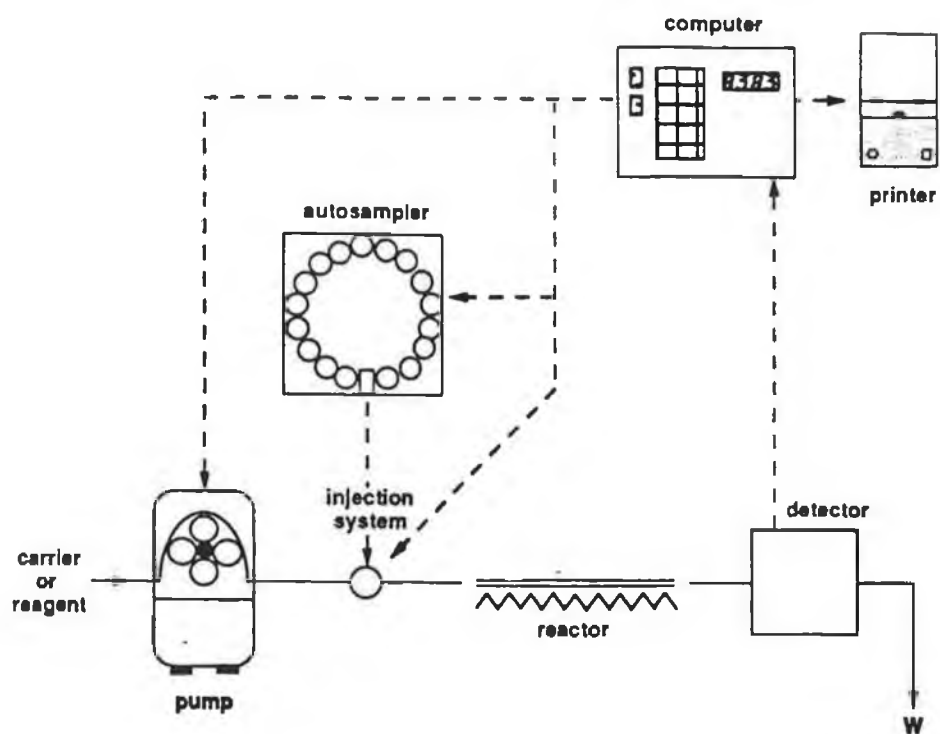


Fig. 3.4 Schematic of the instrumental set up of a FIA system. Dashed lines indicate the components that can be automated.

3.6.1 Pump

Peristaltic pumps which easily accommodate several channels are most commonly used to propel carrier and/or reagent stream(s) at a constant flow rate. An important advantage of this type of pump is the almost instantaneous Start/stop function, while its main drawback is the existence of a pulsating flow. However, if pulse-free FIA systems are required, a pumping device with a pressurised carrier/reagent vessel or piston burette is used. When the FIA system includes pressure building components, e.g., packed bed reactors or a typical HPLC-detector provided with a narrow bore capillary, a high pressure pump will be needed.

3.6.2 Injection Valve

Although several injection systems of varying degrees of complexity have been described e.g., syringe, proportional injector, solenoid valves and others, the six-port rotatory valves provided with an exchangeable fixed volume sample loop are most commonly used. An alternative method of sample injection indicated as 'hydrodynamic injection' and introduced by Ruzicka and Hansen [24], allows accurate and reproducible sample introduction based on controlled sample suction. This approach has been further improved and applied successfully as 'controlled dispersion flow analysis' in clinical applications [25].

3.6.3 Manifold/Reactor System

The use of different manifolds will depend upon the complexity of the chemistry involved in a particular analysis.

The simplest type consists of teflon tubing or a similar material and follows

the early concept of low dispersion single line manifold. The tubing may be simply straight, but when coiled, the dispersion is usually decreased [26]. Reijn et al. [27] have introduced the single bead string reactor (SBSR), a tube packed with glass beads having a diameter of about 70% of the inner tube diameter. This reactor presents certain advantages such as:

- a) increase in the residence time,
 - b) a rather drastic decrease of dispersion, and
 - c) a more stable base line in comparison to the simple teflon tubing,
- probably due to the suppressing effect of the beads on the pulse.

Packed reactors, consist of a zone of tubing which is packed with an inert or chemically active material. Those that have attracted most attention are the chemically active designs such as those incorporating ion exchange, redox and enzymic materials. Heterogeneous reactions involve immobilized enzymes or solid-phase reagents and, consequently the use of packed reactors.

Interferents can be removed on-line by using special devices which allow continuous separation. These techniques have been reviewed by Valcarcel and Luque de Castro [28]. The separation principles commonly employed in FIA systems include dialysis, liquid-liquid extraction, ion-exchange and adsorption. Dialysis is based on the use of a selective membrane through which the analyte in question transfers from a donor stream (flowing to waste) into an acceptor stream (flowing to the detector) [29]. Separation based on liquid extraction needs segmentation of the carrier stream with an organic liquid stream and insertion of a phase separator prior to the detector. Several types of segmentators have been applied [30], and recently, liquid-liquid extraction without phase separation has been introduced [31]. The use of small ion-exchange and adsorption columns facilitates sample clean up and/or

preconcentration when required.

Although, these on-line sample pretreatment steps are frequently applied in techniques such as atomic spectrometry, they can also be applied to FIA systems incorporating electrochemical detectors such as ion-selective electrodes, as will be seen in section 3.9.

3.6.4 Flow Cells and Detectors

Almost any small-volume flow-through detector can be used in FIA. In fact, much of the versatility and popularity of the technique is based on the possibility of easily coupling any type of detection system. Classically, spectrophotometric methods, UV/VIS absorbance, fluorescence and chemiluminescence have received much attention. The most common is atomic spectrometry, which is a widely reported combination [32]. Electrochemical detection including amperometric and potentiometric techniques are also commonly employed, and in this research we have focused on the latter.

3.6.4.1 ISE Flow-through Cells

Several flow-through electrode cell arrangements for the potentiometric determination of ions have been devised. Some commonly used assemblies are shown schematically in Fig. 3.5. The ion-selective electrode in these systems may be part of a small channel zone or alternatively, occupy the whole channel wall. Another approach (Fig. 3.5b) is where the ion-selective electrode protrudes into the sample channel. The electrodes are coupled to cell assemblies as shown in Fig. 3.6. Examples are the well known thin layer cell and tubular membrane flow unit, which are shown in Fig. 3.7a and 3.7b, respectively. Further design considerations of flow-through systems which have

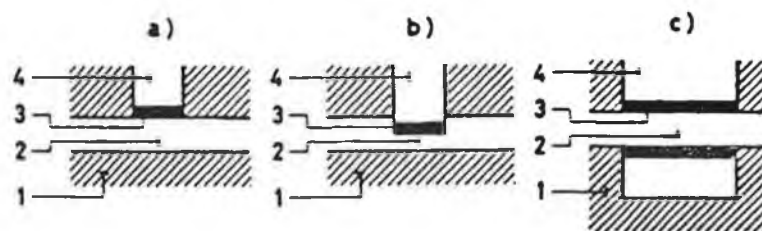


Fig. 3.5 Schematic of ISE flow cells showing the sample channel lining (1), the sample channel (2), the ion selective membrane (3), and the internal reference system (4).

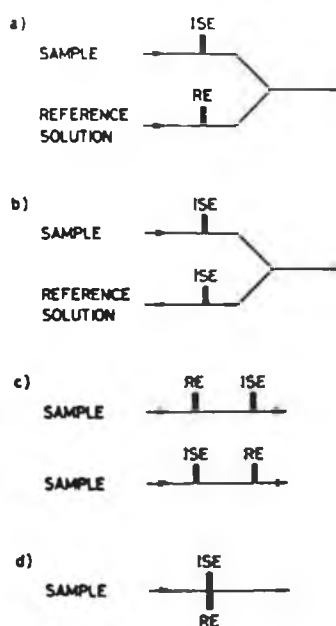


Fig. 3.6 Arrangement of ion-selective electrodes in flow systems. The two channel design are shown for conventional (a) and differential (b) measurement techniques. In the single channel designs the two electrodes can be in series (c) or juxtaposed (d) [33].

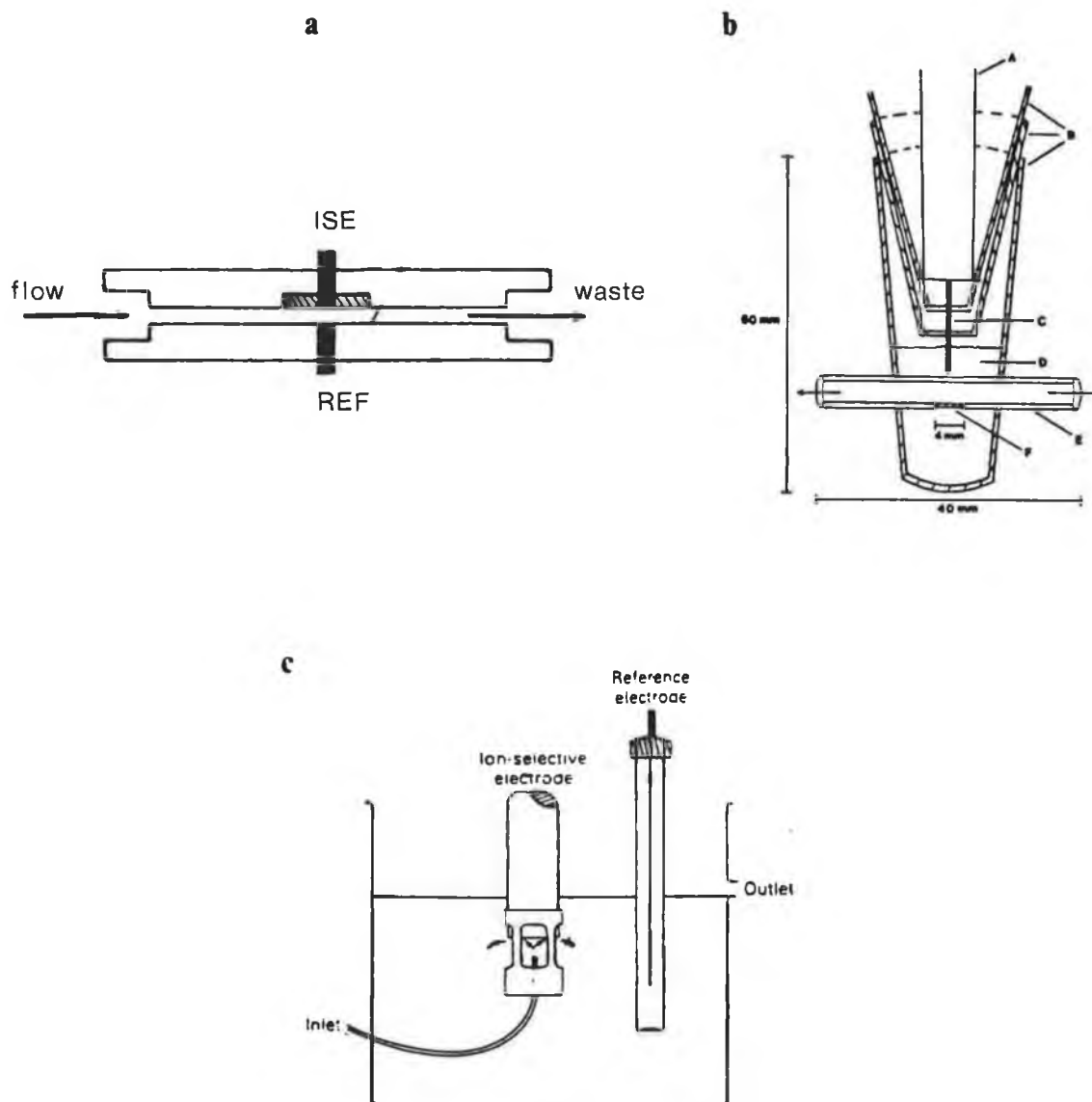


Fig. 3.7 Schematic diagram of different type of flow-through units. (A) thin layer type flow cell; (B) tubular ammonium selective polymer membrane electrode unit: a) coaxial cable, b) plastic pipette tips, c) Ag/AgCl electrode, d) $10^{-2} \text{ mol l}^{-1} \text{ NH}_4\text{Cl}$, e) tubing (0.89 mm), f) PVC-nonactin ammonium selective membrane [54]; (C) large volume wall jet cell.

become widely accepted for use with ISEs are shown in Fig. 7c. In this case, the carrier stream leaves the sample channel close to the vicinity of the sensing electrode before coming in contact with the membrane. Examples of these include: single drop [33], cascade [34] and jet-flow cells [35].

Unfortunately, the variety of existing flow-through cells for ISEs makes it difficult to give a general statement on which design is best. Ruzicka and Hansen, who have contributed extensively to the development of the potentiometric technique in FIA, have employed ISEs in tubular and other arrangements, with the reference electrode located in different zones of the system (although usually after the indicator electrode). The use of ISEs in cascade or series flow cells has permitted the simultaneous determination of several species [36].

According to Frenzel's experience [37], several experimental requirements of ISEs in FIA are met with the wall-jet cell design. His report stresses on the minimum thickness of the hydrodynamic (diffusion) layer and hence fast response obtained with this cell. In order to eliminate liquid junction effects, a large volume wall-jet cell is used. In addition, the reference electrode positioning effects are resolved, while the cell configuration makes it suitable for use with many commercially available electrodes. However, in other applications, such as simultaneous or multidetection and series differential detection (see section 3.8) where it is necessary to ascertain how the flow cell contributes to sample dispersion at a down stream position, tubular or thin layer design would seem to be more appropriate.

The ideal flow-through cell for ISE detection, as outlined by Frenzel [37], should possess low dead volume, fast response, good wash characteristics,

practicability, simple maintenance, ease of construction and compatibility with commercially available electrodes of various sizes and shapes. Moreover, the arrangement of the reference electrode in the cell assembly has to be carefully examined. Difficulties associated with base line drift, liquid junction effects, streaming potential and electrostatic noise are commonly encountered due to the incorrect positioning of the reference electrode. Several of these characteristics will be further discussed in section 3.7.

3.6.4.2 ISFETs

Relatively recent developments in potentiometric detection systems for FIA include the flow-through ISFET detector [38], and the use of an ion-selective electrode array for multi-ion sensing analysis [39].

With respect to ISFETs, there are several important advantages in relation to conventional ISEs in FIA. These include: miniaturisation, low signal/noise ratio, faster response time and less contribution from the detector to the dispersion of the sample. As ISFETs can be miniaturized conveniently, it is possible to place several of them on a single chip, permitting the analysis of multicomponents in FIA systems [40]. Such multi-component determination in FIA has been recently developed for arrays of conventional ISEs. The use of such a system for the determination of potassium, calcium, nitrate and chloride in soil extracts has been described recently [39].

3.6.5 Computerisation

Certain functions in FIA systems such as pumping, injection, and data acquisition may be easily operated by computer control. Several papers dealing with this kind of automation have been reported [41,42]. Furthermore, the

application of chemometric methods in FIA is growing and has been applied to system optimisation [43], and advanced multivariate data evaluation [44].

3.7 SOME CHARACTERISTICS OF ISEs IN FLOWING SYSTEMS

Electrochemical detectors are of importance in hydrodynamic systems due to their selectivity, sensitivity and wide working concentration range. The intrinsic nature of electrochemical processes, which generally occur in membrane surface rather than bulk sample volume, make them attractive and more convenient for detection in miniaturised systems. Another important aspect to be considered is the compatibility of the flow-through principle with the ion-selective electrode membrane. Hence, the permanent carrier stream flowing through the ISE membrane has a conditioning effect over the sensor, which leads to a better stability of the system and increased reproducibility of the emf readings. Also the way in which the sample is presented to the ISE membrane is more closely defined and reproducible under flowing conditions than in the static conditions of batch measurements. This can be further emphasised by the obvious benefit of eliminating any chemical and mechanical interference arising from normal electrode operation procedures (washing, cleaning, changing solution etc.,) commonly associated with stationary measurements. Dynamic characteristics are usually improved with flowing methods since with suitable cell designs the rate of transport processes is increased.

3.7.1 Response Time

Among the processes that contribute to the dynamic response behaviour of membrane electrodes, the diffusion of the sample ions through the stagnant layer is of important consideration in flowing systems. The streaming of the sample

solution is beneficial since it reduces the thickness of the Nernstian diffusion layer which, together with the diffusion coefficient D of the ion considered, affect the time constant t (eqn. 3.3) characterising the response time of any ISE.

$$\tau = \frac{4 \delta^2}{\pi^2 D} \sim \frac{\delta^2}{2 D} \quad (3.3)$$

Thus, flow-through ISE detectors generally exhibit a high speed of response [45].

3.7.2 Liquid-Junction and Reference Electrode

Additional factors which must be considered for any ISE measurement are the form, type and position of the reference electrode and its liquid junction potential [33]. Recognising that it is a key component influencing the performance of flow-through cells, it has been suggested [33] that free-flowing liquid-junctions lead to the highest reproducibility of the liquid-junction potentials and therefore to the highest emf stability. Reproducibilities in the emf measurements of about $25 \mu\text{V}$ have been achieved [46]. To maintain the values of liquid-junction potentials as low as possible, equi-transferent solutions of high concentration should be used as reference electrolytes in contact with the sample solution. However, even in some cases when using saturated KCl or 1.0 M KNO_3 , this potential can amount to several millivolts [47]. Here, the preferred remedy is a constant ionic background in the sample. Although clinical samples like blood plasma or serum usually have a

fairly regulated ionic composition, the use of concentrated equi-transferent solutions is still suggested. Finally, in flowing systems the reference electrode can often be positioned down stream from the indicator electrode, and hence the electrolyte diffusing from the reference electrode cannot contaminate the sample solution.

3.7.3 Streaming Potential

In FIA systems in which ISEs are used as detectors, oscillations in the measuring potential caused by the pump actuation are always present. This is due to the fact that when a liquid is forced through a narrow capillary, a potential difference is set up between the two ends of the capillary tubing. This potential described by eqn. (3.4), is called the streaming potential, under laminar flow conditions:

$$E_s = \frac{2d\epsilon\zeta l}{\pi^2 r^4 \lambda} \quad (3.4)$$

where d is the flow-rate, ϵ is the dielectric constant, ζ the electrokinetic potential, l the length of the tube connecting the ISE with the reference electrode, r the radius of the tube and λ the conductivity. When all parameters in eqn. (3.4) are kept constant, the streaming potential remains constant and is simply added to the emf of the cell. However, this is not normally the case, since the flow-rate always tends to pulsate to a certain extent, provoking oscillations in the value of E_s , which appear in the

signal as periodic noise. One method of suppressing, the streaming potential is to add a large amount of inert electrolyte, so as to increase the conductivity of and lower E_s . This is obviously limited in many cases by the possible interference of the added salt on the electrode response. Other common solutions involve the optimisation of parameters such as d , r , and l , and the incorporation of pulse suppressors in order to decrease the amplitude of the flow-rate oscillations. According to Morf and Simon [33], E_s is insignificant in typical clinical applications, amounting to a total of only 0.65 μV . Recently, Christopoulos and Diamandis [48] have minimized streaming potentials and proposed flow-through cells for solid-state, liquid and PVC matrix ion-selective electrodes with the reference electrode positioned very close to the sensing membrane of the ISE. However, their proposed arrangement only assures a base line noise of $<0.2 \text{ mV}$, which for some practical clinical applications (e.g. Na^+ , Ca^{2+} determination) would obviously introduce significant uncertainty.

3.8 POTENTIALS OF FIA

FIA applications involving the use of ion-selective electrodes can be subdivided into three categories:

- (i) Automated sample processing: the simplest application of the flow injection technique is its use as an automated sample introduction procedure.
- (ii) Automated sample processing and solution handling: wet chemical batch assays based on selective chemical reactions and transformed to flow-injection methods. Here, a reagent stream is needed, and several reagent streams can easily be used.
- (iii) Automated sample (pre)treatment: In this case, extraction units,

dialysers and small packed columns have been inserted in the flow system.

Moreover, the FIA approach inherently offers advantages which can not be achieved by batch methods. For example, several gradient techniques [49] have been developed based on the well-defined concentration profile. This technique allows controlled amplification or dilution [50], zone sampling [51] and pseudo titration methods [52]. The stopped-flow mode, which is usually based on intermittent (stop-go) pumping, can also be applied. In this case the sample plug may be stopped in the detector cell and the sample/reaction is monitored over a period of time.

Series differential detection is another approach which can enhance sensitivity. The concept of this approach is shown in Fig. 3.8 together with a calibration curve for fluoride ions performed by the same technique. The shape of each type of signal is determined by the response time of the particular ISE, the carrier flow rate, the injection volume and the length of the connection between the two ISEs. The advantages of series differential detection methods lie in the improvement in sensitivity, the simpler evaluation of the signal and the fact that no reference electrode is required. Modified reverse flow injection analysis has been recently considered by Frenzel as another potential use of ISEs in a flow injection system. In this case, a branch stream feeds the injection loop of a flow injection manifold. The technique is a novel approach in that the information gathered from the sample and the standard solution is obtained almost simultaneously. The principle is shown in Fig. 3.9 together with the recorder output for various potential applications. Characteristics, advantages and differences of the modified reverse flow injection analysis approach in comparison to classical FIA procedures have been reviewed by Van der Linden [53].

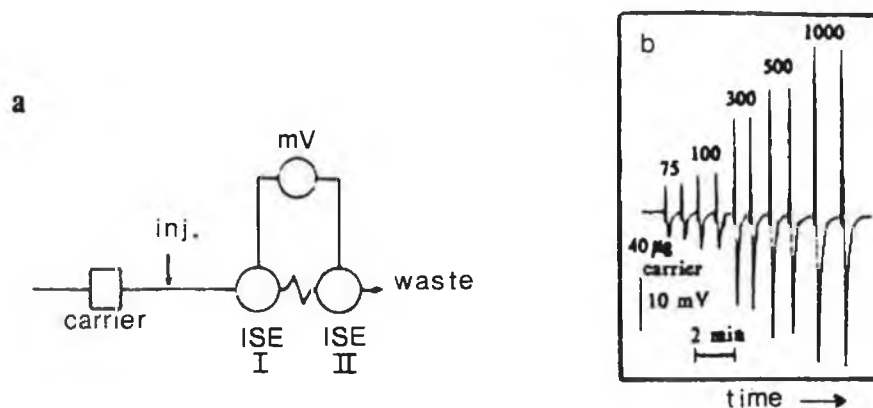


Fig. 3.8 Principle of series differential detection with two ion-selective electrodes (a). Calibration curve for fluoride determination at the $\mu\text{g ml}^{-1}$ level by series differential detection (b) [37].

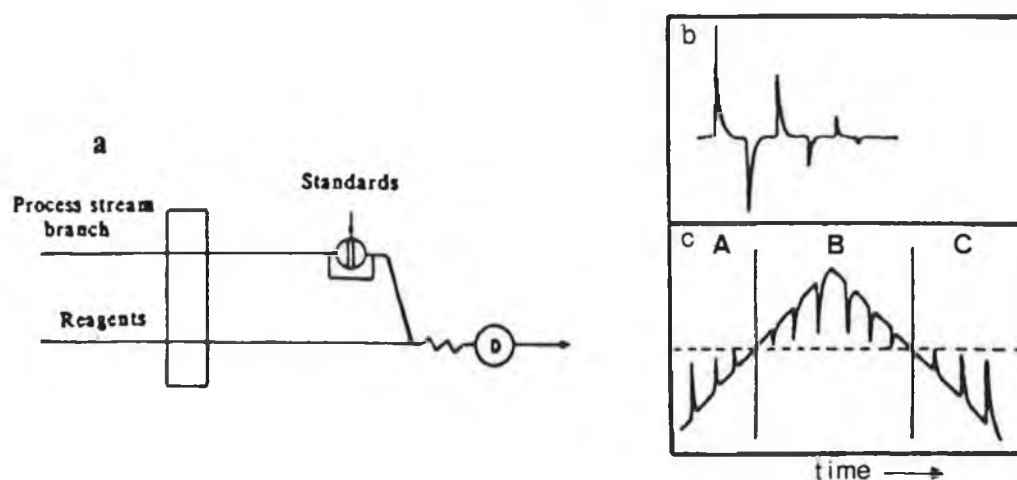


Fig. 3.9 Modified reverse FIA technique for continuous monitoring and process analysis. (a) Flow manifold. (b) Representation of the recorder output after successive injection of standards, the concentrations of which are chosen to equal that of the samples (i.e., the process stream branch). (c) Schematic depiction of a triangle shaped concentration change of the sample with repeated injections of the same standard solution. In (A) and (C) the concentration of the sample is lower than that of the standard; in (B) it is higher than that of the standard injected; and at the two points of intersection with the broken line it is equal. An obvious application is the monitoring of species to control either the deviation from a pre-set value (broken line) or the infringement of a limiting value [37].

3.9 SOME APPLICATIONS OF ISEs IN FLOW INJECTION SYSTEMS

The use of FIA in clinical chemistry is an important and expanding field in which the development of automated assays can be carried out. Potentiometric detection has been frequently employed in FIA-based clinical analysis. Ruzicka and co-workers [36] have demonstrated the advantages of ISEs by applying the flow injection technique to the determination of potassium and sodium in blood serum. Both analytes are measured simultaneously in one stream, obtaining a sampling rate of 125 samples/h with a R.S.D. of 0.8%. Gas dialysis has been successfully applied in FIA for the determination of ammonia in blood samples [54]. The ammonium electrode based in a solvent polymeric membrane is able to measure the analyte in the 10^{-5} to 10^{-3} M range. Similarly, tubular-type electrodes have been used for the determination of chloride and cyanide in blood serum [55]. The determination is carried out in a configuration incorporating two $\text{Ag}_2\text{S}/\text{AgCl}$ electrodes directly connected in such a way that the potential difference generated by one channel containing the sample against another containing the background electrolyte is measured. Other analytes of biological interest such as calcium [56], lithium [57] and hydrogen [58] have also been measured using different flow-through cells. The development of ISFETs has permitted a reduction in the size of these potentiometric detectors to an extent where it is now possible to introduce them into a hypodermic syringe or a catheter, hence allowing the determination of several parameters in-vivo [59]. The fruitful combination of chromatography-FIA with potentiometric detector has also been employed in clinical chemistry for the determination of copper [60]. The stripping potentiometric technique has also found grounds in this field for the determination of mercury in urine and residue samples by using a gold electrode [61].

Another area where ISEs have been used as FIA detectors is in environmental chemistry. The development of methods for the determination of many cations and anions in waste and drinking waters, nutrition plants and rain have been proposed. Hansen et al [62] have determined nitrate in residual waters, air and extracts of soils and fertilizers employing ISE based detection. Despite the rather large sample volume (0.3 ml) a high sample throughput was obtained 90 samples/h. Calcium and pH have also been measured simultaneously in the same stream by these workers [34]. Thomas et al [63] have adapted an Ag_2S electrode in a FIA system for the analysis of sulphur in industrial water processes. A multi-ion sensor cell and data-acquisition system for flow injection analysis has been demonstrated for the simultaneous determination of potassium, calcium, nitrate and chloride in soil extracts achieving both good precision and fast sample throughput[39]. The same workers [64] have developed a FIA system incorporating two hydrogen sensitive PVC membrane electrodes in the same detector cell which can cover the pH range 1-13. Although no application has been presented, solution ionic strength and buffer capacity on the pH measurement are discussed. Frenzel et al [65] have used a metallic silver wire electrode in the presence of cyanide in connection with gas diffusion FIA. Interferences of sulphide, sulphite and nitrite have been removed by on-line oxidation of these compounds before entering the gas diffusion unit. By using the same electrode Frenzel has also reported [66] the potentiometric determination of sulphide by converting hydrogen sulphide passing through a diffusion membrane into the sulphide anion in an acceptor stream containing ammonium sulfate and sodium hydroxide. The fluoride electrode has been extensively studied by Frenzel[67] in FIA systems. Measurements at low concentration levels indicate that 60 to 180 samples/h at the 1 ug ml^{-1} level

can be obtained. The same fluoride ISE has proven useful for indirect determination of aluminium by direct sample injection. The results showed that trace amounts of aluminium were determined with high sensitivity, precision and fast sampling rate in a FIA system [37]. Two configurations of copper ISEs (i.e. a dismountable and a disposable flow-through electrode have been employed for the determination of copper in drinking water [68].

3.10 EXPERIMENTAL WORK

A sodium ion selective membrane based on methyl-p-t butylcalix[4]aryl acetate and its application to the determination of sodium in plasma samples has already been described in chapters 1 and 2. The present experimental work involves the study of some characteristics of this calixarene membrane electrode when incorporated in a flow-injection system. Emphasis will be given to the instrumental set up and its optimisation owing to the key role these parameters play in the efficient functioning of the system.

The detector unit comprises a thin-film polymeric ion-selective membrane which is incorporated in a Technicon flow-through cell. The approach to optimisation of the cell response will be described in terms of the physical, electrical and hydrodynamic parameters which affect its performance. Some characteristics of the electrode such as its response and inherent influence over the flowing conditions in regards to this system will be discussed. The same instrumental set up will serve to demonstrate the feasibility of applying the calixarene polymeric membrane to the analysis of sodium. The advantageous implications of a FIA system regarding precision and accuracy as well as the potential high sample throughput will be demonstrated with respect to the analysis of sodium in clinical samples i.e. blood plasma.

Finally, it will be shown that with this approach, good precision and accuracy can be achieved for a difficult analysis using very simple and inexpensive instrumentation.

3.11 APPARATUS

A Technicon flow-through cell which incorporates the ion-selective electrode membrane was employed as the detection cell. A peristaltic or alternatively a chromatographic pump (Waters Associates) equipped with a rotatory injection valve with interchangeable sample volume loops served to propel the carrier stream. The bridge electrolyte solution passing through the reference electrode was pumped with a computer controlled precision solvent delivery system. The measuring device used was a Phillips PW 9421 pH-millivolt meter which was connected to a Linseis 16512 chart recorder. A third platinum auxiliary electrode to reduce noise level associated with the measurement completed the required electrochemical system.

The analysis of plasma samples by flame photometry was carried out with a IL 943 flame photometer.

3.12 MATERIALS AND SAMPLES

All chemicals used for electrolyte solutions (NaCl , LiCl , KCl , CaCl_2 , MgCl_2) were of analytical reagent grade and the solutions prepared in distilled-deionized water. Salts of tris buffer were obtained from Sigma. The calixarene ionophore employed was from the same source as for the work presented in chapters 1 and 2. The plasticiser mediator 2-nitrophenyl octyl ether (2-NPOE), the lipophilic additive potassium p-tetrakis-chlorophenyl borate (KpTCIPB), poly(vinyl chloride) (PVC) and tetrahydrofuran (THF) were all supplied by Fluka.

Plasma samples were obtained from the Biochemistry department at St. James Hospital, Dublin. The hospital provided the results for the sodium analysis performed with the Smac Technicon 3 analyser.

3.13 MEMBRANE AND ELECTRODE PREPARATION

For the thin film membranes, a master membrane was prepared according to the following procedure: in a 5 ml glass sample bottle, 6 mg of ionophore were dissolved in 600 mg of solvent mediator together with 1.5 mg of ion exchanger. The mixture was stirred and slightly heated on a hot plate magnetic stirrer for approximately 5 minutes. When the added salts were completely dissolved, 300 mg of PVC was added to the mixture. Under continuous vigorous stirring about 2 ml of THF was added to this solution. The resulting solution was allowed to settle to eliminate bubbles formed during the stirring stage and the resulting volume divided and poured into 2.0 x 1.5 cm glass moulds set on glass plates. The moulds containing the liquid cocktail were covered with tissue to absorb the THF vapour and subsequently a heavy object was placed on top to prevent the cocktail leaking from the mould. After approximately 24 hours the THF had evaporated leaving a yellowish transparent flexible membrane around 0.1-0.2 mm thick. Disks of 9 mm diameter were cut out using a cork borer and placed on a plastic plate which acted as a support. Thereafter a small round container which holds the internal filling solution (0.1 M NaCl) was positioned on top of the membrane plate, and clipped in place pressing the membrane against the perspex block.

3.14 FIA ARRANGEMENT

A simple single-line FIA arrangement was used throughout this investigation. The initial approach taken was to assess the output signal stability from the ISE cell to the chart recorder. It is a well known fact that almost all of the parts of the FIA system affect the general stability and noise level of the response signal. The ISE membrane, electrical leads,

connecting manifold filled with high conducting electrolyte, pump and valve actuation, positioning of the reference electrode and so forth are key aspects to be considered. These aspects were carefully taken into account in designing the system layout.

PVC tubing in 2 cm diameter coils around a tube support (25 cm long) was connected to the outlet of the chromatographic pump and then to the injection port. In the same way the outlet of the bridge electrolyte delivery system was connected to the inlet of the detector cell by a 40 cm long coiled (2 cm diameter) PVC tube 0.5 mm i.d. A gas cylinder containing air acted as a source of pressure for pumping the bridge electrolyte. A pressure transducer was placed in a 1 liter glass container and the container filled half of its volume with bridge reference electrolyte (0.1 M KCl) solution. The transducer was connected to a gas solenoid valve which was in turn connected to a differential amplifier and to a BBC microcomputer. The software enabled the computer to detect any drop in the pressure pumping the salt bridge electrolyte from the reservoir, and to compensate by opening the gas solenoid valve. Hence the bridge electrolyte flowed at a constant rate without any pulsation.

In order to eliminate undesirable noise it was decided to use a third auxiliary electrode. This was achieved by introducing a 1.5 cm platinum wire, soldered to a metallic conductor, through an opening made in the tubing going to waste. The orifice was then sealed with epoxy resin and the electrode connected to earth.

In general the use of a third auxiliary electrode has been suggested as an alternative to eliminate undesirable electrostatic action generated by the pump and valve actuation. Another approach widely recognised as a solution to reduce electrostatic interferences is the isolation of the detection system

in a faraday cage. Although this option can be equally efficient it seemed less convenient from a practical point of view.

However, to further minimize interfering noise the detection cell was completely isolated by mounting it inside an aluminium box which acted as a faraday cage. Appropriate holes were drilled in the box to permit the communication of tubing with the cell. The box was then grounded from at least two different points and closed with an aluminium lid.

To prevent noise associated with the injection valve actuation two earthing wires connected it to the faraday cage.

Another important contribution to the noise level in the system is the positioning of the reference electrode in a FIA system. This aspect may become crucial and therefore must be carefully considered [69]. A maximum distance of 10 cm between the ISE and reference electrode can be considered acceptable for most cell configurations when both electrodes must remain separated. However, in the present experimental conditions the reference electrode remained about 2 cm away from the ISE membrane and no further contribution was expected from this source.

A schematic of the FIA set up is shown in Fig. 3.10. Previous to the functioning of the FIA system the electrode design unit dictated the necessity of establishing the flow rate of the bridge electrolyte solution. The optimum flow rate had to be fast enough so as to avoid contamination of the reference electrolyte channel by the carrier stream and relatively slow to enter the waste channel together with the sample rather than passing by the ISE membrane. Accordingly, the velocity of both streams was assessed in a broad margin of flow rates by passing a dye solution either as a carrier stream or as a reference electrolyte and observing the possible back-diffusion in either

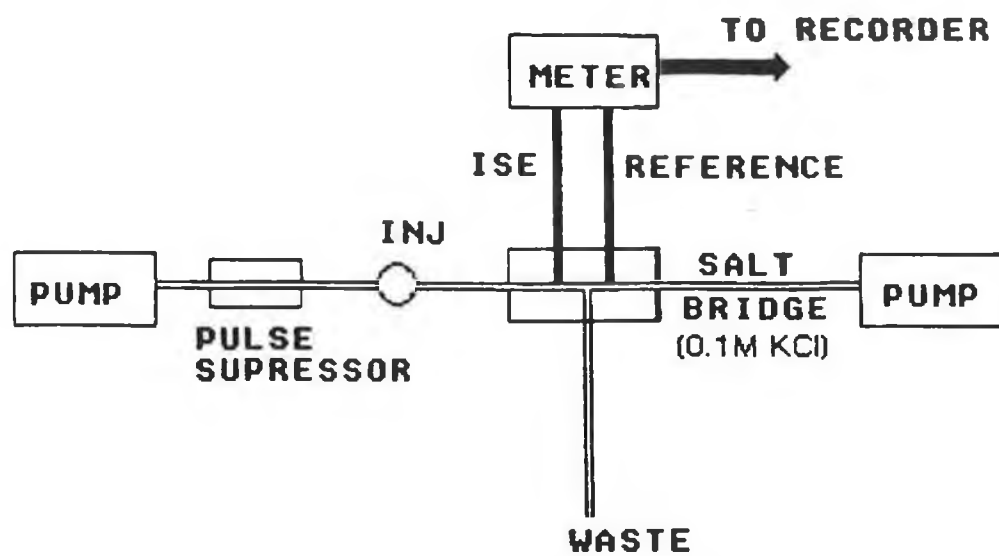


Fig. 3.10 Schematic diagram of the flow injection measuring system.

direction. The results of this work showed that the contamination of one or the other channel stream did not occur at any extent in a wide range of flow rates used. Only when the reference electrolyte flow rate was as low as 0.3 ml min^{-1} and the carrier stream passed at flow rates above 3.4 ml min^{-1} was the dye solution seen to invade the reference electrode channel and produce colouring of the bridge electrolyte solution.

Before incorporating electrodes into the system they were calibrated by determining their slopes under steady-state conditions in NaCl solutions ranging from $1 \times 10^{-4} \text{ M}$ to $1 \times 10^{-1} \text{ M}$. In all cases electrode membranes with slopes over $55.0 \text{ mV decade}^{-1}$ were used.

The membranes were placed on the plastic plate and left to condition in a beaker containing 0.1 M NaCl for at least half an hour prior to use.

3.15 ELECTRODE RESPONSE

The general stability and noise level was experimentally assessed by exposing the membrane electrode to a carrier stream containing $1 \times 10^{-3} \text{ M NaCl}$ and $1 \times 10^{-1} \text{ M LiCl}$. The incorporation of sodium in the carrier composition prevented the membrane from being redundant, provided a more stable base-line response, improved dynamic factors influencing response time to sodium injections and provided a more efficient wash out cycle. Lithium at relatively high concentration decreases streaming potentials and acts as an ionic strength adjustor. In all instances, the carrier stream solutions employed were filtered in a millipore system and degased for 15 minutes in an ultrasonic bath.

A considerable degree of noise was observed when the HPLC pump was switched on. This delivered the carrier stream through the electrode at a flow

rate of 1.0 ml min^{-1} . A stabilisation time of at least one hour was found to be necessary under the stated conditions with this pump. However, a continuous monotonous base line drift of 3.0 to 4.0 mV per hour and occasional baseline fluctuations were still observed even when the system reached its maximum stability.

A new ion-selective electrode may tend to shed the sample stream solution because of the high surface tension of the membrane [36]. In this respect Ruzicka et al [36] have suggested the addition of a non-ionic neutral surfactant or 1 % glycerine to the conditioning solution as well as to the carrier stream to ensure an even coverage of the membrane. However the introduction of surfactant was not considered either in the carrier stream or the conditioning solution and the conditions stated above marked the initial stage of this work.

To determine the basic response properties of the electrode in the FIA system, repetitive injections of 25 μl of 1×10^{-3} to 1×10^{-1} M NaCl were introduced in the carrier stream by loading the sample loop with a manual syringe. The length of the tubing from injection port to detection cell was 50 cm. The injections gave rise to large responses in every case but with very poor discrimination between concentrations (Fig. 3.11). Despite this inconvenience peak heights were reproducible to repeated injections of the test solutions and almost instantaneous responses were observed from the time the sample was injected until it reached the top of the peak. However, return to base line was incomplete and achieved only after a few minutes for the 0.1 M injection.

Although a high concentration of lithium is present in the carrier stream (0.1 M) in relation to a much lower concentration of sodium (10^{-3} M)

the selectivity coefficient K_{NaLi}^{pot} -2.45 (separate solution method) would still appear to permit a favourable response to sodium ions, at least under steady-state conditions. However, this composition, although proving to be advantageous from the point of view that it was without periodic noise, (perhaps owing to the high electrolyte concentration) seemed to suggest that the electrode response to lithium ions cannot be overcome quickly enough to permit the rapid passing sodium solutions to dominate the electrode response. Only when the flow rate was lowered to 0.3 ml min^{-1} was the size and discrimination between calibration peaks improved. The presence of double peaks implied some interferent was present. Consequently, the lithium ions were removed from the carrier stream. Double peaks have been commonly related to the response of the electrode to an interfering substance. The exclusion of Li^+ from the carrier stream, maintaining 10^{-3} M NaCl improved the discrimination among peaks for injections of the same test solutions. However a more noisy base line was introduced. The use of a short C_{18} chromatographic column was used to decrease the pulse caused by the pump. Although, the column did reduce the base line noise only slightly the main problem presented was the build up of pressure when higher flow rates than 2 ml min^{-1} were attempted. Another attempt to reduce noise involved interposing a glass pulse suppressor immediately before the injection valve. Although, this did not remove noise completely, did provide a more acceptable baseline.

The addition of small amounts of K^+ , Ca^{2+} and Mg^{2+} at concentrations of 5.0, 1.0 and 1.0 mmol l^{-1} respectively (all chloride salts) and the replacement of $1 \times 10^{-3} \text{ M}$ concentration of sodium with 0.1 M in the carrier stream composition greatly enhanced the quality of the signal in relation to drift and noise. 50 μl of 0.14 M NaCl sample solutions were

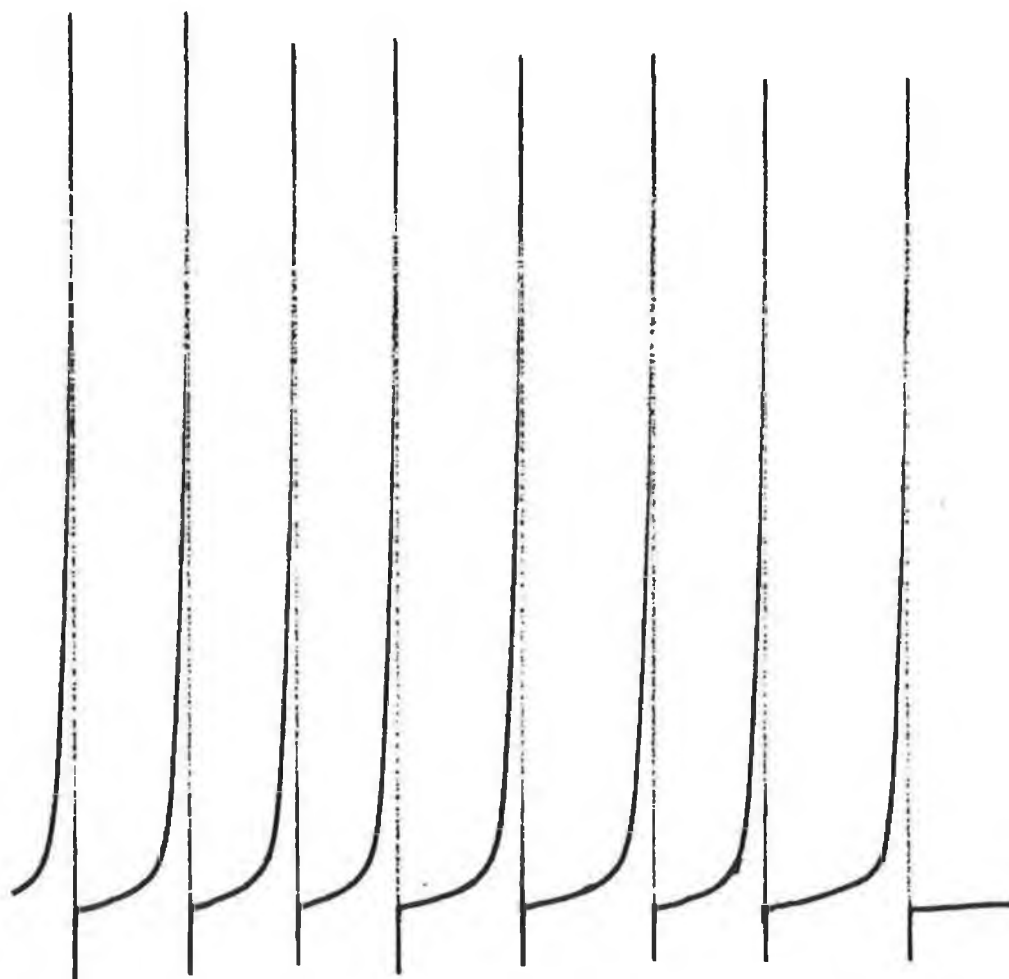


Fig. 3.12 Depiction of the response of the Na^+ ISE detector cell to 0.14 M Na^+ injections. Carrier stream (mmol l^{-1}): K^+ (5.0), Ca^{2+} (1.0), Mg^{2+} (1.0), Na^+ (100.0); flow rate: 1 ml min^{-1} ; tubing length: 50 cm (i.d. 0.5 mm) sample volume: $50 \mu\text{l}$.

injected and the resulting peaks recorded (Fig. 3.12). A rapid, reproducible and relatively stable response was then obtained corroborating some of the basic characteristics of the sensor already found in batch experiments.

3.16 OPTIMISATION OF THE ISE RESPONSE IN TRANSIENT CONDITIONS

From an analytical point of view, there are two important peak parameters which must be controlled in every FIA system namely the peak height and the time taken to re-establish the original base line. These parameters define two aspects which are fundamentally important for the success of any analytical method; e.g. sensitivity and sample throughput. The influence of experimental variables on the dispersion and therefore on the peak shape had therefore to be fully investigated.

3.16.1 Injection Volume

To examine the influence of sample volume on the analytical signal response, injections of 20, 50, and 100 μl of test solutions containing 1×10^{-2} M NaCl were introduced into a carrier stream with an ionic background of KCl 5.0 mmol l^{-1} , CaCl_2 1.0 mmol l^{-1} , MgCl_2 1.0 mmol l^{-1} and tris buffer pH 7.4. The results are listed in table 3.1. Figure 3.13 shows that increasing the injection volume produces a larger analytical signal. On the other hand the larger the sample volume is, the longer it takes to pass through the detector. These longer sample residence times increase the possibility of attaining the steady-state (Nernstian) potential. The attainment of a steady state is, of course unnecessary in flow injection and is achieved at the cost of sample throughput and higher consumption of sample and reagent volumes. Figure 3.13 shows typical recorded peaks for injections of the same

concentration at increasing sample volumes and a trace denoting the maximum value corresponding to the steady-state signal. A 100 μl sample gives about 81 % of the equilibrium potential value at a flow rate of 1.5 ml min^{-1} . The assumption that larger sample volumes will permit the attainment of steady-state condition can not be generalised owing to the time response dependency of the ISE. In fact, it has been shown that at high concentrations of F^- in carrier streams i.e. above 1 mg l^{-1} , the fluoride ion-selective electrode can attain steady-state potentials with sample volumes of 100-200 μl , while at lower concentrations, even a 5 ml sample may not bring the response to a steady state condition [67].

Sample volume	Peak height	% equilibrium
	mV	potential
20 μl	39.0	44.5
50 μl	57.2	65.2
100 μl	71.1	81.0

Table 3.1 Influence of sample volume on the electrode response.
Sample concentration is 1×10^{-2} M NaCl.

3.16.2 Effect of Flow Rate

The effect of flow rate was investigated with constant volume of sample solution. The sample containing 1×10^{-2} M of Na^+ was injected in the same carrier stream as that described above in section 3.15.1. The length of the manifold between injection port and detection cell was 37.5 cm and the

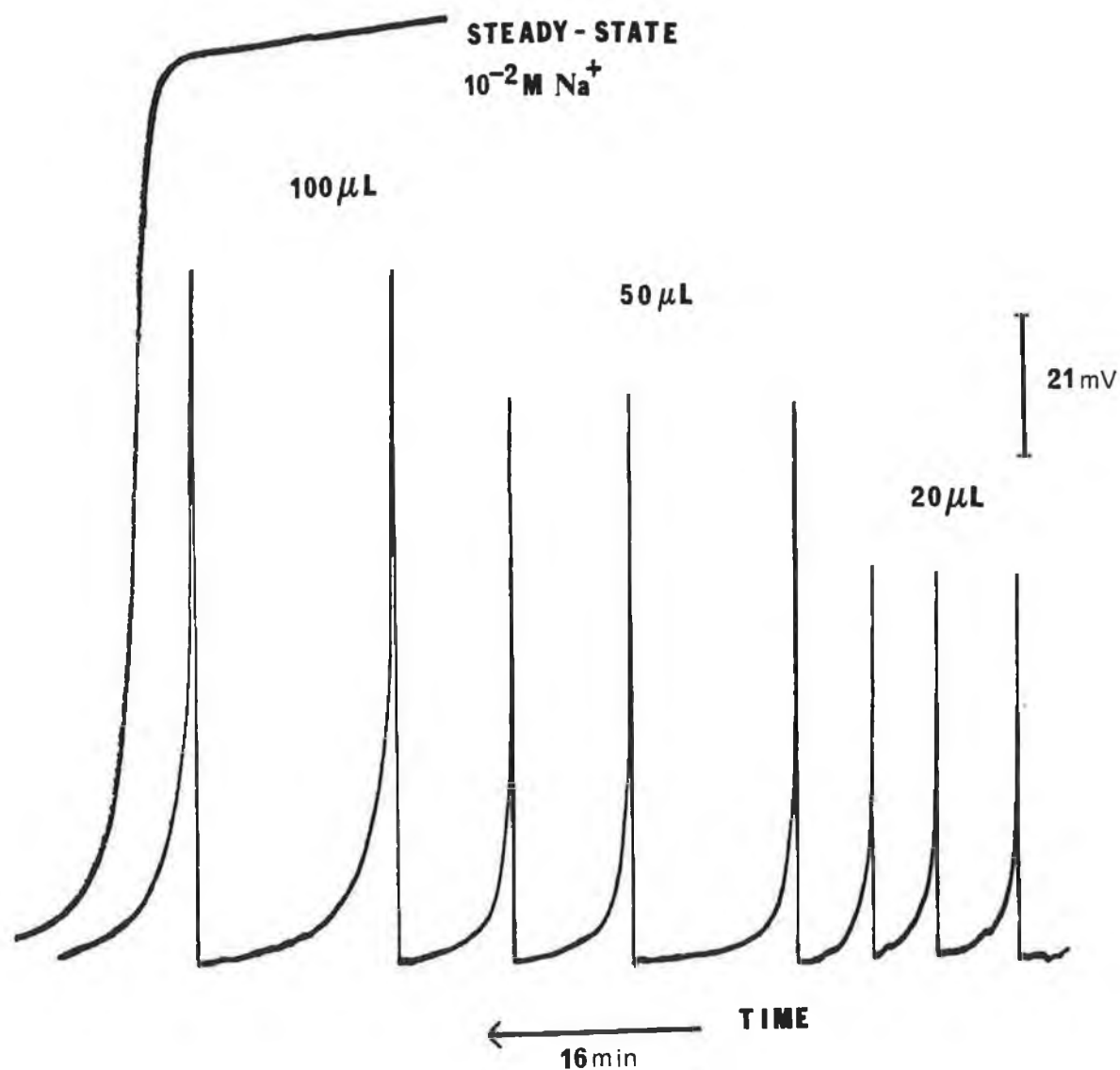


Fig. 3.13 FIA scans for calixarene based ISE illustrating the effect of sample volume on the electrode response.

injected volume $50\ \mu\text{l}$. According to the results recorded in Fig. 3.14, when a constant volume of sample is introduced, the residence time is inversely proportional to the flow rate. In fact at three different flow rates (0.5 , 1.5 and $2.8\ \text{ml min}^{-1}$), the responses in peak height for those peaks obtained at $2.8\ \text{ml min}^{-1}$ were about 89 % of the peaks recorded at $1.5\ \text{ml min}^{-1}$, and the latter about 71 % of the ones recorded at $0.5\ \text{ml min}^{-1}$. According to this relationship, one would think that the lowest flow rates would most likely lead to values near to, or at, the steady state condition. However, this may not be the case, since lower flow rates would also lead to longer response times, owing to the thicker stagnant layer at the boundary of ISE membrane and sample solution. The optimal conditions will be dependent on all the factors influencing the response time of the electrode e.g., the condition of the membrane electrode, the concentration of Na^+ ions in the carrier, the direction of the concentration change, the magnitude of the concentration jump, etc..

This was partly demonstrated by examining the influence of flow rate under different conditions to those already described. $100\ \mu\text{l}$ injections of $0.155\ \text{M NaCl}$ were injected in the same carrier stream mentioned above except that in this case it contained $0.1\ \text{M NaCl}$, and the distance between injection port and the ISE was $30\ \text{cm}$ long. As can be seen from Fig. 3.14 a decrease is observed with increasing flow rate because the response time of the electrode is not fast enough to follow the step change in concentration. However, as flow rate increases, specifically over $2.7\ \text{ml min}^{-1}$ the signal tends to increase and approximate to those values of $1.0\ \text{ml min}^{-1}$. This opposite behaviour to that shown in Fig. 3.13 would suggest that the decrease in the response time of the electrode due to a thinner stagnant layer is more

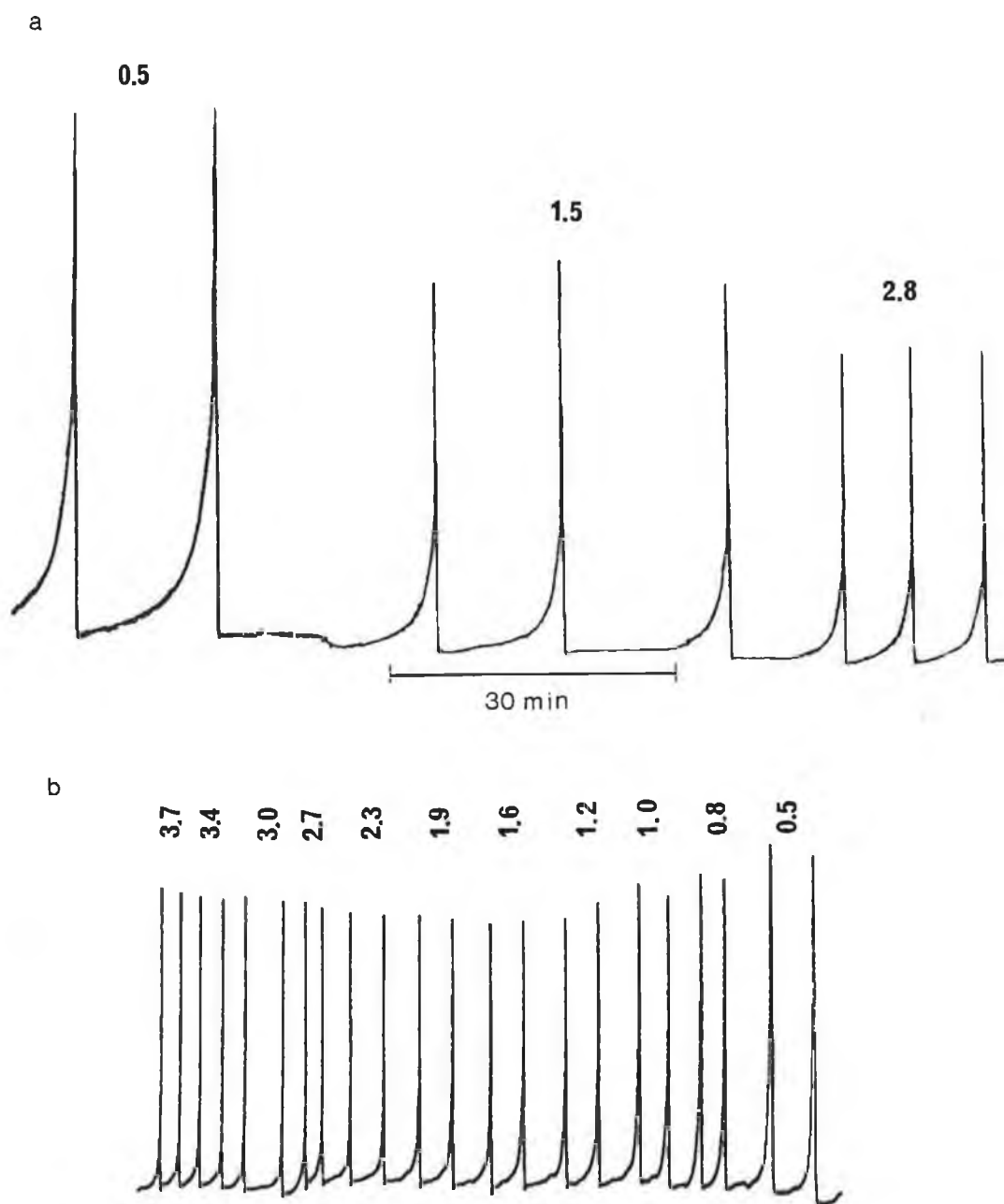


Fig. 3.14 Effect of different flow rates on the response of Na⁺ ISE in a flow injection system. (a) 0.5, 1.5 and 2.8 ml min⁻¹; carrier stream: K⁺, Ca²⁺ and Mg²⁺ at usual concentrations (all chloride salts) and tris buffer at pH 7.4; injections: 50 l l x 10⁻² NaCl; tubing length: 37.5 cm; (b) 0.5, 0.8, 1.0, 1.2, 1.6, 1.9, 2.3, 2.7, 3.0, 3.4, 3.7 ml min⁻¹; carrier stream: as in (a) with further addition of 0.1 M NaCl; injections: 100 l 0.155 M NaCl; tubing length: 30 cm).

significant than the effect produced by a shorter residence time of the sample under these conditions. As can be seen from these results the overall magnitude of the peak height will depend on the experimental conditions adopted.

A consideration in relation to flow rate is that the width of peaks decrease with increasing flow rates. This is obviously an advantage when high sample throughput is required, although this should be weighed against the lower sensitivity obtained and the possibility of cross-contamination between samples when very fast flow rates are employed.

3.16.3 Manifold Length

The effect on variation of the length of the single manifold used was investigated. The experiments consisted in interposing three different lengths of coiled and non-coiled PVC tubing (14.0, 30.0, and 52.0 cm, all 0.5 mm i.d.), between the injection valve and the detection cell and recording the size of the signal at increasing flow rates. Table 3.2 shows that there was almost no influence on peak height arising from these variations in tubing geometry and configuration except for a slight decrease in sensitivity observed when injections are made in the 50 cm manifold system. Further attempts to obtain an enhancement of the signal by coiling the tubing proved unsuccessful at the three lengths investigated.

3.16.4 Carrier Composition

During the course of the experimental work with FIA, problems associated with differences in matrix composition of test solutions injected and the carrier stream were constantly faced. Transient signals which did not result from changes in analyte concentration were often encountered. These

Flow Rate ml min ⁻¹	Tubing length (cm)			
	14	32	50	50(coiled)
	peak height (cm)			
0.5	11.9	12.5	12.1	12.0
0.8	10.8	11.2	11.0	10.9
1.2	10.4	10.2	10.1	10.2
2.0	9.0	9.2	9.1	8.7
2.4	8.7	8.6	8.4	8.4
2.8	8.5	8.2	8.0	7.9
3.2	8.0	8.0	7.6	7.7
3.6	7.5	7.5	7.1	7.0

Table 3.2 Effect of different tubing length on peak heights

problems have been also reported by other workers [69] and it has been suggested that these transients may appear either as a result of anomalous ISE behaviour [69] or due to transient liquid junction and streaming potentials [70]. To minimise these effects the composition of the carrier stream should be as similar as possible to that of the samples. With view to analytical applications in plasma samples, the main aspects to be considered involve the pH and ionic strength of samples. Although, the physiological pH of plasma samples varies in a very reduced range (7.35 - 7.45) there is still need for adjustment even if normal patient plasma is being determined. The universally employed tris buffer [71] is useful in this case. As for ionic strength, the obvious need to reduce the rather large and varying effect of interionic

interactions in plasma samples requires the addition of some plasma electrolytes to the carrier stream.

The effect of several carrier stream compositions on the electrode response was studied with view to determine which would suit best the requirements of Na^+ plasma determination. Taking into consideration that the main cationic components of the plasma sample matrix should be added, an approach similar to that taken by other workers was followed [72]. This involved the addition of KCl (5.0 mmol l^{-1}), CaCl_2 (1.0 mmol l^{-1}) and MgCl_2 (1.0 mmol l^{-1}). Tris buffer (pH 7.4) was also added to the carrier as well as 10 mmol l^{-1} of LiCl to increase the ionic strength of this mobile phase. The results shown in Fig. 3.15a were recorded after injection of $100 \mu\text{l}$ of test samples containing pure sodium solutions ranging from $1 \times 10^{-4} \text{ M}$ to $1 \times 1.5^{-1} \text{ M}$ at a flow rate of 1.6 ml min^{-1} through a 30 cm manifold. Additionally, the same conditions were used to record peaks obtained after including the same background electrolyte present in the carrier stream to the test samples (Fig. 3.15b). In both cases the response signals measured over the base line are almost identical for concentrations above $1 \times 10^{-2} \text{ M}$, indicating that the overall response of the electrode is dominated by the amount of sodium present in the sample. Transient signals appearing below the base line are not related to the concentration of the analyte, although they increased with the sample concentration. However, the importance of matrix matching becomes apparent when one compares samples where the sodium concentration is below 10^{-2} M . Injections of pure sodium chloride at 10^{-4} M (i.e. matrix not matched) produce a large initial artifact which masks any analytical information (Fig. 15a; injection 1) while at the 10^{-3} M level, a small analytical peak is just observable immediately after the artifact

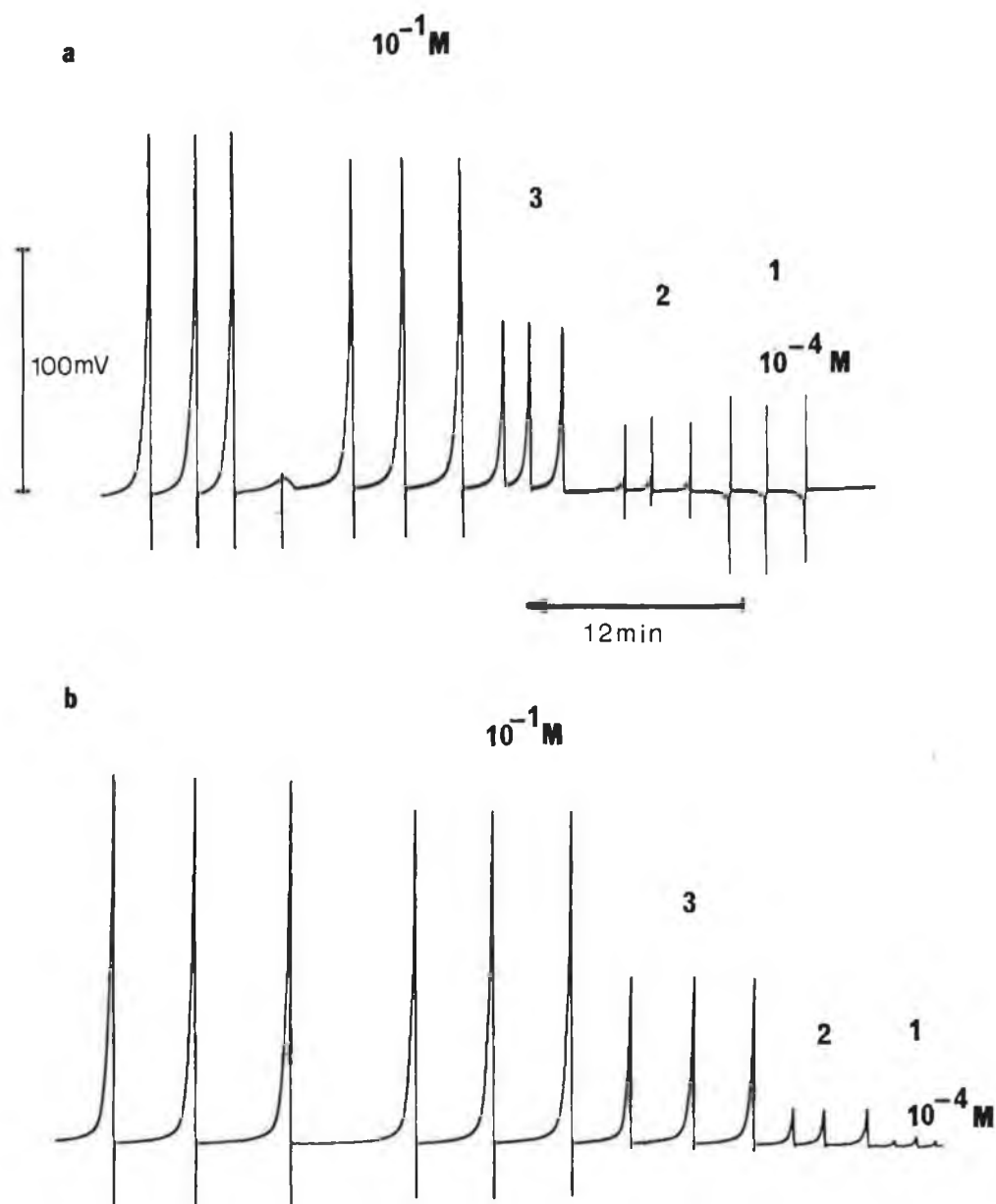


Fig. 3.15 FIA peaks for calixarene based ISE according to its response to two different standards: (a) $1 \times 10^{-4} \text{ M}$ to $1.55 \times 10^{-1} \text{ M}$ pure NaCl injections; (b) $1 \times 10^{-4} \text{ M}$ to 1.55 M sodium injections in the presence of ionic background as in the carrier stream. Carrier stream contains KCl 5.0, CaCl_2 1.0, MgCl_2 and LiCl 10.0 mmol l^{-1} . pH adjusted to 7.4 with tris buffer.

(Fig. 15a; injection 2). With the matched matrix samples, the results are much better, with the analytical peaks for 10^{-4} M and 10^{-3} M sodium chloride injections being clearly resolved (Fig. 15b, injections 1 and 2 respectively).

Slanina et al [73] have reported the benefits of including a background concentration of the measured ion to improve the response time of nitrate ISEs at low analyte concentrations. Although, the addition of this background concentration causes a faster electrode response, straightens the calibration curves to some extent, and allows fast measurements near the detection limit of the electrodes, it also shortens the dynamic linear range of the ISE. So, as is invariably the case in any analytical method, the final operation conditions chosen will represent a compromise between conflicting analytical parameters.

Bearing this in mind, increasing amounts of NaCl ranging from 1×10^{-4} M to 0.1 M were added to the same carrier composition described above and injections of the same concentrations of NaCl solutions fixed with the carrier ionic background performed under the conditions already stated. As indicated in section 3.15, the presence or absence of sodium in the carrier stream as well as that of other substances and their concentration will certainly affect the response of the ISE.

Table 3.3 shows that the direction of the concentration change has an important effect on the observed response. For example an injection of 10^{-1} M sodium chloride into a 10^{-3} M sodium chloride carrier (matrices matched) produce a response of 92.2 mV, whereas an injection of 10^{-3} M sodium chloride into a 10^{-1} M sodium chloride carrier (matrices matched) gave a response of only -33.0 mV. In other words, the peak heights (table 3.3) given by the Na^+ injections show that when the concentration of Na^+ in the sample is higher

		Peak Height (mV)			
Injected	Carrier Stream Composition (Na ⁺ mol l ⁻¹)				
sodium	I. B.	1x10 ⁻⁴	1x10 ⁻³	1x10 ⁻²	1x10 ⁻¹
mol l ⁻¹		+ I. B.	+ I. B.	+ I. B.	+ I. B.
1.0x10 ⁻⁴	2.6	—	10.2	24.4	36.4
1.0x10 ⁻³	14.0	13.4	—	20.6	33.0
1.0x10 ⁻²	66.6	59.6	38.0	—	26.2
1.0x10 ⁻¹	134.0	126.2	92.2	42.8	—
1.5x10 ⁻¹	147.2	137.8	104.4	52.2	7.8

Table 3.3 Effect of carrier stream composition on the Na⁺ electrode response to triplicated 100 ul injections of varying amounts of NaCl. Ionic background (I. B.): K⁺ 5.0, Ca²⁺ 1.0 and Mg²⁺ 1.0 mmol l⁻¹ and tris buffer pH 7.4.

than in the carrier, the response of the electrode to a particular step change in concentration is larger than that of a similar concentration change in the opposite direction. The progressive subtraction of the background signal as the amount of sodium increases in the carrier composition (table 3.3) eventually leads to a response signal which varies over a range of about 20 millivolts for concentrations of sodium in simulated plasma samples ranging from 100 mmol l⁻¹ to 180 mmol l⁻¹. With such millivolt span, work in the highest sensitivity mode of the chart recorder scale is feasible for practical applications such as the determination of sodium in plasma samples. In addition, another advantage of this approach is the much more steady base line signal obtained with high background concentrations of Na⁺ in the carrier

		Δ emf. (mV)			
$-\log[\text{Na}^+]$		Carrier composition (mol l^{-1})			
(step	I.B.	1×10^{-4}	1×10^{-3}	1×10^{-2}	1×10^{-1}
change/M)		+ I.B.	+ I.B.	+ I.B.	+ I.B.
4 - 3	11.4	13.4	-10.2	- 3.8	- 3.4
3 - 2	52.6	46.1	38.0	-20.6	- 6.8
2 - 1	67.4	66.6	54.2	42.8	-26.2
1 - 0.824	13.2	11.6	12.2	9.4	7.8

Table 3.4 Millivolt potential difference for concentration steps of different carrier streams containing background electrolyte and varying amounts of sodium.

stream. Typical fluctuations in base line of the order of ± 0.1 mV were observed when using either 1×10^{-2} or 0.1 M Na^+ in the carrier stream.

In addition, from the same set of experiments, it was seen that the return to base line heavily depended on the concentration of sodium present in the carrier stream (Fig. 3.16), the fastest return being that observed when the carrier sodium concentration was 0.1 M.

Although the above approach to improving the response characteristics of the ISE by incorporating rather high concentrations of the analyte in the stream does look attractive, the main disadvantage is the reduction in sensitivity. As seen from table 3.4, for a step change in concentration involving 55 mmol l^{-1} of sodium, a typical response of 7.8 mV in a carrier stream containing 1×10^{-1} M NaCl (i.e. column 5; $100\text{-}155 \text{ mmol l}^{-1}$) corresponded only to a 59.0 % of the signal found when no sodium was present in

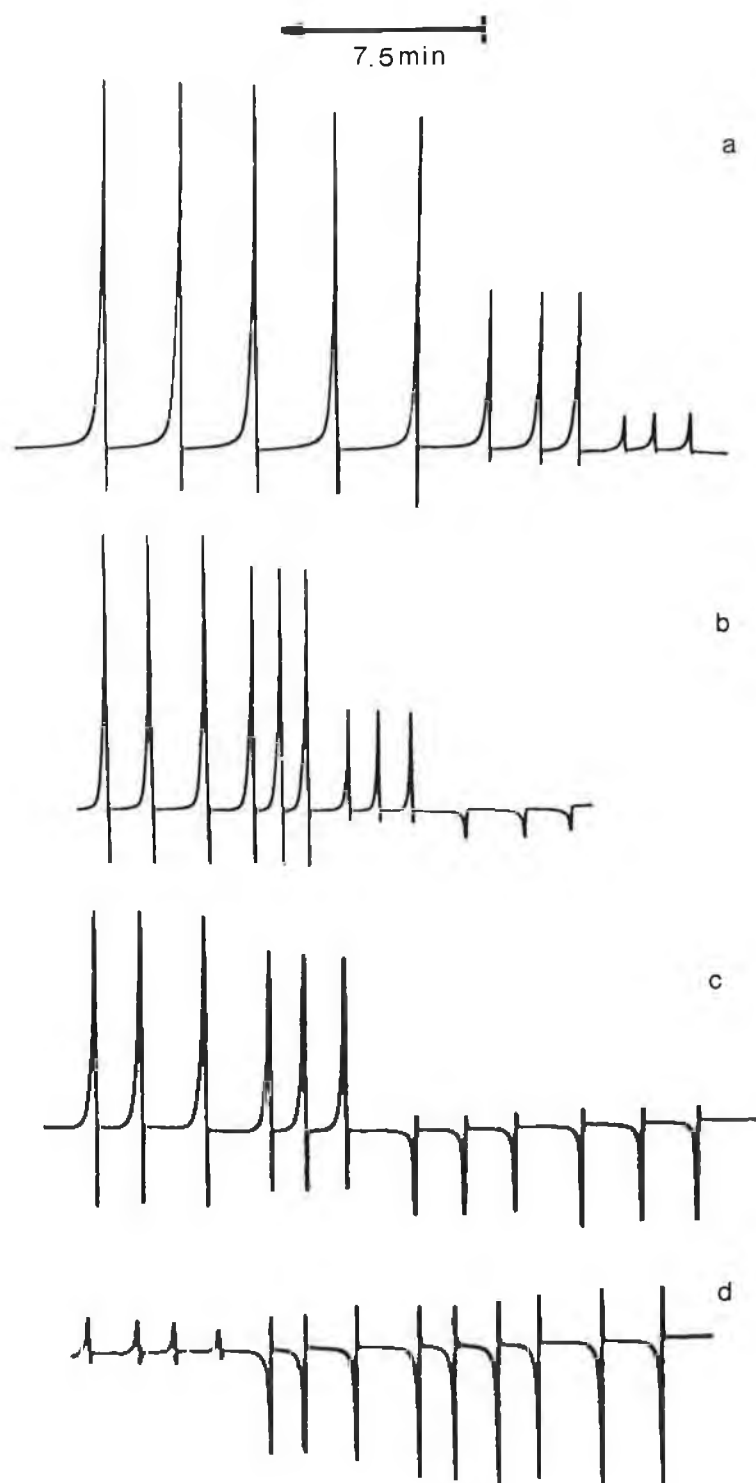


Fig. 3.16 Transient responses for different concentrations of sodium injected into a flowing stream containing K^+ , Li^+ , Ca^{2+} , Mg^{2+} , tris buffer pH 7.4 and varying amounts of (a) 1×10^{-4} , (b) 1×10^{-3} , (c) 1×10^{-2} , (d) 1×10^{-1} M NaCl.

the carrier (13.2 mV). In fact a steady decrease in sensitivity is observed at each concentration step with the lowest values occurring at the highest sodium carrier concentration.

3.17 ANALYTICAL PROCEDURE

3.17.1 Calibration

All conditions involved in the response time of an ion-selective electrode in a FIA system will certainly influence the type of calibration plot obtained for a particular application. These conditions can be optimised to suit the required working range. As demonstrated in section 3.15, the incorporation of sodium in rather high concentrations (0.1 M) in the carrier stream markedly affected both the response time and the general stability of the electrode system. Although these characteristics are particularly important in practical applications, limiting factors which are introduced by the presence of sodium i.e. the reduction of the working range and hence the decrease in sensitivity, must be also considered.

Bearing in mind that the concentration of the analyte in the carrier stream should be below the low end of the calibration curve, and that the lowest limit of sodium in blood samples is around 110 mmol l^{-1} , a flowing stream consisting of 85 mmol l^{-1} sodium plus, the usual ionic background concentration with tris buffer (pH 7.4) was chosen for calibration procedures. With particular emphasis on the normal physiological concentration range of sodium in blood plasma (135 to 145 mmol l^{-1}), sodium standards were prepared containing 110.0 , 125.0 , 140 , 155 , 180 mmol l^{-1} of sodium chloride. The standards also incorporated an ionic background and tris buffer as in the carrier stream. Under optimised conditions of volume (100 l) and tubing

length (14cm), the standards were injected into the carrier stream passing at a flow rate of 2.7 ml min^{-1} . This flow rate, although not being the optimum, provided a suitable compromising between sensitivity and standard throughput. From the peaks depicted in Fig. 3.17 it can be seen that excellent discrimination was obtained between the various standard solutions and the response proved to be near-Nernstian (slope 55.1 mV dec^{-1}) and linear ($r = 0.999$) in the range of concentrations assayed. Response to injections was almost instantaneous and return to base line was complete within about 30 s. The sample throughput, reproducibility and precision are intimately related in a FIA system. Generally speaking, the higher the sampling rate, the larger the probability of contamination between the injected sample and the preceding one (carry-over. This contamination will be revealed in a calibration curve by:

- (a) the instability of the base line and
- (b) the difference in the peak maximum value.

The fact that the base line (Fig. 3.17) varied less than 0.3 mV from the start of the injections, plus a variability of no more than 0.1 mV at the top of the peak for triplicated injection suggests that no contamination between standards was present. However, this problem tends to become more noticeable in samples such as plasma which have a more complex matrix. The high viscosity of samples (owing to the presence of proteins) produces a more sluggish return to base line. This was clearly observed when plasma samples were directly injected into the carrier stream immediately after running the calibration curve discussed above. In fact under those conditions the plasma samples did not return to base line and a stable potential, was only observed several minutes after injection. Although small tubing diameters and manifold lengths will most certainly yield the highest sensitivity and best sample

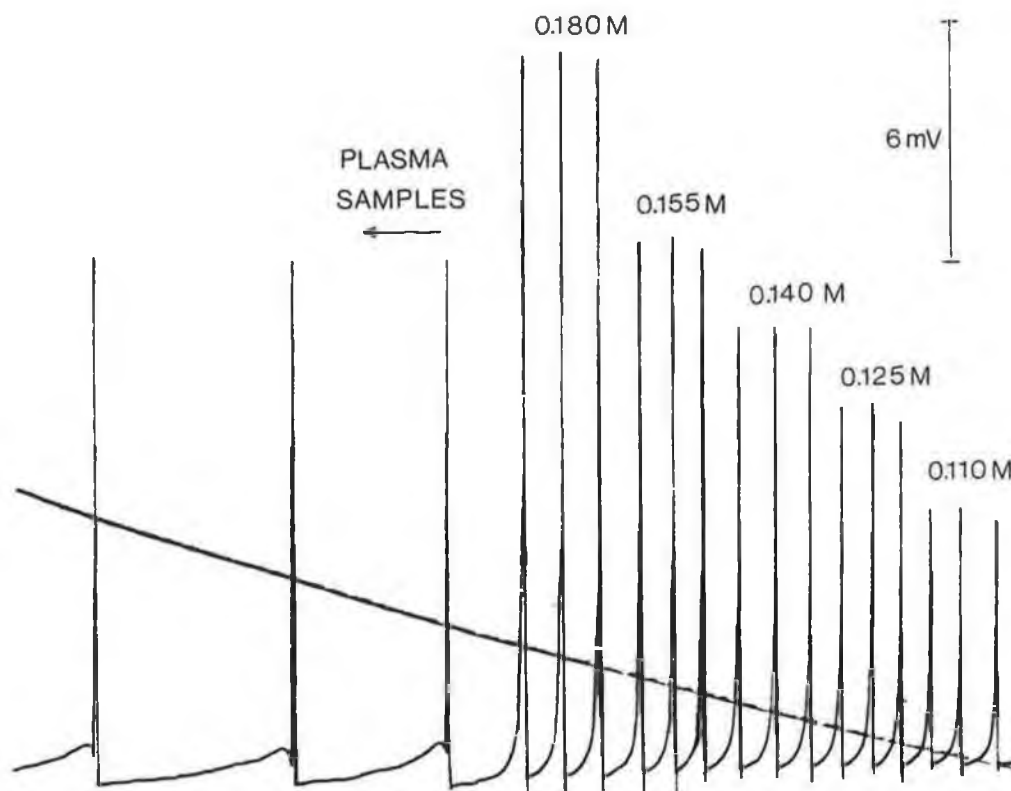


Fig. 3.17 Calibration curves for sodium (0.11 to 0.18 M) as performed in a FIA system with a sodium calixarene based ISE. Injection of plasma samples can be seen at the far end of of the calibration curve. Conditions: flow rate 2.7 ml min^{-1} ; sample volume 100 μl ; tubing length 14 cm (i.d. 0.5 mm).

throughput, such conditions are not sufficient to permit an adequate dispersion of plasma samples in the flowing stream by the time the sample plug reaches the detector cell.

Under four different flow rate conditions, calibration curves were obtained sequentially (Fig. 3.18). Unfortunately at this stage, problems arose with the pressure transducer of the gas pump, and a more unstable and noisy signal was produced. Despite this inconvenience, in every case the calibration curves were linear for the concentration range considered, showing good correlation coefficients, and gave good discrimination between different sodium standards. As expected, the highest sensitivity was seen at low flow rates and the highest sample throughput at higher flow rates.

Due to the rather unstable base line and periodic noise encountered, a peristaltic pump replaced the chromatographic pump and a new pressure transducer was incorporated. These changes re-established the original quality of the base line previously observed.

3.17.2 Analysis of Blood Plasma Samples

In an effort to try to reduce the delay in re-establishing baseline conditions produced by injections of plasma, 10 ml/l of Technicon surfactant was added to the carrier stream. This approach failed owing to the drastic decrease in the magnitude of the signal while return to base line was only slightly improved. Consequently, a ten-fold pre-dilution was considered for the amount of Na^+ and ionic background present in the carrier stream as well as for calibration solutions and plasma samples. Accordingly, 500 μl of plasma and calibration solutions (110, 125, 140 155 and 170 mmol l^{-1} sodium chloride, in the presence of K^+ 5.0 mmol l^{-1} , Ca^{2+} 1.0 mmol l^{-1} and

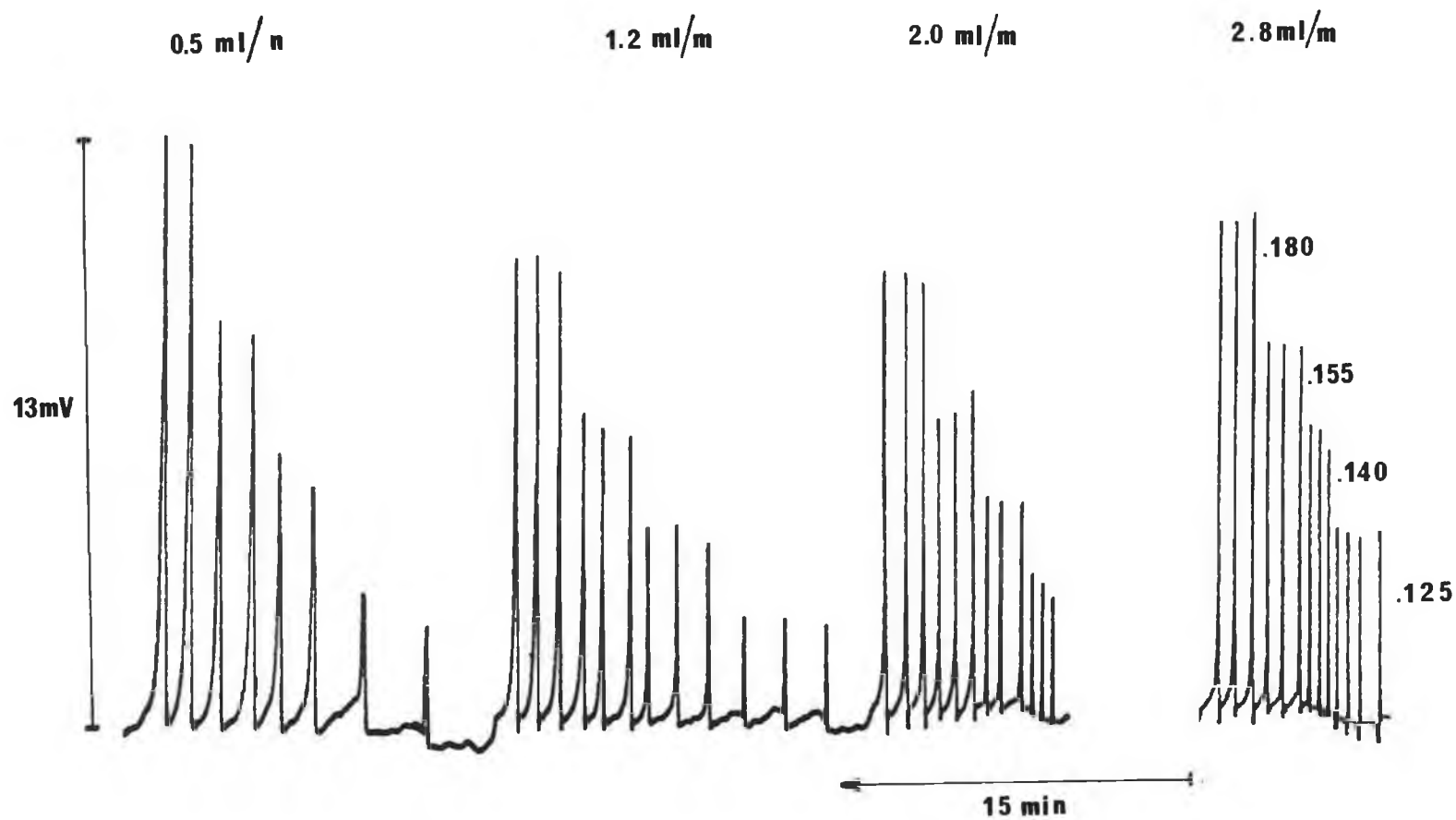


Fig. 3.18 Calibration curves under different flow rates for a calixarene based ISE. (a) 0.5 ml min⁻¹; (b) 1.2 ml min⁻¹; (c) 2.0 ml min⁻¹; (d) 2.8 ml min⁻¹. Other conditions as in Fig.117

Mg²⁺ 1.0 mmol l⁻¹ as chlorides) were diluted ten-fold with tris buffer at pH 7.4. A new calibration curve was then obtained under the same conditions mentioned above, except that this time the flow rate was lowered to 2.0 ml min⁻¹ and the resulting curve was not Nernstian. In principle, Nernstian behaviour would be expected if the electrode response is very fast and the concentration of the analyte is appropriate. Nevertheless, the response was linear with a correlation coefficient $r = 0.9999$ and the base line was stable and without noise (Fig. 3.19). Injections of plasma samples this time showed complete recovery of base line after a short time. These conditions were then adopted to analyse a batch of 10 freshly obtained plasma samples. A further change in flow rate to 0.5 ml min⁻¹ was considered to allow the readout at the top of the peak by following the millivolt change in a pH meter.

In order to avoid carry over, injections were made after return to baseline. To avoid any contamination between samples in the loop, the 100 μ l loop was washed out carefully between injections with 1 ml of milli-Q water followed by approximately 5-fold sample volume.

Although a rather unstable base line was observed, owing to a new problem arising in the gas pump, this seemed not to affect the response of the electrode to repeated injection of samples. The results obtained for a batch of 10 samples injected in triplicate (table 3.5, Fig. 3.20) indicated excellent correlation when compared to the Smac Technicon Analyser in the range of concentrations determined. The resulting linear regression equation, calculated according to Deemings method [74] is given by:

$$Y = 0.94 X + 7.82; (r = 0.980, n = 10)$$

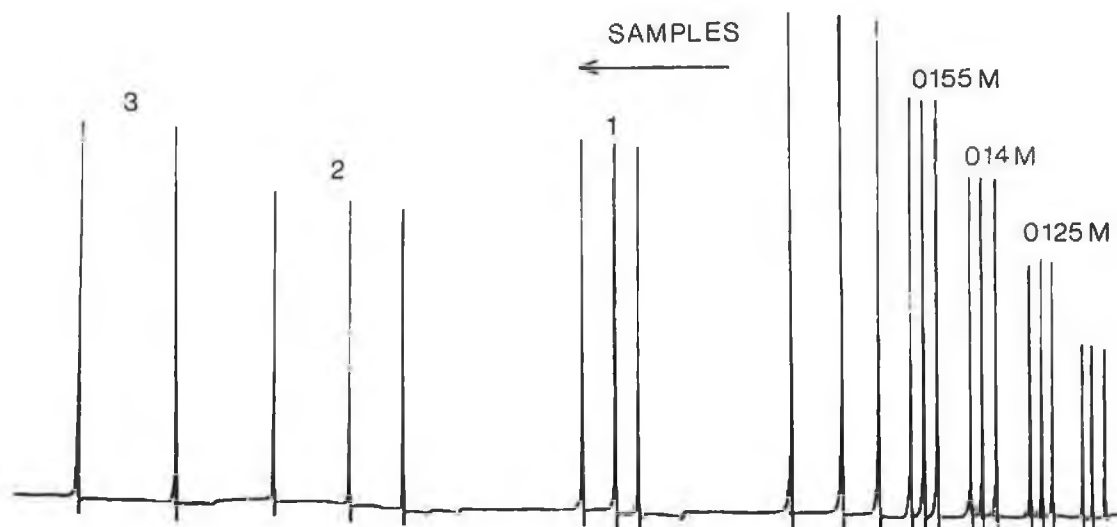


Fig. 3.19 Injections of sodium calibration solutions (0.11 M to 0.17 M) in the presence of an ionic background of K^+ 5.0, Ca^{2+} 1.0 and Mg^{2+} 1.0 mmol l⁻¹ and plasma samples after a ten fold dilution with tris buffer 7.4.

Na ⁺ Concentration mmol l ⁻¹		
Sample	FIA	Smac Technicon
1	139	140
2	126	125
3	140	142
4	143	143
5	141	140
6	139	139
7	140	140
8	132	134
9	141	142
0	141	142

Table 3.5 Sodium plasma concentration as performed by a tetrameric calixarene based ISE in a FIA system and the sodium glass electrode in the Smac Technicon Analyzer, residual standard deviation = 1.1 mmol/l.

where the intercept is given in mmol l⁻¹.

3.17.2.1 Flame Photometry

For the determination of sodium by flame photometry the measurements were carried out using the autosample mode of an IL 943 flame photometer employing an air/propane flame. The cycle basically consists of the aspiration of 20 l of plasma sample together with a 2.0 ml caesium diluent, and the detection of the sodium signal from the corresponding atomic emission wavelength. This is compared with the caesium atomic signal which serves as an internal standard.

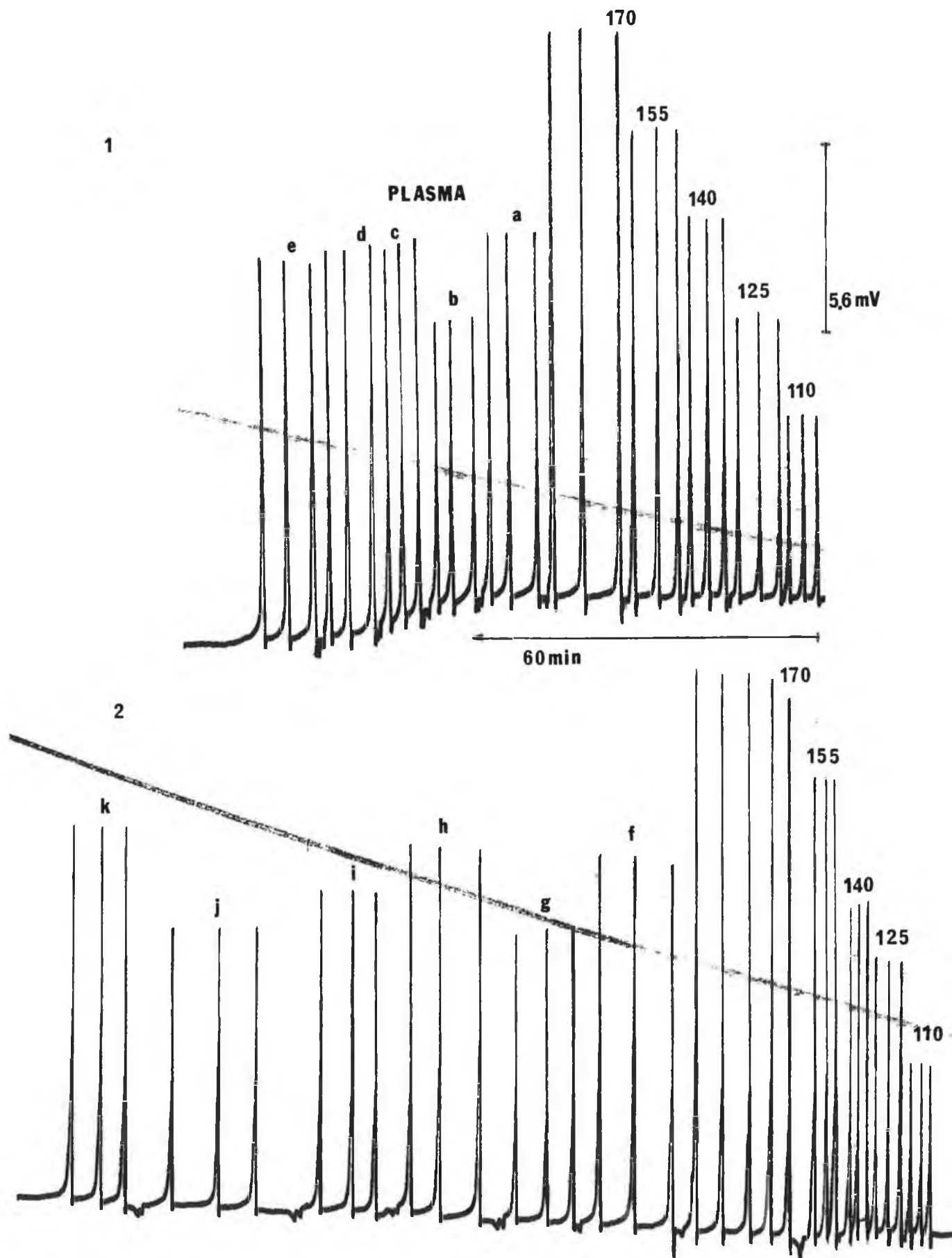


Fig. 3.20 Calibration curves and plasma samples run obtained in a FIA system using methyl p-t-butylcalix[4]arene based ISE. Experimental conditions as in text.

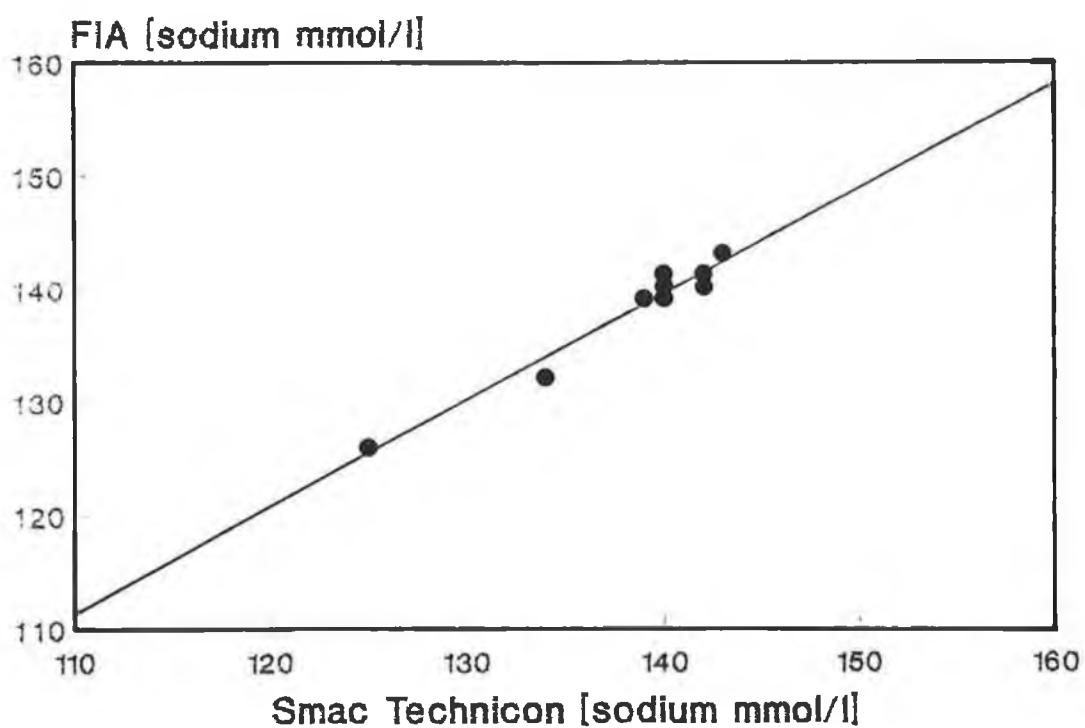


Fig. 3.21 Correlation between Smac Technicon Analyser and a FIA system for the determination of sodium in plasma samples. Slope = 0.94; Correlation coefficient = 0.98 (n = 10).

The electronic amplification of the signal followed finally by the data check and computation completes the analysis. The calibration of the instrument was performed with the 1.5 mmol l^{-1} CsCl internal standard and 140 mmol l^{-1} NaCl.

A batch of 22 samples was analysed by flame photometry and then by FIA. Each sample was divided in two aliquots and the analysis was carried out during the same day. For the FIA determination, the procedure already described (section 3.16.2) was followed. Calibration curves were obtained before the sample run and after assessing the 12th plasma sample.

The results obtained by flame photometry and the FIA system together with the corresponding values of the Smac Technicon Analyser are shown in table 3.6.

From these data, it can be seen that the FIA produced excellent agreement with the standard flame photometry technique as also again with the Smac Technicon Analyser. In fact, the regression analysis for the FIA and flame photometry gave a high correlation between both techniques ($r = 0.94$, $n = 22$), with a residual standard deviation of 0.88 mmol l^{-1} and a slope of 1.09 (Fig. 3.22). The peaks depicted in Fig. 3.23, showed excellent reproducibility in the peak maximum value and a stable base-line (especially for the calibration runs) with the exception of one or two samples after the second calibration curve (the instability being due mainly to some lack of control over the gas pump flow rate).

A clear shift in the base line towards higher values was observed when plasma samples were injected. As seen from Fig. 3.23, the shift occurred immediately after the first plasma injection and amounted 0.5 mv at the end of the sixth injection. The shift in base-line potential is most likely to be attributed to the adsorption of biological components (i.e. proteins) onto the

Sample	Na ⁺ concentration mmol l ⁻¹		
	FIA	Flame	Smac
		Photometry	Technicon
1	141	142	142
2	144	144	143
3	132	132	132
4	142	142	142
5	141	141	139
6	141	140	141
7	139	141	141
8	141	140	139
9	133	134	134
10	143	142	143
11	137	138	138
12	144	147	146
13	136	138	137
14	137	138	136
15	143	141	140
16	135	136	136
17	140	141	141
18	140	140	140
19	142	140	141
20	131	133	133
21	138	139	138
22	143	143	142

Table 3.6 Concentration of sodium in plasma samples as performed by 3 different methods.

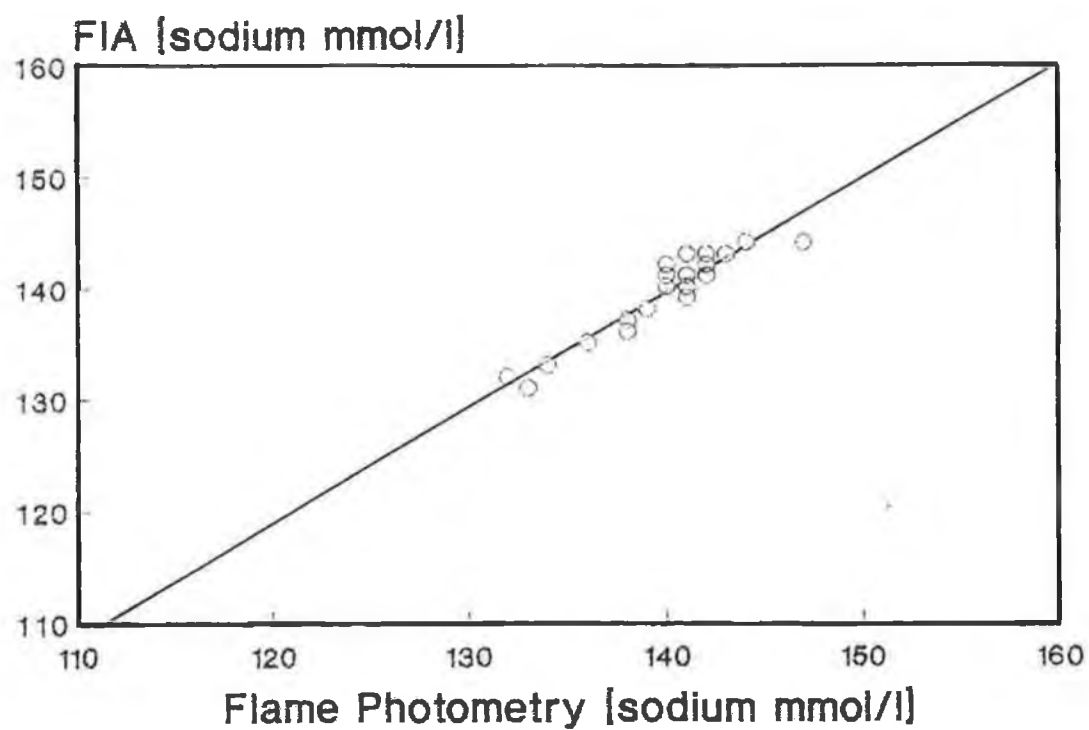


Fig. 3.22 Correlation between flame photometry and FIA system incorporating methyl p-t-butylcalix[4]aryl acetate ionophore in the ISE membrane. For experimental conditions see text.

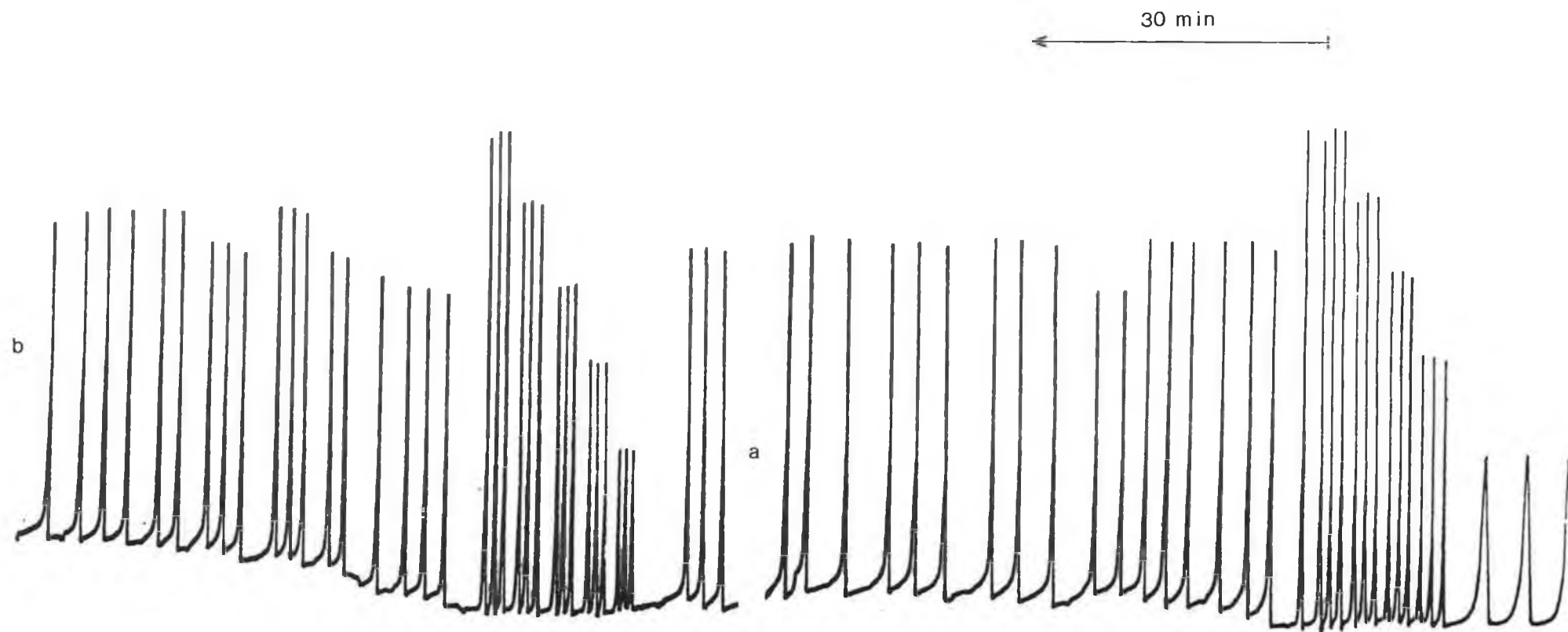


Fig. 3.23 Sodium calibration solutions and plasma sample injections. The first three injections corresponding to the 1.1×10^{-2} M calibrant is shown at a lower chart speed (20 cm/h). Standard and samples were obtained sequentially as in figure except that at point a and b, 5 and 4 samples have been removed respectively for depiction purposes.

surface of the ISE membrane. This effect has been encountered by other workers [75] and was discussed previously (see section 2.4.1, chapter 2). In addition to the base line shifts, a slight decrease in ISE sensitivity occurred. In fact the calibration curve performed after the twelfth plasma sample showed that the values in the peak magnitude decreased uniformly by about 0.2 - 0.3 millivolts for every injection, although the correlation of the calibration curve was maintained. It was noticed however, during the assessment of another batch of samples (Fig. 3.24) performed under the same conditions and with the same ISE membrane, that the original magnitude of values for injection of standards was re-established if the carrier stream was passed through the system for about 20 minutes at high flow rates (i.e. 3.0 ml min^{-1}). Thus the higher flow rates seem to add a more efficient washout cycle to the ISE membrane provided that the injection of samples is done after a complete recover of base-line. In Fig. 3.24 it can also be observed that the shift in potential stabilises after the initial injections and the subsequent new base-line remains relatively constant.

Additional observations from the injection of plasma samples (Fig. 3.20, 3.23, 3.24) showed that return to base line was slower in comparison to aqueous solutions. However, a high sample throughput can be obtained for the system at higher flow rates as depicted in Fig. 3.19.

3.18 CONCLUSIONS

The development of a FIA system and the potential use of a calixarene based ion-selective electrode in a flowing stream for the analysis of sodium in plasma samples was the main goal of the research presented in this chapter. The system developed proved efficient despite some instability arising from the

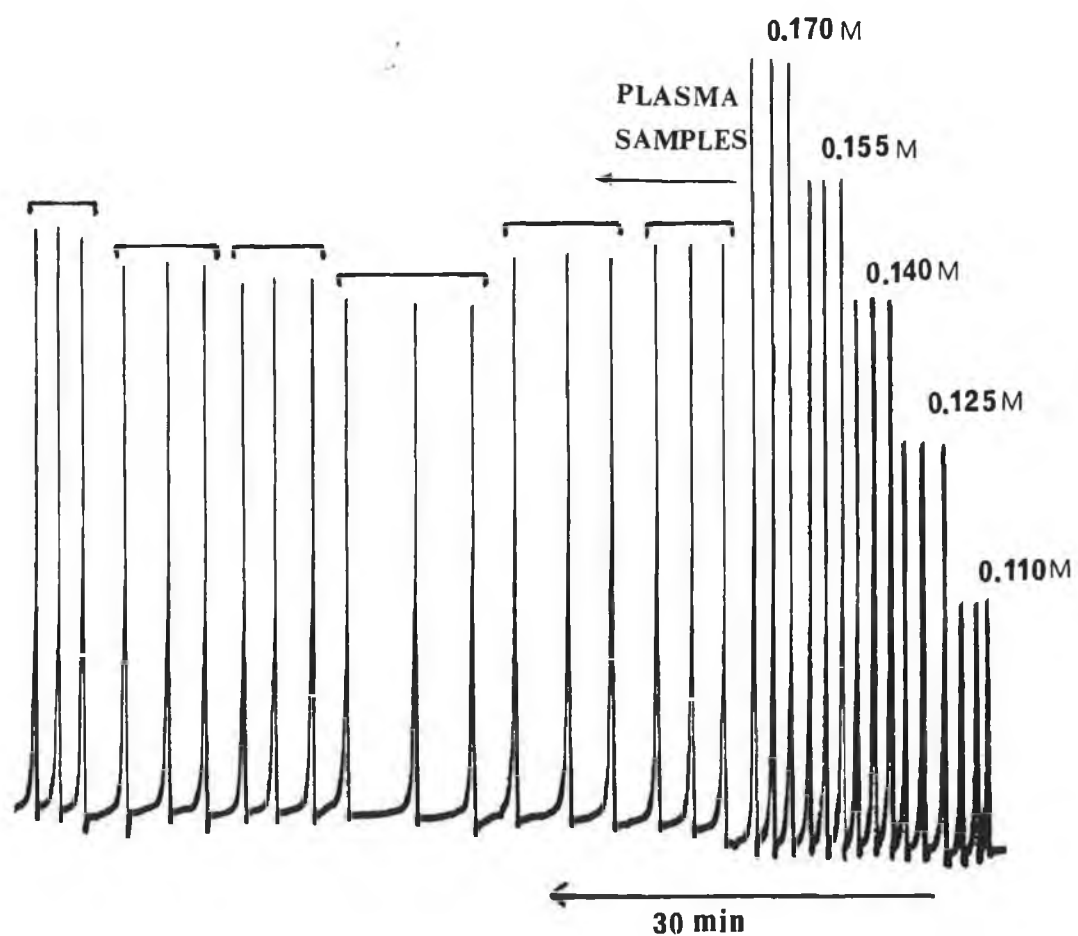


Fig. 3.24 Calibration curve and plasma samples as performed in a FIA system incorporating the methyl ester calix[4]arene based ion-selective electrode.

gas delivery system. A rapid start and stabilisation of the signal within the first 15 minutes from one day to another was a characteristic when using a peristaltic pump. The membrane electrode based on methyl p-t-butylcalix[4]aryl acetate ionophore functioned well in the system, in accordance with theoretical descriptions of the physical and dynamic properties of FIA. The optimum conditions for plasma sodium determination were studied, and as is always the case, a compromise between analytical requirements for the specific determination and the system efficiency had to be adopted. The response of the electrode proved to be fast and with optimised conditions for sample throughput, a large number of samples can be analysed. The overall performance of the methyl p-t-butylcalix[4]arene acetate based ISE in plasma samples was excellent as demonstrated by the high correlation obtained when the results were compared to two well established methods for sodium determination. In fact, the advantages of the FIA approach over batch methods are clearly indicated by the improvement in the precision and accuracy of the determination as compared to the dipping technique previously used (chapter 2). Although, some adsorption of biological components onto the membrane surface was observed, it seemed not to have any major adverse effect on the electrodes performance. However in order to determine to what extent this interference accounts for deviations of the results from the reference method (analyser), further work must be carried out. In addition, improvements in the precision of the analysis can be obtained by means of computer based signal acquisition and processing techniques which can average the signal noise, correct base line drift and obtain digitally the read out at the top of the peak.

3.19 REFERENCES

1. Skeegs, L.T., Am. J. Pathol., 1957, 28, 311.
2. Lutsgarten, J.A., Wenk, R.E., Byrd, C. and Hall, B., Clin. Chem., 1974, 20, 1217.
3. Pungor, E., Toth, K. and Hrabeczy-Pall, A., Trac., 1984, 3, 28.
4. Trojanowicz, M., Anal. Chem. Symp. Ser., 1984, 18, 189.
5. Ruzicka, J. and Hansen, E., Anal. Chim. Acta, 1975, 78, 145.
6. Ruzicka, J. and Hansen, E., Anal. Chim. Acta, 1978, 99, 37.
7. Kalizaki, T., Hasebe, K. and Yoshida, H., Fresenius Z Anal Chem., 1987, 326, 214.
8. Stone, D.C. and Tyson, J.F., Analyst, 1987, 112, 515.
9. korenaga, T., Shen, F.H., Yoshida, H., Takahashi, T. and Stewart, K.K., Anal. Chim. Acta, 1988, 214, 97.
10. Stults, C.L.M., Wade, A.P. and Crouch, S.R., Anal. Chim. Acta, 1987, 192, 301.
11. Stone, D.C. and Tyson, J.F., Anal. Proc., 1986, 23, 23.
12. Hansen, E.H., Anal. Proc., 1981, 18, 261.
13. Tyson, J., Fresenius Z Anal. Chem., 1988, 329, 675.
14. Horvai, G. and Pungor, E., Cri. Rev. Anal. Chem. 1987, 17, 231.
15. Van Veen, J.J.F., Van Opstal, M.A.J., Reijn, J.M., Van Bennekon, W.P. and Bult, A., Anal. Chim. Acta, 1988, 204, 29.
16. Kolev, S.D. and Pungor, E., Anal. Chim. Acta, 1988, 208, 117.
17. Kolev, S.D. and Pungor, E., Anal. Chim. Acta, 1988, 208, 133.
18. Kolev, S.D. and Pungor, E., Anal. Chem., 1988, 60, 1700.
19. Clark, G.D., Hungerford, J.M. and Christian, G.D., Anal. Chem., 1989, 61,

973.

20. Hungerford, J.M. and Christian, G.D., Anal. Chim. Acta, 1987, 200, 1.
21. Christopoulos, T.K. and Diamandis, E.P., Anal. Chem., 1989, 61, 504.
22. Patton, C.J. and Crouch, S.R., Anal. Chim. Acta, 1986, 179, 189.
23. Lazaro, F., Luque de Castro, M.D. and Valcarcel, M., J. Chromatogr., 1988, 448, 173.
24. Ruzicka, J. and Hansen, E.H., Anal. Chim. Acta, 1983, 145, 1.
25. Riley, C., Rocks, B.F. and Sherwood R.A., Anal. Chim. Acta, 1986, 179, 69.
26. Wada, H., Sawa, Y., Morimoto, M., Ishizuki, T. and Nakagawa, G., Anal. Chim. Acta, 1989, 220, 293.
27. Reijn, J.M., Van der Linden, W.E. and Poppe, H., Anal. Chim. Acta, 1983, 123, 229.
28. Valcarcel, M. and Luque de Castro, M.D., J. Chromatogr., 1987, 393, 344.
29. Baadenhuijsen, H. and Seuren-Jacobs, H.E.M., Clin. Chem., 1979, 25, 443.
30. Luque de Castro, M.D., J. Autom. Chem., 1986, 8, 56.
31. Canete, F., Rios, A., Luque de Castro, M.D. and Valcarcel, M., Anal. Chem., 1988, 60, 2354.
32. Tyson, J.F., Anal. Chim. Acta, 1988, 214, 57.
33. Morf, W.E. and Simon, W., Anal. Chem. Symp. Ser., 1982, 33.
34. Hansen, E.H., Ruzicka, J. and Ghose, A.K., Anal. Chim. Acta, 1978, 100, 151.
35. Lindner, E., Toth, K. and Pungor, E., Anal. Chem., 1976, 48, 1071.
36. Ruzicka, J., Hansen, E.H. and Zagatto, E.A., Anal. Chim. Acta, 1977, 88, 1.
37. Frenzel, W., Analyst, 1988, 113, 1039.
38. Alegret, S., Alonso, J., Bartroli, J., Domenech, J., Jaffrezic-Renault, N.

- and Duvault-Herrera, Y., *Anal. Chim. Acta*, 1989, 222, 373.
39. Cardwell, T.J., Cattrall, R.W., Hauser, P.C. and Hamilton, I.C., *Anal. Chim. Acta*, 1988, 214, 359.
40. Ramsing, A.U., Janata, J., Ruzicka, J. and Levy, M., *Anal. Chim. Acta*, 1980, 118, 45.
41. Keller, J.W., Gould, T.F. and Aubert, K., *J. Chem. Educ.*, 1986, 63, 709.
42. Thijssen, P.C., Prop, L.T.M., Kateman, G. and Smith, H.C. *Anal. Chim. Acta*, 1985, 174, 27.
43. Del Valle, M., Alonso, J., Poch, M. and Bartroli, J., *J. Chemometr.*, 1988, 3, 285.
44. Lukkari, I. and Lindberg, W., *Anal. Chim. Acta*, 1988, 211, 1.
45. Lindner, E., Toth, K. and Pungor, E., *Anal. Chem.*, 1976, 48, 1071.
46. Meier, P.C., Ammann, D., Morf, W.E. and Simon, W. in "Medical and Biomedical Applications of Electrochemical Devices", J. Koryta (Ed.), John Wiley & Sons, Chichester, New York, Toronto, 1980.
47. Morf, W.E. in "The Principles of Ion-Selective Electrodes and of Membrane Transport", *Studies in Analytical Chemistry*, Vol. 2, E. Pungor, W. Simon and J. Inczedy (Eds.), Akademiai Kiado, Budapest, 1981; Elsevier, Amsterdam, 1981.
48. Christopoulos, T.K. and Diamandis, E.P., *Analyst*, 1987, 112, 1293.
49. Hansen, E.H., *Fresenius Z Anal. Chem.*, 1988, 329, 656.
50. Rios, A., Lazaro, F., Luque de Castro, M.D. and Valcarcel, M., *Anal. Chim. Acta*, 1987, 199, 15.
51. Toei, J., *Anal. Lett.*, 1988, 21, 633.
52. Tyson, J.F. *Analyst*, 1987, 112, 523.
53. Van der Linden, W.E., *Anal. Chim. Acta*, 1986, 179, 91.

54. Fraticelli, Y.M. and Meyerhoff, M.E., *Anal. Chem.*, 1981, 53, 992.
55. Muller, H., 3^{ird} Symposium on ISEs, Matrafured (Hungary), 1980.
56. Anker, P., Wieland, E., Ammann, D., Dohner, R.E., Asper, R. and Simon, W., *Anal. Chem.*, 1981, 53, 1970.
57. Gadzekpo, V.P., Moody, G.J. and Thomas, J.D.R., *Anal. Proc.*, 1986, 23, 62.
58. Erne, D., Ammann, D. and Simon, W., *Chimia (Switzerland)*, 1979, 33, 88.
59. Janata, J. and Huber, R.J., *Ion Sel. Electrode Rev.*, 1979, 1, 31.
60. Loscombe, C.R., Cox, G.B. and Daiziel, J.A.W., *J. Chromatogr.*, 1978, 166, 403.
61. Jagner, D. and Aren, K., *Anal. Chim. Acta*, 1982, 141, 157.
62. Hansen, E.H., Ghose, A.K. and Ruzicka, J., *Analyst*, 1977, 102, 705.
63. Duffield, E.J., Moody, G.J. and Thomas, J.D.R., *Anal. Proc.*, 1980, 533.
64. Hauser, P.C., Cardwell, T.J., Cattrall, R.W., Tan, S.S. and Hamilton, I.C., *Anal. Chim. Acta*, 1989, 221, 139.
65. Frenzel, W., Liu, C.Y. and Oleksy-Frenzel, J., *Anal. Chim. Acta*, in press.
66. Frenzel, W., *Fresenius J Anal. Chem.*, 1990, 336, 21.
67. Frenzel, W. and Bratter, P., *Anal. Chim. Acta*, 1986, 185, 127.
68. Van der Linden, W.E. and Oostervink, *Anal. Chim. Acta*, 1978, 101, 419.
69. Frenzel, W., *Fresenius Z Anal. Chem.*, 1989, 335, 931.
70. Toth, K., Linder, E. and Pungor, E., *Anal. Chem. Symp. Ser.*, 1980, 135.
71. *In Vitro and in Vivo Effects of Amine Buffers. Ann. N.Y. Acad. Sci.* 1961, 92, 333.
72. Moody, G.J., Saad, B.B. and Thomas, J.D.R., *Analyst*, 1989, 114, 15.
73. Slanina, J., Lingerak, W., and Bakker, F., *Anal. Chim. Acta*, 1980, 117, 91.
74. Cornbleet, P.J. and Gochman, N., *Clin. Chem.*, 1979, 25, 432.
75. Oesch, U., Ammann, D. and Simon, W., *Clin. Chem.*, 1986, 32, 1448.

CHAPTER 4

Adsorptive Stripping Voltammetric

Behaviour of

Pipemidic Acid

4.1 INTRODUCTION

The rational use of patient therapy through drug administration (chemotherapy) requires knowledge of the mechanism by which drugs act in the body. Such action is strongly affected by the manner in which drugs are absorbed, distributed, metabolised and excreted [1]. In order to understand these complex processes, it is necessary to have techniques that allow one to determine the concentration of the drug in blood, urine and other biological fluids and tissues, and also to establish its metabolic paths, thus identifying and quantifying its metabolites.

The absorption and distribution of drugs in the body is frequently affected by multiple factors which modify their availability and produce unsatisfactory therapeutical effects [2]. The analytical determination of drug concentrations in biological fluids permits the clinician to adjust the dose adequately to the individual characteristics of a patient. The analytical control of drugs (therapeutic drug monitoring) is an ever expanding area of research. The main reason for this lies in the fact that there is an increased utilisation of drugs capable of producing serious undesirable effects when their concentration levels are higher than their predetermined therapeutical levels in blood. Drug monitoring is also important in those patients whose pathological condition, e.g., renal failure, may affect and modify the normal pharmacokinetics of the drug. In these cases the analytical determination of the drug permits a notable reduction of the risks involved without renouncing the benefits of the therapy. Another prime reason for quantitative analysis in a given therapy results from the need to establish the drug/dose effect. This is mostly the case of antibacterial drugs for which it necessary to have

is necessary to have certain levels of a particular drug in a specific fluid, in order to reach minimal inhibitory concentrations of that drug. Therapeutic drug monitoring is therefore regarded as an important area of clinical chemistry.

Pipemidic acid, chemically known as 8-ethyl-5,8-dihydro-5-oxo-(1-piperazinyl) pyrido[2,3-d]pyrimidine-6-carboxylic acid [3] is a well established antibacterial agent (Fig. 4.1) synthesised in the early 70's. Most Gram-negative pathogens including, *Escherichia coli* and *Klebsiella*, *Enterobacter*, *Proteus* and *Citrobacter* species are susceptible to pipemidic acid. The high activity of the drug against the most important urinary pathogens, together with its pharmacokinetic characteristics e.g. being excreted into urine in a bacteriologically active form at concentrations higher than the plasma level, has allowed its effective use in urinary infections [4]. In patients given a single dose, average urinary concentrations are the highest in 2 to 4 h or 4 to 6 h urine, the average levels of which are 1,116, 2,441 and 1,949 ug/ml at doses of 0.5, 1, and 2 g, respectively. High concentrations above 100 ug/ml have been detected even in 12 to 24 h urine at therapeutic doses above 1 g. According to Shimizu et al. [5] the percentage of urinary recovery of unchanged pipemidic acid for 24 h ranges between 68.3 to 87.8 %.

In general, these concentrations can be detected by most chromatographic methods developed so far in urine samples [6-8]. Although some of the methods have also been developed for plasma, the clinical significance is rather limited since the levels reached in this fluid are low and bacteriologically and therapeutically insignificant.

Pharmaceutical analysis is another field in which the analytical

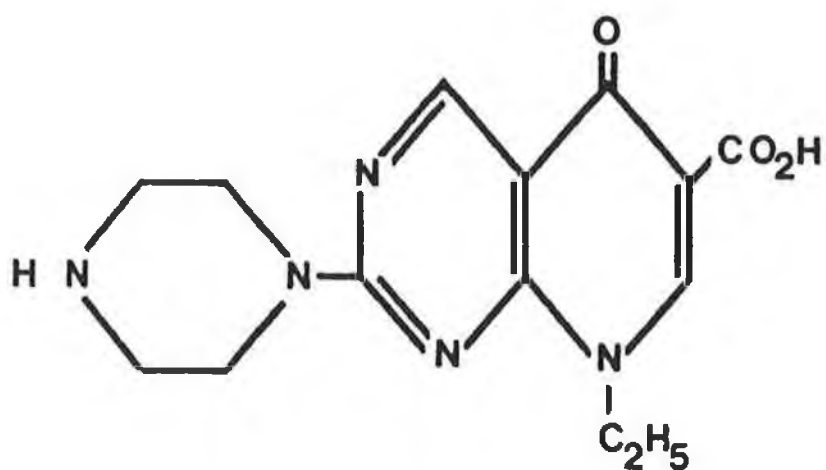


Fig. 4.1 Chemical structure of pipemidic acid.

determination of drugs is highly regarded. Here, quantitative analysis of drugs is mandatory in production processes and required to meet legal regulations which rule the marketing and use of drugs. Typical examples in pharmaceutical analysis are the determination of drugs of possible degradation products in pharmaceutical formulations. In this respect, polarography has been successfully applied to the determination of pipemidic acid in pharmaceutical formulations [9].

Electrochemical methods of analysis offer attractive advantages in clinical chemistry. Some of these advantages will be discussed in this chapter, as they form an important part in the practical considerations adopted for the subsequent experimental work. The objective of the present chapter is to describe briefly electrochemical techniques commonly employed in pharmaceutical analysis, and to examine some electrochemical characteristics of pipemidic acid at hanging mercury drop electrodes. These characteristics have been the basis to further develop an analytical method for the determination of pipemidic acid in urine using adsorptive stripping voltammetry (AdSV).

4.2 ELECTROCHEMICAL ANALYSIS IN CLINICAL CHEMISTRY

The application of electroanalytical techniques to the determination of biomolecules and drugs dates back to the development of polarography. The results of that development were reviewed at that time by Brezina and Zuman [10].

Classical direct current (DC) polarography, which was the fundamental technique of the time, did not possess sufficient sensitivity to determine organic species at trace levels in biological matrices. Consequently, the methods developed for these type of samples were only of limited value for

application to pharmacokinetic studies and drug monitoring. However, they proved to be more efficient in toxicological analysis, where the relatively high concentration of the toxic species could be measured by polarography, sometimes obviating the need for prior separation. The polarographic determination of drugs in pharmaceutical formulations was less affected by sensitivity requirements and was, therefore widely used at that time.

During the 1960's, the development of chromatographic and optical methods of analysis, which offered superior sensitivities compared to DC polarography, produced a strong decline in polarography as a suitable technique in analytical practice.

Nevertheless, the technique remained of considerable interest in academic circles. Paradoxically, it was during this time that the theoretical basis for the development of modern voltammetric techniques were laid. These techniques, whose development owed much to the advances in electronic technology of the time, offered enormous advantages compared to classical polarography.

Under the collective name of 'modern voltammetric methods', the following techniques are included [11,12]:

- pulse polarography and differential pulse polarography
- alternating current polarography
- linear sweep voltammetry
- stripping voltammetry
- square wave polarography.

One characteristic of these techniques, with the exception of stripping

voltammetry, is that they may all use the dropping mercury electrode (DME). For all of the techniques listed, a stationary mercury or solid electrode can also be used as the working electrode. In the following theoretical considerations, the term "polarography" shall be reserved for those voltammetric techniques which employ the DME as working electrode. The application of these electroanalytical techniques to the determination of organic species generally requires the molecule to have an electroreducible or electrooxidisable moiety in its molecular structure [13].

4.2.1 ORGANIC POLAROGRAPHY

4.2.1.1 Electroreducible Molecules

Molecules included in this group usually possess unsaturated groups such as multiple carbon-carbon bonds, carbonyl groups, carbon-nitrogen bonds, nitrogen-nitrogen multiple bonds and nitrogen-oxygen bonds. Numerous heterocyclic compounds (e.g. purines, pyrimidines, pteridines, etc.), and organosulphur compounds, and carbon-halogen compounds are also electroactive.

Mercury electrodes are most often employed for the analysis of such compounds, although solid electrodes might also be employed. The number of molecules and drugs included in this group is very large. Smyth and Franklin Smyth [13] have reviewed the reduction mechanism and analytical applications of the most important groups of these molecules.

4.2.1.2 Electrooxidisable Molecules

The molecules that may undergo oxidation in the range of potentials available over mercury electrodes are rather scarce. Nevertheless, some important biomolecules and drugs present such behaviour e.g. ascorbic acid,

a-tocopherol, folic acid, phenothiazines, etc.). Oxidation of most organic molecules occur at potentials where the use of carbon solid electrodes or noble metals are required. Phenolic compounds, aromatic amines and numerous heterocycles are included in this group.

4.2.1.3 Molecules which originate anodic processes due to the formation of complexes or insoluble salts with the metal of the electrode

Typical examples of molecules belonging to this group are the mercaptans, pyrimidines and thioamides. Zuman [14] has compiled a list of functional groups which are likely to undergo these processes.

4.2.1.4 Molecules capable of originating catalytic processes

A classical example of this type of electroactivity are the Brdicka waves given by serum proteins in the presence of ammonia solutions of cobalt II. They have been extensively studied and are importantly considered as diagnostic criteria in several diseases [15].

4.2.1.5 Molecules which are capable of adsorption at mercury electrodes and originate tensammetric processes

Several surfactants have been determined by this procedure. Kalvoda [16] has combined the accumulation by adsorption on stationary electrodes with tensammetric analysis of the adsorbed species, which has resulted in analytical methods of high sensitivity for substances of this type.

4.2.1.6 Derivatisation

For molecules that do not possess suitable functional groups, and

therefore cannot be included in any of the groups already mentioned, it is possible to introduce electroactive functional groups by means of chemical reactions. This procedure is useful in pharmaceutical analysis [17], and there are abundant reaction procedures described for this purpose. In analysis at trace levels in biological matrices, these procedures are less frequently applied. Smyth and Smyth [17] have reviewed the most usual procedures of functionalisation of non-electroactive molecules.

4.2.2 General Features of Voltammetric Techniques

Modern electroanalytical techniques possess in general a high sensitivity and give rise to low limits of detection based on discrimination of the background current. Differential pulse polarography can normally reach limits of detection in the range of concentrations 10^{-7} - 10^{-8} M. Square wave polarography may increase this limit of detection over one order of magnitude. These sensitivities are comparable, or slightly superior, to those of spectrofluorimetry or gas chromatography. Stripping voltammetric techniques and liquid chromatography with electrochemical detection allows one to obtain sensitivities which are inaccessible to most of the current instrumental analytical techniques available for analysis of organic compounds.

Sensitivity is one of the characteristics most valued in analytical applications within the field of clinical chemistry. In pharmaceutical analysis, most sensitive voltammetric techniques are used for the determination of traces of drug degradation products in commercial preparations.

An important drawback constitutes the apparent lack of selectivity of voltammetric techniques. Interferences in the determination of drugs in biological matrices might result from the presence of endogeneous compounds

which originate processes at a potential close to that of the drug or its metabolites. An interesting aspect to be considered in an analytical method for the determination of drug species is their capacity to measure selectively the drug in the presence of its metabolites. Metabolic transformations may modify the electroactivity of the drug, or even suppress it by affecting the nature of the functional group or the structure responsible for this activity.

Although direct determinations of drugs in serum and urine by voltammetric techniques are found in the literature without previous separations [18], this procedure is not generally valid, unless this has a toxicological objective rather than a clinical one i.e., drugs which have been administered to produce serum concentrations higher than 10 ug ml^{-1} [19]. In the analytical control of a certain therapy and in pharmacokinetic studies, the analytical problem is a determination at the ultra-trace level with typical concentrations in the range of ng ml^{-1} . Here, previous separations are indispensable.

The precision of modern polarographic techniques is high. Voltammetric techniques with stationary mercury electrodes also present good precision. In this respect, problems are presented by solid electrodes, due to the non-renewable character of the surface, which is a cause of bad reproducibility.

In pharmaceutical analysis, differential pulse polarography has found extensive applications. The determination of drugs in the presence of non-electroactive excipients permits one to carry out direct analysis, and errors of 1-2% together with relative standard deviations of the same order are easily attainable.

Voltamperometric techniques can be easily automated for analytical

procedures. The recent introduction of computerised instrumentation permits a large number of samples to be processed with minimum attention by the operator. From an economic standpoint, these techniques offer a utility/price relation that is highly attractive. The instrumentation is simple and obviates the need for expensive single components with limited life time. This reduces maintenance cost to a minimum.

4.3 THEORY OF ELECTROANALYTICAL TECHNIQUES

4.3.1 Introduction

Electrochemical analysis has a fundamental theoretical basis of great complexity. This section aims only to explain some theoretical basis and applications of techniques used in the experimental part of this thesis. No detailed discussion of fundamentals or applications of these techniques will be treated, as these are explained systematically in comprehensive books of electrochemistry. In this case those texts will be cited where necessary.

4.3.2 Polarographic Techniques

4.3.2.1 Classic Direct Current (DC) Polarography

As in all voltammetric techniques, DC polarography involves the application of varying the applied potential ($< 10 \text{ mV s}^{-1}$) with time at a DME, and recording of the current intensity response as a function of the potential applied.

The study of DC polarographic waves allows one to obtain a large amount of information on the nature of the processes taking place at the electrode. The interpretation of these waves is based on an extensively developed theory treated by Heyrovsky and Kuta [20], and Meites [21]. The most recent

development of the technique (i.e. Tast polarography) has been well discussed by Bond [11]. Zuman [14] has written a classical book on organic polarographic analysis, and has reported the principles on which the application of this technique is based for the study of the mechanism of electrode processes [22].

4.3.2.2 Differential Pulse Polarography

The main characteristic of this technique lies in the utilisation of an application of successive potential pulses of constant amplitude and short duration (typically 60 ms), which are imposed on the slow linear potential sweep. The application of the pulse is produced at the end of the life time of the drop (controlled drop time) and the response current is processed in a way that the output signal is given by the difference between the intensities measured about 15 ms before the drop falls and that at an equal time before the pulse is applied. The technique makes use of the fact that the capacitive current decreases exponentially with time after the application of the potential pulse, while the faradaic current decays proportionally to $t^{-1/2}$, i.e. at a slow rate. The ratio of faradaic current/capacitive current at the end of the pulse is therefore very favourable, thus permitting the measurement of very small currents produced by substances which are present in solution at very dilute concentration. The waves so obtained are presented as a peak due to the differential recording of the current. The equations that express the relationship intensity-potential with respect to the characteristic parameters of the technique, e.g. pulse amplitude, pulse duration, have been laid out by Parry and Osteryoung [23]. The theory for reversible processes has been treated by Bond [11] and the criteria for reversibility in this technique has been established by Birke [24].

4.3.2.3 Alternating Current Polarography

The wave form used in this case consists of a small-amplitude sinusoidal alternating potential superimposed onto the usual potential ramp used in DC polarography. The current in the cell contains AC and DC components constituting the response to the sinusoidal tension and to the linear potential scan respectively. The DC component is eliminated by recording solely the AC current with the same frequency as the applied sinusoidal potential. The resulting plot constitutes an AC polarogram.

The recorded current contains both faradaic (i_f) and capacitive (i_c) components. The alternate faradaic current responds to the periodic variation in the concentration relationship between the oxidised and reduced forms of the electroactive species at the electrode-solution interface. For fast reversible electrode processes, the resulting alternating current intensity will be large, while a small response will be expected for sluggish processes.

4.3.2.4 Square Wave Polarography

This technique involves the application of a small amplitude square wave voltage instead of the sinusoidal one used in AC polarography. The alternating current detection is effected by sampling the current near the end of each square wave half-cycle, and the current-voltage curve consists of a plot of the alternating current sampled during the positive and negative square wave half-cycles versus the DC potential. Discrimination against the charging current, which results from the growth of the mercury drop, is minimised by measuring the current at the end of the drop life where the rate of area change is very small. The change in charging current is exponential and is a function of time, with the decay being proportional to e^{-t/RC_d} (where R is the ohmic

resistance of the circuit, t is time, and C_{dl} is the capacity of the double layer). When square wave pulses are superimposed onto the DC potential, the faradaic current changes as a function of $t^{-1/2}$, implying that decay in charging current is faster than that of the faradaic current. In essence the technique discriminates greatly against charging current based on the smaller RC time constant associated with the double layer charging process relative to the faradaic process. Square wave polarography is basically equivalent to sinusoidal AC polarography, although having greater sensitivity. Discussion on square wave polarography is available in several books [25,26].

4.3.2.5 Stripping Voltammetry

In conventional polarographic and voltammetric techniques the intensity of the analytical signal is limited by the diffusion of analyte from the bulk of the solution to the surface of the electrode. At very low concentrations, the availability of electroactive material during the potential sweep is generally insufficient to produce a response that differentiates well enough from the capacitive current. This physical limitation of the voltammetric techniques to sensitivity can be overcome by controlled accumulation of the analyte on the surface of the working electrode before the voltammetric measurement is taken. Several techniques have been developed regarding this approach under the name of "stripping voltammetry". They are characterised by their extraordinary sensitivity, while maintaining other favourable characteristics of voltammetric techniques such as precision, ease of automation, and the possibility of simultaneous determination of several elements.

Fundamentals common to all stripping voltammetric techniques is, as

already mentioned, the accumulation of either the analyte or a species generated from it by means of a chemical or electrochemical reaction, on the surface or within the working electrode. Under rigorously controlled hydrodynamic and electrochemical conditions, it is possible to establish well defined relationships between the amount of analyte accumulated and its concentration in the bulk of the solution. The voltammetric response generated by the stripping or electrochemical transformation of such a deposit constitutes a measure of the concentration of analyte in solution.

Classification of stripping voltammetric methods is based on two criteria:

1. The nature of the accumulation process according to the electrochemical or chemical reactions involved. Undoubtedly, this is the most important aspect which states the most significant differences among the various techniques.
2. The voltammetric technique employed in the measurement of the accumulated species. Here, it is advisable to remember that potentiometric methods have also been used, specially in simultaneous determination of various elements.

According to the nature of the accumulation process three techniques can be clearly defined.

4.3.2.5.1 Anodic Stripping Voltammetry (ASV)

ASV is the most extensively used technique in the determination of heavy metal ions in environmental and biological samples. The accumulation step takes place by cathodic electrodeposition at a potential corresponding to the diffusion plateau of the reduction wave of the analyte at the working electrode. The metal is reduced in the form of an amalgam (mercury electrode)

or in the form of an adhered (film if a solid electrode is employed). The measurement is performed by scanning the potential in the positive direction and the analytical signal is constituted by the anodic peak appearing at the potential in which the deposited metal is reoxidised. The corresponding electrochemical reactions are:



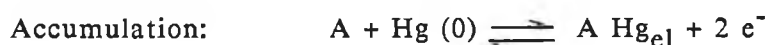
In practice, the field of application of ASV is restricted to the determination of heavy metals. However, it would be possible to expect that this technique can be applied to the determination of organic compounds belonging to redox systems in which the reduced form is electroactive and able to adsorb strongly on the working electrode. Although numerous systems of this kind have been extensively studied with regards to their adsorption behaviour (methylene blue, riboflavin), examples of analytical applications to the determination of organic species are rather few.

4.3.2.5.2 Cathodic Stripping Voltammetry

This technique presents two variables which are characterised by the use of either non-inert or inert electrodes. In the first instance, which is only important with regards to the determination of organic molecules, the analyte is accumulated at the surface of the working electrode in the form of either a sparingly soluble salt or an adsorbed coordination compound formed between the substance to be determined and the ions coming from the dissolution

of the working electrode material. During the accumulation step the potential is kept at a value at which the electrode is oxidised in the presence of the analyte. In the measurement step, the potential is scanned in the negative going direction, and the analytical signal consists of a cathodic peak that appears at the potential at which either the anion or ligand bound to it is reduced.

The corresponding electrochemical reaction are as follows:



The most frequently used electrode materials are mercury and silver. The application field comprises several inorganic anions capable of forming sparingly soluble salts with mercury and silver, as well as with organic species containing certain functional groups (mercaptans, thioamides, pyrimidines) which interact with mercury ions. In the second instance, inert electrodes made up of carbon or noble metals are used for the determination of ions such as Mn (II) or Pb (II) which can be accumulated as oxides.

4.3.2.5.3 Adsorptive Stripping Voltammetry (AdSV)

The main characteristic of this technique is that the analyte is accumulated and later measured as is, without any previous electrochemical transformation to another chemical species. The accumulation step takes place without any electron transfer at the electrode-solution interface; accordingly, it is not necessary, in general, to keep the electrode at a too highly positive

or negative potential during the accumulation step. In fact, although the extent of the accumulation may show a dependence on the accumulation potential, it is feasible to carry out an effective accumulation of the analyte under open circuit conditions.

The main advantage of this technique versus ASV lies in the fact that the former avoids the electrodeposition of traces of metallic impurities present in the background electrolyte, which could provoke serious interferences in the measurement step. When compared with CSV, adsorptive stripping voltammetry shows a notably superior sensitivity, which can be understood by taking into account that the adsorptive accumulation is not limited by the solubility of the mercury salt.

Kalvoda [27] has reviewed the analytical applications of adsorptive stripping voltammetry, pointing out the wide range of application of this technique. This includes organic ions, as well as both electroactive and non-electroactive species.

Adsorptive stripping voltammetry may be applied to the determination of any species that can be accumulated by adsorption in a controlled manner onto any kind of electrode. This implies that clear and well defined relationships should exist between the surface concentration of the adsorbed species, Γ , its concentration in the bulk of the solution, C_0 , and the accumulation time, t_{acc} . Such a defined relationship exists when the two following conditions are met [28]:

- 1) the adsorption rate is very large in relation to the transport rate of the species from the bulk of the solution to the surface of the electrode;
- 2) the adsorption equilibrium lies strongly in favour of the adsorbed species.

Phillips [29] has shown that the surface concentration of the adsorbed species 0 can be expressed in terms of the concentration in the bulk of the solution, the diffusion coefficient (D) and the accumulation time as follows:

$$\Gamma_0 = 1.128 C_0 D_0^{1/2} t_{acc}^{1/2} + C_0 D_0 (t_{acc} / r) \quad (4.1)$$

which is fulfilled for spherical electrode of radius r when the transport of substance takes place under pure diffusion conditions. Valenta [30] has shown that the second term of equation 4.1 is negligible for small values of t_{acc} . Accordingly, the Koryta equation [31] could be considered as a limiting situation of equation 4.1 for small values of t_{acc} , e.g. accepting the slightly smaller value of the numeric coefficient of the first term.

When the accumulation process takes place under convective mass transport conditions, the hydrodynamic conditions of the cell exert a determining influence on the dependence of Γ_0 upon C_0 and t_{acc} . If magnetic stirring is used, as frequently occurs to be, the Nernst diffusion layer hypothesis [32] leads to an expression of the following type:

$$\Gamma_0 = K C_0 t_{acc}$$

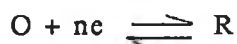
where, K is a coefficient depending upon the geometry of the cell and the stirring conditions, both of which are assumed to be invariable.

Once a relationship between Γ_0 and C_0 has been established, any voltammetric technique giving rise to a response proportional to Γ_0 will be

valid, at least in principle, for analytical purposes.

The voltammetric behaviour of adsorbed species presents notable peculiarities with respect to those substances being reduced under diffusion-controlled conditions. These peculiarities will yield important advantages from an analytical point of view, as will be seen later on.

Given a redox system:



in which both oxidised and reduced forms adsorb strongly on the electrode. It is assumed that:

- 1) all the adsorption sites on the electrode surface are equivalent (homogeneous surface)- this hypothesis is rigorously fulfilled by mercury electrodes;
- 2) the adsorption processes of both species O and R obey the Langmuir isotherm, which means that interactions among molecules in the adsorbed phase are negligible- such an hypothesis is acceptable in the case of low coverage values.
- 3) the surface concentrations Γ_O and Γ_R vary with the potential in accordance with the Nernst equation.

A surface standard potential, $E^{0'}$, can be defined as:

$$E^{0'} = E^0 - (G_R - G_O) / nF$$

where, $E^{0'}$ is the standard potential of the system in solution and G_R and G_O are the adsorption standard free energies of the reduced and

oxidised species respectively.

The application of the Nernst equation to the system leads to :

$$= \exp [(nF / RT) (E - E^{0'})] =$$

Laviron [33,34] has established the equations for the voltammetric curves obtained by linear sweep voltammetry or cyclic voltammetry for the system and conditions described above. The expression for the linear sweep voltammogram is as follows:

$$[i] = (F^2 n^2 v A \Gamma / RT) [(1 +)^2]$$

where v is the potential scan rate, A is the area of the electrode and Γ is the global surface concentration of both species. The curve present a maximum for $\alpha = 1$, that is to say for $E = E^{0'}$. The voltammetric peak potential is the same as the surface standard potential. The peak is symmetrical with respect to the line parallel to the ordinates axis that crosses the potential $E^{0'}$. The cyclic voltammetric curve shows an anodic peak symmetrical to the cathodic peak. Both peaks have a width at their half height of $90/n$ mV at 25°C .

The peak intensity shows a linear dependence on the potential scan rate. This characteristic, together with the symmetrical shape of the cyclic voltammogram, allows for an easy differentiation of this kind of process from those which are diffusion-controlled, whose peak intensities show a linear

dependence with the half power of the scan rate [35].

For higher surface concentrations, it is not possible to describe the interactions among the adsorbed molecules; a Frumkin isotherm being necessary to describe the adsorption process [34].

In the case of predominant attractive forces, the peak potential undergoes a displacement to more negative values, owing to the fact that it is necessary to provide additional energy to overcome the attraction interactions. For sufficiently intense interactions, the peak becomes thinner and sharp [33]. In the cyclic voltammogram, a hysteresis effect appears [36], which consists in a separation of the cathodic and anodic peaks differing now in their peak potentials. Under these conditions no mathematical description of the curve can be made.

The advantages of adsorptive stripping voltammetry over those techniques operating under diffusion control are not restricted to the accumulative adsorption of the substance onto the electrode, which results in an improved analytical signal. The fact that the peak intensity varies linearly with v rather than $v^{1/2}$ prohibits a drastic fall in the ratio of faradaic to capacitive current to occur when higher scanning rates are used, with the subsequent gain in sensitivity and time of analysis.

The high sensitivity shown by adsorptive stripping voltammetry, together with its excellent precision and instrumental simplicity, make of this technique an attractive tool for the determination of drugs in biological samples at low level concentrations. However, the development of this kind of application finds difficulties arising from the extremely complex nature of biological materials, and particularly from the presence of large amounts of surfactants (proteins, lipids, etc.) that are able to adsorb on the working

electrode hindering the accumulation of the analyte of interest.

Kalvoda [37] has discussed the general conditions for the application of this technique to determine electroactive organic molecules, paying special attention to the effect caused by the presence of other surfactants upon both the accumulation process and the voltammetric behaviour of the adsorbed electroactive species. Kalvoda points out that the competitive coverage of the electrode surface by the interferent surfactants makes the analytical response to decrease and can even fully suppress the accumulation process. The longer the accumulation time the more acute the interference of surfactants. This can be explained owing to the fact that the time required to reach a complete coverage of the electrode is inversely proportional to the surfactant concentration in solution [38].

The paramount importance of this phenomenon when applying adsorptive stripping voltammetry to analysis in biological samples has urged various authors to study in certain detail the effect of several surfactants upon the adsorptive voltammetric behaviour of the analytes of interest. Thus, Osteryoung and co-workers [39] have examined the reduction behaviour of the antihistaminic drug cimetidine when adsorbed in the presence of human serum and Triton X-100. They found a similar suppression effect for both of them. The authors recommended a previous chromatographic separation before the determination of cimetidine in serum.

Wang et al. [40] have studied the systems riboflavin-camphor and flavine-mononucleotide-gelatin, reporting that 5 ppm of either surfactant suppresses the stripping peak of the nucleotide and diminishes the stripping peak of the flavine to 45% of its original value. Neither of the surfactants modify either the peak potential or its morphology.

Fernandez et al. [41] have reported an extensive study on the suppression effect of anionic, cationic and non-ionic surfactants on the adsorptive stripping voltammetric behaviour of folic acid. The authors pointed out the marked effect of the mass transport conditions on the suppressing role of the surfactants; thus a preconcentration step carried out in unstirred solutions yields stripping peaks whose shape and intensity remain essentially unaltered in the presence of gelatin.

Kalvoda [37] has shown that the determination of 1×10^{-7} M nitrazepam is feasible in the presence of 5 ppm of gelatin for accumulation times shorter than 15 s, whereas the use of t_{acc} longer than 60 s produces a total suppression of the analytical signal.

Some conclusions can be drawn from the above cited references:

(i) it is not feasible for direct determination of organic species by adsorptive stripping voltammetry in matrices containing high concentration of surfactant materials (e.g. serum), in which case it is necessary to carry out a previous separation of interferent species.

(ii) the suppressing effect of surfactants is lessened by using shorter accumulation times or unstirred solutions.

(iii) although there exists a rapid growing number of papers that apply this technique to the determination of molecules of biological importance, the analytical applications in biological samples is still rather scarce.

4.4 EXPERIMENTAL WORK

4.4.1 Apparatus

Voltammetric experiments were carried out using either a computerised electrochemical measurement system (Inelecsa, Seville, Spain) or alternatively, a Metrohm E-611 potetioestat coupled to a Metrohm E-612 scanner. The linear sweep voltammograms produced by the latter instrument were recorded on a Graphtech WX-4421 X-Y recorder. A Metrohm EA-410 hanging mercury drop electrode (HMDE) was used throughout as the working electrode. The drop size corresponded to three divisions of the micrometric dial of the electrode. A platinum wire was used as the auxiliary electrode with a saturated calomel reference electrode. The solutions were stirred using a 12-mm magnetic stirring bar (Metrohm, Herisau, Switzerland).

4.4.2 Materials

Pipemidic acid was obtained from Prodes Pharma Laboratories (Barcelona, Spain). Stock solutions (1.0×10^{-2} M) of pipemidic acid were prepared in 5.0×10^{-2} M NaOH each week. Solutions were stored at 4°C and protected from the light. Britton-Robinson (B-R) buffers, of constant ionic strength adjusted to 0.3 M with KCl, and standardised 0.1 M HClO_4 solutions were used as background electrolytes. All other reagents were of analytical reagent grade (Merck, Darmstadt, FRG) and purified water was obtained by passing distilled water through a Milli-Q (Millipore-Waters, Milford, MA, USA) system.

4.4.3 Method

For voltammetric investigations, the test solution (20 ml) was de-aerated with oxygen-free argon for 15 minutes (and for a further 30 s before each new measurement). An equilibrium time of 10 s was allowed to elapse between the end of the stirring and the start of the potential scan. The potential unless stated otherwise, was scanned at 1 Vs^{-1} .

4.5 RESULTS AND DISCUSSION

4.5.1 Cyclic Voltammetry

Pipemidic acid undergoes two main reduction processes at the HMDE as seen from the cyclic voltammogram shown in Fig. 4.2, obtained for a $5.0 \times 10^{-5} \text{ M}$ solution of the drug in Britton-Robinson buffer pH 3.04. The resultant peaks, namely peak 1 appearing at -569 mV and 2 at -892 mV, are symmetrical in shape with a width at their half height of 30.3 and 63.4 mV respectively, indicating adsorption controlled processes. At higher concentrations, i.e. $2.0 \times 10^{-4} \text{ M}$, the shape of the curves changed into waves which showed typical diffusion plateaus, indicating that the processes are diffusion controlled under these conditions. Maintaining the same procedure, but lowering the concentration of the drug to $2.0 \times 10^{-7} \text{ M}$, resulting in the voltammograms showing a rather negligible current for the second process while the first was not visible at all. However, when the potential scan was performed after allowing a period of accumulation of 75 s under electrolysis, process 2 appeared as a well defined peak, while process 1 remained unseen. This phenomena, although only an assumption at this stage, indicates the possibility of adsorptive accumulation of pipemidic acid at the HMDE.

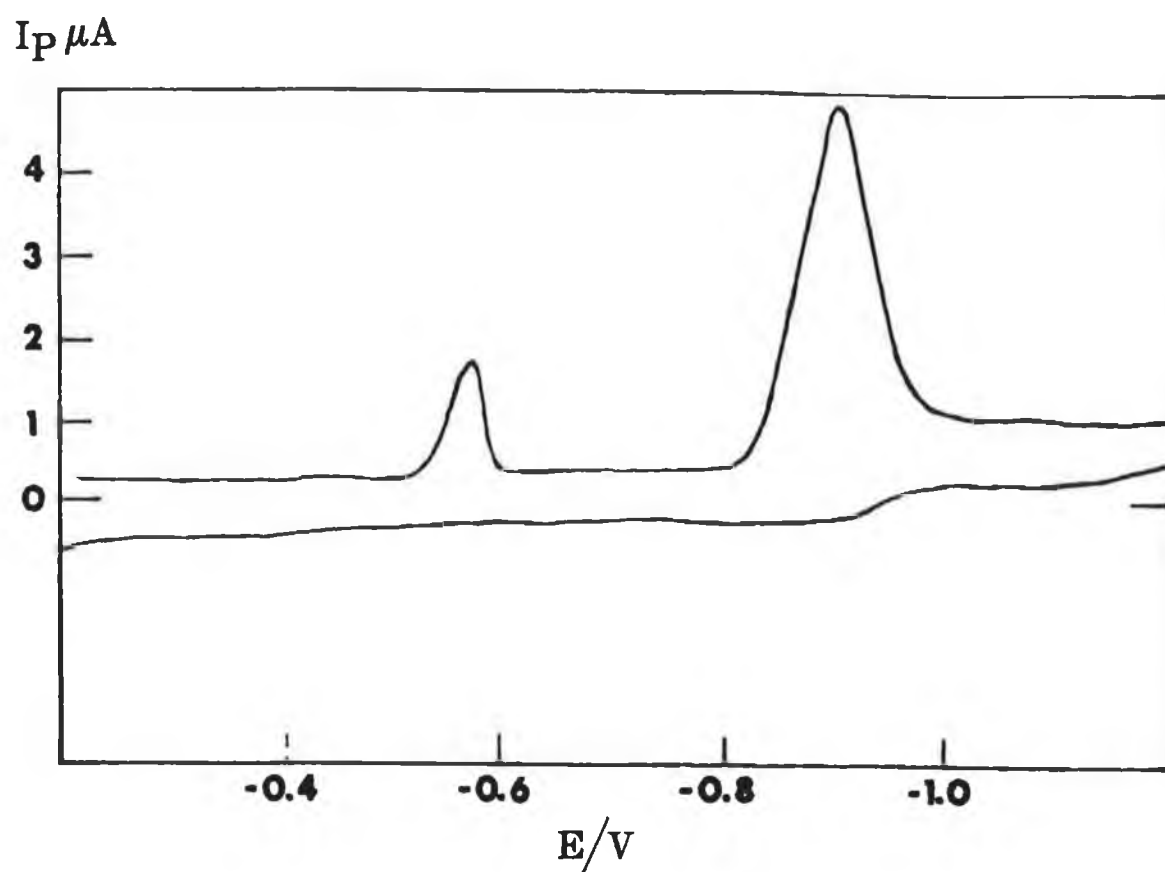


Fig. 4.2 Linear sweep solution phase voltammograms obtained for 5.0×10^{-5} M of pipemidic acid in Britton - Robinson buffer pH 3.04 at a scan rate of 1 V/s.

4.5.2 Influence of pH

The influence of pH was studied in Britton-Robinson buffers ranging from pH 2 to pH 11. Such solutions had an ionic strength adjusted to 0.3 with KCl. 0.1 M Perchloric acid was also employed during this study to examine the behaviour of the drug at pH 1. Solutions of pipemidic acid (2.0×10^{-4} M) were prepared and voltammograms were recorded as described in the experimental section.

The resulting voltammograms showed that process 1 takes place between pH 1 and 5 (1, Fig. 4.2), while process 2 exists over the whole range of assayed pH values, i.e. 1-11. At pH values above 7, the shape of peak 2 changed somewhat. Thus, at pH between 8 and 9 the wave splits into two waves (Fig.4.3) at pH 10 it reassumes the single wave morphology and, finally, at pH 11 the wave appears split again. This behaviour resembles closely the work of Hoffmann and Dybowski [9] who have previously reported on the DC polarographic characteristics of pipemidic acid.

Peak currents for process 1 showed little dependence on pH (Fig. 4.4), whereas pH had a marked influence upon peak currents for process 2 (Fig. 4.4), with 0.1 M HClO_4 yielding the maximum analytical signal. From this it was readily concluded that peak 2 was the most important for analytical purposes in the pH region from 1 to 7, where peak currents for this process were improved compared to peak 1 by a factor of about 3. Accordingly, the rest of the study was concentrated on peak 2, whose peak potential, E_p , varied linearly with pH in the range 1 to 5 according to the equation:

$$E_p(\text{mV}) = -66.7 \text{ pH} - 715.7$$

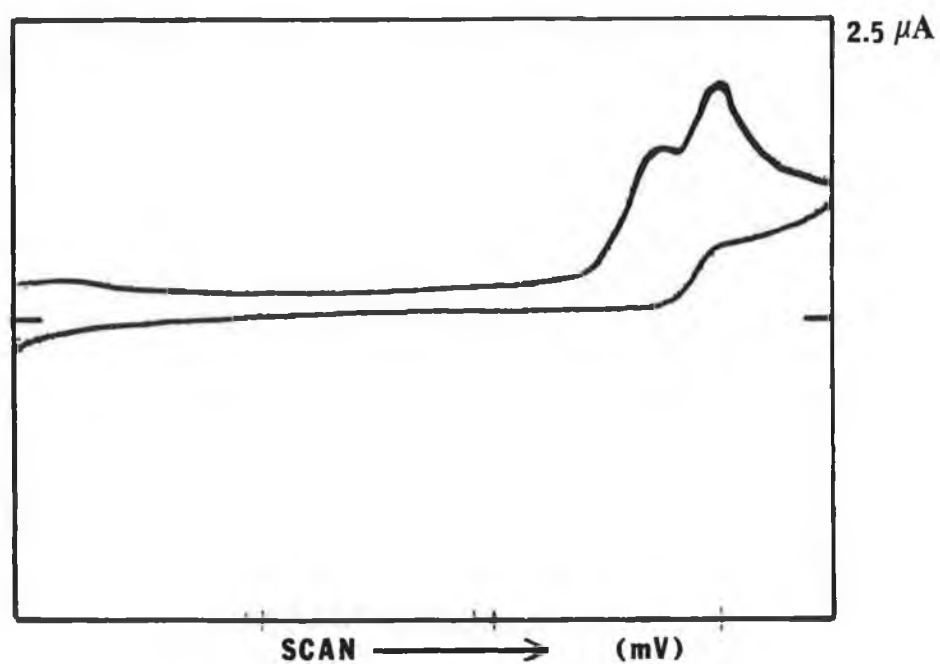


Fig. 4.3 Reduction wave of pipemidic acid at pH 8.

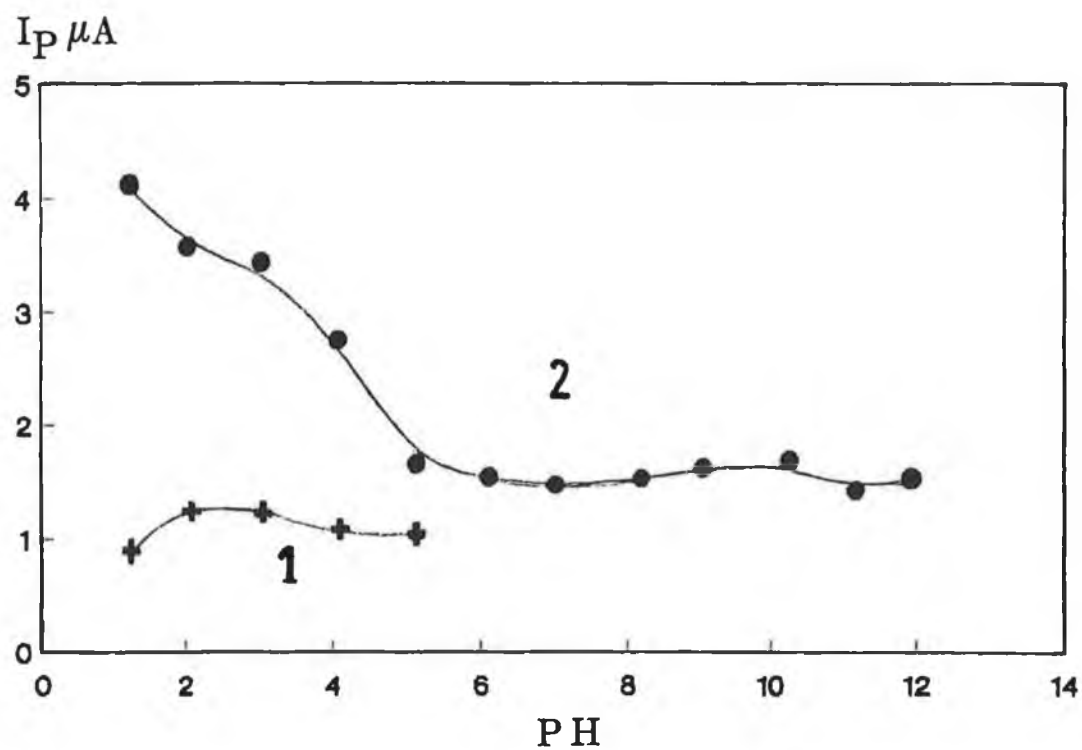


Fig. 4.4 Effect of pH on peak current.

With respect to peak 1 it was observed that a cyclic voltammogram recorded to potentials less negative than those at which process 2 appears gave rise to a new peak in the anodic region of the voltammogram. This would imply a certain degree of reversibility for process 1. In fact it could be ascribed to the reversible reduction of the semiquinone which has been reported to take place in acidic media at about this potential [42]. Nevertheless, when the potential was allowed to reach values more negative than those at which the second reduction process occurs, no peak appears in the reverse scan of the voltammogram. This seems to indicate that the second reduction process is related with the first one in such a way that it would result in the hindering of the reoxidation to the semiquinone. In relation to the second reduction peak, its nature has not been further investigated and all the rest of the work reported here will be focused on process 2 using 0.1 M HClO_4 standardised solutions as background electrolyte.

4.5.3 Adsorptive Stripping Voltammetric Behaviour of Pipemidic Acid

The adsorptive stripping voltammetric behaviour of pipemidic acid was studied in detail at low concentrations i.e. typically in the region of 10^{-7} M where the process is clearly adsorption-controlled. Consequently, the dependency of the voltammetric signal of the drug upon accumulation potential, preconcentration regime (forced mass transport or semi-infinite linear diffusion), preconcentration electrolytic conditions (under either electrolysis or open circuit), scan rate, accumulation time and concentration were examined.

4.5.3.1 Effect of Accumulation Potential

The measurements were carried out for 1.0×10^{-6} M solution of pipemidic acid with an accumulation time of 15 s under electrolysis. A period of 10 s as 'rest time' was permitted after the stirring was turned off. The potential was varied between +200 mV to -600 mV and swept at a scan rate of 1000 mVs^{-1} . The results from the curve shown in Fig. 4.5 indicate that the peak intensity is practically independent of the accumulation potential (E_{acc}) over a broad range. Except for a range of E_{acc} between +200 and 0.0 mV, which produces lower peak currents, variations in peak intensities for accumulation potentials varying between 0.0 and -600 mV are insignificant in this range of potentials. Although the adsorption of organic species at mercury electrodes generally presents dependence on the accumulation potential, there are examples of accumulation behaviour as the one described here [32]. This is undoubtedly advantageous for analytical purposes, when dealing with real samples that contain a myriad of potentially interferent substances. The fact of being able to preconcentrate at a sufficient negative potential provides one with a means to minimise the effect of those interferents which accumulate at more positive potentials, such as the case of commonly encountered compounds in blood or urine samples like sulphur-containing amino acids, proteins, uric acid, etc.. These compounds are liable to form salts with the mercuric ions generated at positive potentials.

According to these findings further experiments were carried out at E_{acc} of -500 mV, except when otherwise indicated.

4.5.3.2 Accumulation under Convective Transport Conditions

2.0×10^{-7} M solutions of the drug were stirred for 60 s under

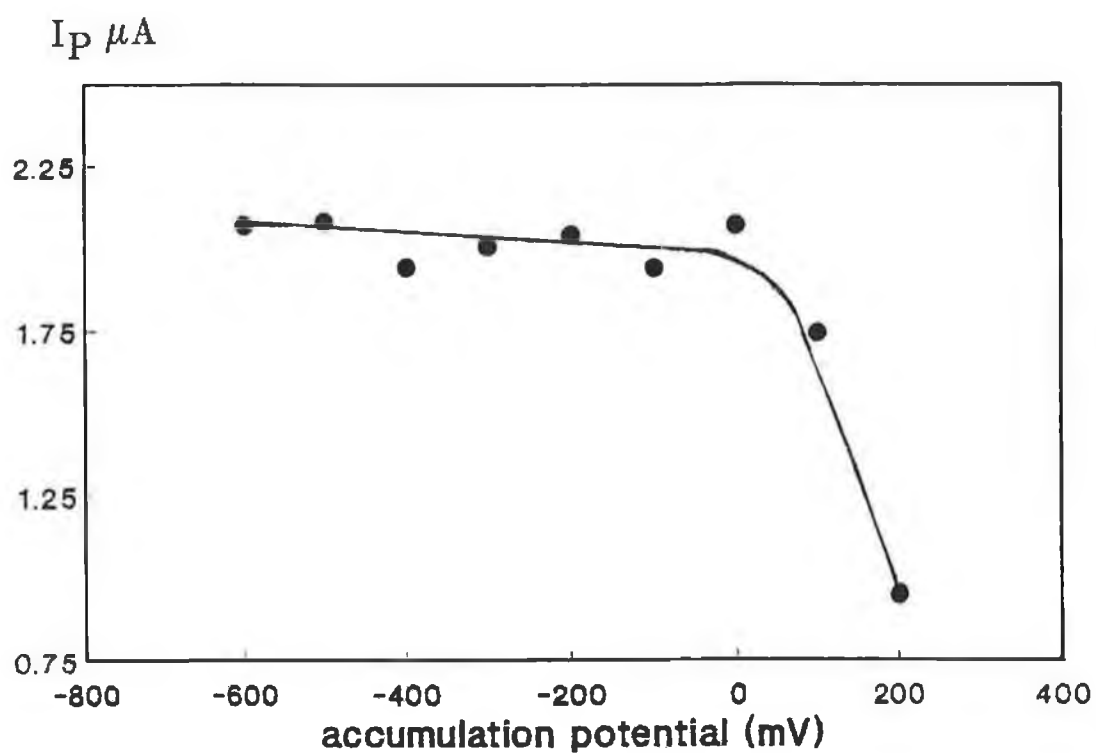


Fig. 4.5 Effect of the accumulation potential on the response signal of pipemidic acid.

electrolysis with 10 s of equilibration time after the stirring ceased.

Previous scans of the blank solution were carried out and found satisfactory during an accumulation period of 120 s. The voltammogram of pipemidic acid obtained at scan rate of 100 mV s^{-1} yielded a peak whose intensity was 1,450 nA in 0.1 M HClO_4 background electrolyte (Fig. 4.6a). In another experiment performed under the same conditions, but in which the mass transport was exclusively due to migration of the drug from the bulk of the solution under semi-infinite linear diffusion yielded a peak current of 350 nA after 120 s of preconcentration (Fig. 4.6b). Thus, these results imply that the rate-determining step of the process is clearly governed by the transport of the drug from the bulk of the solution to the surface of the electrode.

4.5.3.3 Influence of Electrolysis

At E_{acc} of -500 mV and a scan rate of 100 mV s^{-1} , stirred 5×10^{-7} M solutions of the drug were preconcentrated for 60 s, and the accumulation was examined both under electrolysis and in an open circuit mode. The results showed that accumulation did not occur at any significant extent when the preconcentration was carried out under open circuit (Fig. 4.7). In fact, from the values obtained, the accumulation under electrolysis gave a peak whose current was 1,530 nA, well above the value of 96 nA produced under open circuit condition.

4.5.3.4 Effect of Scan Rate

One of the important advantages of voltammetric techniques regarding adsorbed species in comparison to linear sweep voltammetry is that the peak intensity of the absorbed reducing species increases linearly with the scan

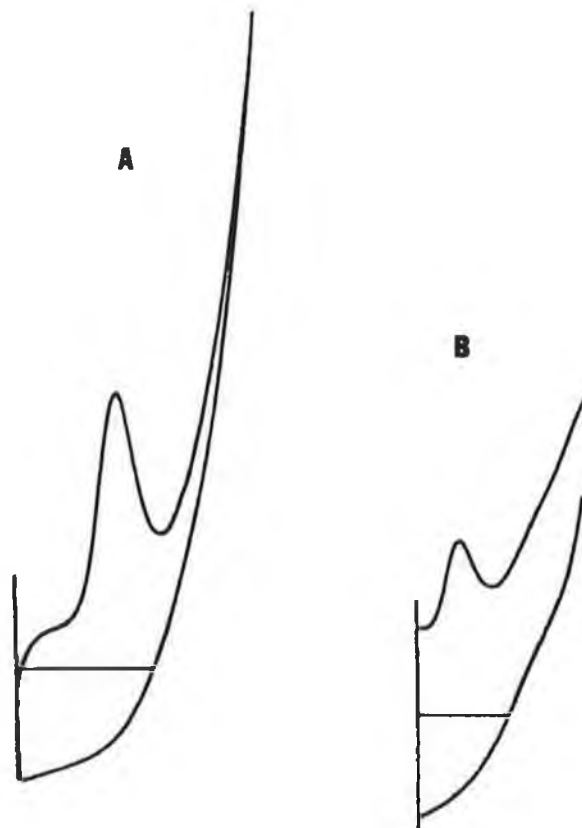


Fig. 4.6 Effect of the transport conditions of pipemidic acid to the surface of the electrode: (A) magnetically stirred solution; (B) stationary conditions.

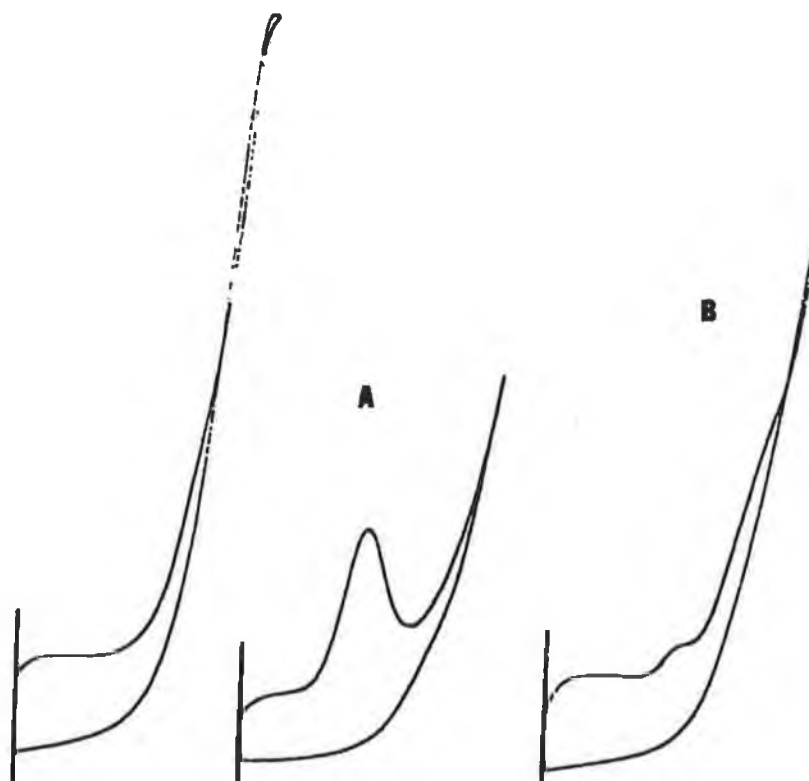


Fig. 4.7 Voltammograms under (A) electrolysis and (B) open circuit mode, for solutions containing 2.0×10^{-7} M pipemidic acid.

rate rather than with $v^{1/2}$. It is possible then to use higher scan rates thus maintaining an acceptable faradaic current/capacitive current ratio, while gaining some degree of sensitivity.

This dependency was demonstrated for the second reduction process of pipemidic acid in stirred solutions (t_{acc} 75 s and E_{acc} -500 mV). The results shown in Table 4.1 and Fig. 4.8, indicate that peak currents increased linearly with the scan rate between 100 and 1000 mVs^{-1} . The equation describing this linear relation is:

$$i_p \text{ (nA)} = 1.09 (v/V \text{ s}^{-1}) - 1.06; r = 0.9997, n = 7$$

$v / mV \text{ s}^{-1}$	i_{pc} / nA	i_f / i_c
100	101	2.26
200	208	2.89
300	312	3.37
400	436	3.79
500	502	3.20
700	766	3.61
1000	1.080	3.41

Table 4.1 Variation of the peak intensity and faradaic/charging current ratio with scan rate for a 2.0×10^{-7} M pipemidic acid solution, (t_{acc} 75 s, E_{acc} -500 mV).

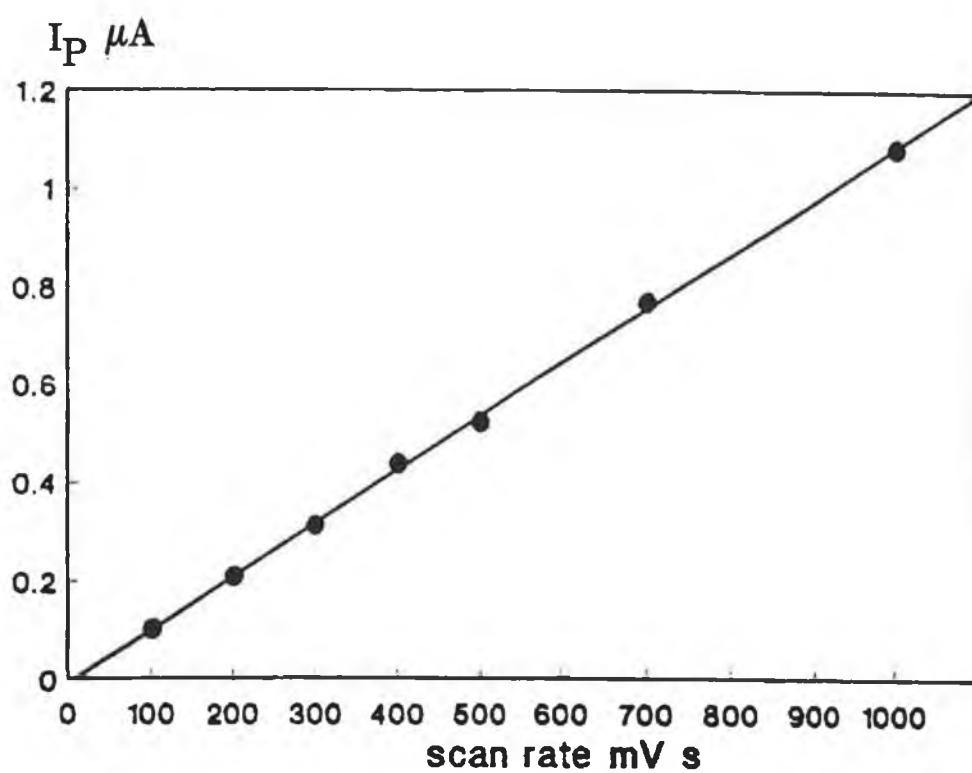


Fig. 4.8 Effect of the scan rate with peak intensity.

4.5.3.5 Effect of Accumulation Time

Under the above optimised parameters, successive accumulation stripping cycles were carried out for six different concentrations of the analyte. The resultant accumulation curves are shown in Fig. 4.9. As expected, the lower the bulk concentration of pipemidic acid, the lower the magnitude of the stripping current and the better the linear relationship between peak intensity and t_{acc} . In addition, a plot of the slope of the initial linear portions of the accumulation curves versus the corresponding concentrations gave rise to a linear graph as expressed by the equation:

$$\text{slope} = 9.04 \times 10^7 \text{ (nA s}^{-1} \text{ mol}^{-1}\text{)}$$

indicating that the adsorption process follows a normal Langmuir-type isotherm in the initial region of the plot. As either the t_{acc} or the assayed concentration take higher values, the peak current ceases to increase. In fact, it shows a trend to diminishing values that can even drop close to those achieved after a very short t_{acc} (Fig. 4.9). This could be explained in terms of an adsorption equilibrium (not a saturation equilibrium) that is a function of the bulk concentration of the drug, which is reached as a compromise between the adsorption forces driving the molecules to the surface of the electrode and the possible repulsion interactions of the molecules in the absorbed state, once a given coverage of the electrode has been reached.

Although there are not many of these phenomena reported in the literature, some examples of similar behaviour for molecules of biological importance are described in the work of Tunon Blanco et al [43], and Cortina Villar et al [44].

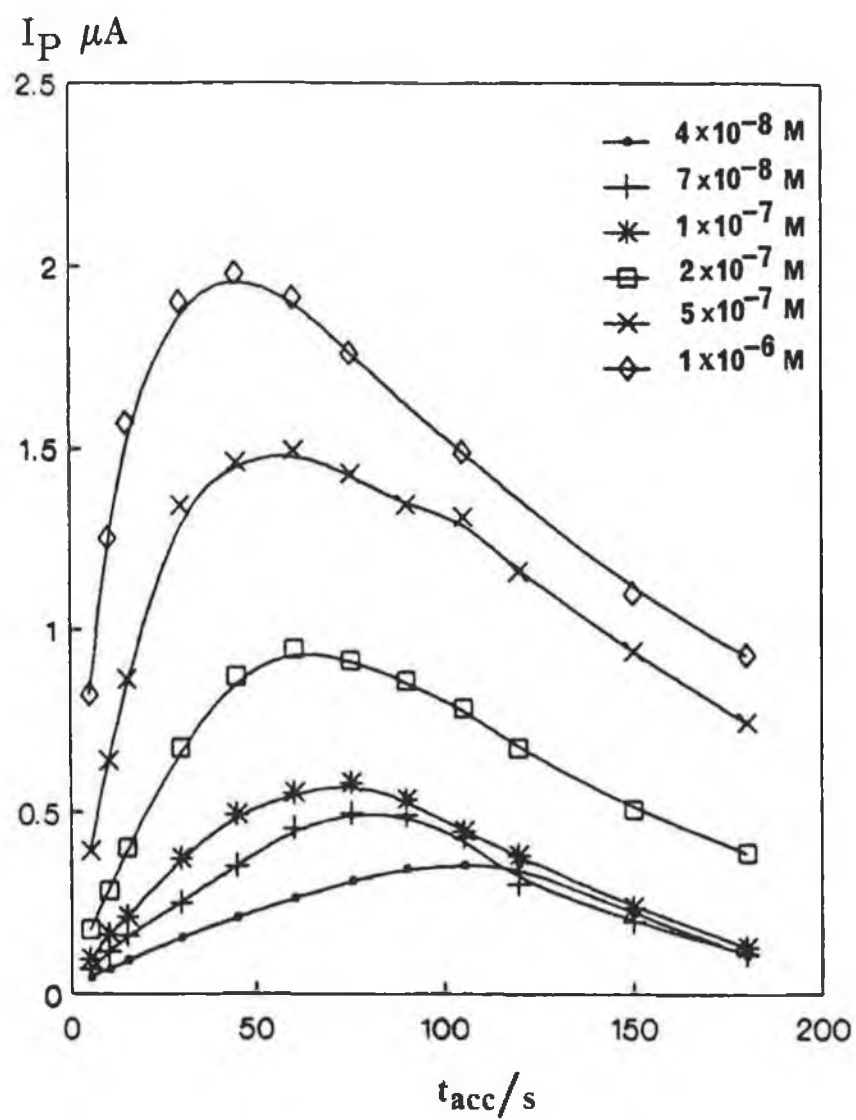


Fig. 4.9 Accumulation curves for different concentrations of pipemidic acid by linear sweep voltametry. E_{acc} -500 mV, scan rate $1.0 V s^{-1}$.

As can be seen from Fig. 4.9, analytically useful relations between peak intensity and concentration exist over the complete range of t_{acc} . However it is better that the quantification of the drug be performed by using those experimental conditions that fall within the initial zone of the accumulation curves where the maximum $i_p : t_{acc} : C$ ratios are attainable. According to this consideration and results shown in Fig. 4.9, it was decided that a t_{acc} of 75 s yielded about the highest degree of adsorption of pipemidic acid onto the surface of the electrode, and therefore the highest sensitivity for the determination of the drug.

In view of the described experiences it can be concluded that:

(i) pipemidic acid generates two reduction processes on mercury electrodes, one of which exists as a well defined single peak in a broad range of pH i.e. 1-7;

(ii) the nature of this reduction process remains unknown, but is likely to be associated with a reduction of the 5-oxo pyrimidine moiety in the molecular structure.

(iii) the drug adsorbs onto the electrode, the rate determining step of which depends on the transport of the drug from the bulk of the solution to the electrode surface;

(iv) the adsorption of pipemidic acid on the electrode seems to follow a normal Langmuir type isotherm for short accumulation times; however, such accumulation drops following some unfavourable adsorption equilibrium, once a certain coverage of the surface has been attained.

4.5.3.6 Effect of the Concentration of Pipemidic Acid in Solution

As mentioned in section 4.3.2.5.3, the use of the adsorptive stripping

voltammetry technique as an analytical approach depends on the existence of a defined and reproducible relation between the concentration of analyte in solution and the intensity of the voltammetric response of the adsorbed substance.

This dependency between the peak intensity and the concentration of the analyte was studied in 0.1 M HClO₄. Linear sweep voltammetry was employed, and the scans were carried out at 1 Vs⁻¹. The accumulation conditions were as follows: E_{acc} -500 mV, mercury drop size corresponding to 3 divisions of the micrometric dial of the electrode, constant stirring rate, t_{acc} 75 s under electrolysis and 10 s resting time.

C / mol l ⁻¹	i _p / nA
2.5 x 10 ⁻⁹	4.00
5.0 x 10 ⁻⁹	18.00
7.5 x 10 ⁻⁹	37.00
1.0 x 10 ⁻⁸	55.00
2.5 x 10 ⁻⁸	141.00
5.0 x 10 ⁻⁸	266.00
7.5 x 10 ⁻⁸	398.00
1.0 x 10 ⁻⁷	508.00

Table 4.2 Effect of concentration of pipemidic acid on the adsorptive stripping voltammetric response signal

The results are summarised in Table 4.2. The reduction peak of

pipemidic acid is 3 times superior in height to that of the base line noise of the background electrolyte for a concentration of 2.5×10^{-9} M. The peak intensity varies linearly with concentration in the range of 7.5×10^{-9} M to 1.0×10^{-7} M. The curve so obtained passes almost through the ordinates of both axis at the origin (Fig. 4.10).

The equation that defines the dynamic linear range is:

$$i \text{ (uA)} = (5.1 \times 10^6) (M) - 4.8 \times 10^{-4}; r = 0.9989$$

The high sensitivity of the adsorptive stripping voltammetric technique is usually accompanied by a good reproducibility of the measurement. This reproducibility was demonstrated by repeating the procedure of accumulation-stripping in a solution containing 2.0×10^{-8} M of pipemidic acid. The experience performed 10 times gave rise to the following values:

-average peak current	96.6 nA
-standard deviation	6.6×10^{-3}
-relative standard deviation	1.7 %

4.5.3.7 Differential Pulse and Square Wave Voltammetry

Although linear sweep voltammetry possesses sufficient sensitivity to determine pipemidic acid in urine samples, as will be shown in the next sections, it was decided to explore alternative potential scan modes that might provide with an even better analytical response. Several experiments were carried out using both differential pulse and square wave techniques.

As indicated in sections 4.3.2.2 and 4.3.2.4, irreversible processes are commonly better studied by applying either of the mentioned techniques.

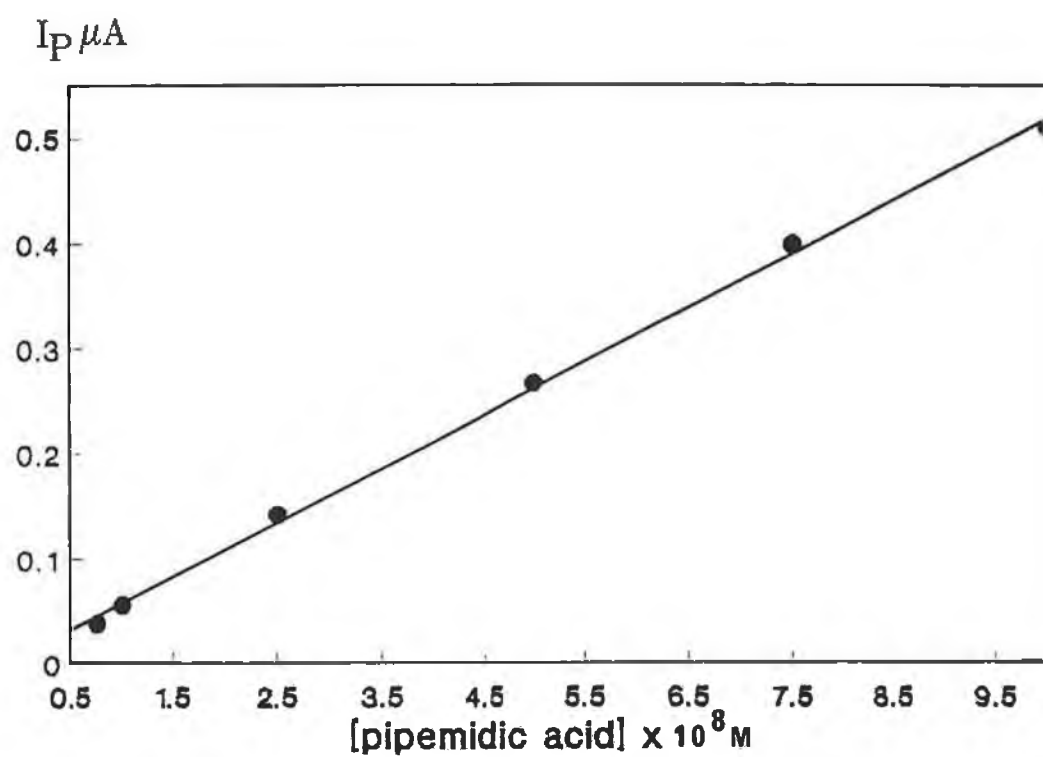


Fig. 4.10 Calibration curve of pipemidic acid in 0.1 M HClO_4 background electrolyte solutions.

Nevertheless, situations have been reported in which these techniques do not provide with more sensitive signals than those offered by linear sweep voltammetry, when applied to the stripping of substances strongly adsorbed on the surface of the working electrode.

With this in mind, inherent parameters of both techniques were optimised for the analytically relevant reduction process before calibration curves were constructed using differential pulse and square wave voltammetry.

4.5.3.7.1 Differential Pulse Voltammetry

The effect of pulse amplitude was examined for a 4.0×10^{-7} M concentration of pipemidic acid in 0.1 M HClO_4 for values between 10 and 100 mV. At 75 s after accumulation, the differential intensity of the peak proved to be linear for values within 10 to 50 mV. At higher values the curve levels off and the peak current remains constant for pulse amplitudes over 60 mV (see Fig. 4.11a).

Studies of the accumulation of the drug on the surface of the electrode were carried out for a 4.0×10^{-7} M solution of the drug. The conditions adopted were: pulse amplitude 50 mV and scan rate 1 Vs^{-1} .

As seen from Fig. 4.11b the drug accumulates onto the surface of the electrode in a trend similar to that followed by LSV.

The linearity between peak intensity and concentration was then examined in concentrations ranging from 1.1×10^{-8} M to 7.5×10^{-8} M. The measurements were performed under the following conditions: t_{acc} 75 s, E_p -500, scan rate 1 Vs^{-1} , pulse amplitude 50 mV. The linear regression analysis of this data gives an intercept of 2.8×10^{-3} μA and a slope of

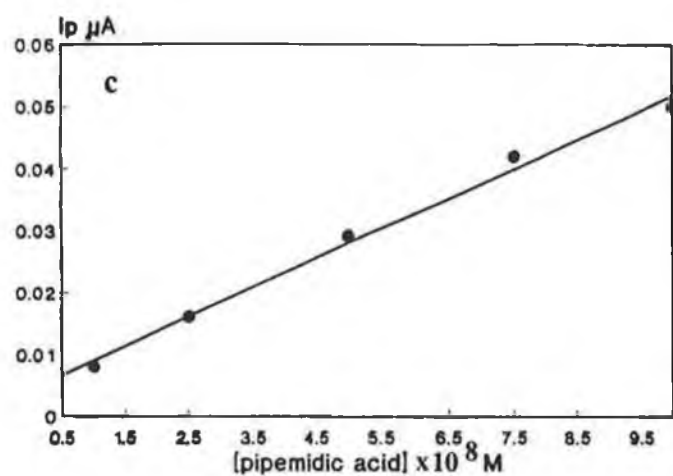
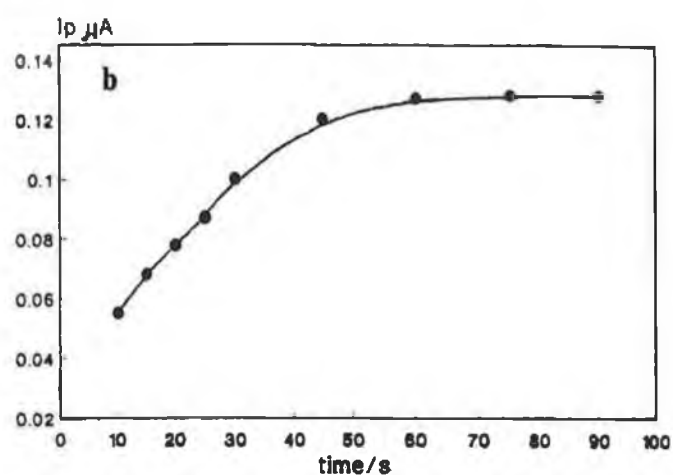
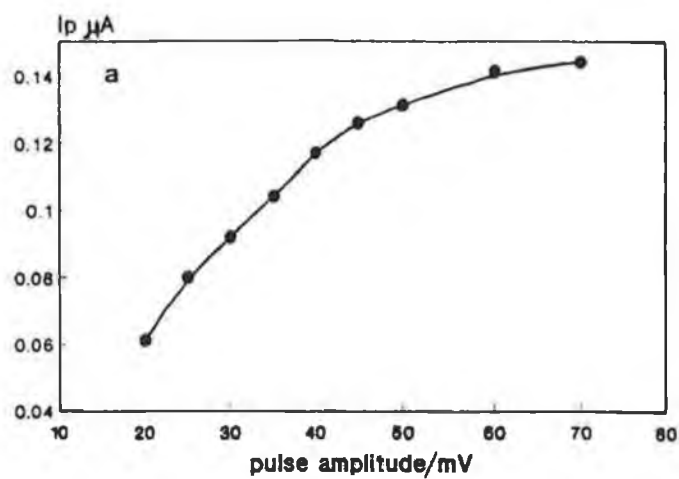


Fig. 4.11 Some characteristics of the response signal of pipemidic acid by differential pulse voltammetry: a) effect of pulse amplitude; b) effect of the accumulation time; c) calibration curve.

5.2×10^5 uA. The regression coefficient found is 0.999. A plot of the calibration curve is presented in Fig. 4.11c.

4.5.3.7.2 Square Wave Voltammetry

As for the differential pulse technique, characteristic parameters of square wave voltammetry were optimised previous to the construction of calibration curves. In 2.0×10^{-7} M stirred solutions of pipemidic acid accumulated for 45 s the optimum conditions of pulse amplitude and frequency were found to be 50 mV and 160 Hz respectively. These conditions, together with an accumulation potential of -500 mV and a scan rate of 1 V s^{-1} gave at variable accumulation times a trend similar to that found previously using either LSV or DPV. Following these conditions and preconcentrating the drug after 1.15 minutes, the limit of detection was 8.0×10^{-9} M and the linear range found extended from 1.1×10^{-8} M to 7.5×10^{-8} M (Table 4.3). The equation describing this linear range is:

$$i/\text{uA} = 3.6 \times 10^6 \text{ C(M)} - 4.5 \times 10^{-2}; r = 0.997$$

Concentration mol l ⁻¹	I _p nA
1.0×10^{-8}	90
2.5×10^{-8}	140
5.0×10^{-8}	250
7.5×10^{-8}	310

Table 4.3 Calibration curve data for pipemidic acid obtained using square wave voltammetry.

4.5.3.8 Application of Adsorptive Stripping Voltammetry to the Determination of Pipemidic Acid in Urine

In bibliographical reviews concerning this technique, no work has been reported that makes reference to the determination of the drug in biological matrices containing surfactants. Although, in principle, such an application must be possible if the determinand is separated, the neoclassicist to employ complex separation methods does not look attractive to tackle the problem.

Apart from proteins, urine contains numerous low molecular weight substances, many of which are electroactive and/or capable of adsorbing onto mercury electrodes. It is then expected that separation methods based on different molecular size will not be efficient enough for this type of matrix.

An alternative to the problem consists in abandoning an exhaustive clean-up of the sample and the use of short accumulation times to minimise the effect of surfactants. The interferences from other substances that do not accumulate may be reduced by diluting the sample, which also decreases the saturation of the drop surface by surfactants. However, it is evident that both procedures are detrimental to the sensitivity of the technique, but it was hoped that this would still be sufficient for the determination in the range of concentrations of clinical importance.

4.5.3.8.1 Extraction Procedure

Attempts were made to carry out a direct determination of pipemidic acid in urine samples. Regarding this approach, a 1 ml urine sample was spiked with the drug to give a concentration 1.0×10^{-4} M and diluted to 20 ml with the background electrolyte (final concentration in cell: 5×10^{-6} M). After

75 s accumulation time the voltammogram recorded under the usual conditions (Fig. 4.12a) did not show at all the reduction peak otherwise obtained for pipemidic acid in 0.1 M HClO_4 (Fig. 4.12b). This experiment reveals the suppressive effect of some of the natural existing components of urine which behave as surfactants, leading to the necessity of applying some sort of clean-up procedure. Separation procedures are a conventional requirement in most analytical methodologies when determining species in biological samples (an exception being the use of potentiometric selective electrodes or biosensors).

Accordingly, a solid-liquid extraction was employed owing to the ease with which it can be carried out, the low cost, as well as the good results obtained with other related analytes [45,46].

The retention characteristics of pipemidic acid onto the packing material of a C_{18} cartridge were studied for a wide range of pH's provided by phosphate/acetate/ammonia buffer solutions i.e., pH between 2 and 9. The results (Fig. 4.13) do not show significant differences with variation in the pH, and recoveries were calculated to be between 98 and 99.5 % in all instances. The best analytical signal was obtained for an extraction accomplished at pH 5, and this was chosen for the extraction of urine samples.

Urine samples consisted of pooled human urines donated from ten healthy individuals. The samples were spiked with an adequate amount of the drug to give the desired final concentration.

The cartridge was previously activated by passing successively 20 ml of water, 10 ml of methanol and 10 ml of the respective buffer. 1 ml of urine sample was diluted to 10 ml with the buffer solution (0.025 M phosphate-acetate

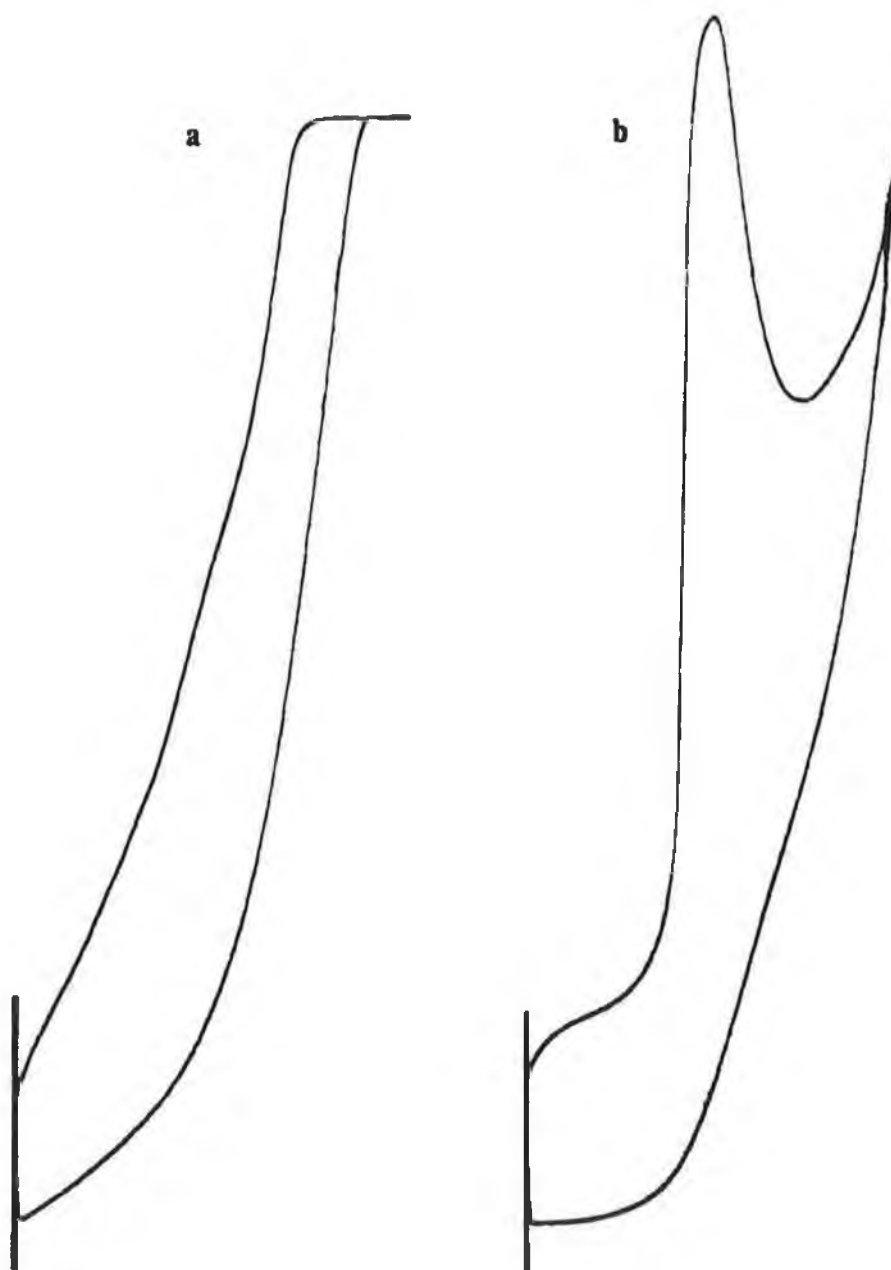


Fig. 4.12 (a) Effect of untreated urine sample on the adsorptive stripping voltammetric behaviour of 5.0×10^{-6} M solution of pipemidic acid after an accumulation time of 75 s. (b) Response signal of the same concentration of the drug previous to addition of urine after an accumulation time of 75 s.

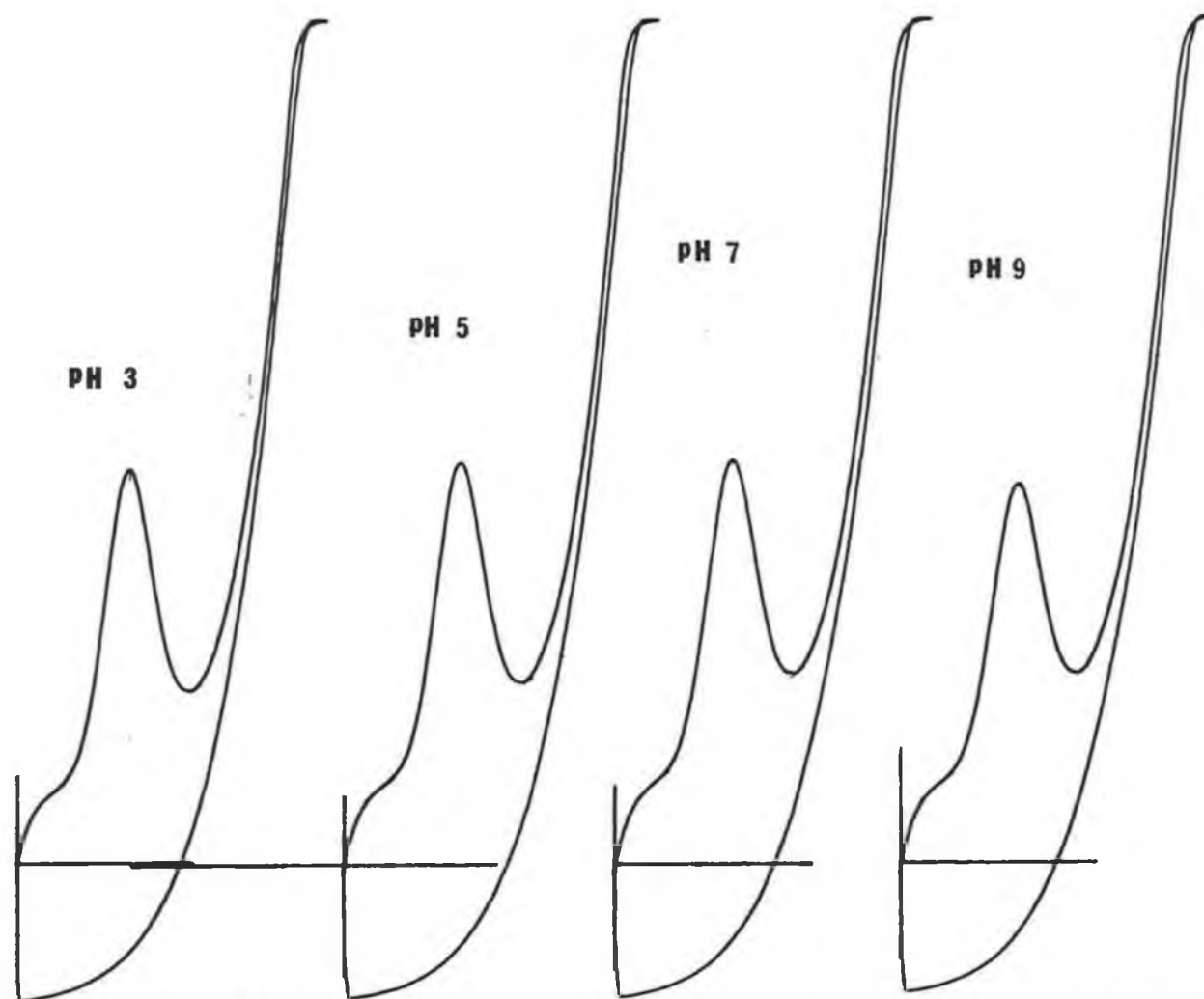


Fig. 4.13 Voltammograms obtained during extraction of aqueous solutions of pipemidic acid at different pH.

buffer adjusted to pH 5 with 0.8 M NaOH). This was mixed carefully to avoid the forming of foam and transferred to a 20 ml syringe. The solution prepared was passed through the cartridge and the eluent discarded. The cartridge was then washed with 20 ml of water and the retained materials were eluted with 3 ml of methanol. Afterwards, the solvent was evaporated in a thermostatted bath at 45°C under an inert gas stream. The dry extract was redissolved in 5 ml of the background electrolyte (0.1 M HClO₄) and mixed by mechanical vibration for 2 minutes. 0.5 ml aliquots were transferred to the polarographic cell and made up to 20 ml with 0.1 M HClO₄ and the voltammograms recorded in the usual fashion.

The extract of urine thus prepared is practically free of proteins and very polar molecules which are eluted from the column by eluting with water.

The main advantage of the separation procedure described is its simplicity. Analogous procedures using reversed-phase C₁₈ or silica microcolumns are becoming very popular during last years for the clean up of biological samples in routine analysis by HPLC.

Extracts were prepared according to the above mentioned procedure and their adsorptive stripping characteristics were examined using linear sweep voltammetry. The voltammograms corresponding to the blanks were first observed, and subsequently varying amounts of the drug were added to the extract dissolved in the background electrolyte. The additions were made with a Hamilton microsyringe to avoid variations in the volume of the cell (20 ml).

The first experiments demonstrated that the accumulation in magnetically stirred solutions were scarcely useful, since no peaks were observed for added amounts of pipemidic acid lower than 6.3 ug (t_{acc} 20 s), which would correspond to a concentration of drug in urine of about 2×10^{-4} M. The

accumulation in stationary solutions produced superior results, being able to detect 0.5 ug of pipemidic acid added to the 0.5 ml urine extract at the same accumulation time.

These preliminary results showed that accumulation in the convective transport mode was not viable for the application. All other experiments were carried out in stationary solutions.

Fig. 4.14 shows the voltammograms obtained for different values of t_{acc} in (a) the urine extract and (b) in the same extract after the addition of 6.3 ug of pipemidic acid to the cell. In the voltammograms corresponding to that of the blank no peak was observed at the potential at which pipemidic acid is reduced. However, two peaks are observed at -645 mV and -911 mV during the cathodic scan whose intensities increase with time. These peaks start to appear after a t_{acc} of 45 s, and at a t_{acc} of 75 s the currents for the unknown peaks are 46 nA and 96 nA respectively.

Accumulation curves obtained for urine extracts spiked with the drug (Fig. 4.15b) showed that maximum adsorption was reached with a shorter t_{acc} than in aqueous solutions, owing to the presence of natural surfactants in the urine which were retained in the C₁₈ cartridge with the drug and compete for the adsorption sites of the electrode. As can be seen from Fig. 4.15, adsorption maxima occur for t_{acc} between 10-20 s. A t_{acc} of 20 s was used throughout for urine samples.

4.5.3.8.2 Effect of Concentration of Pipemidic Acid in the Presence of Urine

Extract

The intensity of the cathodic peak varies linearly with the amount of pipemidic acid added to a blank urine extract. This addition gave rise to

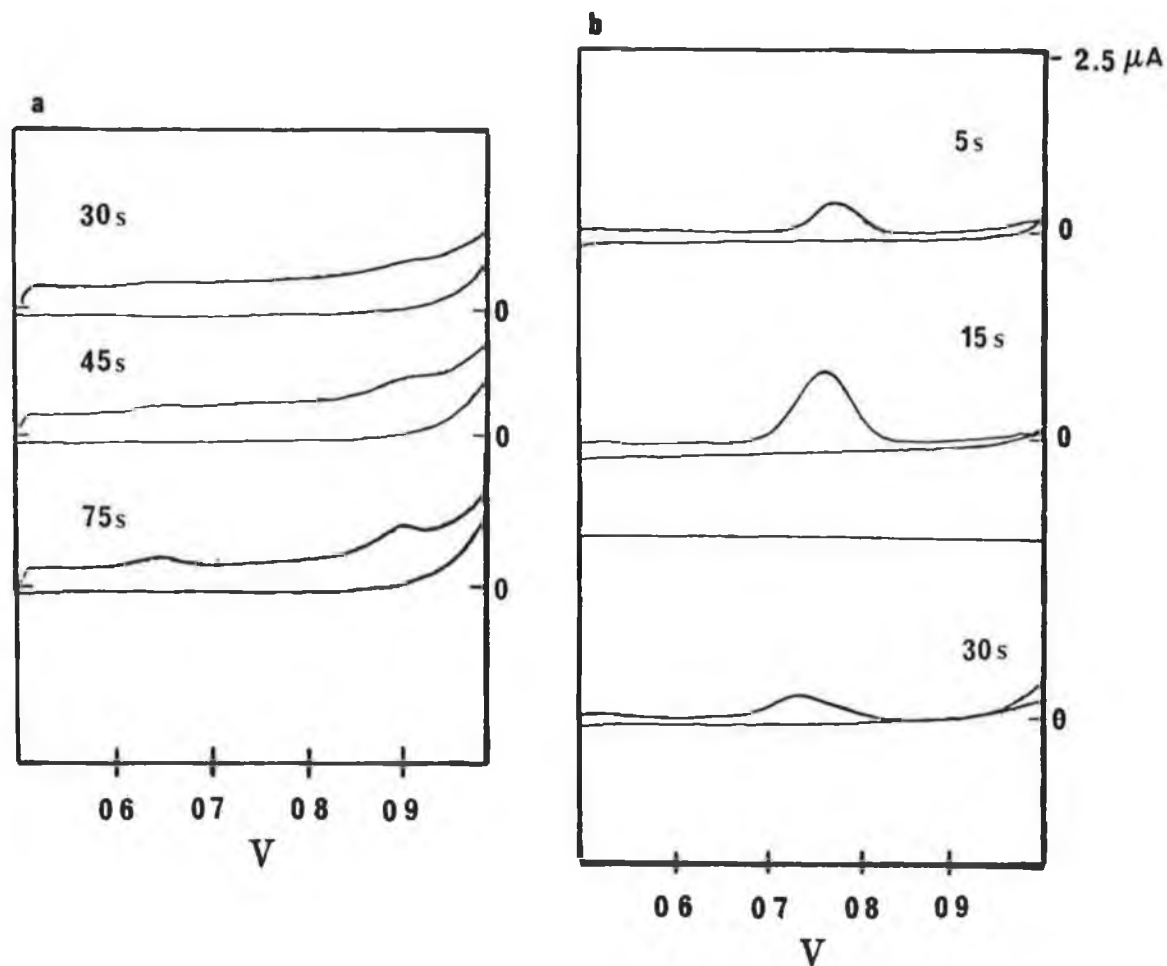


Fig. 4.14 Voltammograms for (a) blank urine extracts, and (b) pipemidic acid additions, at different accumulation times.

$I_p \mu A$

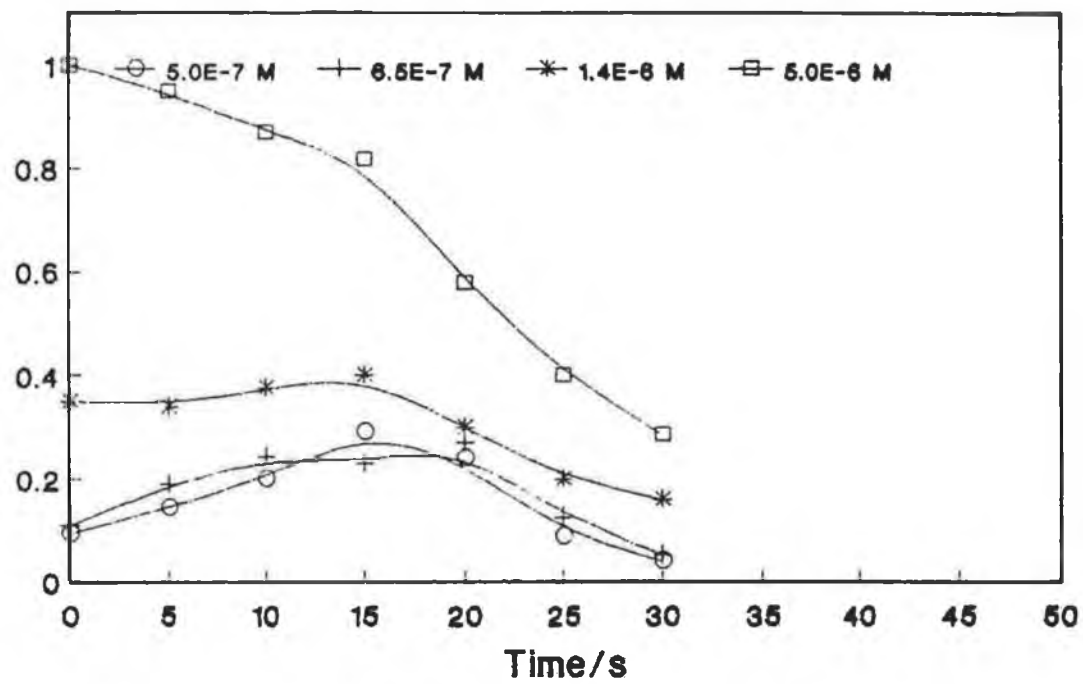


Fig. 4.15 Accumulation curves for different concentrations of pipemidic acid in urine samples.

a wide range of linearity covering almost 2 orders of magnitude from 2.0×10^{-7} M to 1.0×10^{-5} M in the cell (Fig. 4.16), as expressed by the following equation:

$$i_p (\mu\text{A}) = 6.3 \times 10^4 C (\text{M}); r = 0.999, n = 11$$

A calibration graph was also constructed using direct responses i.e. 5 s without stirring. The calibration plot obtained in this case showed a shorter linear range of linearity from 1.0×10^{-7} M to 1.0×10^{-6} M.

4.5.3.8.3 Standard Addition

The excellent linearity of the response signal allows one to use the method of standard addition.

The voltammogram of a blank urine extract obtained following the extraction procedure mentioned in section 4.5.3.8.1 is shown in Fig. 4.17 (line 0), together with a urine sample extract (line 1) containing $30.35 \mu\text{g ml}^{-1}$ of pipemidic acid. Quantitation of the urine content of the drug was accomplished by the standard addition method (Fig. 4.17, lines 2 to 4).

To further establish the precision of the method, 5 aliquots of urine were spiked with the same amount of drug and processed according to the proposed method. The compiled results (table 4.4) show that at this concentration level, the recovery attained was 82% and the assay precision expressed in terms of the relative standard deviation was 5.2%.

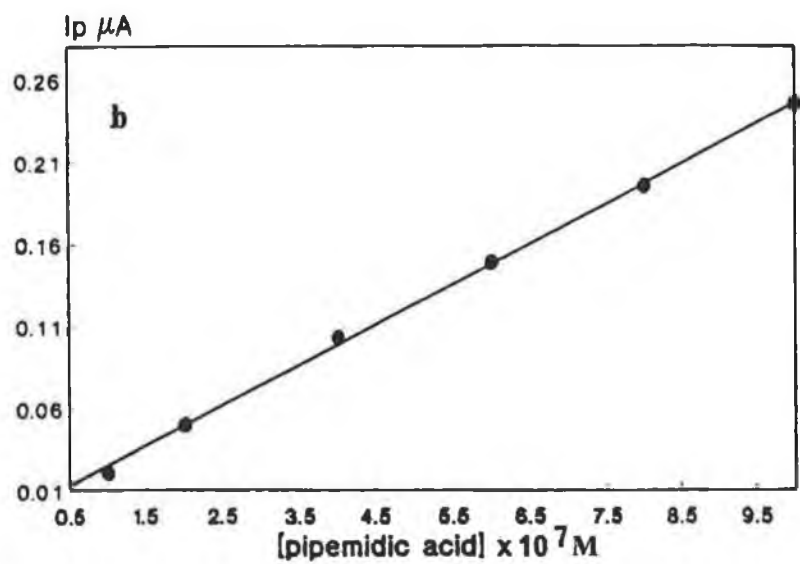
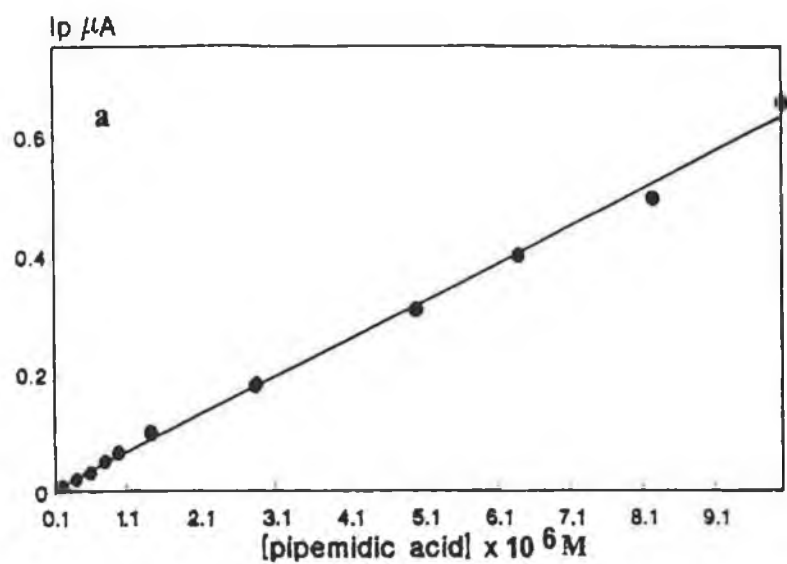


Fig. 4.16 Calibration curves of pipemidic acid in urine samples by standard addition: (a) t_{acc} 20 s; (b) t_{acc} 5 s.

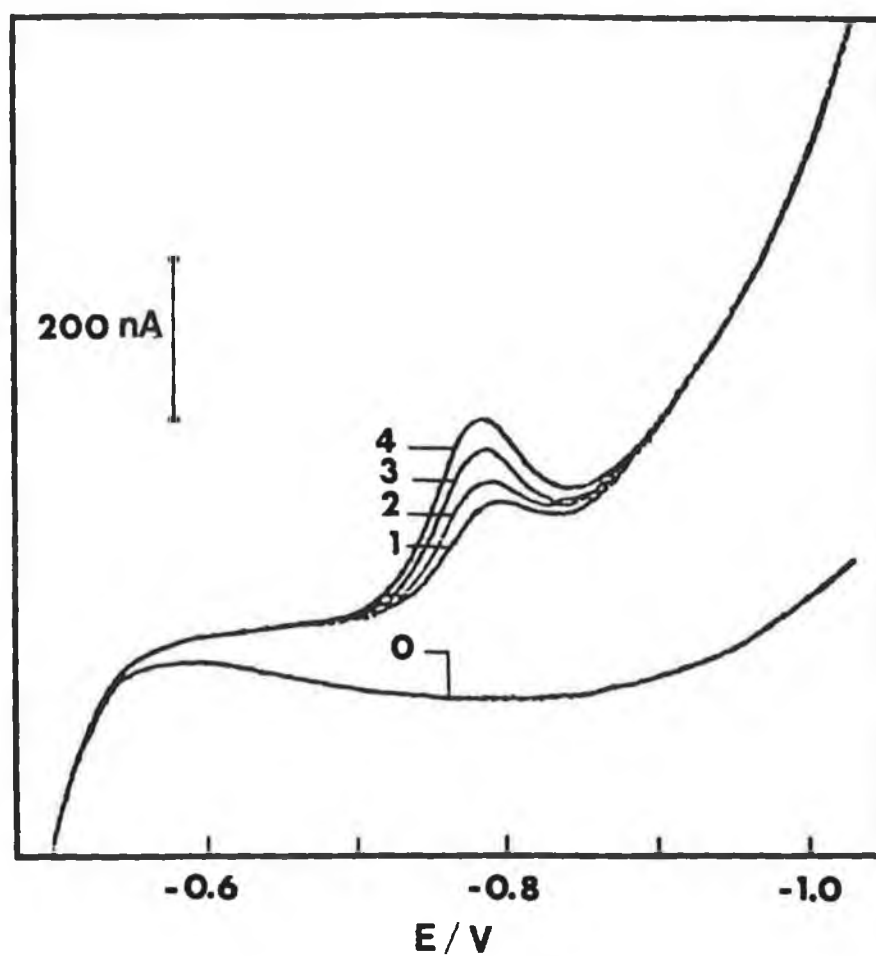


Fig. 4.17 Linear sweep voltammograms obtained for urine extracts of a urine sample. 0 a blank; and 1 containing 30.35 ug ml^{-1} of pipemidic acid. Curves 2 - 4 are successive standard additions of $1.5 \times 10^{-7} \text{ M}$ of the drug.

Sample	Concentration found mol l ⁻¹
1	4.40 x 10 ⁻⁷
2	4.09 x 10 ⁻⁷
3	4.17 x 10 ⁻⁷
4	3.88 x 10 ⁻⁷
5	3.89 x 10 ⁻⁷

Table 4.4 Precision data for the method.

4.5.3.9 Conclusions

Pipemidic acid is reduced on mercury electrodes, the number of processes being dependent on the pH of the solution. The main process observed under optimised conditions by linear sweep voltammetry was used for analytical purposes.

The drug can be accumulated by adsorption on hanging mercury drop electrodes. The accumulation process is controlled by the transport of the drug to the surface of the electrode. The voltammetric response of the adsorbed species presents a maximum current intensity at pH 1.

The voltammograms of pipemidic acid adsorbed onto the electrode indicate that the shape and symmetry of the peaks, as well as the dependency on the scan rate, is consistent with an adsorption controlled process.

The determination of pipemidic acid by adsorptive stripping voltammetry in aqueous solutions is feasible for concentrations as low as 7.5 x 10⁻⁹ M. In fact, the dynamic linear range was found to be between 7.5 x 10⁻⁹ M to

1×10^{-7} M. The optimum conditions for the determination are: pH = 1 (0.1 M HClO_4 as background electrolyte); accumulation time 75 s in stirred solution under electrolysis; scan rate 1 V s^{-1} ; accumulation potential -500 mV. Operating under these conditions it is possible to detect 2.5×10^{-9} M pipemidic acid. The reproducibility of the adsorptive voltammetric measurement at a concentration level of 2×10^{-8} M is demonstrated by a relative standard deviation of 1.7 %.

The use of other voltammetric techniques such as differential pulse voltammetry and square wave voltammetry working under optimised conditions did not enhance the response signal of pipemidic acid for this determination.

The adsorptive stripping characteristics of pipemidic acid was examined in the presence of urine extracts obtained following elution through a C_{18} cartridge. The results of these experiments demonstrated that the adsorptive accumulation of the drug takes place in unstirred solutions. For an accumulation time of 20 s in the presence of the extract, the adsorptive stripping response varies linearly in the range of 2.0×10^{-7} M to 1.0×10^{-5} M of pipemidic acid.

On the basis of these results the standard addition technique can be used preferentially for the determination of the drug in urine samples following extraction in a reverse phase C_{18} microcolumn. Accordingly, the results of 5 urine samples containing 30.35 ug ml^{-1} gave a relative standard deviation of 5.2 % for the determination.

4.6 REFERENCES

1. Chamberlain, J., Analysis of Drugs in Biological Fluids, CRC Press, Boca Raton, Florida, 1986.
2. De Leenheer, A. and Nelis, H., Analyst, 1981, 106, 1025.
3. Takase, Y., Nakamura, S., Takae, H., Minami, A., Nakata, K., Inoue, S., Ishiyama, M. and Kubo, Y., Antimicrob. Agents Chemother., 1975, 8, 132.
4. Holmes, B., Brogden, R.N. and Richards, D.M., Drugs, 1985, 30, 482.
5. Shimizu, M., Nakamura, S., Takase, Y. and Kurobe, N., Antimicrob. Agents Chemother., 1975, 7, 441.
6. Fukuhara, K. and Matsuki, Y., J. Chromatogr., Biomed. Appl., 1987, 60, 409.
7. Zio, C.A., Mazzarini, G. and Pietta, P., J. Chromatogr. 1980, 200, 245.
8. Smethurst, A.M. and Mann, W.C., J. Chromatogr., Biomed. Appl., 1983, 274, 421.
9. Hoffmann, H. and Dybowski, M., Fresenius Z Anal. Chem., 1982, 312, 625.
10. Brezina, M. and Zuman, P., Polarography in Medicine, Biochemistry and Pharmacy, Interscience, New York, 1958.
11. Bond, A., Modern Polarographic Methods in Analytical Chemistry, Marcel Dekker, New York, 1980.
12. Flato, J., Anal. Chem., 1972, 44, 75A.
13. Smyth, M.R. and Smyth, W.F., Analyst, 1978, 103, 529.
14. Zuman, P., Organic Polarographic Analysis, Pergamon Press, Oxford, 1964, p. 99.
15. Chowdhry, B., in Polarography of Molecules of Biological Significance, Smyth, W.F. (Ed.), Academic Press, London, 1979, p. 169.

16. Kalvoda, R., *Anal. Chim. Acta*, 1982, 138, 11.
17. Smyth, W.F. and Smyth, M.R., in *Polarography of Molecules of Biological Significance*, Smyth, W.F. (Ed.), Academic Press, London, 1979, p.28.
18. Davidson, I.E. and Smyth, W.F., *Anal.Chem.*, 1977,,49, 1195.
19. Brooks, M., D'Arconte, L., Hackman, M. and de Silva, J., *J. Anal. Toxicol.* 1977, 1, 179.
20. Heyrovsky, J. and Kuta, J., *Principles of Polarography*, Academic Press, New York, 1966.
21. Meites, L., *Polarographic techniques*, Interscience, New York, 1965.
22. Zuman, P., *The Elucidation of Organic Electrode Processes*, Academic Press, New York, 1969.
23. Parry, E. and Osteryoung, R., *Anal. Chem.*, 1965, 37, 1634.
24. Birke, R., Kim, M-H. and Strasfeld, M., *Anal. Chem.*, 1981, 53, 852.
25. Bard, A.J. and Faulkner, L.R., *Electrochemical Methods*, J. Wiley, New York, 1980.
26. Mac Donald, D.D., *Transient Techniques in Electrochemistry*, Plenum Press, New York, 1977.
27. Kalvoda, R. and Kopanica, M., *Pure Appl. Chem.*, 1989, 61, 97.
28. Laviron, E., *Bull. Soc. Chim.*, 1967, 3717.
29. Phillips, S.L., *J. Electroanal. Chem.*, 1966, 12, 294.
30. Valenta, P. and Krzvaric, D., *J. Electroanl. Chem.*, 1977, 75, 437.
31. Korita, J., *Czech. Chem. Commun.*, 1953, 18, 206.
32. Kolpin, C.F. and Swofford, H.S., *Anal. Chem.*, 1978, 50, 916.
33. Laviron, E., *J. Electroanal. Chem.*, 1974, 52, 395.
34. Laviron, E., *J. Electroanal. Chem.*, 1979, 100, 263.
35. Wopschall, R. and Shain, I., *Anal. Chem.*, 1967, 39, 1515.

36. Laviron, E., *J. Electroanal. Chem.*, 1975, 63, 245.
37. Kalvoda, R., in press.
38. Koryta, J., *Coll. Czech. Chem. Commun.*, 1953, 18, 206.
39. Webber, A., Shah, M. and Osteryoung, R., *Anal. Chim. Acta*, 1983, 154, 105.
40. Wang, J., Luo, D., Farias, P. and Mahmoud, J., *Anal. Chem.*, 1985, 57, 158.
41. Fernandez Alvarez, J.M., Costa Garcia, A., Miranda Ordieres, A.J. and Tunon Blanco, P., *J. Electroanal. Chem.*, 1987, 225, 241.
42. Meites, L., Zuman, P. and Rupp, E., *Handbook Series in Organic Electrochemistry*, CRC Press, Boca Raton, Florida.
43. Tunon Blanco, P., Fernandez Alvarez, J.M. and Costa Garcia, A., *Proceedings ElectroFinnAnalysis*, Plenum Press, 1990, in press.
44. Cortina Villar, J.C., Costa Garcia, A., Fernandez Alvarez, J.M. and Tunon Blanco, P., *J. Electroanal. Chem.*, 1990, 280, 167.
45. Fernandez Alvarez, J.M., Costa Garcia, A., Miranda Ordieres, A.J. and Tunon Blanco, P., *J. Pharm. Biomed. Anal.*, 1988, 6, 743.
46. Collier, C., McLeo, S. and Solding, S., *Ther. Drug Monit.*, 1982, 4, 371.

CONCLUDING REMARKS

The construction and characterisation of ion-selective electrodes based on several calixarene neutral molecules has led to the development of successful electrodes for caesium and sodium ions. Simple and convenient design of catheter type electrodes with tip dimensions of about 2 mm was used in most part of this research. These electrodes were used to assess the performance of two hexameric calixarenes with respect to electrode response function, dynamic characteristics and selectivity against a common range of interfering ions. Both electrodes behaved relatively well with near-Nernstian responses to changes in caesium concentration. The electrodes responded quickly to changes in concentration and steady state response was obtained within a few seconds. Selectivity coefficients for both electrodes were determined for common alkali and alkaline earth metal ions, indicating that one is superior in its preference with respect to rubidium and potassium ions. Although a few caesium electrodes have been described in the literature, the applications of caesium electrodes in chemical analysis tends to be limited mainly to the analysis of caesium in nuclear fission processes.

Catheter type, macroelectrodes and coated wire electrodes based on PVC membranes incorporating either a methyl ester or a methyl tetraketone tetrameric calixarenes were studied. The sodium responsive electrodes all exhibited Nernstian behaviour. The stability and reproducibility of the electrodes were determined in aqueous sodium solutions and were found to be excellent in every case. The life time of the electrodes was examined by measuring the electrode response function and resistance over a prolonged period of time. Results showed that operational life times of at least several

months can be obtained. The rapid response of the electrodes is an additional requirement of these devices for most applications. Although responses are almost instantaneous, accurate measurements could not be performed due to limitations posed by the experimental set up. However, responses of less than 10 seconds were estimated for both electrodes for decade changes in sodium activity. The selectivity coefficients determined for both electrodes indicated that the preference against lithium, potassium and hydrogen is superior to other existing electrodes based on solvent polymeric membranes. In general these selectivities can be regarded as comparable to the sodium glass electrode with the exception of a much improved discrimination against hydrogen ions (an extremely important characteristic). The ammonium selectivity is improved for the methyl tetraketone electrode in comparison to its methyl ester counterpart. Both electrodes were applied to the determination of sodium in blood plasma samples and the results compared to automated analysers and to flame photometry. The measurements made by the dipping measuring technique at steady-state equilibrium gave very similar results to the reference methods. The precision of the measurements was within a few mmol per liter. The manual method represented the limiting factor for better precision in this type of analysis.

The development and optimisation of a flow injection analysis system incorporating the methyl ester calix[4]arene electrode was carried out and proved successful for the determination of sodium in plasma samples. The results obtained were compared to the manual technique employed previously and were found to greatly improve the precision and accuracy. The results typically showed residual standard deviations of less than 1 mmol per liter in comparison to flame photometry. According to these results this particular

electrode can be considered as a successful alternative to the sodium glass electrode for clinical applications. Not only are the desirable features of solvent polymeric membranes met with the calixarene based electrodes but in addition these membrane electrodes should prove less expensive compared to the traditional glass electrodes.

In another part of these research modern voltammetric techniques were employed to study the electrochemical behaviour of pipemidic acid. The drug is reduced on mercury electrodes, the number of processes being dependent on the pH of the background electrolyte. The main reduction process observed under optimised conditions was used to develop an analytical method by adsorption stripping voltammetry. The determination of pipemidic acid in human urine of patients undergoing pipemidic acid therapy proved successful, with this technique providing with a useful quantitative analysis for monitoring patients in the therapeutical useful concentration range of pipemidic acid.